Calhoun
Institutional Archive of the Naval Postgraduate School

Calhoun: The NPS Institutional Archive

DSpace Repository

Theses and Dissertations | 1. Thesis and Dissertation Collection, all items

1985

Mean flow and turbulence in complex terrain

Buell, Michael J.

http://hdl.handle.net/10945/21425

Downloaded from NPS Archive: Calhoun

http://www.nps.edu/library

Calhoun is the Naval Postgraduate School's public access digital repository for research materials and institutional publications created by the NPS community. Calhoun is named for Professor of Mathematics Guy K. Calhoun, NPS's first appointed -- and published -- scholarly author.

Dudley Knox Library / Naval Postgraduate School
411 Dyer Road / 1 University Circle
Monterey, California USA 93943

DUDLEY KNOX LIBRARY
NAVAL POSTGRADUATE SCHOOL
MONTEREY, CALIFORNIA 93943-5002

NAVAL POSTGRADUATE SCHOOL
Monterey, California

THESIS

MEAN FLOW AND TURBULENCE IN COMPLEX TERRAIN

by

Michael J. Buell

March 1985

Thesis Advisor: Gordon E. Schacher

Approved for public release; distribution unlimited

T230154

REPORT DOCUMENTATION PAGE

READ INSTRUCTIONS BEFORE COMPLETING FORM

1. REPORT NUMBER

2. GOVT ACCESSION NO.

3. RECIPIENT'S CATALOG NUMBER

4. TITLE (and Subtitle)
Mean Flow and Turbulence in Complex Terrain

5. TYPE OF REPORT & PERIOD COVERED
Master's Thesis
March 1985

6. PERFORMING ORG. REPORT NUMBER

7. AUTHOR(s)
Michael J. Buell

8. CONTRACT OR GRANT NUMBER(s)

9. PERFORMING ORGANIZATION NAME AND ADDRESS
Naval Postgraduate School
Monterey, California 93943

10. PROGRAM ELEMENT, PROJECT, TASK AREA & WORK UNIT NUMBERS

11. CONTROLLING OFFICE NAME AND ADDRESS
Naval Postgraduate School
Monterey, California 93943

12. REPORT DATE
March 1985

13. NUMBER OF PAGES
270

14. MONITORING AGENCY NAME & ADDRESS(if different from Controlling Office)

15. SECURITY CLASS. (of this report)
Unclassified

15a. DECLASSIFICATION/DOWNGRADING SCHEDULE

16. DISTRIBUTION STATEMENT (of this Report)
Approved for public release; distribution unlimited

17. DISTRIBUTION STATEMENT (of the abstract entered in Block 20, if different from Report)

18. SUPPLEMENTARY NOTES

19. KEY WORDS (Continue on reverse side if necessary and identify by block number)
Turbulence
Diffusion

20. ABSTRACT (Continue on reverse side if necessary and identify by block number)

Atmospheric models used to describe horizontal diffusion in the surface layer depend upon a detailed characterization of the mean flow and standard deviation of wind direction fluctuations ($\sigma\theta$). Meteorological data were collected from 12 towers located across the coastal complex terrain of Vandenberg AFB, CA. from August 1983 to July 1984 in order to

#20 - ABSTRACT - (CONTINUED)

analyze these mean and turbulence parameters as a function of stability, time averaging, wind direction, wind speed, elevation and terrain.

Three stability cases were chosen from Richardson Number criteria and found representative of specific flow regimes. $\sigma\theta$ was a function of stability with the largest values associated with the unstable (sea breeze) case and lower values with the stable (land breeze/drainage flow) and neutral (postfrontal) cases. All three stability cases showed varying degrees of $\sigma\theta$ dependence on time averaging, wind direction, wind speed, elevation, and terrain with greater time averaging dependence found in the unstable case, greater wind direction and terrain dependence noted in the stable case, and greater lower level height dependence found in both the stable and unstable cases. In contrast to most findings over homogeneous terrain, $\sigma\theta$ dependence on wind speed was found in all three stability cases with this dependence most important in the netural case.

Approved for public release; distribution is unlimited.

Mean Flow and Turbulence in Complex Terrain

by

Michael J. Buell
Captain, United States Air Force
B.S., Pennsylvania State University, 1980

Submitted in partial fulfillment of the
requirements for the degree of

MASTER OF SCIENCE IN METEOROLOGY

from the

NAVAL POSTGRADUATE SCHOOL

March 1985

-thesis
B5974
c.1

ABSTRACT

Atmospheric models used to describe horizontal diffusion in the surface layer depend upon a detailed characterization of the mean flow and standard deviation of wind direction fluctuations ($\sigma\theta$). Meteorological data were collected from 12 towers located across the coastal complex terrain of Vandenberg AFB, CA. from August 1983 to July 1984 in order to analyze these mean and turbulence parameters as a function of stability, time averaging, wind direction, wind speed, elevation and terrain.

Three stability cases were chosen from Richardson Number criteria and found representative of specific flow regimes. $\sigma\theta$ was a function of stability with the largest values associated with the unstable (sea breeze) case and lower values with the stable (land breeze/drainage flow) and neutral (post-frontal) cases. All three stability cases showed varying degrees of $\sigma\theta$ dependence on time averaging, wind direction, wind speed, elevation, and terrain with greater time averaging dependence found in the unstable case, greater wind direction and terrain dependence noted in the stable case, and greater lower level height dependence found in both the stable and unstable cases. In contrast to most findings over homogeneous terrain, $\sigma\theta$ dependence on wind speed was found in all three stability cases with this dependence most important in the neutral case.

TABLE OF CONTENTS

I. INTRODUCTION ---------- 16

II. BACKGROUND ---------- 19

A. PRIOR WORK (TWO EXAMPLES) ---------- 19

B. THEORETICAL CONSIDERATIONS ---------- 20

III. VANDENBERG SITES AND SENSORS ---------- 24

A. SENSOR CHARACTERISTICS ---------- 24

B. TERRAIN FEATURES ---------- 25

IV. VANDENBERG CLIMATOLOGY ---------- 36

A. GENERAL FEATURES ---------- 36

B. SEASONAL CLIMATOLOGY ---------- 38

C. WIND CLIMATOLOGY ---------- 41

V. DATA ACQUISITION AND PROCESSING ---------- 46

A. DATA ACQUISITION ---------- 46

1. Vandenberg System ---------- 46

2. NPS System ---------- 46

B. DATA PROCESSING ---------- 47

1. Processing and Storage ---------- 47

2. Quality Control ---------- 50

VI. DATA ANALYSIS ---------- 52

A. GENERAL PURPOSE ---------- 52

B. BINNING ---------- 52

C. METHODOLOGY ---------- 54

VII. DEVELOPMENT OF CASE STUDIES ---------- 56

VIII. RESULTS ---------- 61
A. REFERENCE INFORMATION ---------- 61
B. UNSTABLE CASE STUDY (2/7/84, 1000-1700) ---- 61
1. Synoptic Situation/Mean Flow ---------- 61
2. σθ Dependence on Time Averaging -------- 65
a. General Results ---------- 65
b. Power Law Relationship ---------- 65
c. Height Dependence ---------- 69
d. Site/Sensor Elevation Dependence --- 73
3. σθ Dependence on Wind Direction -------- 73
a. General Results ---------- 73
b. Site/Sensor Elevation Dependence --- 82
4. σθ Dependence on Wind Speed ---------- 82
a. General Results ---------- 82
b. Site/Sensor Elevation Dependence --- 82
5. Terrain Dependence ---------- 101
C. STABLE CASE STUDY (2/12/84, 0200-0800) ----- 105
1. Synoptic Situation/Mean Flow ---------- 105
2. σθ Dependence on Time Averaging -------- 107
a. General Results ---------- 107
b. Power Law Relationship ---------- 107
c. Height Dependence ---------- 114
d. Site/Sensor Elevation Dependence --- 116
3. σθ Dependence on Wind Direction -------- 116
a. General Results ---------- 116
b. Site/Sensor Elevation Dependence --- 125

4. σθ Dependence on Wind Speed ---------- 125
a. General Results ---------- 125
b. Site/Sensor Elevation Dependence --- 135
5. Terrain Dependence ---------- 135
D. NEUTRAL CASE STUDY (3/17/84, 0900-1800) ---- 149
1. Synoptic Situation/Mean Flow ---------- 149
2. σθ Dependence on the Averaging --------- 155
a. General Results ---------- 155
b. Power Law Relationship ---------- 155
c. Height Dependence ---------- 156
d. Site/Sensor Elevation Dependence --- 160
3. σθ Dependence on Wind Direction -------- 160
a. General Results ---------- 160
b. Site/Sensor Elevation Dependence --- 170
4. σθ Dependence on Wind Speed ---------- 170
a. General Results ---------- 170
b. Site/Sensor Elevation Dependence --- 170
5. Terrain Dependence ---------- 188
E. INTERSTABILITY COMPARISON ---------- 192
IX. DISCUSSION AND INTERPRETATION ---------- 201
A. GENERAL REMARKS ---------- 201
B. UNSTABLE CASE ---------- 201
C. STABLE CASE ---------- 205
D. NEUTRAL CASE ---------- 208
E. INTERSTABILITY COMPARISON ---------- 210
X. SUMMARY AND CONCLUSIONS ---------- 213
XI. APPLICATIONS TO DIFFUSION MODELING ---------- 218

APPENDIX A: DAILY SYNOPTIC ANALYSIS (1 Aug 1983-22 Jul 84) ---------- 220

APPENDIX B: SITE SPECIFIC σθ DEPENDENCY TABLES (UNSTABLE CASE) ---------- 234

APPENDIX C: SITE SPECIFIC σθ DEPENDENCY TABLES (STABLE CASE) ---------- 241

APPENDIX D: SITE SPECIFIC σθ DEPENDENCY TABLES (NEUTRAL CASE) ---------- 248

APPENDIX E: SITE/ELEVATION SPECIFIC σθ DEPENDENCY TABLES (INTERSTABILITY) ---------- 254

APPENDIX F: SENSOR SPECIFIC σθ CHARACTERIZATION TABLES (INTERSTABILITY) ---------- 259

LIST OF REFERENCES ---------- 267

INITIAL DISTRIBUTION LIST ---------- 269

LIST OF TABLES

I. Vandenberg Meteorological Sensor Characteristics ---------- 26

II. Sensor Measurement Capabilities and Heights --- 27

III. Vandenberg Sensor and Site Locations ---------- 31

IV. Vandenberg Site Characterizations ---------- 34

V. Vandenberg Data Binning ---------- 53

VI. Vandenberg Case Studies ---------- 59

VII. Analysis of Missing $\sigma\theta$ Data ---------- 62

VIII. VBG Mean Flow--By Site (2/7/84 (1000-1700)--Unstable) ---------- 66

IX. VBG Mean Flow--By Height (2/7/84 (1000-1700)--Unstable) ---------- 67

X. $\sigma\theta$ Dependence on Time Averaging (2/7/84 (1000-1700)--Unstable) ---------- 68

XI. $\sigma\theta$ vs TAVG (All Sensors) (2/7/84(1000-1700)--Unstable) ---------- 69

XII. $\sigma\theta$ vs TAVG (All Sites) (2/7/84 (1000-1700)--Unstable) ---------- 73

XIII. $\sigma\theta$ Dependence on Wind Direction (2/7/84 (1000-1700)--Unstable) ---------- 83

XIV. $\sigma\theta$ Dependence on Wind Speed (2/7/84 (1000-1700)--Unstable) ---------- 92

XV. VBG Mean Flow--By Site (2/2/84 (0200-0800)--Stable) ---------- 108

XVI. VBG Mean Flow--By Height (2/2/84 (0200-0800)--Stable) ---------- 109

XVII. $\sigma\theta$ Dependence on Time Averaging (2/2/84 (0200-0800)--Stable) ---------- 111

XVIII. $\sigma\theta$ vs TAVG (All Sensors) (2/2/84 (0200-0800)--Stable) ---------- 114

XIX. σθ vs TAVG (All Sites) (2/2/84 (0200-0800)--Stable) ---------- 116

XX. σθ Dependence on Wind Direction (2/2/84 (0200-0800)--Stable) ---------- 126

XXI. σθ Dependence on Wind Speed (2/2/84 (0200-0800)--Stable) ---------- 136

XXII. VBG Mean Flow--By Site (3/17/84 (0900-1800)--Neutral) ---------- 152

XXIII. VBG Mean Flow--By Height (3/17/84 (0900-1800)--Neutral) ---------- 153

XXIV. σθ Dependence on Time Averaging (3/17/84 (0900-1800)--Neutral) ---------- 154

XXV. σθ vs TAVG (All Sensors) (3/17/84 (0900-1800)--Neutral) ---------- 155

XXVI. σθ vs TAVG (All Sites (3/17/84 (0900-1800)--Neutral) ---------- 156

XVII. σθ Dependence on Wind Direction (3/17/84 (0900-1800)--Neutral) ---------- 169

XVIII. σθ Dependence on Wind Speed (3/17/84 (0900-1800)--Neutral) ---------- 179

XXIX. σθ vs TAVG (Interstability--All Sensors) ------ 195

LIST OF FIGURES

1. Geographical Location of Vandenberg AFB and General Features ---------- 28

2. Vandenberg Topography and Meteorological Tower Sites ---------- 29

3. South-Central California Coastal Wind Trajectories under a Predominant Northwesterly Flow Regime ---------- 43

4. Vandenberg Monthly Wind Roses ---------- 44

5. Flow of Data Through the Arrays From Acquisition to Storage ---------- 49

6. VBG Synoptic Situation (2/7/84--Unstable) --------- 63

7. VBG Mean Flow (2/7/84 (1000-1700)--Unstable) ------ 64

8. (a) Power Law Relationship (All Sensors) (2/7/84 (1000-1700)--Unstable) ---------- 70

   (b) Power Law Ratio (All Sensors (2/7/84 (1000-1700)--Unstable) ---------- 71

9. $\sigma\theta$ vs TAVG (All Sites) (2/7/84 (1000-1700)--Unstable) ---------- 72

10. $\sigma\theta$ vs TAVG (2/7/84 (1000-1700)--Unstable)
    (a) Site 102, (b) Site 300, (c) Site 200,
    (d) Site 301, (e) Site 052, (f) Site 054,
    (g) Site 101, (h) Site 055 ---------- 74

11. $\sigma\theta$ vs WD (2/7/84 (1000-1700)--Unstable)
    (a) Site 102, (b) Site 300, (c) Site 200,
    (d) Site 301, (e) Site 052, (f) Site 054,
    (g) Site 101, (h) Site 055 ---------- 84

12. $\sigma\theta$ vs WS (2/7/84 (1000-1700)--Unstable)
    (a) Site 102, (b) Site 300, (c) Site 200,
    (d) Site 301, (e) Site 052, (f) Site 054,
    (g) Site 101, (h) Site 055 ---------- 93

13. (a) $\sigma\theta$ vs TAVG (Terrain Analysis) (2/7/84 (1000-1700)--Unstable) ---------- 102

(b) σθ vs WD (Terrain Analysis) (2/7/84 (1000-1700)--Unstable) ---------- 103

(c) σθ vs WS (Terrain Analysis) (2/7/84 (1000-1700)--Unstable) ---------- 104

14. VBG Synoptic Situation (2/2/84--Stable) ---------- 106

15. VBG Mean Flow (2/2/84 (0200-0800)--Stable) -------- 110

16. (a) Power Law Relationship (All Sensors) (2/2/84 (0200-0800)--Stable) ---------- 112

(b) Power Law Ratio (All Sensors) (2/2/84 (0200-0800)--Stable) ---------- 113

17. σθ vs TAVG (All Sites) (2/2/84 (0200-0800)--Stable) ---------- 115

18. σθ vs TAVG (2/2/84 (0200-0800)--Stable)
(a) Site 102, (b) Site 300, (c) Site 200,
(d) Site 301, (e) Site 052, (f) Site 054,
(g) Site 014, (h) Site 055 ---------- 117

19. σθ vs WD (2/2/84 (0200-0800)--Stable)
(a) Site 102, (b) Site 300, (c) Site 200,
(d) Site 301, (e) Site 052, (f) Site 054,
(g) Site 014, (h) Site 055 ---------- 127

20. σθ vs WD (2/2/84 (0200-0800)--Stable)
(a) Site 102, (b) Site 300, (c) Site 200,
(d) Site 301, (e) Site 052, (f) Site 054,
(g) Site 014, (h) Site 055 ---------- 137

21. (a) σθ vs TAVG (Terrain Analysis) (2/2/84 (0200-0800)--Stable) ---------- 145

(b) σθ vs WD (Terrain Analysis) (2/2/84 (0200-0800)--Stable) ---------- 146

(c) σθ vs WS (Terrain Analysis) (2/2/84 (0200-0800)--Stable) ---------- 147

22. VBG Synoptic Situation (3/17/84 (0900-1800)--Neutral) ---------- 150

23. VBG Mean Flow (3/17/84 (0900-1800)--Neutral) ------ 151

24. (a) Power Law Relationship (All Sensors) (3/17/84 (0900-1800)--Neutral) ---------- 157

(b) Power Law Ratio (All Sensors) (3/17/84 (0900-1800)--Neutral ---------- 158

25. σθ vs TAVG (All Sites) (3/17/84 (0900-1800)--Neutral) ---------- 159

26. σθ vs TAVG (3/17/84 (0900-1800)--Neutral)
(a) Site 102, (b) Site 300, (c) Site 200,
(d) Site 301, (e) Site 052, (f) Site 054,
(g) Site 014, (h) Site 055 ---------- 161

27. σθ vs WD (3/17/84 (0900-1800)--Neutral)
(a) Site 102, (b) Site 300, (c) Site 200,
(d) Site 301, (e) Site 052, (f) Site 054,
(g) Site 014, (h) Site 055 ---------- 171

28. σθ vs WS (3/17/84 (0900-1800)--Neutral)
(a) Site 102, (b) Site 300, (c) Site 200,
(d) Site 301, (e) Site 052, (f) Site 054,
(g) Site 014, (h) Site 055 ---------- 180

29. (a) σθ vs TAVG (Terrain Analysis) (3/17/84 (0900-1800)--Neutral) ---------- 189

(b) σθ vs WD (Terrain Analysis) (3/17/84 (0900-1800)--Neutral) ---------- 190

(c) σθ vs WS (Terrain Analysis) (3/17/84 (0900-1800)--Neutral) ---------- 191

30. (a) Power Law Interstability Comparison ---------- 193
(b) σθ vs TAVG (Interstability--All Sensors) ----- 194
(c) σθ vs TAVG (Interstability--12' Sensors) ----- 196
(d) σθ vs TAVG (Interstability--54' Sensors) ----- 197
(e) σθ vs TAVG (Interstability--102' Sensors) ---- 198
(f) σθ vs TAVG (Interstability--204' Sensors) ---- 199

TABLE OF SYMBOLS AND ABBREVIATIONS

$\sigma\theta$	-	Standard deviation of wind direction fluctuations
σv	-	Standard deviation of lateral wind fluctuations
σy	-	Cross-wind diffusion parameter
θ	-	Wind direction
θ_l	-	Potential temperature
Γ	-	Dry adiabatic lapse rate
BP	-	Barometric pressure
dT	-	Temperature difference
DP	-	Dewpoint
g	-	Gravitational constant
ON	-	Onshore
OFF	-	Offshore
PG	-	Pressure gradient
Ri	-	Gradient Richardson number
Ri_o	-	Ri (adjusted)
SW	-	Shortwave radiation
TAVG	-	Time averaging
TEM(T)	-	Temperature
U	-	Horizontal mean wind speed
VI	-	Visibility
WD	-	Wind direction
WS	-	Wind speed
Z	-	Height
Z_0	-	Local roughness length

ACKNOWLEDGEMENTS

The author acknowledges the assistance and advice provided by Professor Gordon E. Schacher, Chairman, Physics Department, Naval Postgraduate School and Professors Soren Larsen, Torben Mikkelsen and Gene Takle, also associated with the Naval Postgraduate School, in the preparation of this thesis. Their expertise and experience in the field of turbulence measurement and analysis provided me with a wealth of knowledge and information. The author also expresses gratitude to Mr. Chuck S. Skupniewicz of the Naval Postgraduate School Physics Department whose work was invaluable in providing the computer programming essential for the analysis of the data within this report.

I. INTRODUCTION

Air pollution meteorology over complex terrain has become one of the leading problems of our day. One of the most important but least understood areas of research for characterizing plume movement and pollutant concentration variations with time is the characterization of turbulence. Since turbulence drives diffusion, understanding turbulence is a necessity in diffusion modeling.

The purpose of the work reported here is to characterize both mean flow and turbulence over complex terrain. The area chosen for this study was Vandenberg Air Force Base (VBG), California, an area containing both complex and coastal terrain. From August 1983 to July 1984, meteorological data were collected from sensors located on towers throughout the Vandenberg terrain. Current and future analyses of these data will support diffusion modeling programs which have been developed by both the military and civilian organizations. Current users of these data are the Air Force Space Division for Space Shuttle impact modeling, the Army Atmospheric Science Lab for validation of 3-dimensional flow models, and the Naval Postgraduate School (NPS) for investigating coastal meteorology and parameterizing a complex terrain puff model.

The meteorological data examined in the work reported here were obtained from a total of 30 sensor arrays located

on 12 towers throughout the Vandenberg terrain. The data include wind speed, wind direction, air temperature, dew-point temperature, barometric pressure, visibility, and long and short-wave radiation. Means of these quantities and the standard deviation of wind direction fluctuation parameters ($\sigma\theta$) were processed and recorded. Schacher and Stanton [Ref. 1] provide a complete description of the data acquisition, processing, and storage.

As $\sigma\theta$ values are related to turbulence intensity, this parameter has been examined as a function of stability, time averaging, wind speed, wind direction, elevation and terrain. Richardson Number stability criteria were used to specify cases of near-homogeneous stability conditions for all sensors. For given stability calssifications, this study investigated the importance of the other meteorological parameters in describing turbulence over the Vandenberg terrain.

Although the primary purpose of diffusion modeling for Vandenberg is to assess the impact of the Space Shuttle exhaust, the Vandenberg terrain is varied enough and sufficient atmospheric conditions were encountered over the one year period that the data should prove useful for general model development.

The following chapters detail the strategy involved in characterizing $\sigma\theta$ over a coastal complex terrain area. Following a discussion of prior work in this field of research

and theoretical considerations, specifics involving terrain features and sensor locations are presented along with information concerning Vandenberg seasonal climatology and the synoptic forcing patterns which influenced the area during the period of analysis. After a review of data acquisition, processing, and analysis procedures, the $\sigma\theta$ measurements and relationships are presented and analyzed in an attempt to characterize this parameter for diffusion modeling.

II. BACKGROUND

The following two sections highlight the importance of investigating $\sigma\theta$ as a function of stability, averaging time, wind direction, and wind speed and describe some of the difficulties involved with maintaining both statistical validity and obtaining good spatial resolution in carrying out such an investigation.

A. PRIOR WORK (TWO EXAMPLES)

Numerous studies of flow through complex terrain have been performed. One of the more noteworthy measurement programs was carried out during July 16-28, 1979 in the Anderson Creek basin in the Geysers geothermal area in California. That study was part of the Atmospheric Studies in Complex Terrain (ASCOT) program and involved measurements of drainage winds in complex terrain. While the results of that experiment, Hanna [Ref. 2], proved useful in analyzing nocturnal drainage flows, the period of measurement was not extensive enough to assess the impact of a wide variety of environmental conditions.

A second study involved the collection of temperature and wind data from a single tower located at Motunui, New Zealand between October 1981 and January 1983. Recent analyses of these data by Wratt and Homes [Ref. 3] describe how wind direction and wind speed fluctuations depend on

height. The height dependence was found to be dependent on both stability and wind direction.

While the Anderson Creek experiment involved extensive instrumentation and short time periods, the New Zealand experiment utilized a single tower and long time periods. The work reported here attempted to achieve both statistical validity and good spatial resolution for a wide range of conditions.

B. THEORETICAL CONSIDERATIONS

Atmospheric turbulence consists of random fluctuations of the three-dimensional wind vector, which act to dilute an effluent injected into the atmosphere. The time-averaged value of a given wind statistic is given by

$$\overline{W} = \frac{1}{T} \int_0^T W \, d\tau \qquad (1)$$

where W represents either wind speed, wind direction, or a value of any one of the components, and T is the sampling time. The intensity of turbulence along and perpendicular to the mean direction is defined by

$$i_x = \left(\frac{\overline{u^2}}{U^2}\right)^{1/2} = \frac{\sigma u}{U} \qquad (2)$$

$$i_y = \left(\frac{\overline{v^2}}{U^2}\right)^{1/2} = \frac{\sigma v}{U} \qquad (3)$$

where σ is the standard deviation of the velocity distribution, U is the mean horizontal velocity component and u and v are the fluctuations about the mean. The standard deviation of the azimuthal wind direction angle ($\sigma\theta$) is related to the intensity of turbulence in the crosswind direction (i_y) since

$$\tan \theta' \doteq v/(U+u) = \theta' \text{ (Radians)} \qquad (4)$$

$$\overline{\theta'^2} = \left(\frac{\overline{v^2}}{(U+u)^2}\right) = \left(\frac{\overline{v^2}}{U^2}\left(1 + \frac{u}{U}\right)^{-2}\right) \qquad (5)$$

which, expanding and neglecting higher order terms, yields

$$\overline{\theta'^2} = \frac{\overline{v^2}}{U^2} \text{ or } \sigma\theta = \frac{\sigma v}{U} \qquad (6)$$

The application of a sampling and averaging process to a time series of wind data constitutes a filter, or window, through which only a portion of the total energy in the spectrum of wind fluctuations can be observed. Atmospheric diffusion is related not only to the value of the standard deviation, or variance, of wind direction but also to the frequency distribution of the turbulence. Smaller scale turbulence is evident at the higher frequencies and larger scale turbulence is found in the lower frequencies.

Relationships also exist between $\sigma\theta$ values and wind speed classes. For a given stability condition, values of $\sigma\theta$ for

sampling times greater than a minute or so will always be greater when the wind is light than when it is strong. The low-level wind direction meandering decreases in amplitude very rapidly with height under stable conditions. Although large surface values of $\sigma\theta$ for unstable conditions do not decrease very rapidly with height, the greatest lateral fluctuations during a very unstable thermal structure do occur with very light winds, as in the stable case.

When the value of $\sigma\theta$ for a given sampling time, T_0, is known, the value of $\sigma\theta$ may be estimated for a different sampling time by the following empirical power law relationship:

$$\sigma\theta(T) = \left(\frac{T}{T_0}\right)^x \sigma\theta(T_0) \qquad (7)$$

Although the value of x varies with stability, wind speed, and height above the surface, a value of 0.2 is often used as a working approximation.

Since the standard deviation of the crosswind component distribution (σv) is related to $\sigma\theta$ through the relationship: $\sigma v = (\sigma\theta)(U)$, Slade [Ref. 4] has found the following statements concerning σv dependence on wind speed, stability, and height to be true over homogeneous terrain:

1. At a given height, during neutral conditions, σv is proportional to wind speed.
2. For a given wind speed and height, σv is greater during unstable than during stable conditions.
3. For a given stability condition and at a given height, σv increases with wind speed and surface roughness, most markedly during stable conditions.

4. The value of σv changes rather little with height during any stability condition. During stable conditions, $\sigma\theta$ decreases with height whereas the wind speed increases comparatively rapidly over the same height interval. During unstable conditions, the decrease of $\sigma\theta$ with height is slow and the increase in wind speed is also slow.

Finally, Wratt et al [Ref. 5] found the irregularity of upwind terrain important in the study of horizontal dispersion. Studies by Panofsky [Ref. 6] have shown the sensitivity of $\sigma\theta$ to mesoscale terrain properties. An enhancement of $\sigma\theta$ was found in slightly rolling terrain (versus homogeneous terrain) due to the presence of persistent low frequency horizontal eddies set up by the hills. Complex terrain dictates the use of direct $\sigma\theta$ measurements in the characterization of turbulence and subsequent diffusion modeling.

III. VANDENBERG SITES AND SENSORS

The following information is a summary of site and sensor characteristics for towers located on Vandenberg AFB and is included here for completeness. The reader is referred to Schacher and Stanton [Ref. 1] for more detailed information.

A. SENSOR CHARACTERISTICS

The meteorological sensors from which the data in this report are obtained are attached to a network of towers on Vandenberg AFB which is part of the Weather Information Network and Display (WIND) system. Dwyer and Tucker [Ref. 7] describe the operation of this system as it applies to the Eastern Test Range, Cape Kennedy, Florida. These systems were installed to provide diffusion climatology in dealing with potential toxic hazards arising from launch operations of missiles and other space vehicles with toxic propellants.

The area containing the Vandenberg towers is approximately 10 by 20 miles. The tower heights range from 12 to 300 feet and multiple sensors are located on towers greater than 12 feet in elevation. While wind speed and wind direction are measured on every tower, dew point temperature is obtained from only two sites, one on North Vandenberg and one on South Vandenberg, and barometric pressure, visibility, rain rate, and long and short-wave radiation are measured

at only one tower on South Vandenberg. The characteristics of these sensors are detailed in Table I.

Wind speed and wind direction are measured from sensors located at tower elevations of 12, 54, 102, 204 and 300 feet. Temperature sensors are also installed at these heights with the lowest sensor located at 6 feet rather than 12 feet. The remaining sensors which measure pressure, visibility, radiation, and rain rate are all located at the 6 foot level on the specified towers. Table II summarizes the locations of these sensors.

B. TERRAIN FEATURES

Vandenberg AFB is an ideal location for examining coastal and complex terrain meteorology. The base is situated on the central California coast and is comprised of various types of terrain ranging in elevation from sea level to greater than 2000 feet. The geographical location of Vandenberg and its general features are shown in Figure 1. Towers which support the meteorological sensors are located throughout the Vandenberg area in terrain types ranging from river beds to canyons to mountain tops. These sites are shown relative to terrain elevation contour maps of the area in Figure 2.

Sites 102, 200, 300 and 301 are within one mile of the coastline with site 102, the northernmost of the coastal towers, located just northwest of the air field in relatively flat sand dunes. Sites 200, 300 and 301 are situated just east of a fairly high shoreline bluff.

TABLE I

Vandenberg Meteorological Sensor Characteristics

SENSOR	TYPE	CHARACTERISTICS
Temperature	Rosemount Series 78 platinum resistance in Geotech Model 327 aspirated radiation shield	accuracy ± 0.3 deg C
Dew Point	EG&G Model 110S-M cooled mirror system	Range -80 deg F to 120 deg F accuracy ± 0.5 deg F
Wind Speed	Geotech 1564B with 170-41 plastic cups	threshold 0.63 mph distance constant 5 ft accuracy ± 1%
Wind Direction	Geotech 50.2C with 53.1	threshold 0.7 mph at 10 deg distance constant 5.7 ft turning radius 29 in damping ratio 0.4 at 10 deg
Visibility	MRI 1580 A visiometer	range 0-50 mi
Pressure	Yellow Springs, Inst. Series 2014, bellows type	range 909-1073 mbar accuracy ± 0.5 mbar
Short wave	Epley PSP precision pyranometer	range 0-2 Langley accuracy ± 0.1 langley

TABLE II

Sensor Measurement Capabilities and Heights

Site Number	Sensor Height (feet)						
	6	12	40	54	102	204	300
009		WS WD					
014		WS WD					
052	TEM	WS WD		WS WD dT			
103	TEM	WS WD		WS WD dT			
054	TEM	WS WD		WS WD dT			
055	TEM		WS WD	dT			
056	TEM		WS WD				
101	TEM	WS WD		WS WD dT			
102	TEM	WS WD		WS WD dT	WS WD		
200	TEM	WS WD		WS WD dT	WS WD dT	WS WD dT	
299*					WS WD (108 ft)		
300	TEM	WS WD		WS WD dT	WS WD dT	WS WD dT	WS WD dT
301+	TEM DP	WS WD	WS WD dT DP	WS WD dT DP	WS WD dT DP	WS WD dT DP	WS WD dT DP

*Piggyback to site 300
+Also VI, BP, SW

TEM-Temperature
WS- Wind Speed
WD-Wind Direction
VI-Visibility
BP-Barometric Pressure
SW-Shortwave Radiometer
dT-Temperature Difference
DP-Dew Point

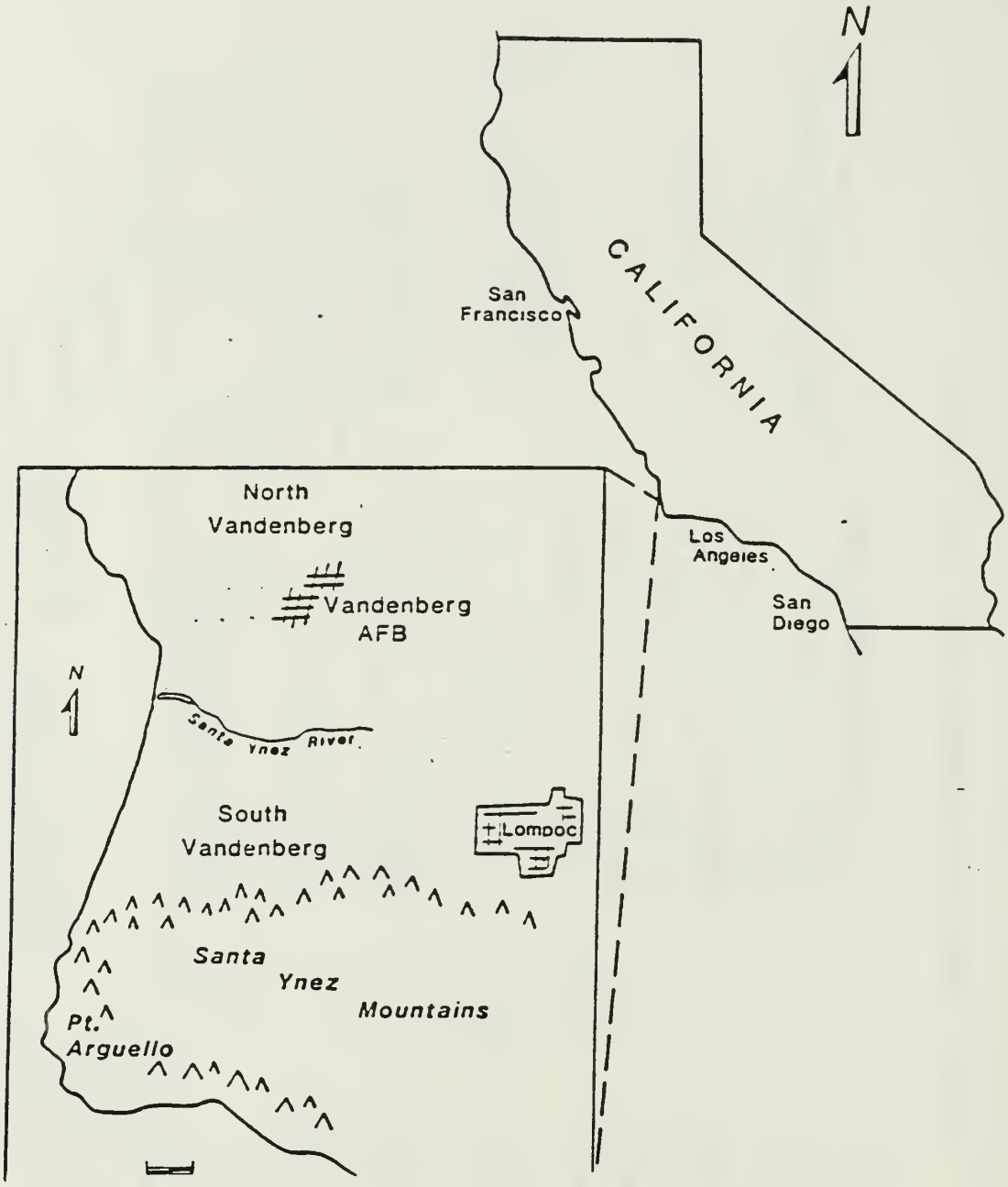

Figure 1. Geographical Location of Vandenberg AFB and General Features

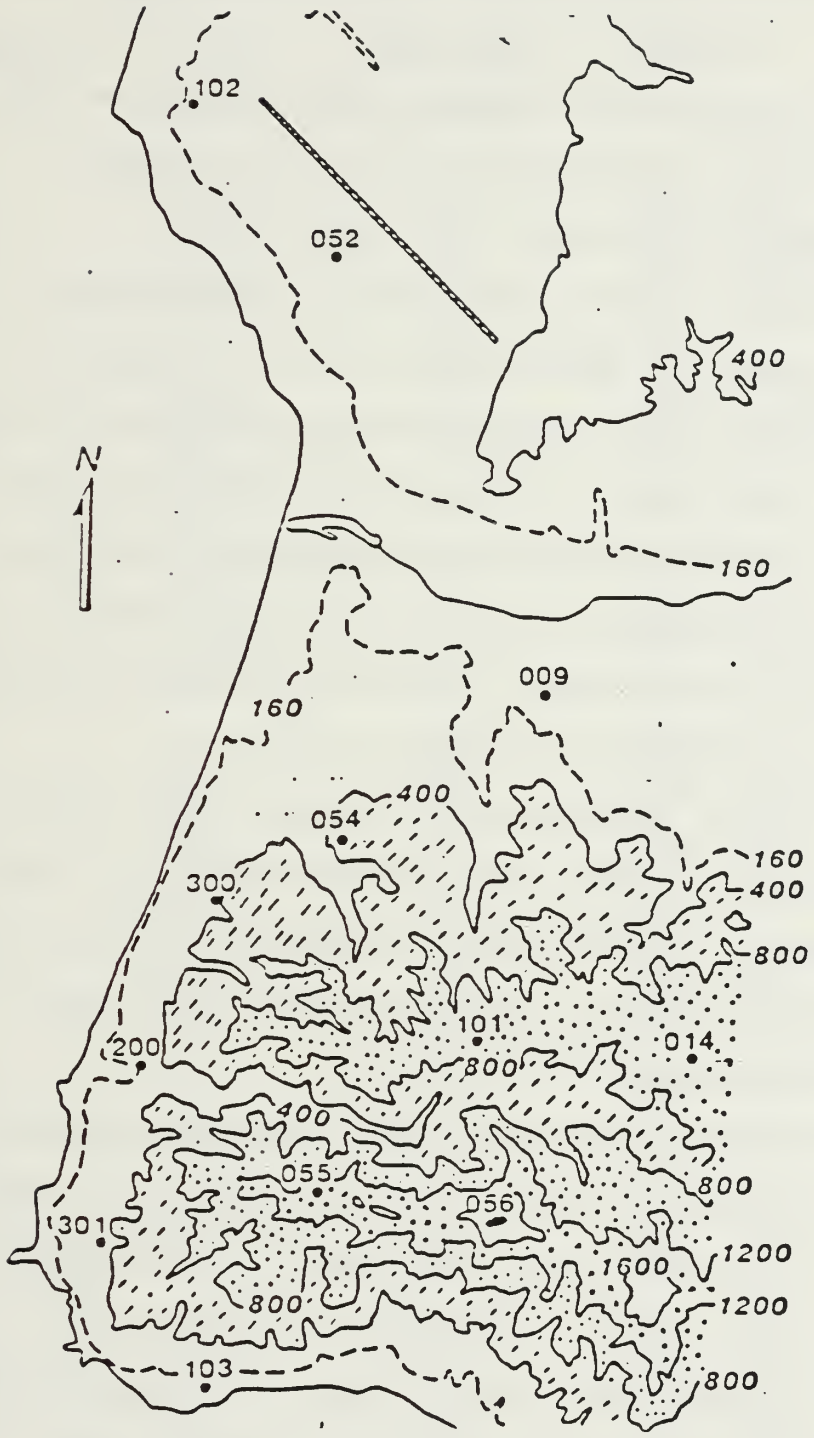

Figure 2. Vandenberg Topography and Meteorological Tower Sites

The sites located on the flattest terrain are 009, 052 and 102. Site 052 is situated near the air field and 009 on a river bed.

To the east of the three coastal sites located on South Vandenberg are rising inland hills. Site 200 is near a canyon which extends four miles into these hills.

In attempting to describe possible air flow obstructions in the vicinity of these towers, it is necessary to further describe the local terrain and any man-made structures which may alter the local air flow. The vegetation in the Vandenberg area includes coastal sage scrub and grassland. Although there are numerous trees in the general area, none of them are located near enough to the sites to be a significant factor in disrupting the local air flow.

Small electronics shelters which are five feet square and eight feet high accompany each of these towers. These structures, however, do not alter the predominant flow since they are located 50 feet away from the base of the tower downwind from the predominant direction.

In addition to these shelters, two gantrys are present in the vicinity of tower site 300. Both gantrys are approximately 300 feet in height with one located at 255 degrees and 193 meters away from the tower and the other at 121 degrees and 346 meters away from the site. Major structures are also located in the vicinity of sites 055 and 056. Table III summarizes the sensor/site terrain features and

TABLE III

Vandenberg Sensor and Site Locations

Sensor No.	Site	Level (Ft)	Remarks
1	009	12	27' Flat & in River Plane
2	014	12	1446' Gentle Slopes
3	052	12	290' Flat & by Airfield
4	054	12	450' Canyon Nearby
5	101	12	1077' Top of Small Knoll
6	102	12	215' Flat & Most North
7	103	12	56' Coastal & Most South
8	200	12	310' Flat & Coastal
9	300	12	385' Flat & Coastal
10	301	12	381' Flat & Coastal
11	052	54	290' Flat & by Airfield
12	054	54	450' Canyon Nearby
13	055	40	1530' Top of Mountain
14	056	40	2136' Top of Mountain
15	101	54	1077' Top of Small Knoll
16	102	54	215' Flat & Most North
17	103	54	56' Coastal & Most South
18	200	54	310' Flat & Coastal
19	300	54	385' Flat & Coastal
20	301	54	381' Flat & Coastal
21	102	102	215' Flat & Most North
22	200	102	310' Flat & Coastal
23	300	102	385' Flat & Coastal
24	299	108	385' Flat & Coastal
25	301	102	381' Flat & Coastal
26	200	204	310' Flat & Coastal
27	300	204	385' Flat & Coastal
28	301	204	381' Flat & Coastal
29	300	300	385' Flat & Coastal
30	301	300	381' Flat & Coastal

TABLE III (CONTINUED)

12 Ft.	Sensors (10)	: 1,2,3,4,5,6,7,8,9,10
40 Ft.	Sensors (2)	: 13,14
54 Ft.	Sensors (8)	: 11, 12,15,16,17,18,19,20
102 Ft.	Sensors (4)	: 21,22,23,25
108 Ft.	Sensors (1)	: 24
204 Ft.	Sensors (3)	: 26,27,28
300 Ft.	Sensors (2)	: 29,30

Notes:

Site 052:	By Airfield
Site 102:	Northernmost
Site 103:	Shielded by Pt. ARguello (Southernmost)
Site 300:	Sensor 24 (Site 299) is 108 ft. level at Site 300
Site 301:	Space Shuttle Complex

Table IV details the natural and man-made wind flow obstacles which are present at each site.

TABLE IV

Vandenberg Site Characterizations

009	Elevation:	27 ft
	Terrain:	flat river flood plane
	Vegetation:	plowed field with grass at tower base, treeline 100 yds to N
	Structures:	electronic shelter to SW, 30 ft high building 100 yds SE
014	Elevation:	1446 feet
	Terrain:	gentle slopes to all sides, 20 ft to canyon S of tower, ridge 1-2 mi W
	Vegetation:	low grass and rock
	Structures:	10 foot shed 30 ft NE
052	Elevation:	290 ft
	Terrain:	flat
	Vegetation:	grass 1-2 ft
	Structures:	2 low huts 300 yds SW, shelter E of tower
054	Elevation:	450 ft
	Terrain:	well-exposed with a gradual slope toward the W, canyon to immediate S and W W dropping off quickly, slight slope to N
	Vegetation:	grass and shrub
	Structures:	launch pads NW and SE of tower 150 ft apart, shelter located ESE of tower
055	Elevation:	1530 ft
	Terrain:	located on top of mountain peak, sharp drop-off 20 ft W, otherwise flat on top
	Vegetation:	concrete and dirt at site itself, otherwise surrounded by chapparal 2-5 ft in height
	Structures:	40 ft telephone pole immediately S, 60 ft radome 70 ft E of tower
	Comment:	Radome will cause severe flow distortion
056	Elevation:	2136 ft
	Terrain:	located on top of mountain peak with sharp drop-off 10 ft around permiter of site
	Vegetation:	concrete and asphalt on pad, surrounded by chapparal shrubbery on sloping hillsides
	Structures:	obstructive 25 feet high buildings 30 ft to SW and NNW of tower, radar dish above SW building
	Comment:	high winds indicative of this site, temperature sensor at 6-foot level has possible heating influence from asphalt, some flow distortion from buildings

TABLE IV (CONTINUED)

101	Elevation:	1077 ft
	Terrain:	tower on top of small knoll with gradual slope to W and N, 12 ft hill 50 ft SE, deep canyon 300 ft S, small canyon to immediate N
	Structures:	buildings on adjacent hill 1/4 mi NNW at same height as tower base
	Comment:	lower wind vane doesn't appear to be influenced by hill to SE
102	Elevation:	215 ft
	Terrain:	flat with gradual slope to beach front
	Vegetation:	grass and sand, 10-foot hill 60 ft E
	Structures:	launch pad 300 yds S, shelter 30 ft SE, two low buildings 400 yds to S
103	Elevation	56 ft
	Terrain:	in center of gentle NS slope, hills 1/4 mi N, coastline 1/4 mi S with 100-ft drop-off
	Vegetation:	grassland 2 ft high
	Structures:	shelter to S, boat house approx 20 ft high located 200 ft ESE
	Comment:	not in operation at start of project
200	Elevation:	310 ft
	Terrain:	immediate location flat, short period rolling terrain to W, deep canyon to immediate S banked by high hills
	Vegetation:	3-5 ft chaparral shrubs
	Structures:	20 foot building 200 ft NW
300	Elevation:	385 ft
	Terrain:	relatively flat, slight grade to N and E of tower, ending in gentle hills, slightly rolling terrain toward the W
	Vegetation:	3 ft chaparral shrubs
	Structures:	tower located between two 300 ft gantries 150 ft apart WNW and ESE of the tower
301	Elevation:	381 ft
	Terrain:	fairly flat, sharply rising hills one-half mi E
	Vegetation:	2-5 foot chaparral shrubs
	Structures:	four-story building 1/4 mi NW, major structures approx. 600 ft E

IV. VANDENBERG CLIMATOLOGY

A. GENERAL FEATURES

Vandenberg AFB is located on the south-central California coast and is dominated by a number of climatological factors. Synoptically, there is a semi-permanent high pressure system over the Pacific Ocean and off the southern California coast which has varying degrees of influence over the strength and direction of the atmospheric pressure gradient flow over the project area. This variability is basically seasonal and is a function of the northward and southward movement of this high pressure system. From spring to fall, the Pacific high is strong enough and close enough to the coast that the Vandenberg local climatology is dominated by occurrences of low temperature inversions and accompanying stratus and/or fog.

The overall moderating influence of the ocean is also a factor in understanding Vandenberg climatology. Although the Pacific Ocean maintains a predominately marine atmospheric boundary layer throughout this area, rapid changes in atmospheric conditions can occur with increasing distance from shore. This is due, in part, to the high hills located along the Vandenberg coastline.

Another seasonal phenomenon which affects Vandenberg climatology is the Santa Ana condition. This condition

generally affects Southern California and results in high temperatures, low humidity, and easterly high winds from the interior deserts. Valleys and canyons may experience extremely high winds under these conditions.

The general year-round climatology at Vandenberg is mild with occasional maximum temperatures of 90 degrees F occurring between August and October. During the winter months, the minimum temperature generally does not drop below 40 degrees F. Similarly, the summer minimum temperatures average above 50 degrees F.

Rainfall in the Vandenberg area generally occurs during the winter months with an average of 12 inches expected between November and April. In contrast, the summer months from May to October average only one inch of rain.

As Vandenberg is a coastal site, differential heating triggers a land-sea-breeze cycle over the area. The sea breeze, which can reach speeds of 15-20 knots during the afternoon hours, is often replaced by an offshore land breeze in the evening. This cycle tends to be strengthened by the evening downslope drainage flow, which is present in the project area due to the hilly terrain.

When a strong atmospheric pressure gradient is present over Vandenberg, the sea breeze cycle may be masked because of its superposition on the gradient wind. Under these conditions, the cycle causes variations in the speed of the onshore flow. The presence of stratus in the area also alters

the diurnal shifting of on and off-shore flow due to the lack of differential heating. Stratus is often associated with steady onshore flow for days at a time.

During the summer months, fog and stratus frequently move inland over the Vandenberg area during the late afternoon hours and remain until mid-morning when it is dissipated due to heating. Such fog and stratus conditions are not likely over this area during the winter months, since frequent frontal passages with occasional strong and gusty winds cause mixing of the atmosphere.

B. SEASONAL CLIMATOLOGY

In addition to noting some of the mesoscale meterological conditions which affect the Vandenberg area, information on seasonal climatology is also important in relating certain synoptic conditions to turbulence modeling.

During the summer months, the synoptic pattern over the project area is controlled by the semi-permanent Pacific high pressure system which is positioned just west of the central California coast. Onshore flow over Vandenberg results from clockwise flow around this high pressure system, enhanced by the local sea breeze and from overland heating which creates an inland heat trough. An inversion aloft is usually present over the area due to strong subsidance. In addition to the local land-sea-breeze circulation, the resulting stratus regime is affected by mesoscale influences such as

local topography, inversion height, and local sea surface temperatures. Large scale synoptic changes are very weak and infrequent during the middle of the stratus season and are usually masked by larger diurnal fluctuations of cloud cover, winds, and temperatures.

In the fall, the marine inversion over the coastal area begins to dissipate as the Pacific subtropical high pressure system off the central California coast begins to recede southward. This results in further southward penetration of frontal systems into the Vandenberg area. In addition, Santa Ana conditions occasionally affect the Vandenberg area during the fall months. The Santa Anas rarely last more than a few days and are characterized by dry desert winds which blow to the coast. Although Santa Ana winds are usually accompanied by excellent operational weather, visibilities may occasionally be restricted by blowing dust and sand and turbulence may become an operational hazard.

During the winter months, frequent frontal passages with strong westerly winds characterize the synoptic pattern over the area. Despite this storm pattern, the Pacific high pressure system, along with its associated subsidence inversion, can reform between frontal passages and the Santa Ana effect can still be felt when the surface pressure in the Great Basin is strong enough.

During the spring, the storm pattern moves north again and the Pacific High, with its associated stratus regime, once again regains control of the synoptic flow.

A summary of synoptic forcing in terms of atmospheric pressure gradient influences over the Vandenberg area during the period August 1983-July 1984 is presented below. Along with an analysis of pressure gradient direction and relative strength, supporting information on local land-sea-breeze circulation, Santa Ana conditions, and frontal activity is derived from this summary and utilized in analysis of the turbulence case studies presented in this report.

SUMMARY OF SYNOPTIC FORCING

PG	Pressure Gradient	( )	Amount of Rainfall in inches
WK	Weak	(T)	Trace of Precipitation
MDT	Moderate	(-)	No significant precipitation
STR	Strong		

AUGUST: No fronts (.02"); Flow direction N-NW; PG strength WK-MDT; no significant PG AUG 15-19.

SEPTEMBER: No fronts (.03"); Flow direction N-NW; PG strength WK-MDT.

OCTOBER: 1 Front (.24"); Flow direction N-NW (till Oct 19) and NE-SE (till Nov 3); PG strength WK-MDT (STR behind fronts); no significant PG Sep 30-Oct 10; possible Santa Anas Oct 25-27.

NOVEMBER: 7 Fronts (2.15"); Flow direction NE-SE (till Nov 3) and SW with postfrontal NW (after Nov 3); PG strength WK-MDT (STR behind fronts).

DECEMBER: 6 Fronts (2.83"); Flow direction VRB; PG strength WK-MDT (STR behind fronts).

JANUARY : 2 Fronts (.03"); Flow direction VRB; PG strength WK-MDT (STR behind fronts); no significant PG Jan 14-20; possible Santa Anas Jan 1-5, 27-29.

FEBRUARY: 5 Fronts(.19"); Flow direction VRB; PG strength WK-MDT (STR behind fronts).

MARCH: 6 Fronts (T); Flow direction VRB (till mid-March) and NW-NE (after min-March); PG strength MDT (STR behind fronts).

APRIL: 5 Fronts (.39"); Flow direction NW-NE; PG strength MDT (STR behind fronts).

MAY: 5 Fronts (T); Flow direction NW-NE; PG strength MDT (STR behind fronts).

JUNE: 1 Front (T); Flow direction N-NW; PG strength MDT-STR; strong PG (NW) Jun 1-21.

JULY: No Fronts (-); Flow direction N-NW; PG strength VRB; no significant PG Jul 15-19.

Total annual VBG frontal passages: 38

Total rainfall amount: 5.88" (approximate)

Most frontal passages: Nov-Dec

Heaviest rainfall: Dec

Basic pressure gradient flow: Jun-Mid Oct (N-NW)
Mid Oct-Early Nov (NE-SE)
Nov (SW-NW)
Dec-Mid Mar (VRB)
Mid Mar-May (NW-NE)

Weakest pressure gradients: Aug 15-19; Sep 30-Oct 10; Jan 14-20; Jul 15-19.

Strongest pressure gradients: Mar, Apr, May, Jun (1-21).

A detailed description of the daily pressure gradient influences and synoptic features affecting the Vandenberg area from 1 August 1983 to 22 July 1984 is presented in Appendix A.

C. WIND CLIMATOLOGY

The importance of the mean wind flow over complex terrain for turbulence characterization should not be

underestimated. The transport of material in the atmosphere is dependent on the mean wind and the rate of diffusion during the cloud travel. In complex terrain, special attention must be paid to the mean transport aspects since the wind flow may deviate substantially from a steady horizontal direction.

A wind climatology is important in assessing seasonal synoptic patterns and predominant air flow. Figure 3 illustrates the average wind trajectories expected along the south-central California coast under general synoptic northwesterly flow conditions. Note the 320-360 degree wind flow along the southwestern corner of the Vandenberg area. Evidence of this phenomenon presents itself in one of the case studies examined later in this report.

The seasonal wind climatology for the Vandenberg area is presented in Figure 4. These seasonal wind roses are for a location near the Vandenberg air strip. The diagrams show a predominantly north-northwesterly flow of air over this area between the months of March and November. From December to February, the wind direction shows an equally high frequency of occurrence in both the northwesterly and southeasterly directions. The high southeasterly wind direction frequencies are primarily due to the Santa Ana effect, although these conditions are typically of short duration. The average number of days per month experiencing Santa Ana winds at Vandenberg range from a maximum of 7-9 between

Figure 3. South-Central California Coastal Wind Trajectories under a Predominant Northwesterly Flow Regime

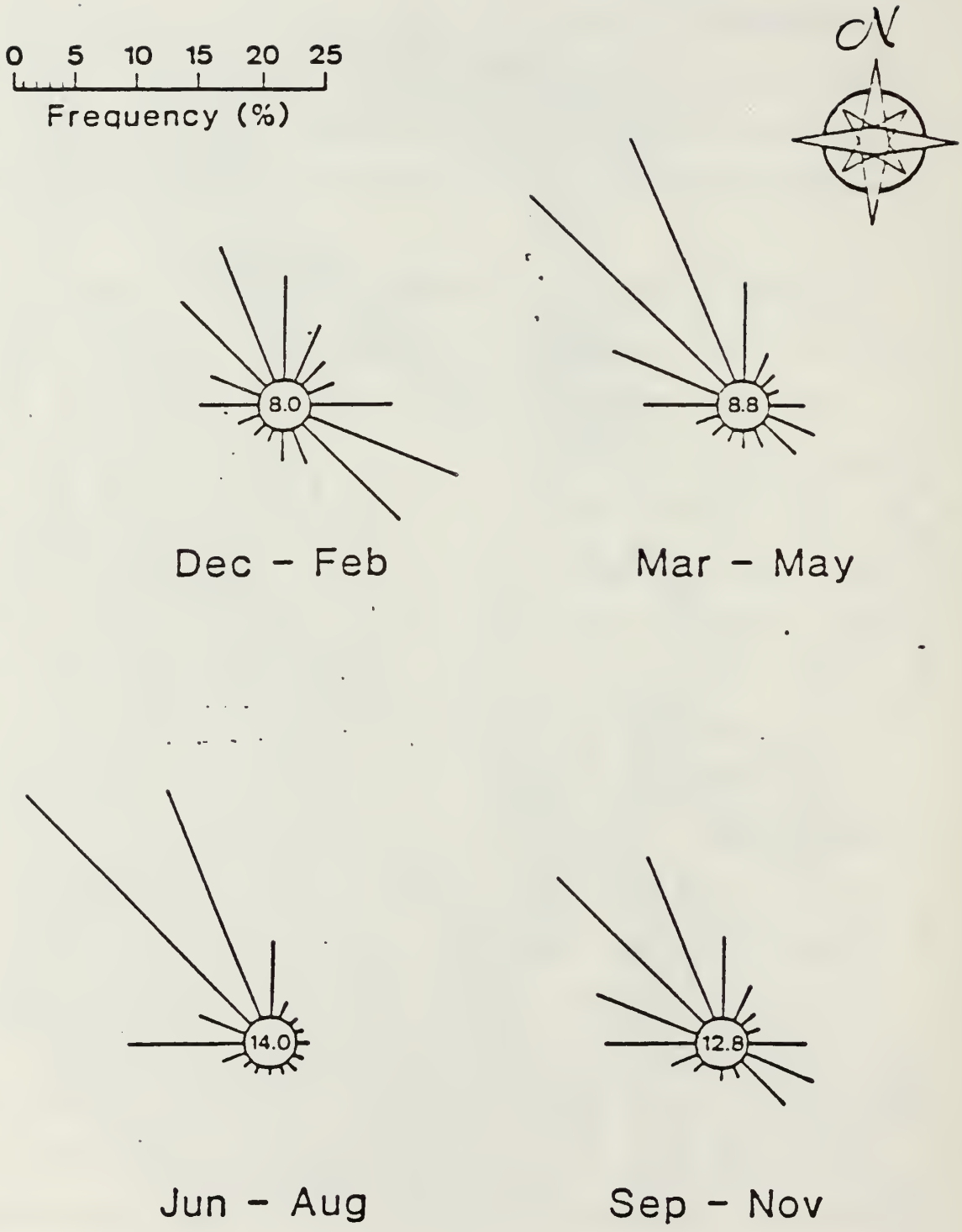

Figure 4. Vandenberg Monthly Wind Roses

November and January to a minimum of zero between June and August.

The spring and summer stratus season generally is characterized by a diurnal oscillation of day time sea breezes and weaker night time land breezes. Despite this overland diurnal wind cycle, winds off the coast generally maintain their direction out of the northwest.

V. DATA ACQUISITION AND PROCESSING

A. DATA ACQUISITION

1. Vandenberg System

The following major components comprise the Vandenberg data acquisition system:

1. central computer which issues commands and interprets data words
2. analog to digital converters at each site
3. transmit and receive modems at each site
4. hard-wire lines from each site to the central computer
5. transmit and receive modems at the central computer

Standard calibration values are established for the measured meteorological parameters of wind speed, wind direction, temperature, temperature difference, dew point, visibility, barometric pressure, and short wave radiation. Calibrations of the total Vandenberg system are performed periodically either by going to the individual sites and manually setting a calibration value or by calling for a predetermined value with the calibration command word.

2. NPS System

The NPS data acquisition system is a passive listener to the Vandenberg system since it cannot be actively involved in this process without upsetting the operation of the Vandenberg system. The NPS system is comprised of the following components:

1. Hewlett Packard 9826 computer
2. Innovative Data Technology 9-track tape deck
3. Hewlett Packard 82901 dual floppy disc drive
4. Hewlett Packard 7281 thermal printer
5. NPS constructed data acquisition unit
6. 16-bit parallel interface

For this study, the output from the NPS system included means and standard deviations for averaging periods of 15 sec, 5 min, 15 min, and 1 hr. Not all of the averaging periods contained the same data since there were two methods of data processing and storage. All averages were stored on 9-track tape and the 15 min data were also stored on floppy disks. The purpose of storing the 15 min data on these disks was for comparison checks with the Vandenberg 15 min printed output. Two full weeks of data at a time were collected and stored on these tapes and disks. Provisions were available for turning off the input from any site if there was a malfunction of the Vandenberg system.

B. DATA PROCESSING

1. Processing and Storage

The NPS system was time synchronized to the Vandenberg clock so that both systems processed the same data. At the end of each data acquisition cycle, all wind sensor data was processed to produce the vector components of the wind for each wind speed/wind direction pair. This information was then added into the appropriate 15 sec storage arrays

for later processing to produce that average. When a 15 sec average was produced, the non-wind data for the last acquisition cycle was added into the long-term average storage array. This resulted in the frequency of acquisition of non-wind sensor data being a factor of 15 less than for the wind data. This was inconsequential, however, in that high frequency spectral information was only required for the wind data.

Figure 5 details the flow of data through the arrays, from acquisition to final storage. The data processing produced means and standard deviations of the wind variables and means for the non-wind sensors. Certain other parameters were also stored to allow calculation of means and standard deviations for time periods longer than 15 sec. The following is a list of these stored parameters:

1. sum of x-component (Mean)
2. sum of y-component (Mean)
3. sum of x-squared (Mean)
4. sum of y-squared (Mean)
5. sum of xy
6. number of data points
7. sum of sensor data (non-wind sensors)
8. number of data points (non-wind sensors)

All processing and storage of wind data was done utilizing vector components. The horizontal wind vector was decomposed with the x-direction representing east and the

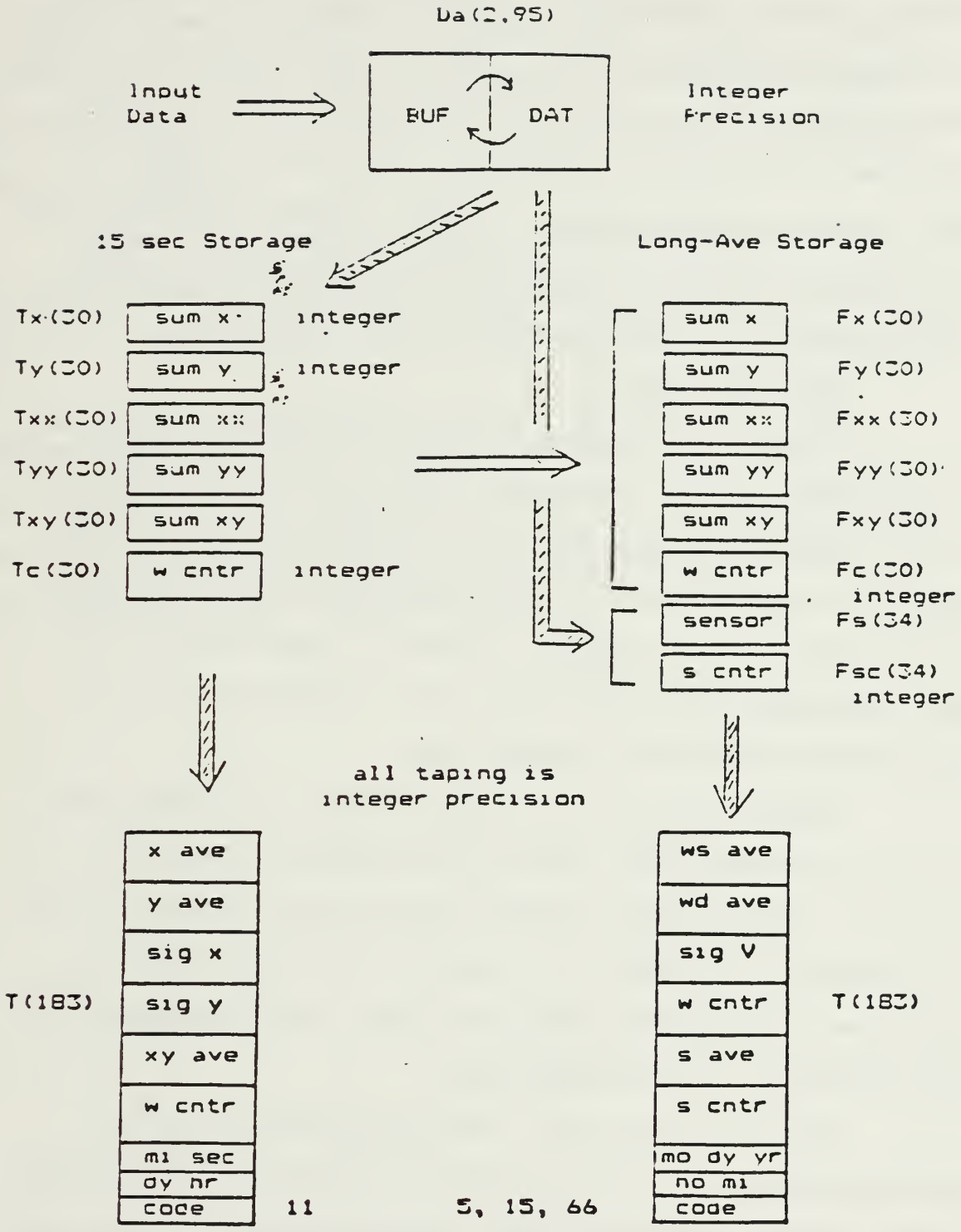

Figure 5. Flow of Data Through the Arrays from Acquisition to Storage

y-direction representing north. The primary advantage in storing vector components is in the formation of parameter averages over varying time periods. For monatomic variables, such as temperature and speed, longer averages may easily be formed from shorter averages as long as the number of data points in each average is known. Vector averaging was necessary, however, in forming longer averages for other meteorological parameters such as wind direction.

2. Quality Control

Obviously erroneous data were rejected at the time of data acquisition. As these checks could not be applied to all sensors due to processing time limitations, other methods of quality control were applied to the data after acquisition. These methods included a comparison of NPS and Vandenberg 15 min averages and an analysis of all of the averages stored on 9-track tape.

Comparison of the 15 min averages was accomplished on-site to detect data acquisition problems as quickly as possible. This method enabled problems with either the NPS or Vandenberg systems to be caught at an early stage and corrected in a minimum period of time. Such erroneous data was eliminated from the data set.

Quality control was also maintained through an extensive analysis of the averages contained on the 9-track tapes. Errors associated with the acquisition of individual data points were smoothed over in the process of data

averaging. The goal of the quality control program was to eliminate those data whose characteristics deviated substantially from the norm, while maintaining natural statistical fluctuations in the data which were representative of atmospheric processes.

Data was considered suspect when constant values of meteorological parameters were evident beyond a certain period of time and when the rate of change of such parameters was too large. Schacher and Stanton [Ref. 8] detail the maximum accepted changes from one averaging period to the next for the wind and temperature sensors. The rate values were set large due to the natural fluctuations occurring in the atmosphere within complex terrain.

VI. DATA ANALYSIS

A. GENERAL PURPOSE

The work reported here examined some of the characteristics of turbulence over the Vandenberg area through an analysis of $\sigma\theta$ values that were obtained from the various sites located throughout the terrain. By concentrating on periods of time when near-homogeneous stability conditions were present for the Vandenberg area, $\sigma\theta$ dependencies on other meteorological and topographical parameters were more clearly defined. Under given stabilities, $\sigma\theta$ values were plotted as functions of averaging time, wind speed and wind direction, as well as location and height. The result of developing schemes highlighting such dependencies was a characterization of $\sigma\theta$ for each sensor at each site within the project area for given stabilities/flow regimes. Not only were site specific dependencies of $\sigma\theta$ on the above parameters revealed, but inter-comparisons between sensor and site $\sigma\theta$ values under given stabilities resulted in additional information regarding terrain influences. The rest of this chapter highlights the binning and methodology used in this study.

B. BINNING

Table V summarizes the data binning procedures utilized in the various $\sigma\theta$ dependency schemes. Stability, through

TABLE V

Vandenberg Data Binning

Stability: Unstable, Neutral, Stable

Averaging Time: TAVG '1' = 15 s, TAVG '2' = 10 m, TAVG '3' = 2 h

TAVG 1 = 15 s	TAVG 5 = 5 m	TAVG 9 = 1 h
TAVG 2 = 30 s	TAVG 6 = 10 m	TAVG 10 = 2 h
TAVG 3 = 1 m	TAVG 7 = 15 m	TAVG 11 = 4 h
TAVG 4 = 2 m	TAVG 8 = 30 m	

Wind Speed (MS^{-1}): WS '1' = 0-4, WS '2' = 4-8, WS '3' = 8+

WS1 = 0-2	WS5 = 8-10	WS8 = 14-16
WS2 = 2-4	WS6 = 10-12	WS9 = 16-18
WS3 = 4-6	WS7 = 12-14	WS10 = 18+
WS4 = 6-8		

Wind Direction (Degrees): 'Onshore' (200-360), 'Offshore' (040-160)

WD1 = 0-40	WD4 = 120-160	WD7 = 240-280
WD2 = 40-80	WD5 = 160-200	WD8 = 280-320
WD3 = 80-120	WD6 = 200-240	WD9 = 320-360

NOTE: s = seconds
m = minutes
h = hours
On = 'Onshore' (200-360 degrees)
Off = 'Offshore' (040-160 degrees)
TAVG = Averaging time (s,m,h)
WS = Wind speed (ms^{-1})
WD = Wind direction (degrees)
$\sigma\theta$ = Standard deviation of horizontal wind direction fluctuations (degrees)
Plotted numbers = Number of data points in given bin

Richardson Number calculations, was classified as either unstable, neutral, or stable. Averaging time was binned either into 11 categories ranging from 15 sec to 5 hr, or into categories of 15 sec, 10 min, and 2 hr, depending on the implemented scheme. Wind speed was classified either into bins of 0-4, 4-8, and 8+ ms^{-1}, or into 10 bins of 2 ms^{-1} width with the tenth bin containing all wind speeds greater than or equal to 18 ms^{-1}. Once again, the implemented scheme dictated which wind speed binning procedure was used. Finally, wind direction was divided either into 9 bins of 40 degree width each or into bins of onshore (200-360 degrees) and offshore (040-160 degrees) flow contingent on the scheme being examined. Elevation and terrain variability was inherent with the location of the various sites and sensors.

C. METHODOLOGY

Each case study presented in this report is representative of a particular stability class and each study presents the same sequence of schemes. Initially, the synoptic situation and mean flow pattern over the Vandenberg area is described for the given stability case. Next, the dependency schemes are implemented as described below:

Scheme 1: $\sigma\theta$ vs TAVG

TAVG: Primary parameter (11 bins)

WD: Secondary (onshore, offshore)

WS: Secondary (0-4, 4-8, 8+ ms^{-1})

Power Law Study

Height analysis (12,54,102, and 204 ft)

Site comparison (15 sec → 2 min)

Scheme 2: $\sigma\theta$ vs WD

WD: Primary parameter (9 bins)

TAVG: Secondary (15 s, 10 m, 2 h)

WS: Secondary (0-4, 4-8, 8+ ms^{-1})

Height analysis (12,54,102, and 204 ft)

Site comparison (4 most populated WD bins)

Scheme 3: $\sigma\theta$ vs WS

WS: Primary (10 bins)

TAVG: Secondary (15 s, 10 m, 2 h)

WD: Secondary (onshore, offshore)

Height analysis (12,54,102, and 204 ft)

Site comparison (4 most populated WS bins)

Finally, an interstability comparison is made of $\sigma\theta$ dependency on time averaging for all sensors and of $\sigma\theta$ dependency on time averaging for sensors at the 12, 54, 102, and 204 foot levels.

VII. DEVELOPMENT OF CASE STUDIES

All of the case studies in the work presented here were selected based on their homogeneous stability characteristics as determined from Richardson Number calculations. Wratt et al [Ref. 9] found that a stability classification scheme based on Richardson Number measurements from towers located in complex terrain led to a useful summary of meteorological data. Teunissen [Ref. 10] has classified the atmosphere according to the following Richardson Number regimes:

$Ri < 0$	unstable air with convective turbulence in addition to mechanical turbulence
$Ri \sim 0$	air termed 'neutral' or 'near-netural' with purely mechanical turbulence
$0 \leq Ri \leq 0.25$	stable air with mechanical turbulence being damped by thermal stratification
$Ri > \sim 0.25$	very stable air in which no turbulence can exist in the vertical direction

The gradient Richardson Number, Ri, is related to the rate at which work must be done in the gravitational field when moving fluid volumes in the vertical direction. It is defined by:

$$Ri \equiv \frac{g(\partial\theta_1/\partial Z)}{\theta_1(\partial U/\partial Z)^2} \qquad (8)$$

where θ_1 is potential temperature, U is the mean wind, and Z is height. Hydrostatic stability principles relate θ to

the actual temperature T by:

$$\frac{1}{\theta_1}\frac{\partial\theta_1}{\partial Z} = \frac{1}{T}\left(\frac{\partial T}{\partial Z} + \Gamma\right) \tag{9}$$

where Γ is the dry adiabatic lapse rate ($\Gamma \approx 1$ degree C/100 meters). Thus, the gradient Richardson Number becomes:

$$Ri = \frac{g}{T}\frac{\left(\frac{\partial T}{\partial Z} + \Gamma\right)}{\frac{u_2-u_1}{\left(\frac{z_2-z_1}{}\right)^2}} = \frac{g}{T}\frac{\left(\frac{\partial T}{\partial Z} + \Gamma\right)}{\frac{u_2^2}{z_2^2}\frac{1-(u_1/u_2)}{\left(\frac{1-(z_1/z_2)}{}\right)^2}} \tag{10}$$

where the subscripts 1 and 2 refer to different heights.

As the 12 and 54 foot level sensors were assumed to be within the surface layer, the 12 foot level was adjusted to the 54 foot level in the Richardson Number calculation (Ri_0) such that:

$$Ri = Ri_0\left(\frac{1-(z_1/z_2)}{1-(u_1/u_2)}\right)^2 \tag{11}$$

where z_1 = 12 feet = 3.6 meters and z_2 = 54 feet = 16.5 meters. This yields:

$$1 - \left(\frac{z_1}{z_2}\right) = 0.778 \tag{12}$$

and, assuming a roughness length (z_0) of 0.1 meter,

$$\frac{u_1}{u_2} = \frac{\ln(z_1/z_0)}{\ln(z_2/z_0)} = \frac{\ln\ (3.6/0.1)}{\ln\ (16.5/0.1)} = 0.7019$$

Finally,

$$Ri = Ri_0\left(\frac{0.778}{0.298}\right)^2 = Ri_0(6.8) \qquad (14)$$

and

$$Ri_0 = Ri/6.8 \qquad (15)$$

The adjusted stability classification became:

Stable: $Ri_0 \geq 0.0038$

Neutral: $-0.015 \leq Ri_0 < 0.0038$

Unstable: $Ri_0 \leq -0.015$

Richardson Number calculations were examined at each tower for the one year's collection of data. Careful analysis of these data yielded specific periods of time when the same stability condition was present throughout the project area. Further investigation revealed that these stability periods were related to specific wind flow regimes. It was found that stable periods which occurred during the evening hours correlated well with land breeze conditions and drainage flow throughout the area. Likewise, the afternoon unstable periods correlated well with onshore sea breeze conditions. Strong wind conditions were found in conjunction with the strongest periods of neutral stability. Table VI lists the

TABLE VI

Vandenberg Case Studies

UNSTABLE CASES

January 14, 1984 (1000-1700 Hrs)

February 6, 1984 (1000-1700 Hrs)

* February 7, 1984 (1000-1700 Hrs)

February 8, 1984 (1000-1700 Hrs)

March 19, 1984 (1000-1700 Hrs)

STABLE CASES

December 12, 1983 (0000-0600 Hrs)

December 29, 1983 (1800-0800 Hrs)

January 31, 1984 (1200-0800 Hrs)

* February 2, 1984 (0200-0800 Hrs)

February 2, 1984 (1800-0800 Hrs)

NEUTRAL CASES

December 12, 1983 (1000-1600 Hrs)

* March 17, 1984 (0900-1800 Hrs)

March 18, 1984 (0900-1800 Hrs)

*indicates case studies analyzed in this report

stability cases which exhibited the greatest stability homogeneity for a given period of time.

1. The unstable case study selected for this study was February 7, 1984 (1000-1700 hours). The synoptic situation showed high pressure over Idaho, low pressure mover northwest Mexico, and no significant forcing over the project area. Analysis of the data showed a nearly constant onshore flow, indicative of a sea breeze condition during this time period.

2. The stable case chosen for this study was February 2, 1984 (0200-0800 hours). Synoptically, high pressure was situated over Idaho with low pressure over southern California. As with the unstable case, no significant pressure-gradient forcing was in evidence over this area during these hours. Data analysis showed the predominant wind direction to be offshore, due apparently to a combination of nocturnal land breeze and drainage flow effects.

3. For the neutral case, March 17, 1984 (0900-1800 hours) was chosen. Synoptically driven strong winds from the north-northwesterly direction were occurring over the Vandenberg area during these hours, primarily due to the passage of a cold frontal system through the area earlier that day. Atmospheric pressure gradient forcing appeared relatively strong with flow aloft from the north-northeasterly direction.

VIII. RESULTS

A. REFERENCE INFORMATION

Summary details regarding Vandenberg sensor/site elevations and locations and specific terrain characteristics are included in Table III for easy reference in analyzing the forthcoming $\sigma\theta$ data. Table V describes the data binning involved with each of the stability case studies examined and an analysis of both missing and 'bad' $\sigma\theta$ data for the sensors in each of the case studies is included in Table VII.

B. UNSTABLE CASE STUDY (2/7/84, 1000-1700)

1. Synoptic Situation/Mean Flow

The Vandenberg weather at this time was dominated by a 1032 mb high pressure center located over southern Idaho. Figure 6 shows very weak easterly pressure gradient forcing over the central California coast with the 500 mb jet well north of the area (over western Canada). There was no precipitation in the Vandenberg area.

Max Temp: 77 °F Min Temp: 49 °F

AVG VBG wind direction (all sensors): onshore (200-360°)

AVG VBG wind speed (all sensors): 0-4 ms^{-1}

Figure 7 illustrates the mean flow occurring at the various sites and sensors in the Vandenberg area. Westerly flow was predominant along the coast with more variable onshore flow (240-320°) occurring with height at site 200

TABLE VII

Analysis of Missing $\sigma\theta$ Data

Unstable Case Study (2/7/84, 1000-1700)

$\sigma\theta$ values missing for sensors: 1,7,9,12,17,30

'bad' data for sensors: 6,14,21

Stable Case Study (2/2/84, 0200-0800)

$\sigma\theta$ values missing for sensors: 1,7,9,17

'bad' data for snesors: 14,15,21,30

Neutral Case Study (3/17/84, 0900-1800)

$\sigma\theta$ values missing for sensors: 1,2,7,9,17

'bad' data for sensors: 11,16,19,23,27,29,30

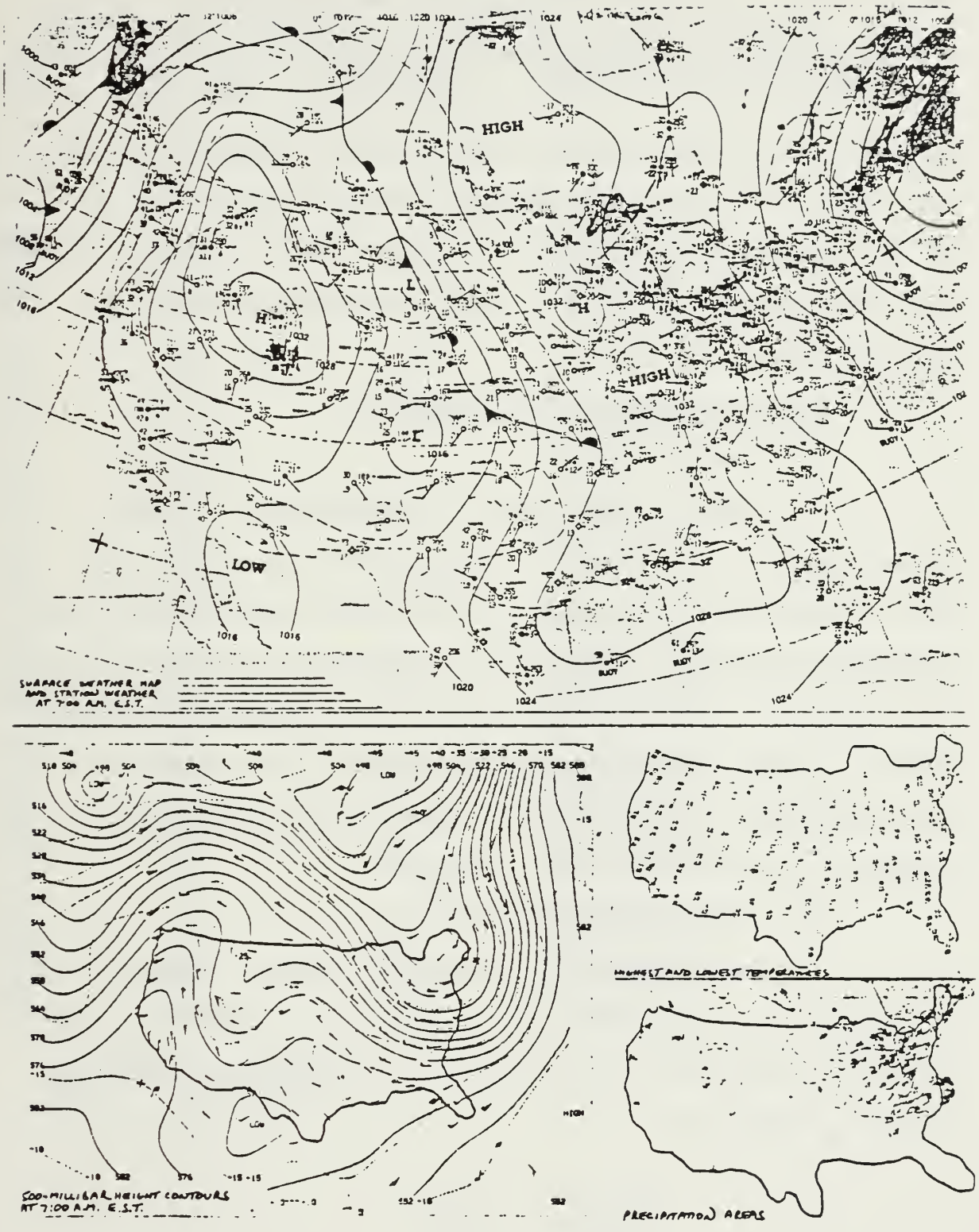

Figure 6. VBG Synoptic Situation (2/7/84--Unstable)

and persistent northwesterly flow (320-360°) in evidence at site 301. Southerly onshore flow was apparent at interior sites 055 and 056 and west-southwesterly flow along the ridge line was evident at site 101. Wind direction was generally uniform with height at each site with the exception of site 200 and wind speed increased with sensor elevation at all sites. Tables VIII and IX list the mean flow wind directions and wind speeds according to site and sensor elevations, respectively.

2. $\sigma\theta$ Dependence on Time Averaging

a. General Results

Table X summarizes $\sigma\theta$ dependence on time averaging for time averages ranging from 15 sec to 5 min. The $\sigma\theta$ values at all sensors at all sites increased as time averaging increased. This was as expected since increasing the averaging time includes more of the fluctuation spectrum. Table XI shows the average value of $\sigma\theta$ for all sensors for the designated averaging time. The standard deviation of the spread in $\sigma\theta$ values is also indicated.

b. Power Law Relationship

As described in an earlier chapter, Chapter II.B, a commonly used expression for the ratio of standard deviations of horizontal wind directions for different sampling times t_a and t_b is:

$$\frac{\sigma\theta(t_a)}{\sigma\theta(t_b)} = \left(\frac{t_a}{t_b}\right)^x$$

TABLE VIII

VBG Mean Flow--By Site (2/7/84 (1000-1700)--Unstable)

Site	Level (Ft)	Sensor No.	Predominant Flow (WD/WS)
009	12	1	
014	12	2	200-240/2-4
055	40	13	160-200/2-4
056	40	14	----------
052	12	3	240-280/2-4
052	54	11	240-280/2-4
054	12	4	240-280/2-4
054	54	12	----------
101	12	5	200-240/0-2
101	54	15	200-240/0-2
103	12	7	----------
103	54	17	----------
102	12	6	280-320/2-4
102	54	16	240-280/2-4
102	102	21	----------
200	12	8	280-320/0-2
200	54	18	200-240/2-4
200	102	22	240-280/0-2
200	204	26	280-320/4-6
300	12	9	----------
300	54	19	240-280/2-4
300	102	23	240-280/2-4
299	108	24	240-280/2-4
300	204	27	240-280/2-4
300	300	29	240-280/2-4
301	12	10	320-360/2-4
301	54	20	320-360/2-4
301	102	25	320-360/2-4
301	204	28	320-260/2-4
301	300	30	----------

Note: WD (degrees)
WS (ms^{-1})

TABLE IX

VBG Mean Flow--By Height (2/7/84 (1000-1700)--Unstable)

Level (Ft)	Sensor No.	Site	Predominant Flow (WD/WS)
12	1	009	----------
12	2	014	200-240/2-4
12	3	052	240-280/2-4
12	4	054	240-280/2-4
12	5	101	200-240/0-2
12	6	102	280-320/2-4
12	7	103	----------
12	8	200	280-320/0-2
12	9	300	----------
12	10	301	320-360/2-4
40	13	055	160-200/2-4
40	14	056	----------
54	11	052	240-280/2-4
54	12	054	----------
54	15	101	200-240/0-2
54	16	102	240-280/2-4
54	17	103	----------
54	18	200	200-240/2-4
54	19	300	240-280/2-4
54	20	301	320-360/2-4
102	21	102	----------
102	22	200	240-280/0-2
102	23	300	240-280/2-4
102	25	301	320-360/2-4
108	24	299	240-280/2-4
204	26	200	280-320/4-6
204	27	300	240-280/2-4
204	28	301	320-360/2-4
300	29	200	240-280/2-4
300	30	301	----------

Note: WD (Degrees)
WS (ms^{-1})

TABLE X

$\sigma\theta$ Dependence on Time Averaging (2/7/84 (1000-1700)--Unstable)

		TIME AVERAGING				
Sensor	Site-Ht	15 sec	30 sec	1 min	2 min	5 min
3	052-12'	8.7	10.2	12.9	13.6	18.3
4	054-12'	9.7	10.7	11.9	12.8	14.0
5	101-12'	10.3	11.7	13.7	15.3	18.9
6	102-12'	8.7	13.4	19.8	21.7	30.6
7	200-12'	13.6	15.6	17.8	20.1	22.3
10	301-12'	19.6	22.2	24.8	34.0	34.3
13	055-40'	8.5	8.9	14.8	19.4	15.9
11	052'54'	7.5	8.5	9.6	10.8	12.5
15	101-54'	8.1	9.3	10.7	11.8	14.7
16	102-54'	12.9	13.7	14.4	15.2	15.5
18	200-54'	11.5	13.3	15.3	16.7	18.7
19	300-54'	7.9	9.0	10.1	11.3	13.2
20	301-54'	9.0	10.8	12.6	14.2	16.6
22	200-102'	11.0	12.8	14.6	15.9	17.7
23	300-102'	8.7	10.0	11.1	12.2	13.4
25	301-102'	8.9	10.4	12.3	13.4	15.3
24	299-108'	8.8	10.6	12.0	13.3	14.8
26	200-204'	8.5	10.0	11.4	12.7	14.5
27	300-204'	8.6	10.2	11.6	12.6	13.7
28	301-204'	9.5	11.3	13.6	15.2	16.7
29	300-300'	8.0	9.4	10.7	12.0	13.7

Note: Most representative values listed above ($\sigma\theta$ in degrees)
Wind direction onshore (200-360 degrees)
Wind speed 0-4 ms^{-1} except sensor 26 (4-8 ms^{-1})

TAVG = 15 sec: Mean $\sigma\theta$(DEG) = 9.9 Standard deviation (DEG) = 2.7

TAVG = 30 sec: Mean $\sigma\theta$(DEG) = 11.5 Standard deviation (DEG) = 3.0

TAVG = 1 min: Mean $\sigma\theta$(DEG) = 13.6 Standard deviation (DEG) = 3.5

TAVG = 2 min: Mean $\sigma\theta$(DEG) = 15.4 Standard deviation (DEG) = 5.0

TAVG = 5 min: Mean $\sigma\theta$(DEG) = 17.4 Standard deviation (DEG) = 5.4

TABLE XI

$\sigma\theta$ vs TAVG (All Sensors) (2/7/84 (1000-1700)--Unstable)

TAVG	$\sigma\theta$ (Deg)	S.D. (DEG)
15 s	9.9	2.7
30 s	11.5	3.0
1 m	13.6	3.5
2 m	15.4	5.0
5 m	17.4	5.4

where an empirical value for x obtained over homogeneous terrain is 0.20.

In this case study, t_a was set to 5 minutes and t_b to 15 seconds. By calculating the average values of $\sigma\theta$ at 15 second and 5 minute time averaging, an observed value of x was determined. Figure 8(a) shows the relationship between the average observed power law value of x (x = 0.19) and the empirical x value (x = 0.20). In general, most of the sensors had x values between 0.16 and 0.21. Figure 8(b) shows ($\sigma\theta$ (T)/$\sigma\theta$ (15 s)) vs TAVG along with the associated mean values and standard deviations. Very little difference exists between these two curves either at short time averaging values (high frequencies) or at long time averaging values (low frequencies).

c. Height Dependence

A summary of $\sigma\theta$ dependences on time averaging as a function of sensor elevation is shown in Table XII/Figure 9.

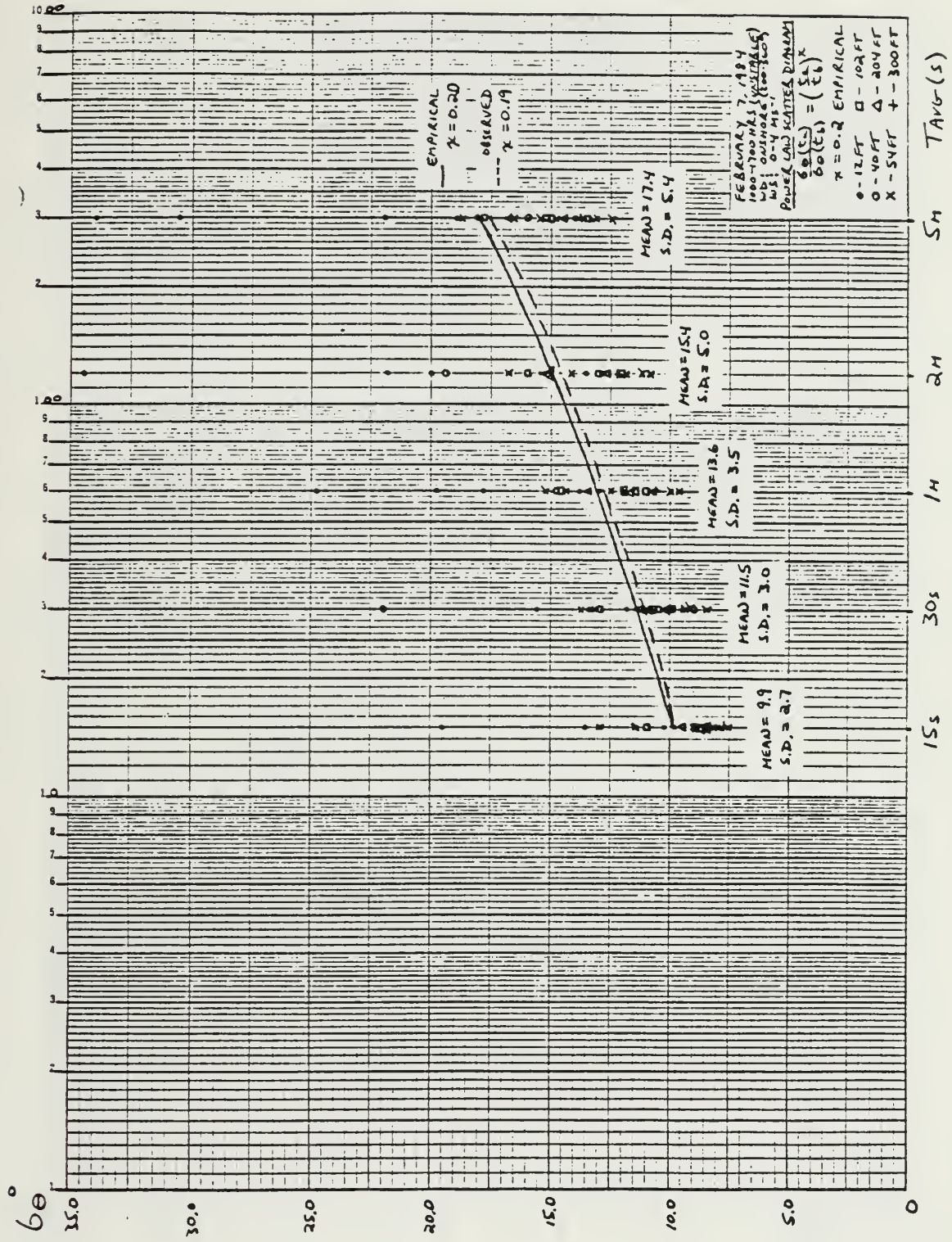

Figure 8(a). Power Law Relationship (All Sensors) (2/7/84 (1000-1700)--Unstable)

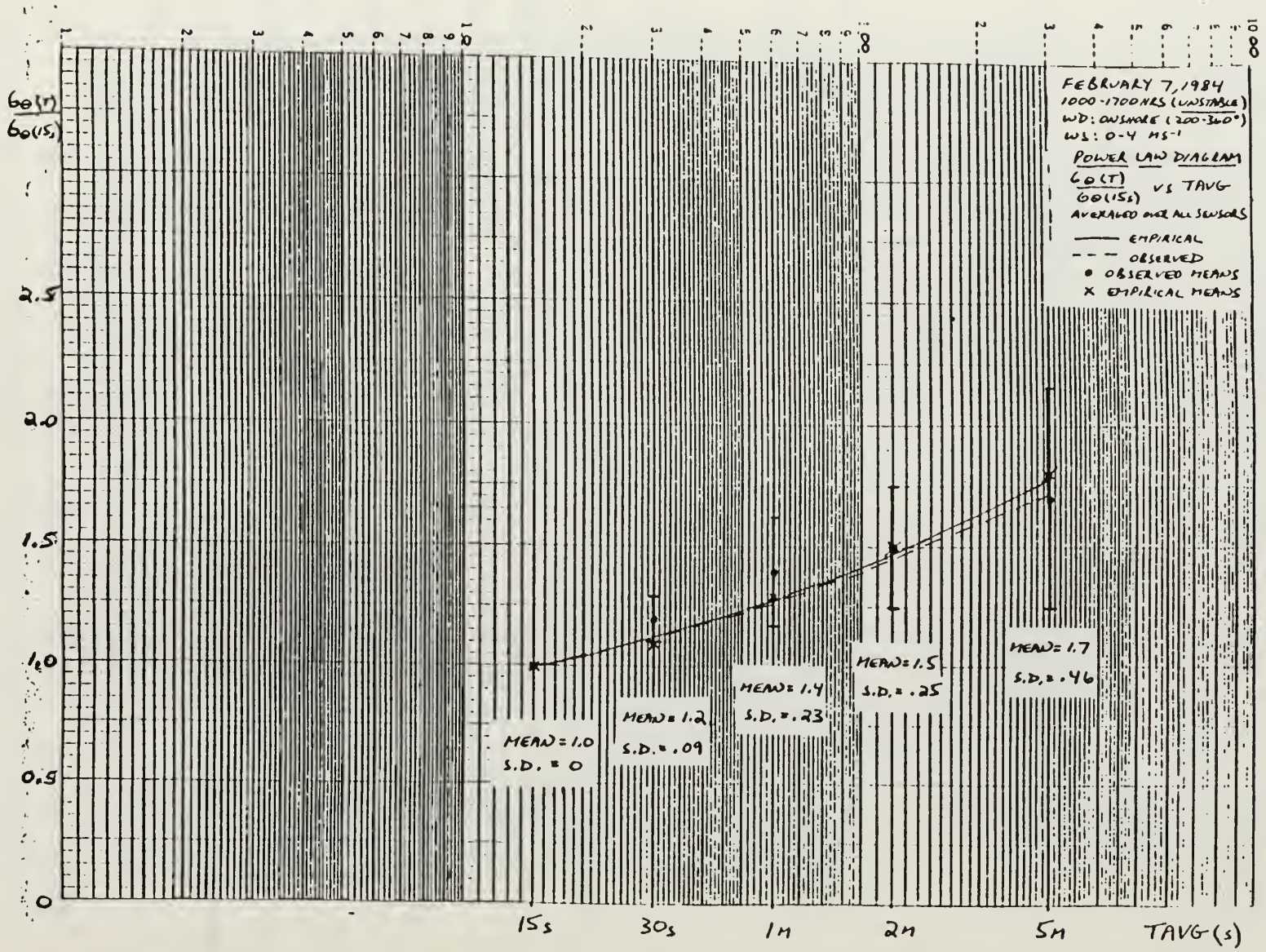

Figure 8(b). Power Law Ratio (All Sensors) (2/7/84 (1000-1700)--Unstable)

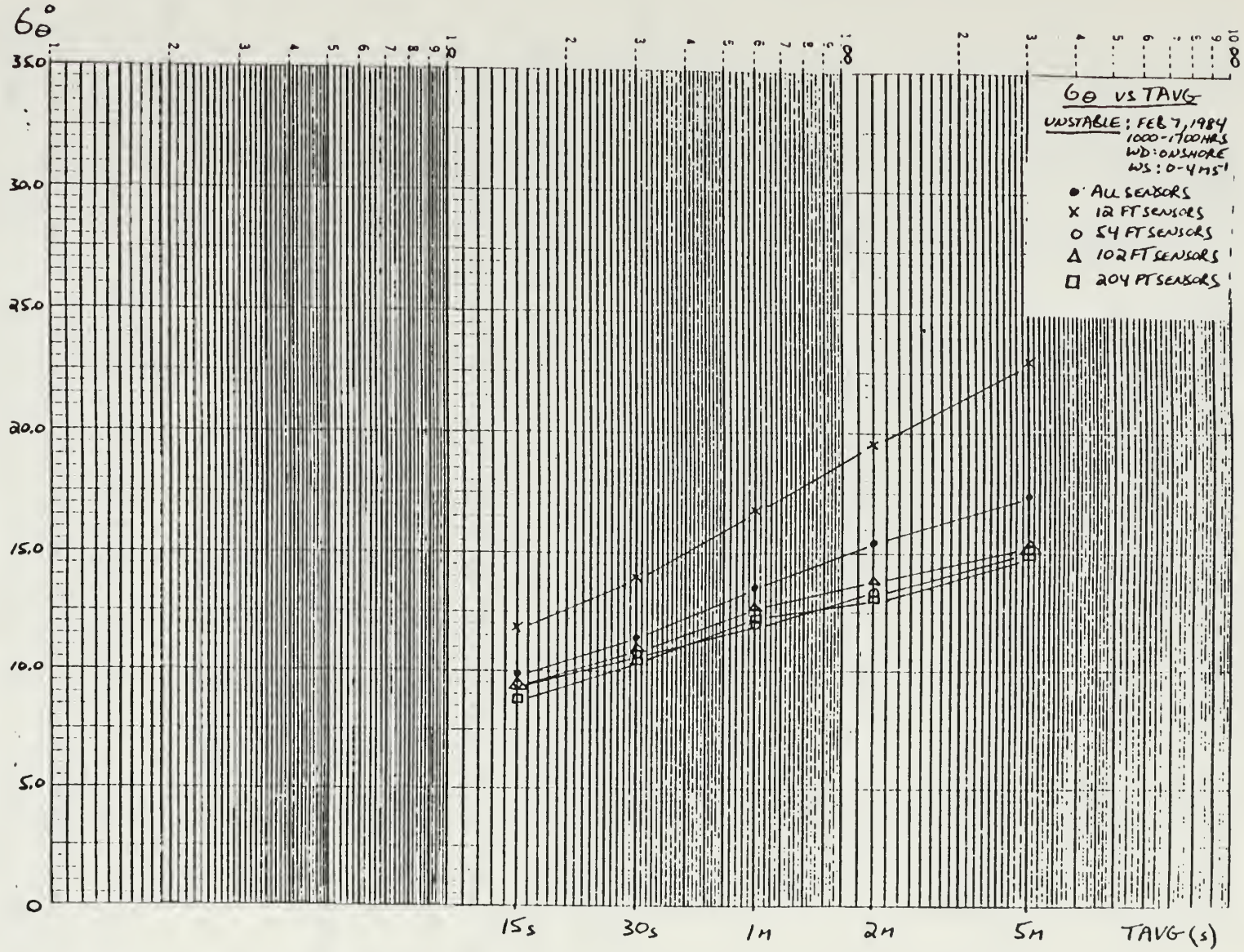

Figure 9. σθ vs TAVG (All Sites) (2/7/84 (1000-1700)--Unstable)

TABLE XII

$\sigma\theta$ vs TAVG (All Sites) (2/7/84 (1000-1700)--Unstable)

	Sensor Elevation (Ft)			
TAVG	12	54	102	204
15 s	11.8	9.5	9.5	8.9
30 s	14.0	10.8	11.1	10.5
1 m	16.8	12.1	12.7	12.2
2 m	19.6	13.3	13.9	13.5
5 m	23.1	15.2	15.5	15.0

d. Site/Sensor Elevation Dependence

Figures 10(a-h)/Tables B-(1-8) show site specific $\sigma\theta$ dependences on time averaging for various sensor elevations. Sites 102, 300, 200 and 301 are arbitrarily classified as 'coastal' sites, with sites 052, 054, and 101 classified as 'inland' sites, and site 055 classified as an 'inland elevated' site. A terrain analysis later in this chapter will collectively examine $\sigma\theta$ differences between sites and dependences on time averaging relative to each site.

3. $\sigma\theta$ Dependence on Wind Direction

a. General Results

For the case of onshore sea breeze flow associated with the unstable case, $\sigma\theta$ values throughout the terrain generally appeared to be lower when the wind was blowing from the north-northwest (280-360°). The predominant winds, however, were blowing from the west (240-280°) with the exception of

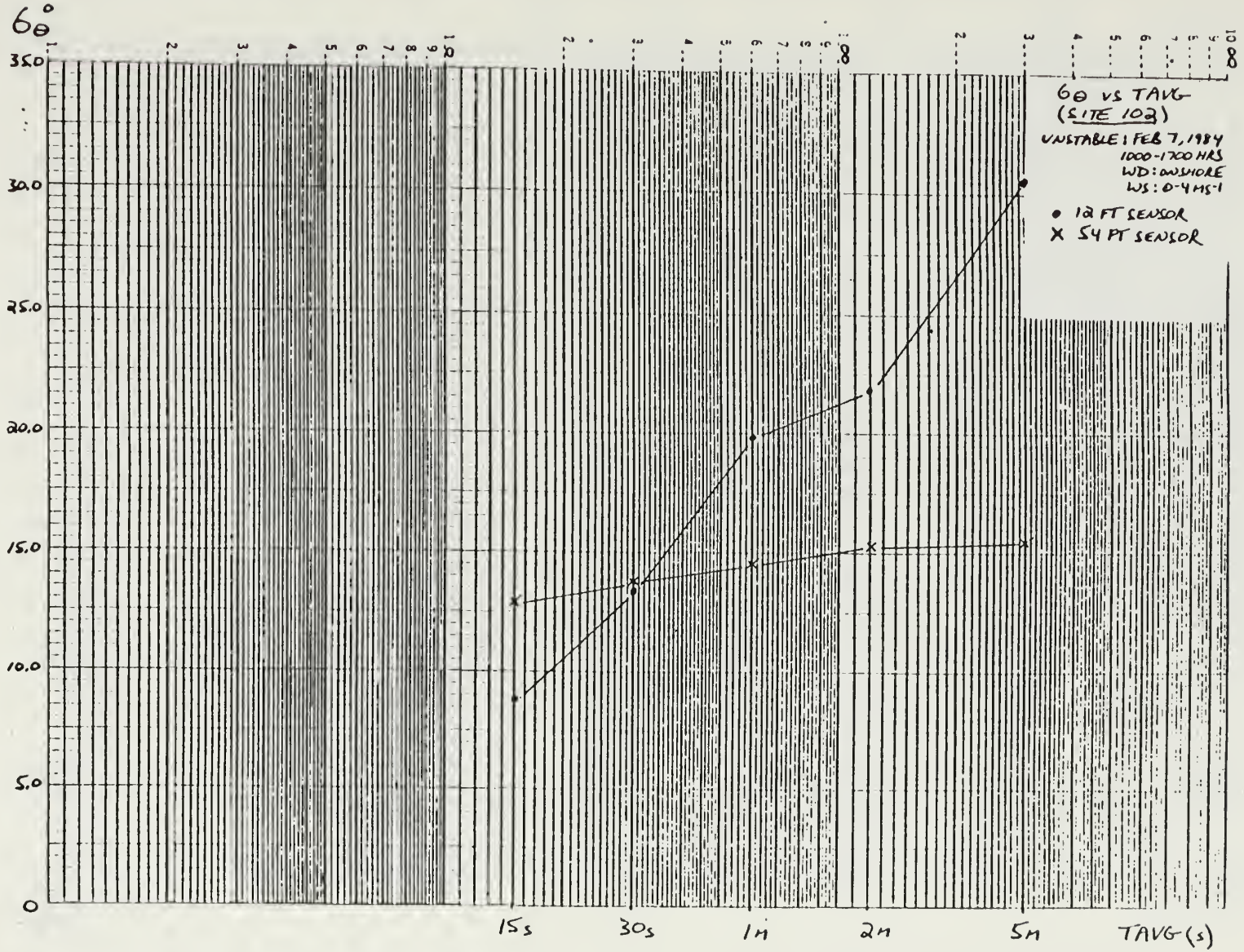

Figure 10(a). σθ vs TAVG (Site 102) (2/7/84 (1000-1700)--Unstable)

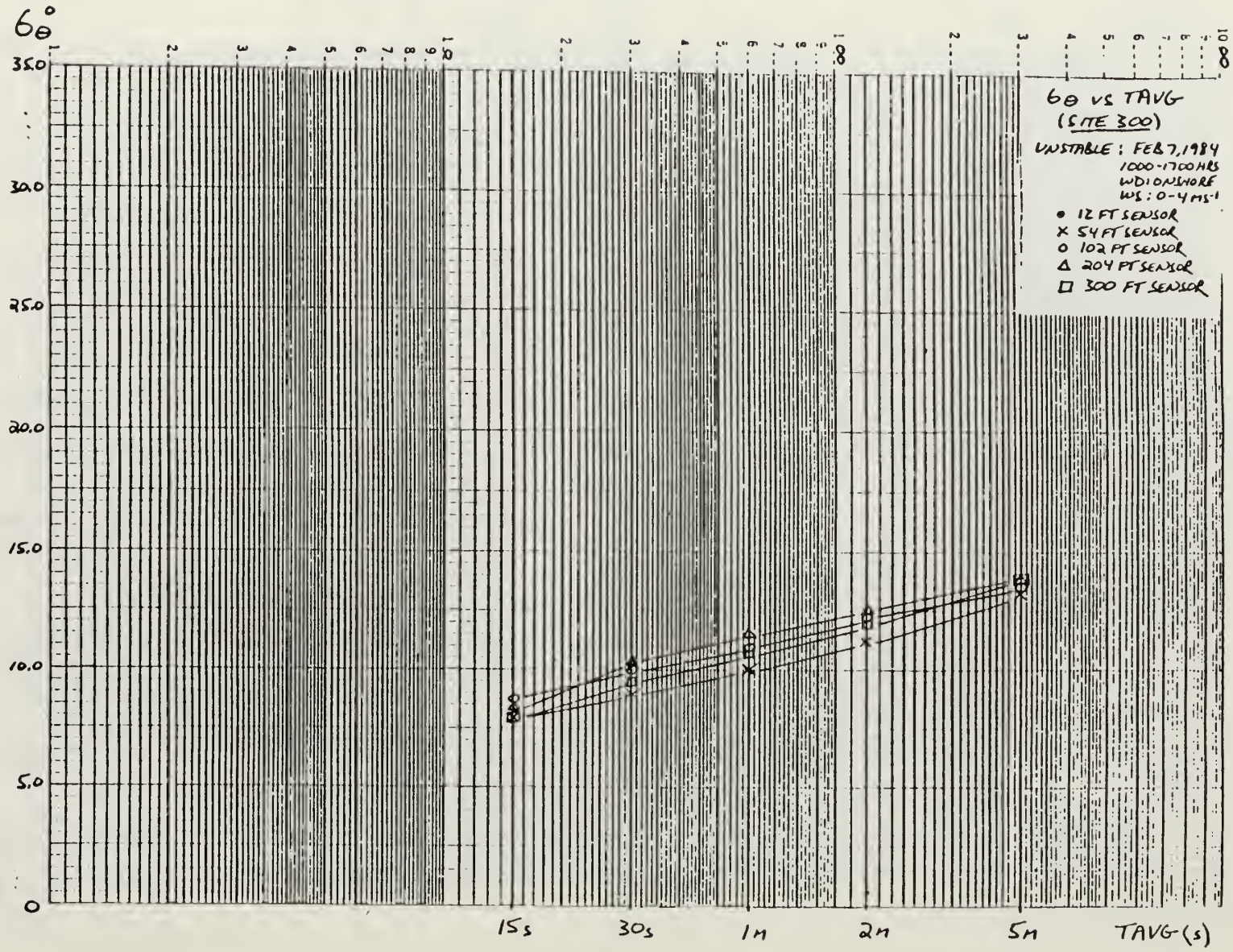

Figure 10(b). σθ vs TAVG (Site 300) (2/7/84 (1000-1700)--Unstable)

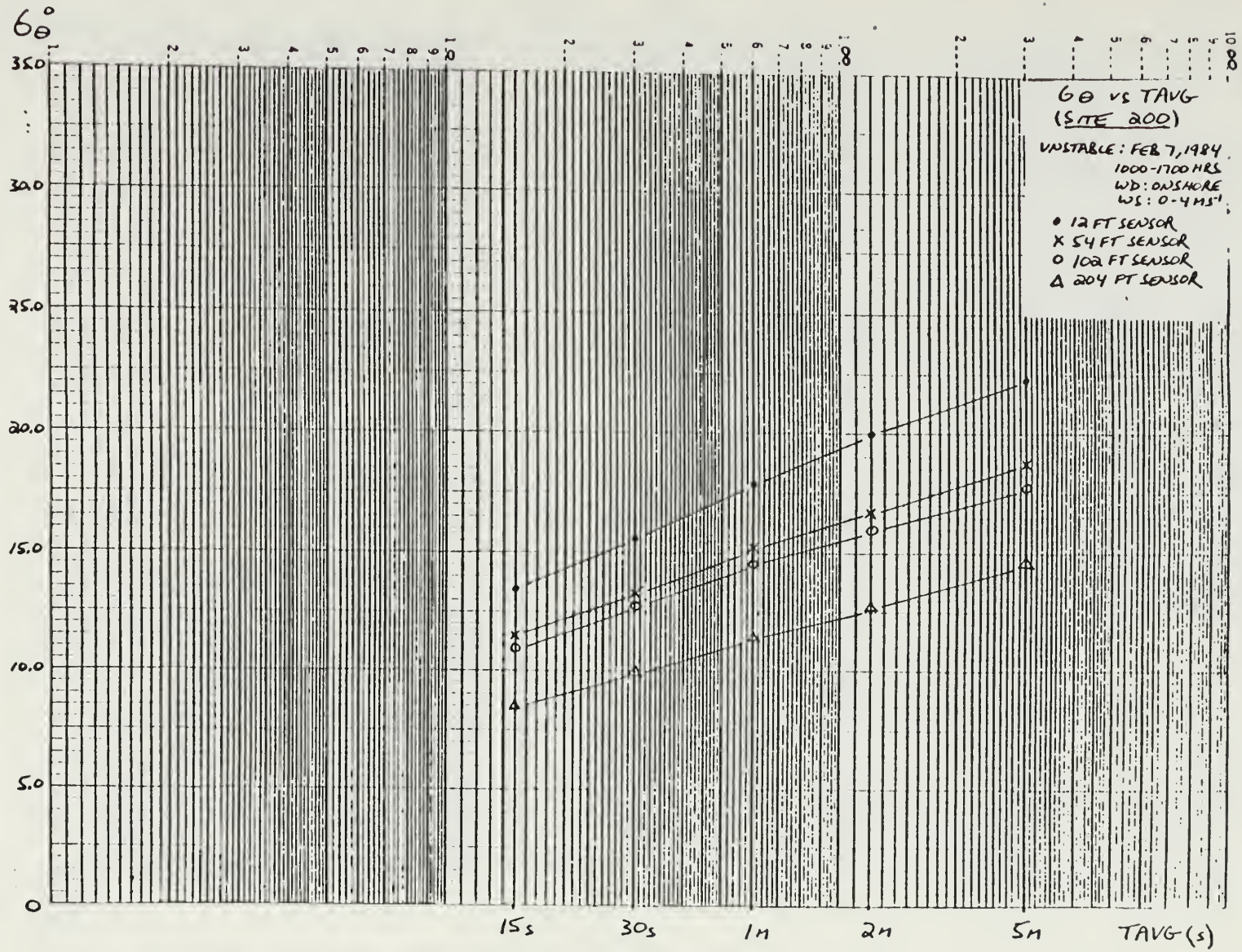

Figure 10(c). σθ vs TAVG (Site 200) (2/7/84 (1000-1700)--Unstable)

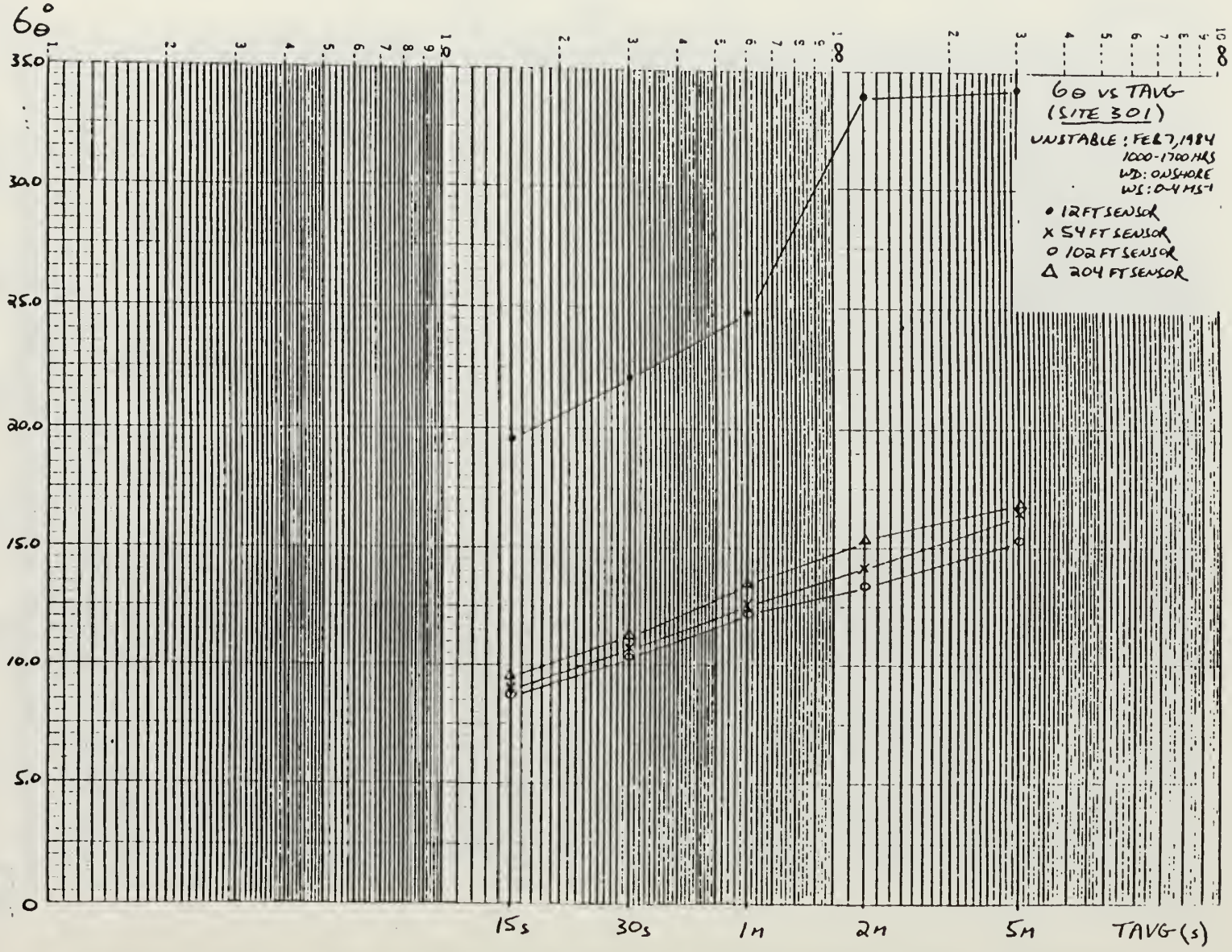

Figure 10(d). σθ vs TAVG (Site 301) (2/7/84 (1000-1700)--Unstable)

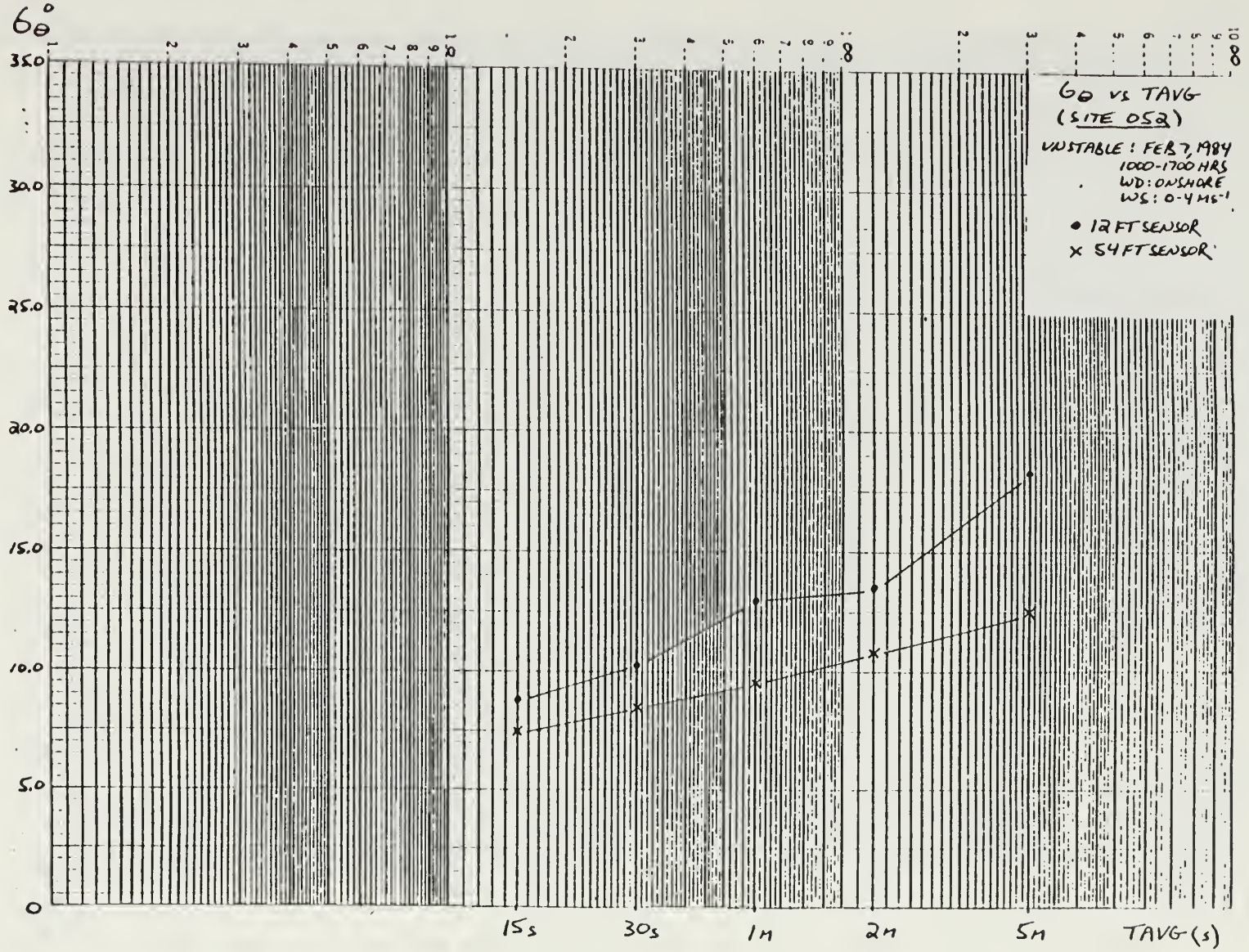

Figure 10(e). σθ vs TAVG (Site 052) (2/7/84 (1000-1700)--Unstable)

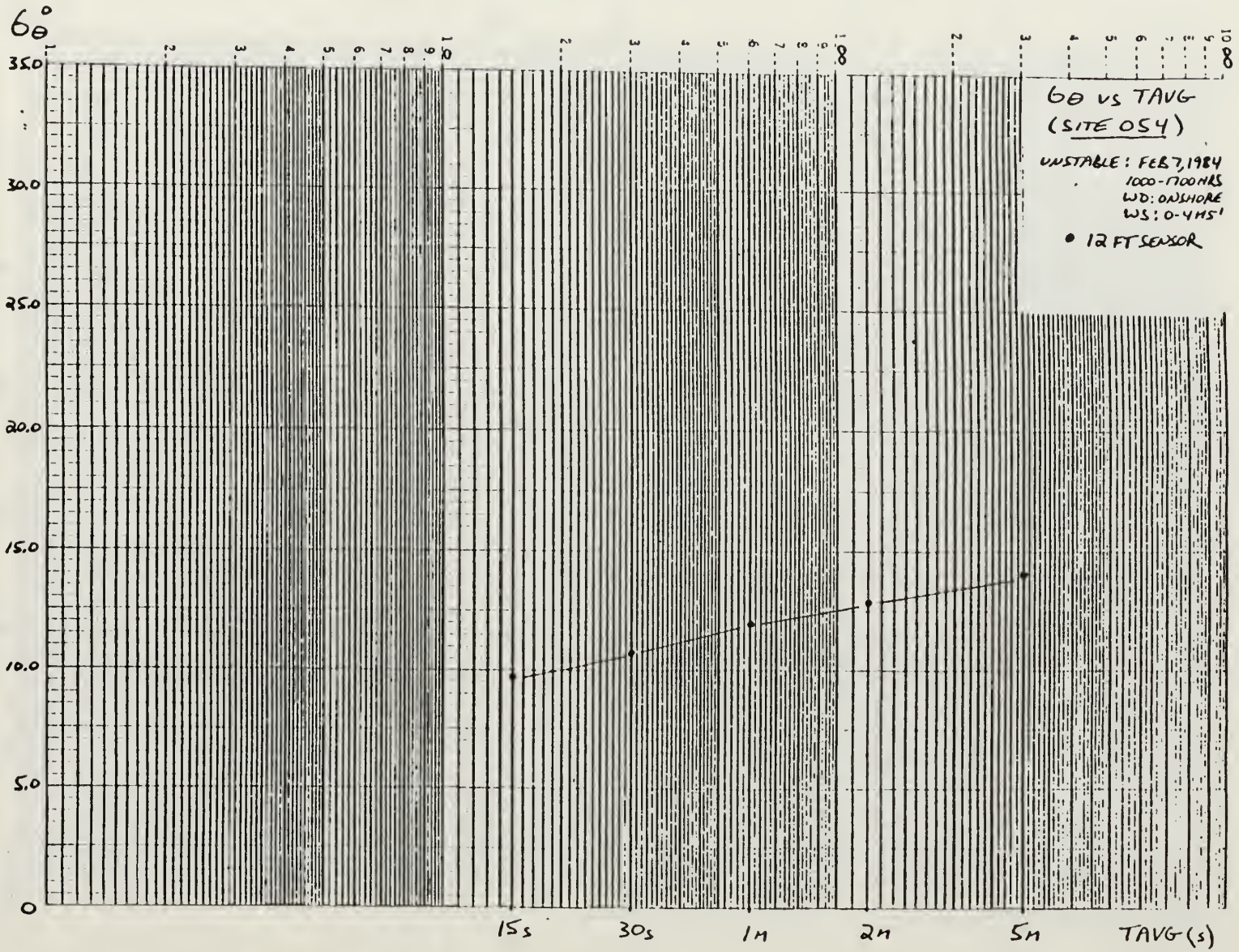

Figure 10(f). σθ vs TAVG (Site 054) (2/7/84 (1000-1700)--Unstable)

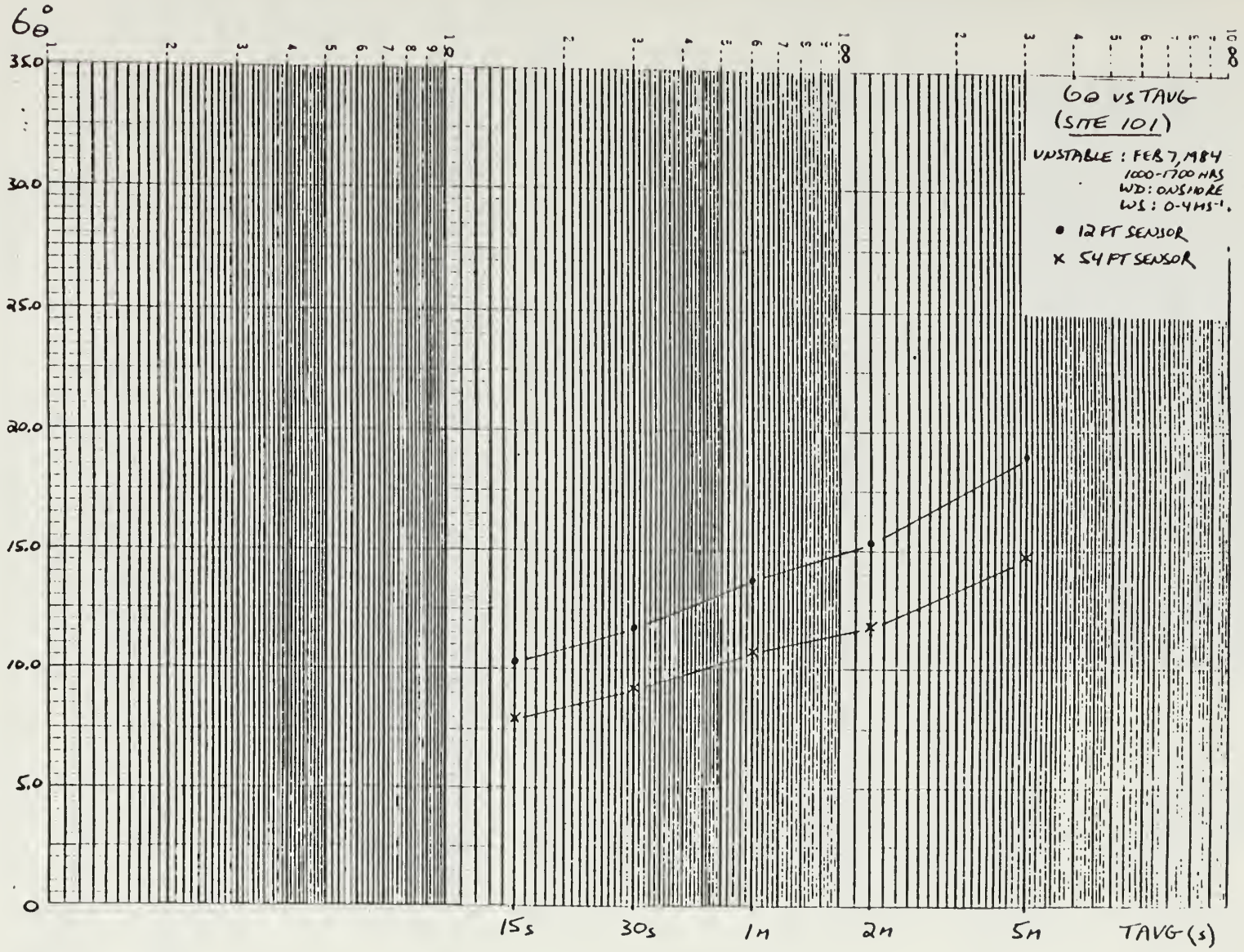

Figure 10(g). σθ vs TAVG (Site 101) (2/7/84 (1000-1700)--Unstable)

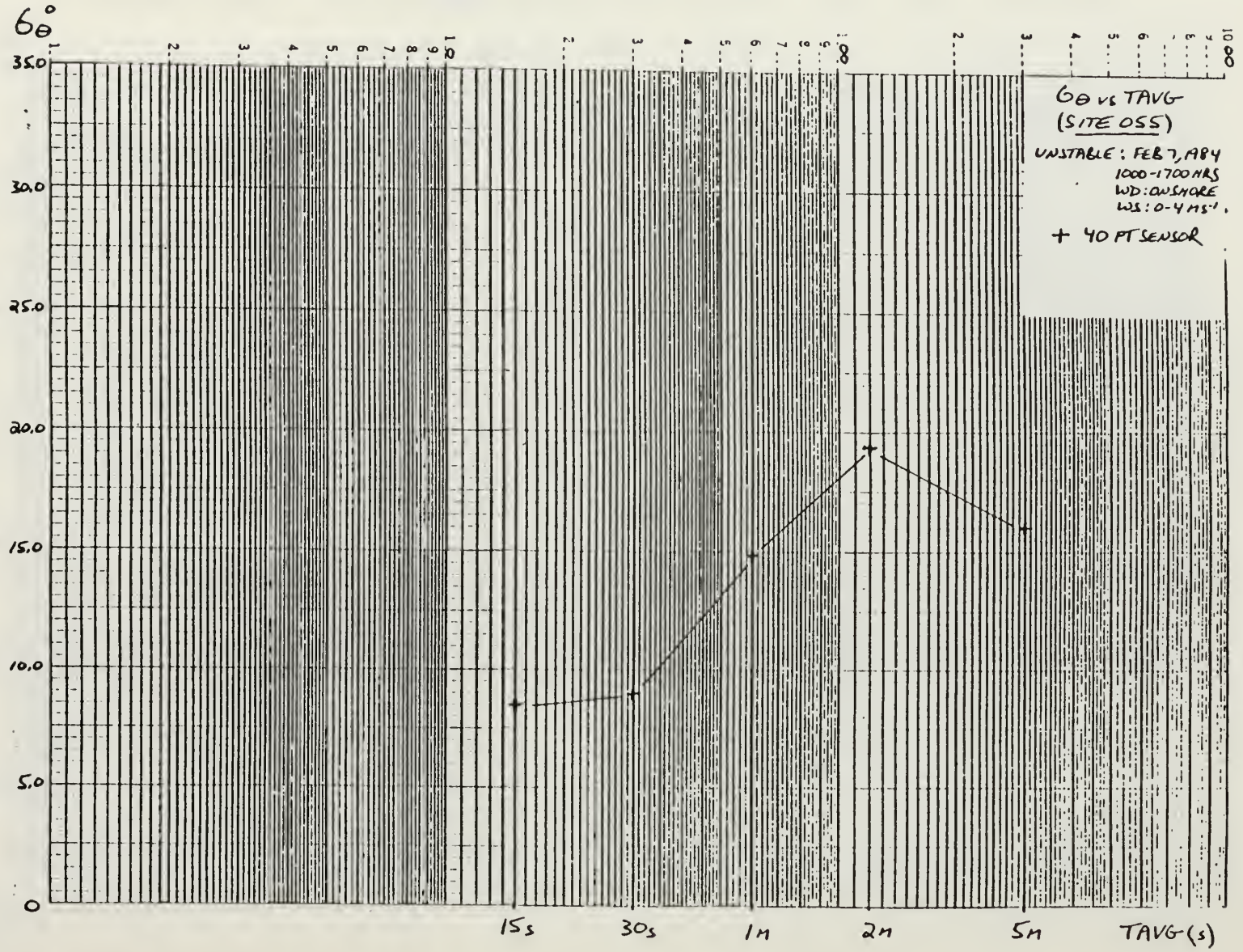

Figure 10(h). σθ vs TAVG (Site 055) (2/7/84 (1000-1700)--Unstable)

southerly onshore winds prevailing at site 055 and 056. Table XIII describes the $\sigma\theta$ dependence on wind direction for all sensors and indicates from which direction the predominant wind was blowing as well.

b. Site/Sensor Elevation Dependence

Figures 11(a-h)/Tables B-(9-16) show the dependence of $\sigma\theta$ on wind direction for various sensor elevations at specific sites (* = Predominant Wind Direction). A terrain analysis later in this chapter will collectively examine $\sigma\theta$ differences between sites and $\sigma\theta$ dependences on wind direction relative to each site.

4. $\sigma\theta$ Dependence on Wind Speed

a. General Results

The predominant wind speed at all sensors was 2-4 ms^{-1} with the exception of sensors 101-12' and 54' and 200-12' and 102' which experienced predominant wind speeds of 0-2 ms^{-1} and sensor 200-204' which had a prevailing wind speed of 4-6 ms^{-1}. In general, all sensors exhibited a decrease in $\sigma\theta$ values with increasing wind speed. This is expected since higher wind speeds cause neutral conditions and lower turbulence intensity levels. Table XIV describes the $\sigma\theta$ dependence on wind speed for all sensors and indicates the predominant wind speed at each sensor as well.

b. Site/Sensor Elevation Dependence

Figures 12(a-h)/Tables B-(17-24) describe $\sigma\theta$ dependence on wind speed for various sensor elevations at

TABLE XIII

$\sigma\theta$ Dependence on Wind Direction
(2/7/84 (1000-1700)--Unstable)

		WIND DIRECTION				
Sensor	Site-Ht	5	6	7	8	9
3	052-12'	9.1	7.7	8.7*	9.3	8.6
4	054-12'	----	17.5	9.8*	9.4	8.5
5	101-12'	11.1	11.1*	12.6	9.9	7.8
6	102-12'	----	13.1	9.8	7.8*	8.8
8	200-12'	15.7	135.	15.6	13.2*	11.7
10	301-12'	----	18.0	24.5	25.1	16.0*
13	055-40'	5.0*	----	----	----	----
11	052-54'	6.4	7.8	7.5*	7.4	7.1
15	101-54'	10.1	8.9*	10.0	6.8	6.3
16	102-54'	----	14.0	13.8*	10.2	30.6
18	200-54'	10.1	10.8*	13.9	11.0	7.5
19	300-54'	7.7	9.0	7.4*	7.4	9.9
20	301-54'	13.7	9.5	8.8	10.0	8.6*
22	200-102'	6.5	11.4	11.5*	12.3	6.8
23	300-102'	9.0	10.1	7.7*	5.8	----
25	301-102'	9.0	8.9	10.4	11.1	7.6*
24	299-204'	10.5	10.5	8.9*	7.3	----
26	200-204'	----	7.0	8.9	10.2*	5.4
27	300-204'	9.0	9.4	8.6*	6.5	----
28	301-204'	8.1	13.0	10.9	11.5	7.9*
29	300-300'	6.4	7.6	8.3*	7.7	10.8

Note: Most representative values listed above ($\sigma\theta$ in degrees)

* = Predominant wind direction

Time averaging 15 seconds

Wind speed 0-4 ms^{-1} except sensors 13 and 26 (4-8 ms^{-1})

Wind direction 5: 160-200 degrees

Wind direction 6: 200-240 degrees

Wind direction 7: 240-280 degrees

Wind direction 8: 280-320 degrees

Wind direction 9: 320-360 degrees

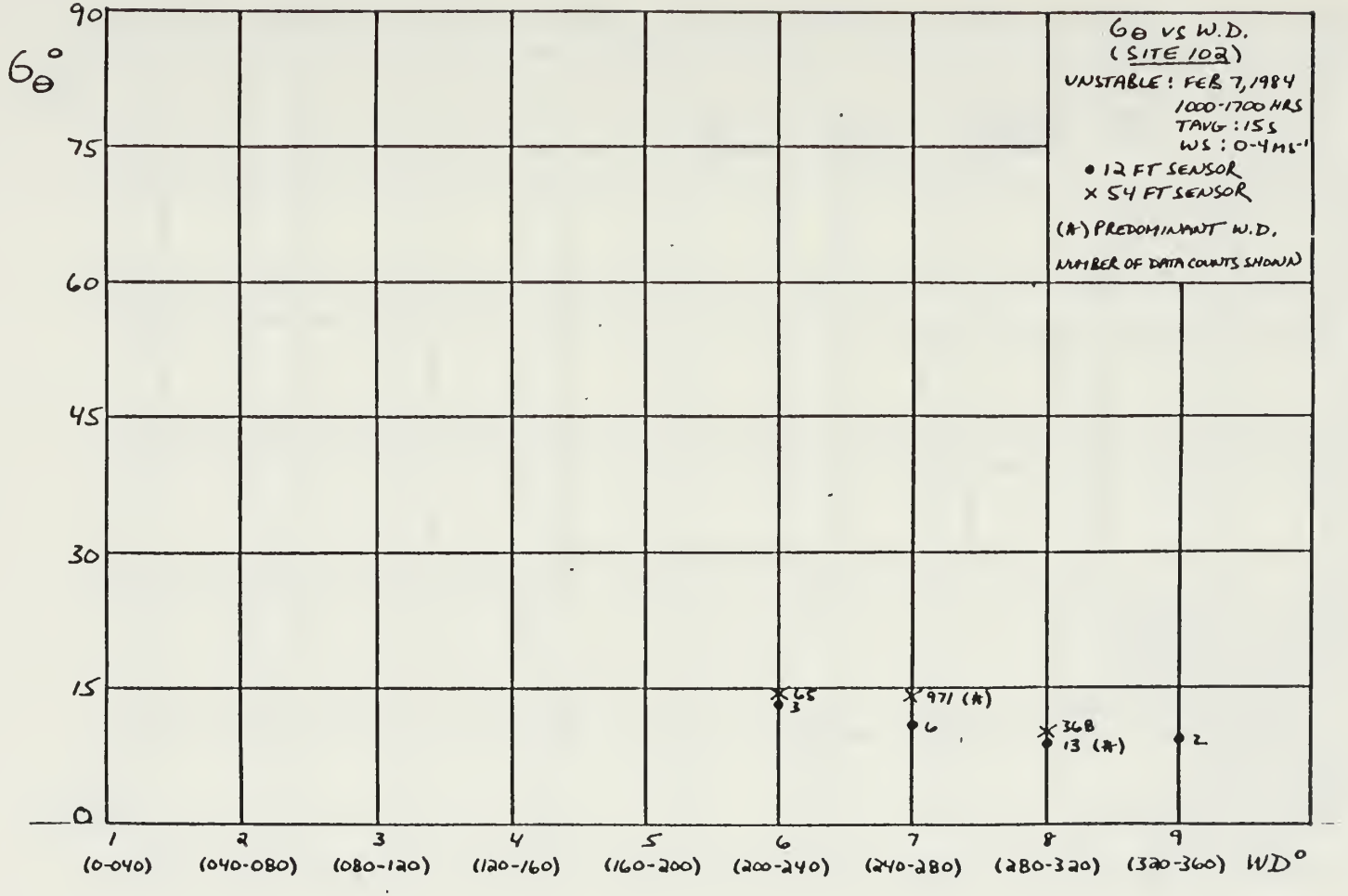

Figure 11(a). $\sigma\theta$ vs WD (Site 102) (2/7/84 (1000-1700)--Unstable)

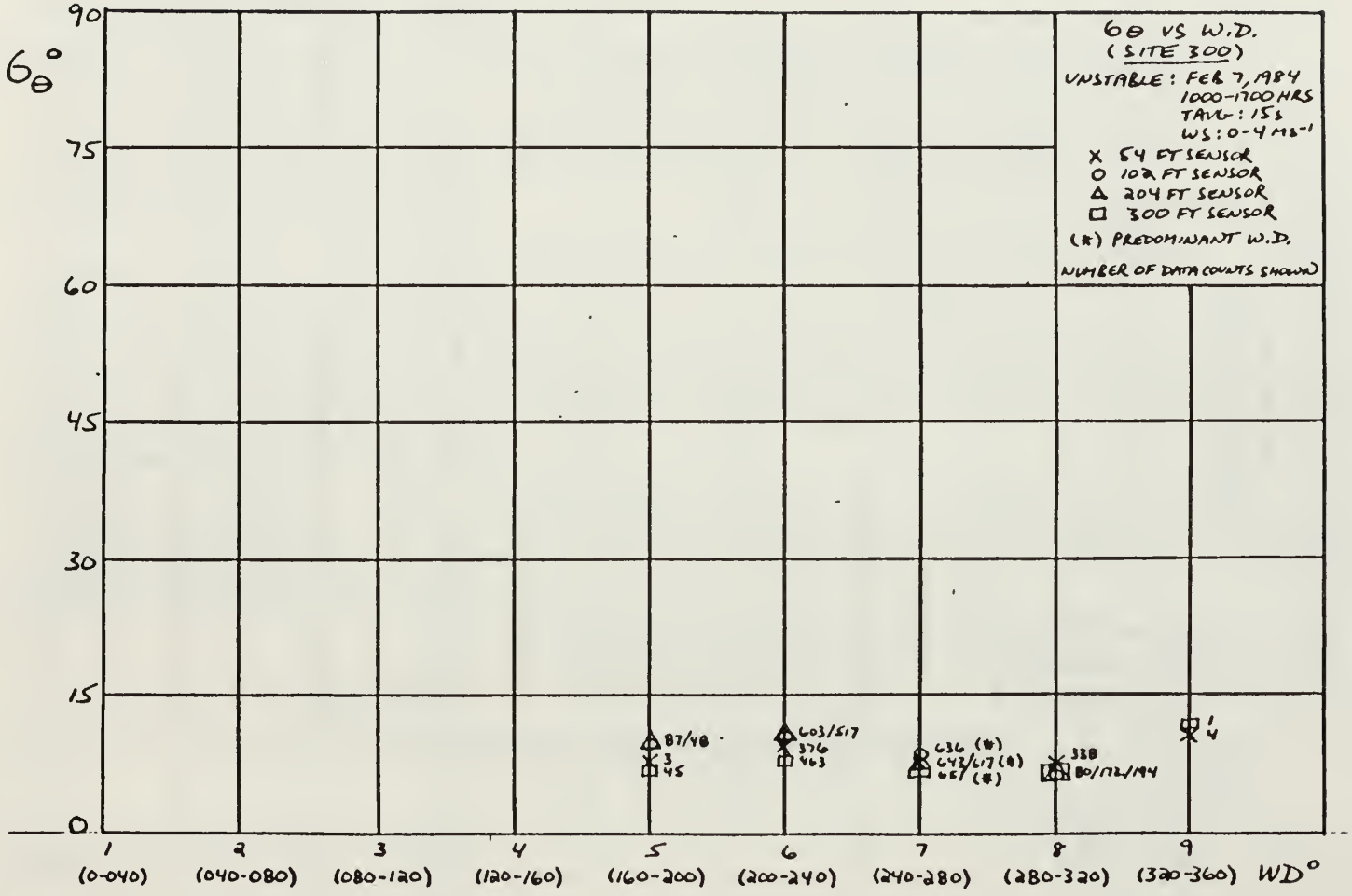

Figure 11(b). σθ vs WD (Site 300) (2/7/84 (1000-1700)--Unstable)

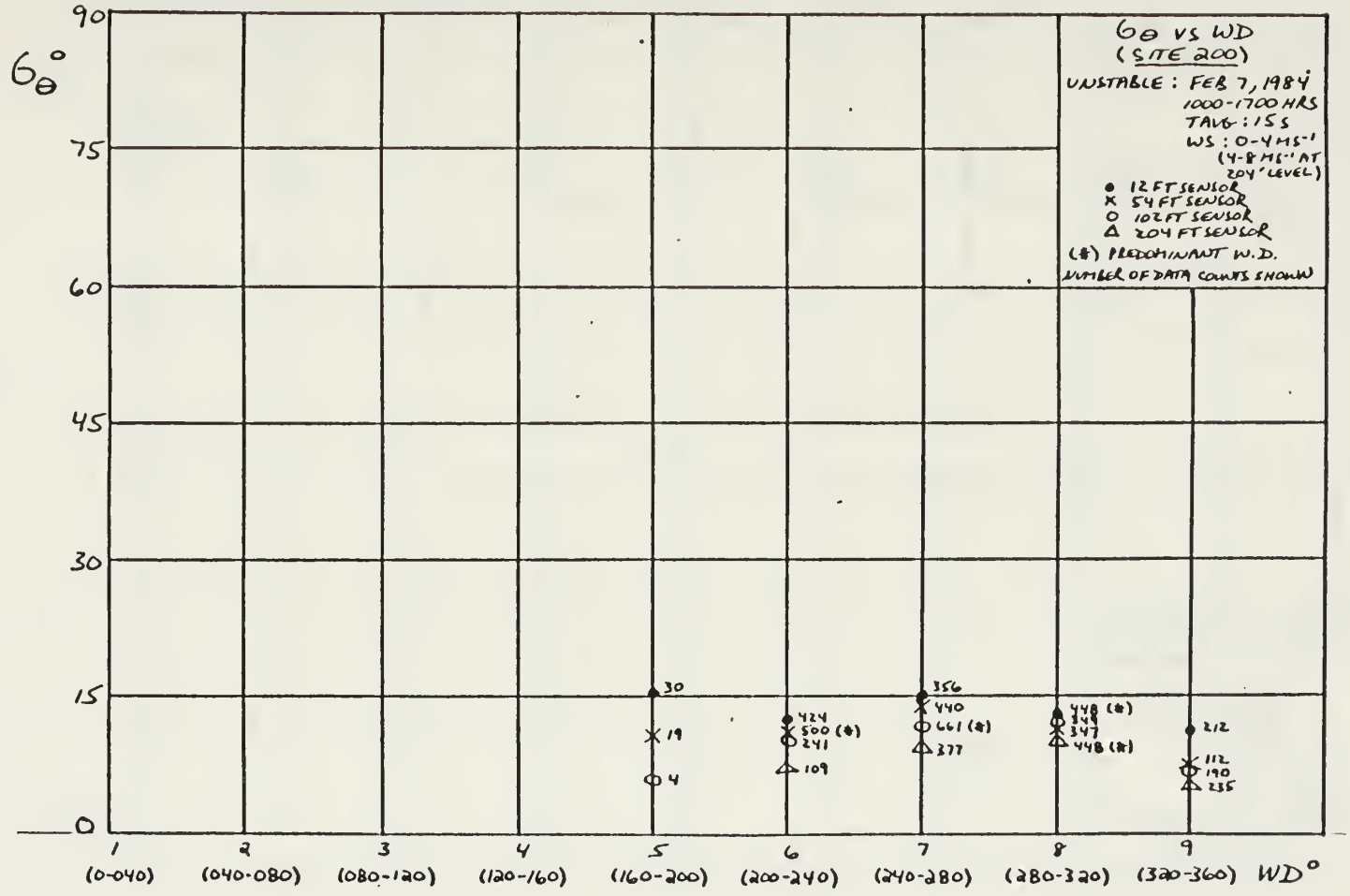

Figure 11(c). σθ vs WD (Site 200) (2/7/84 (1000-1700)--Unstable)

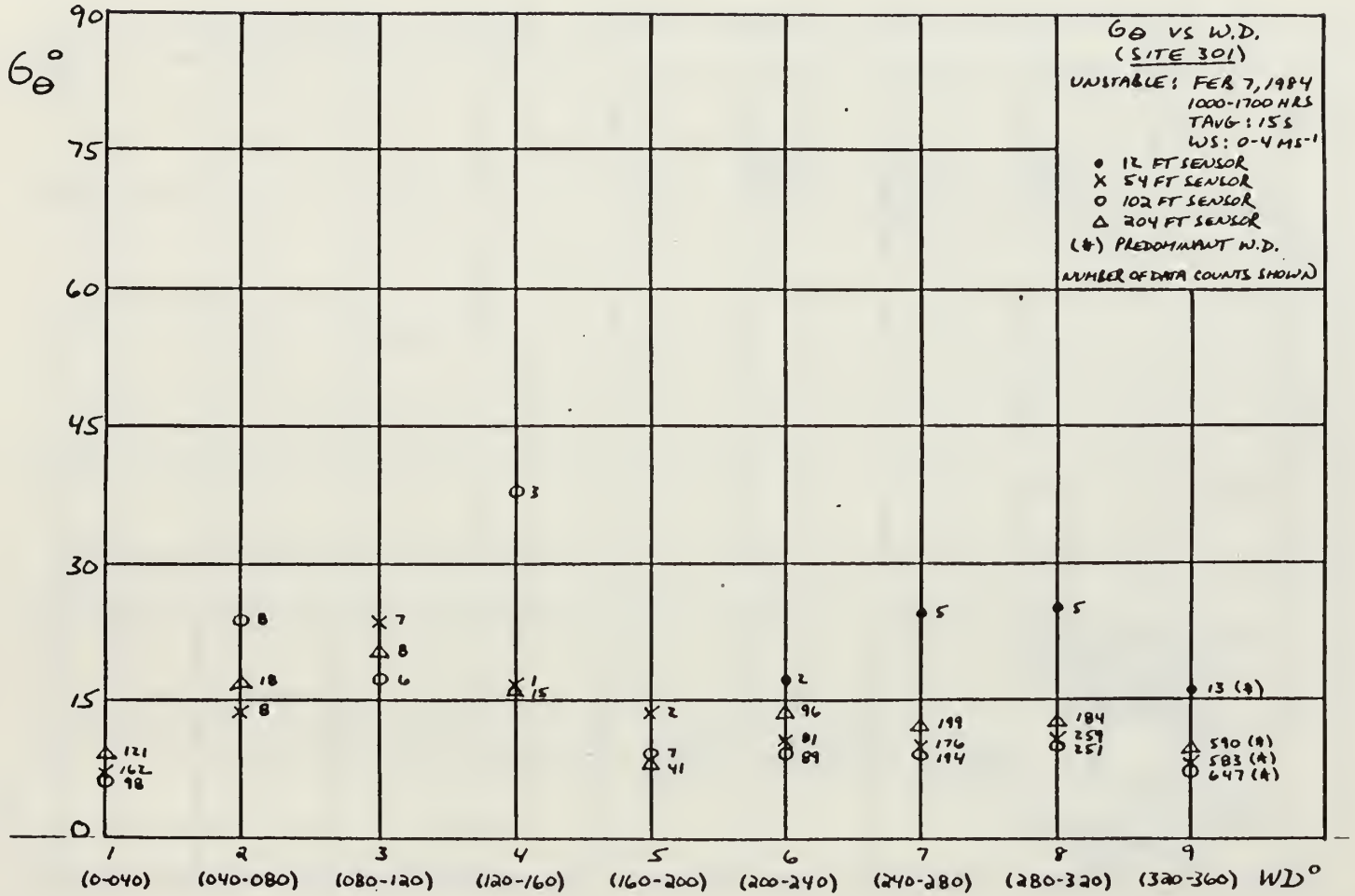

Figure 11(d). σθ vs WD (Site 301) (2/7/84 (1000-1700)--Unstable)

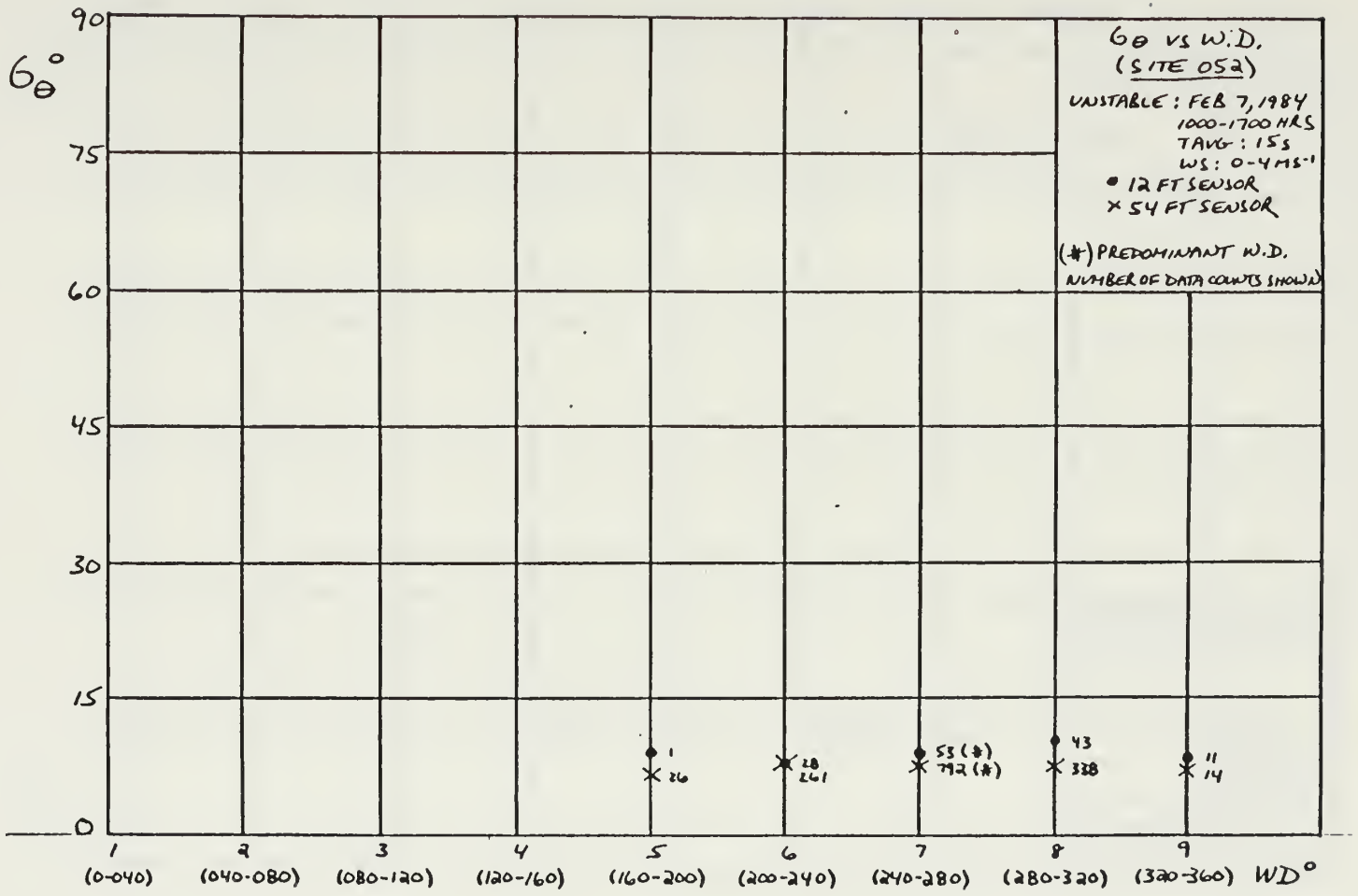

Figure 11(e). $\sigma\theta$ vs WD (Site 052) (2/7/84 (1000-1700)--Unstable)

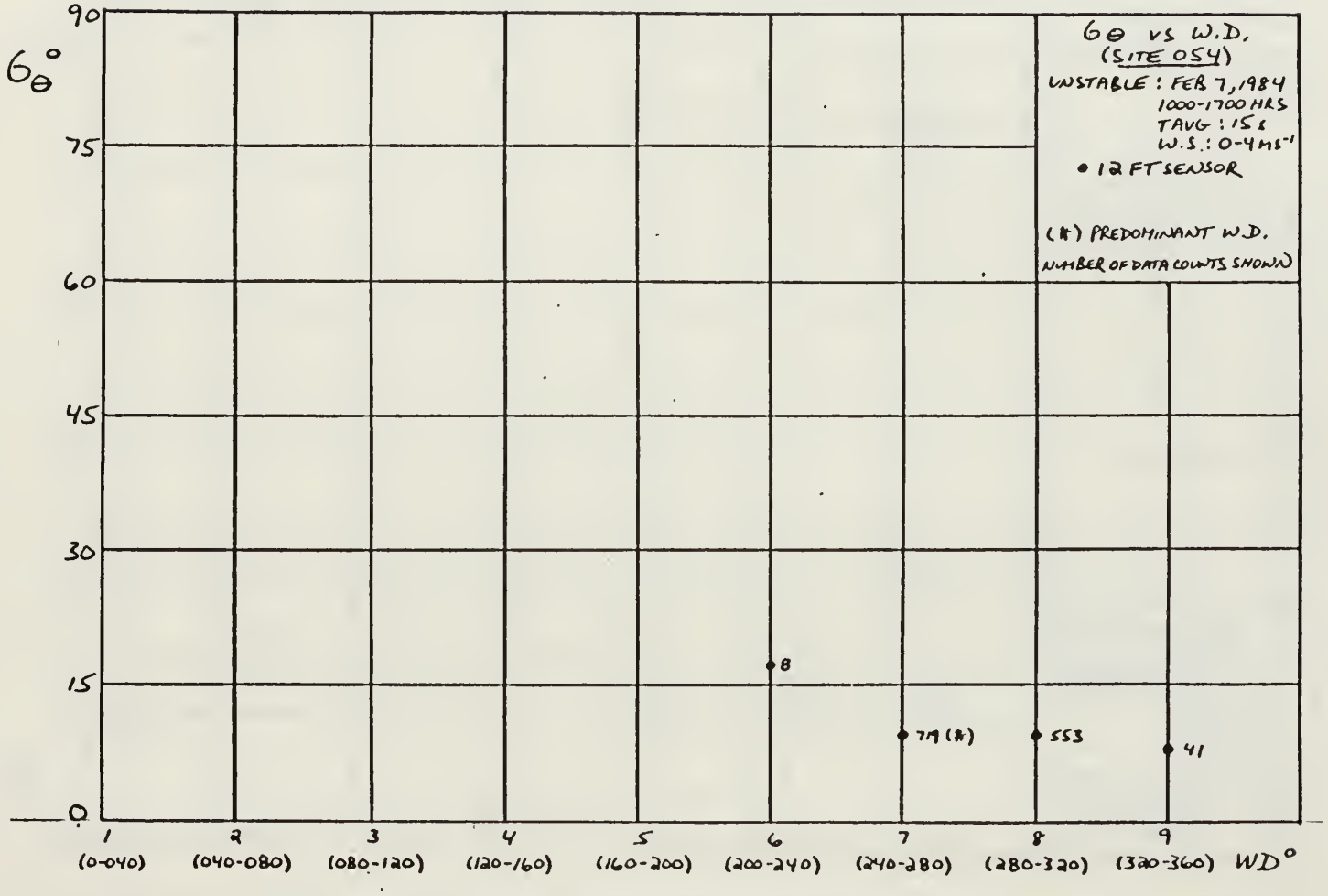

Figure 11(f). σθ vs WD (Site 054) (2/7/84 (1000-1700)--Unstable)

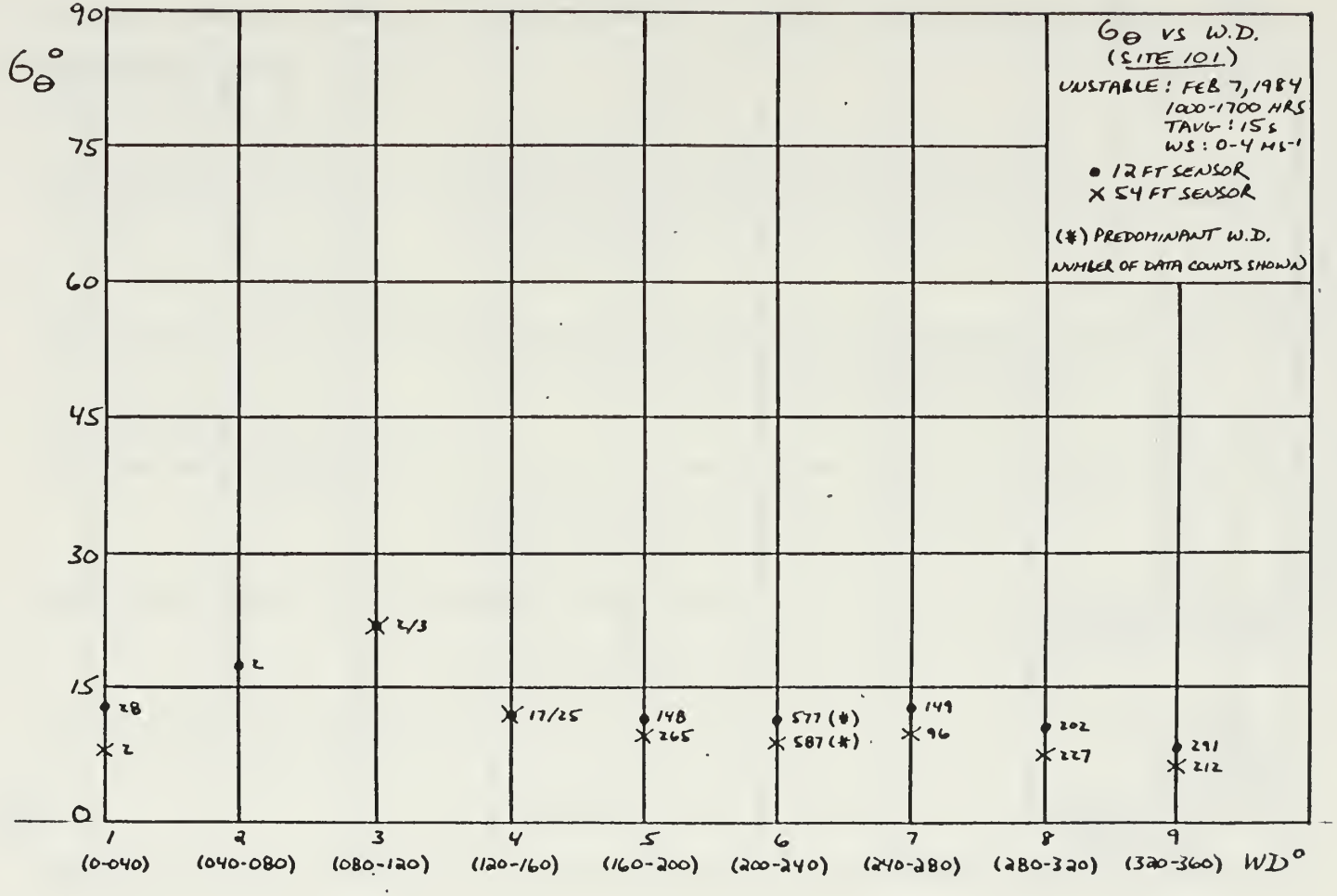

Figure 11(g). $\sigma\theta$ vs WD (Site 101) (2/7/84 (1000-1700)--Unstable)

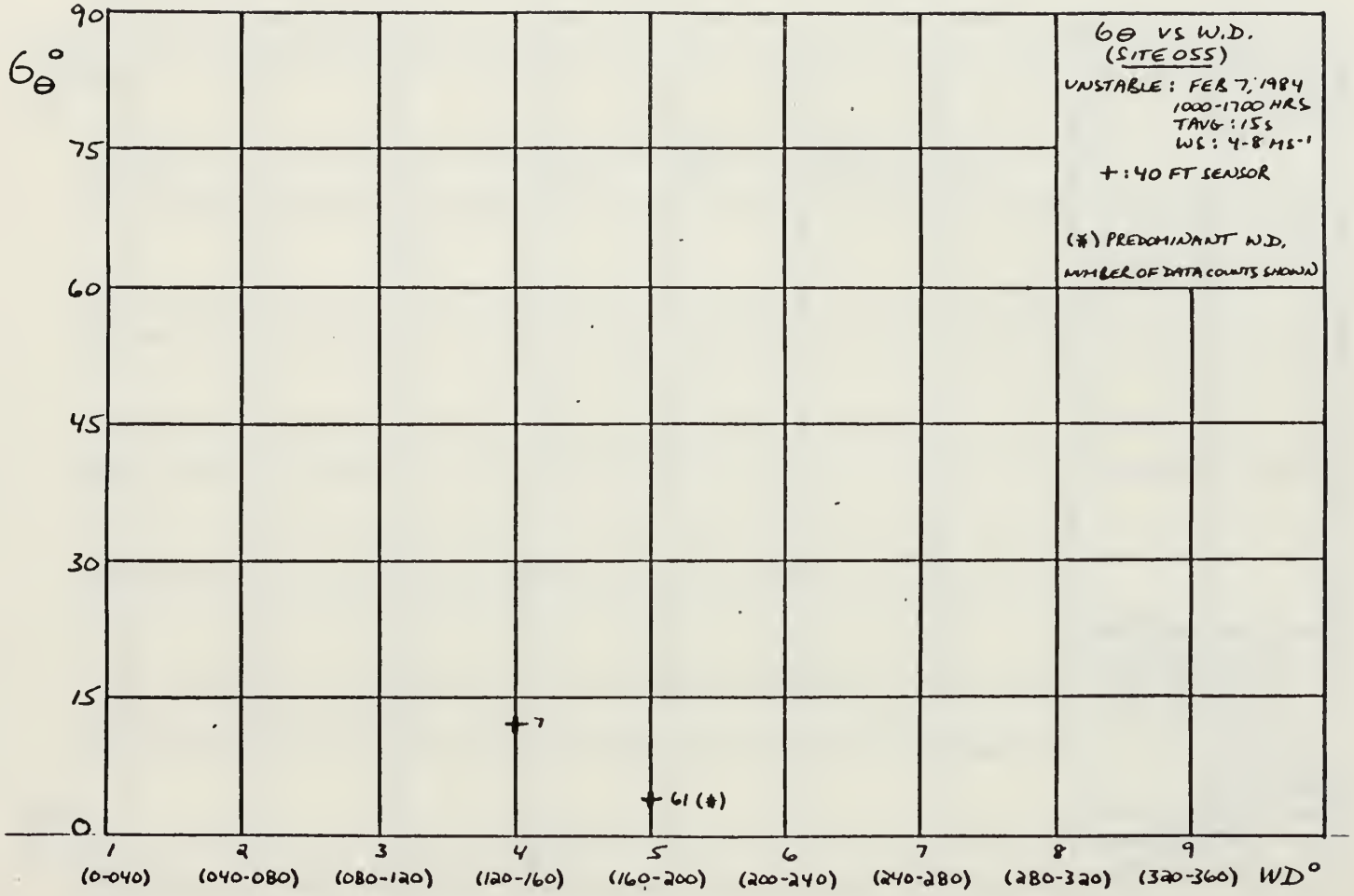

Figure 11(h). σθ vs WD (Site 055) (2/7/84 (1000-1700)--Unstable)

TABLE XIV

$\sigma\theta$ Dependence on Wind Speed
(2/7/84 (1000-1700)--Unstable)

UNSTABLE CASE: February 7, 1984 (1000-1700 hours)

		WIND SPEED			
Sensor	Site-Ht	1	2	3	4
3	052-12'	11.9	8.1*	----	----
4	054-12'	10.2	9.5*	6.6	----
5	101-12'	11.4*	8.2	10.7	----
6	102-12'	10.9	6.8*	8.7	----
8	200-12'	15.0*	9.9	----	----
10	301-12'	29.1	10.9*	----	----
13	055-40'	12.4	6.1*	10.5	----
11	052-54'	11.9	7.3*	4.6	----
15	101-54'	8.8*	6.4	----	----
16	102-54'	16.7	10.6*	5.9	----
18	200-54'	17.8	10.3*	7.0	----
19	300-54'	9.8	7.3*	9.1	----
20	301-54'	12.6	7.7*	4.7	3.6
22	200-102'	12.7*	9.2	6.8	----
23	300-102'	10.1	8.0*	6.2	----
25	301-102'	12.0	7.0*	3.1	2.4
24	299-108'	10.4	8.6*	7.2	5.5
26	200-204'	----	13.9	8.6*	5.9
27	300-204'	10.7	7.8*	6.7	----
28	301-204'	12.5	7.3*	2.8	1.9
29	300-300'	10.3	6.8*	5.7	----

Note: Most representative values listed above ($\sigma\theta$ in degrees)

* = Predominant wind speed

Time averaging 15 seconds

Wind direction onshore (200-360 degrees)

Wind speed 1: 0-2 ms^{-1}

Wind speed 2: 2-4 ms^{-1}

Wind speed 3: 4-6 ms^{-1}

Wind speed 4: 6-8 ms^{-1}

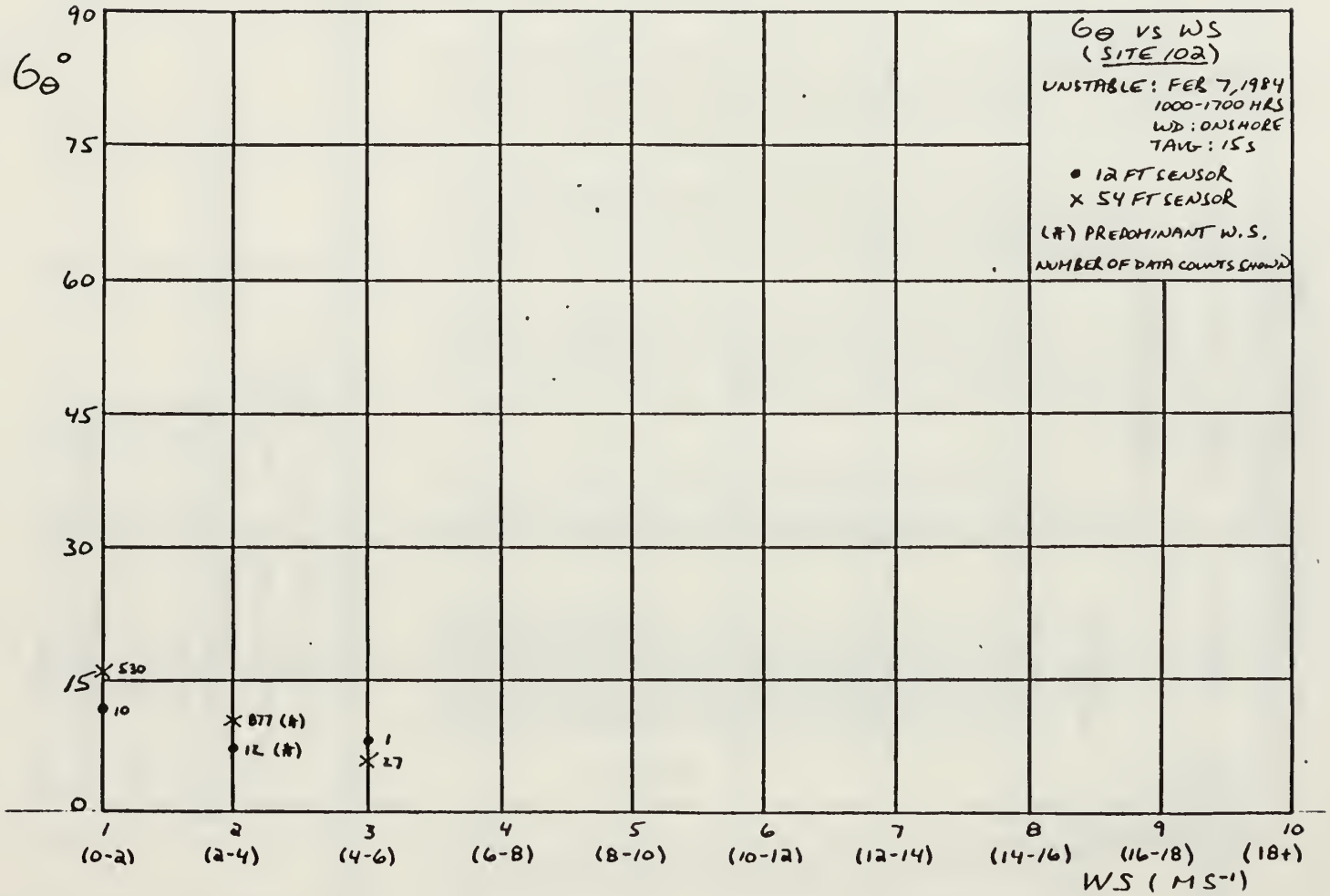

Figure 12(a). $\sigma\theta$ vs WS (Site 102) (2/7/84 (1000-1700)--Unstable)

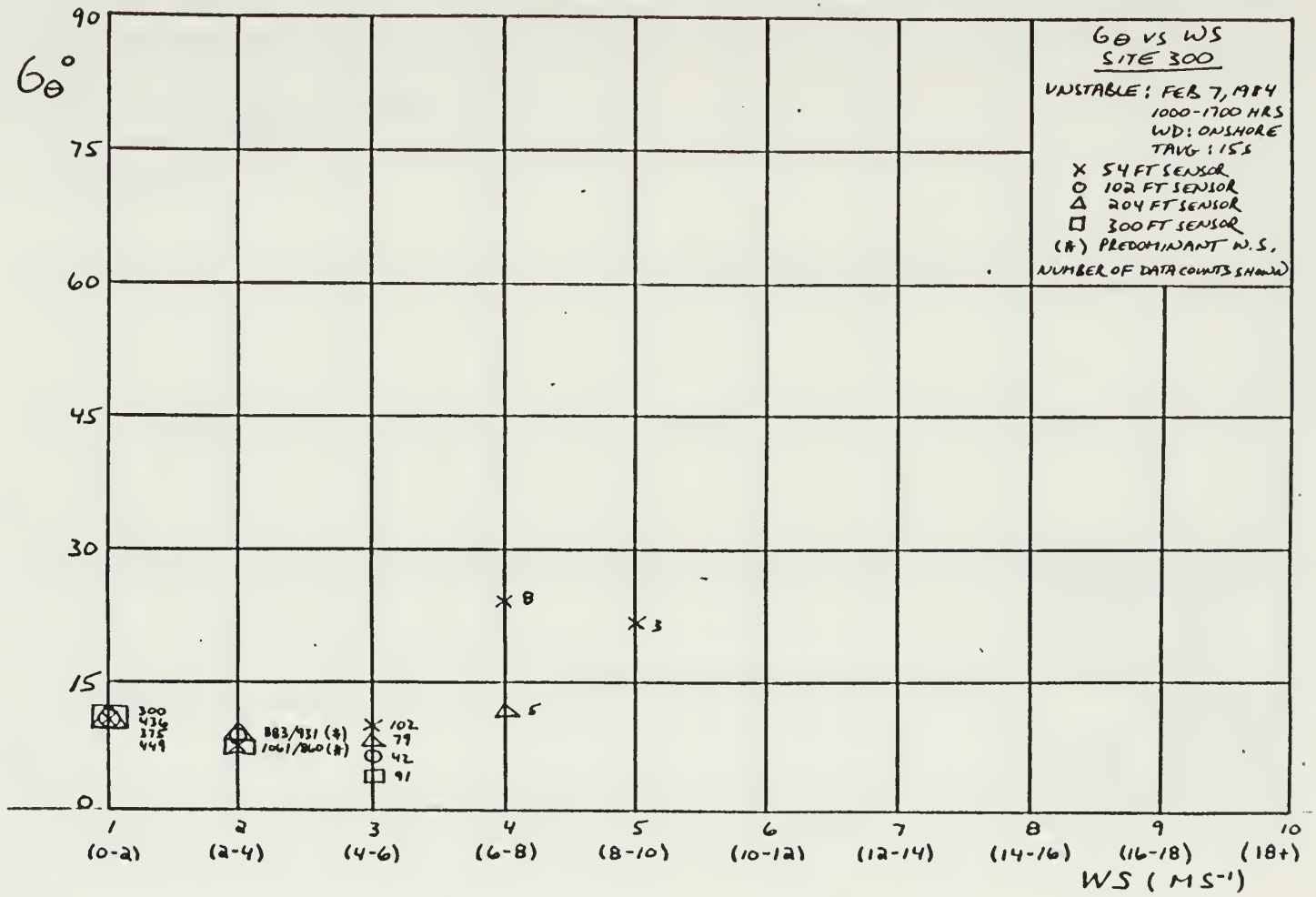

Figure 12(b). σθ vs WS (Site 300) (2/7/84 (1000-1700)--Unstable)

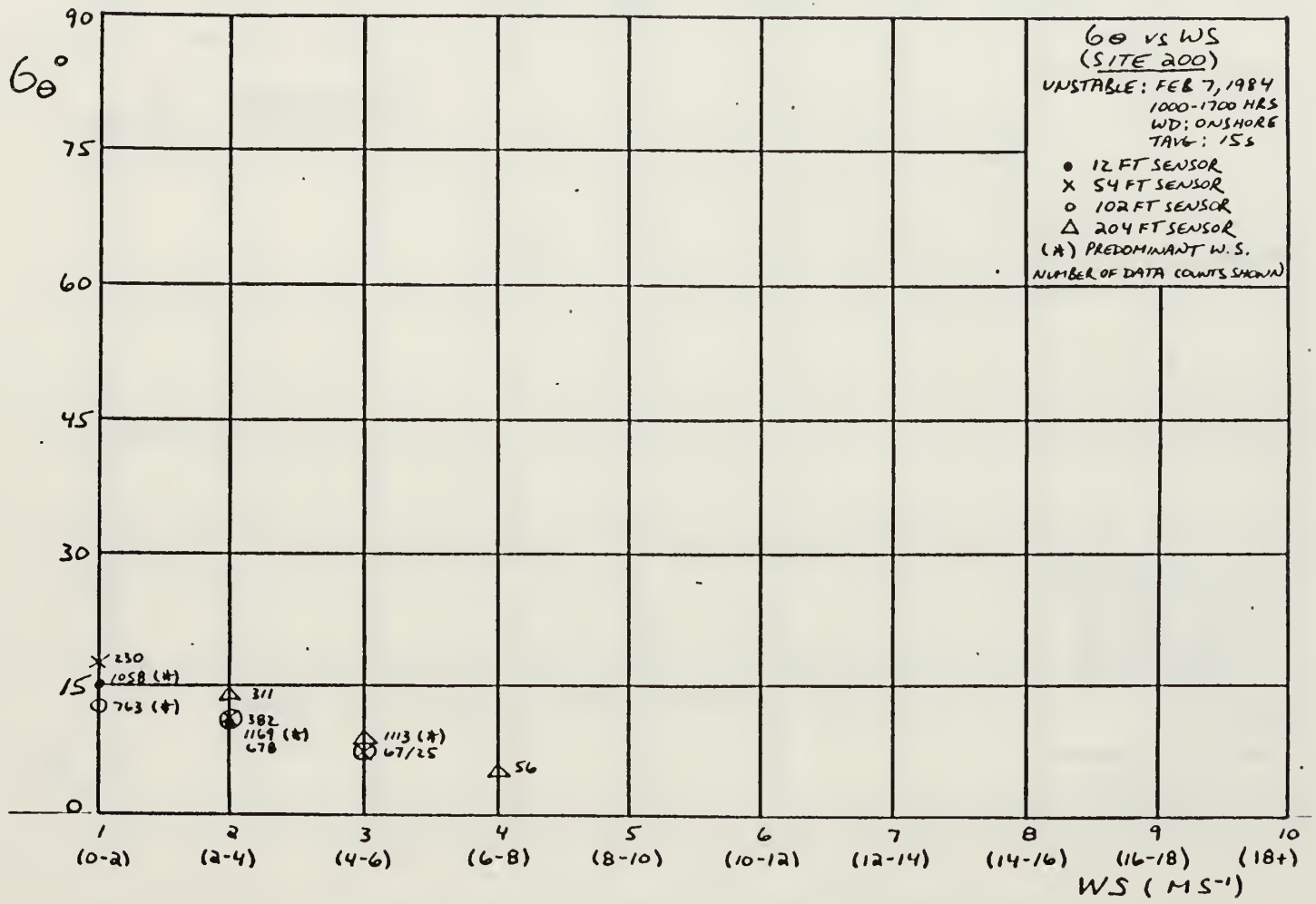

Figure 12(c). $\sigma\theta$ vs WS (Site 200) (2/7/84 (1000-1700)--Unstable)

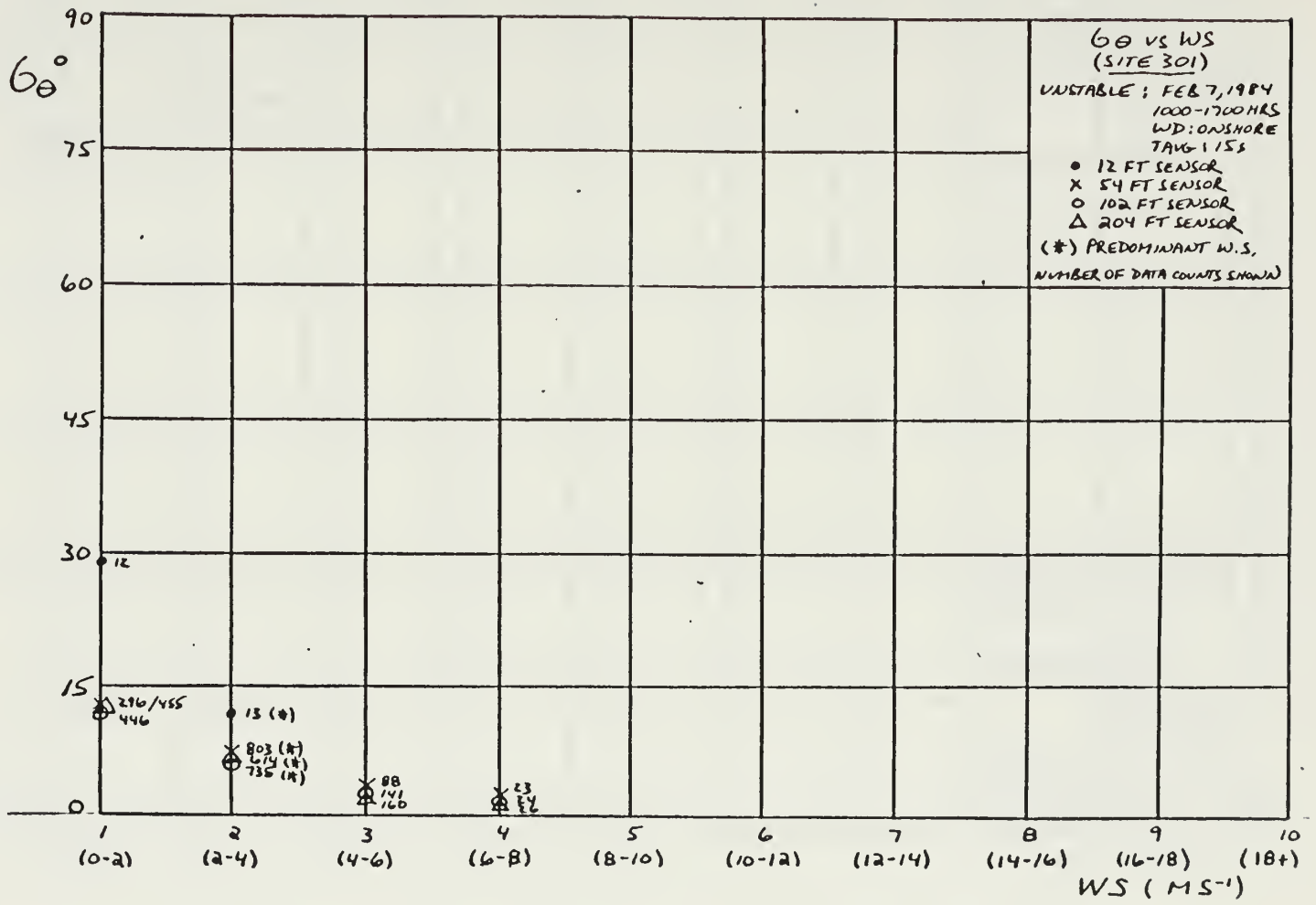

Figure 12(d). σθ vs WS (Site 301) (2/7/84 (1000-1700)--Unstable)

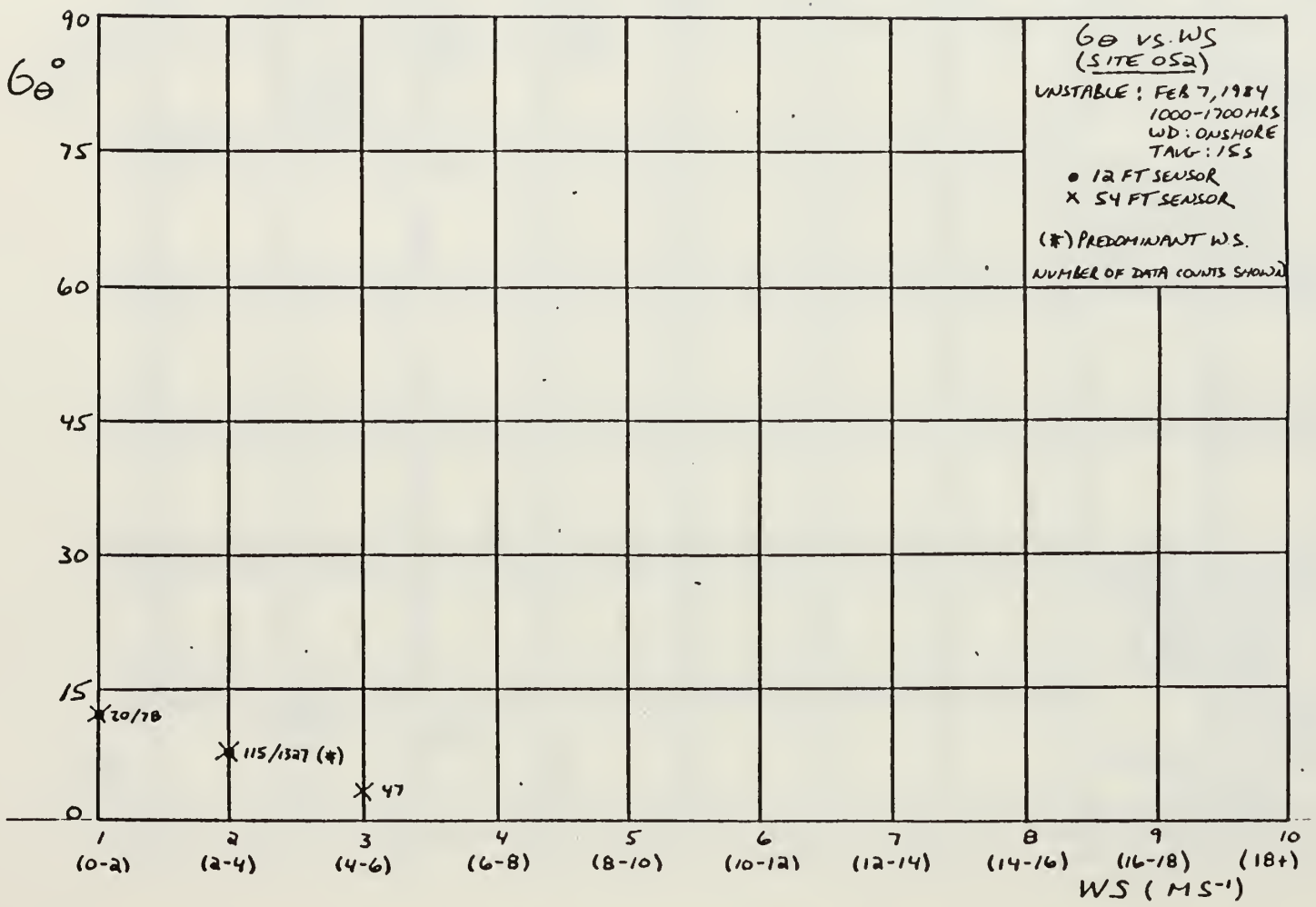

Figure 12(e). $\sigma\theta$ vs WS (Site 052) (2/7/84 (1000-1700)--Unstable)

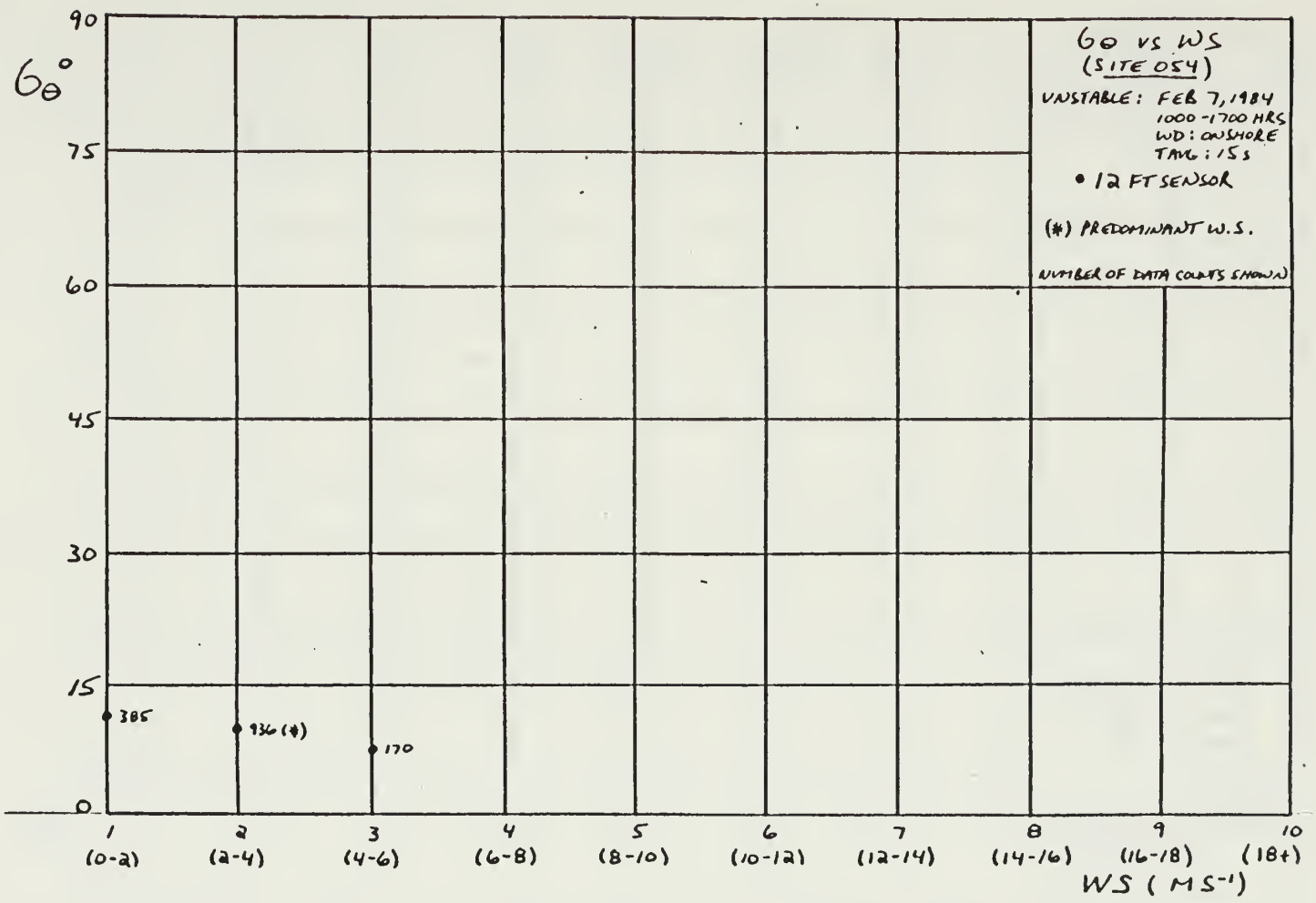

Figure 12(f). σθ vs WS (Site 054) (2/7/84 (1000-1700)--Unstable)

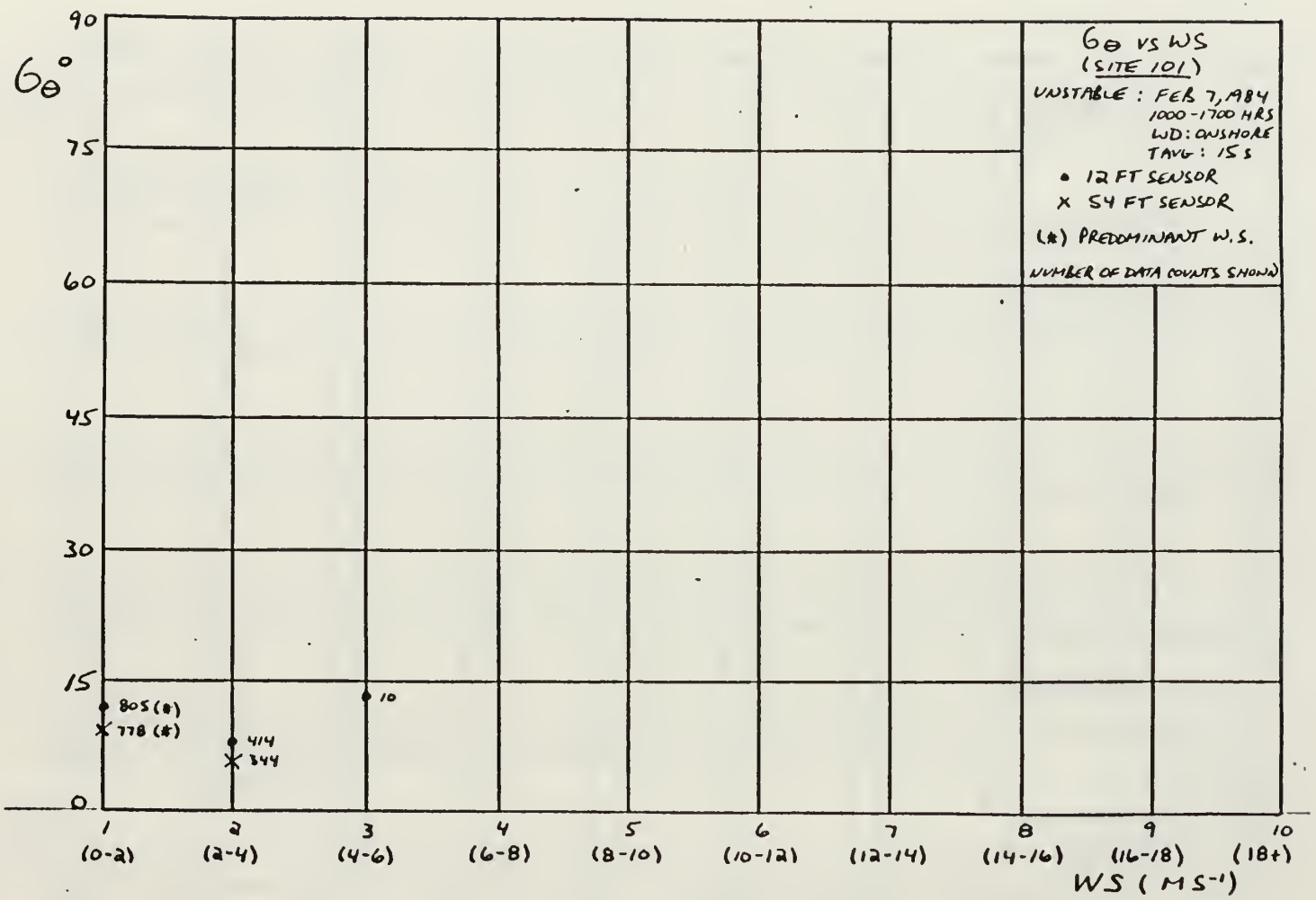

Figure 12(g). $\sigma\theta$ vs WS (Site 101) (2/7/84 (1000-1700)--Unstable)

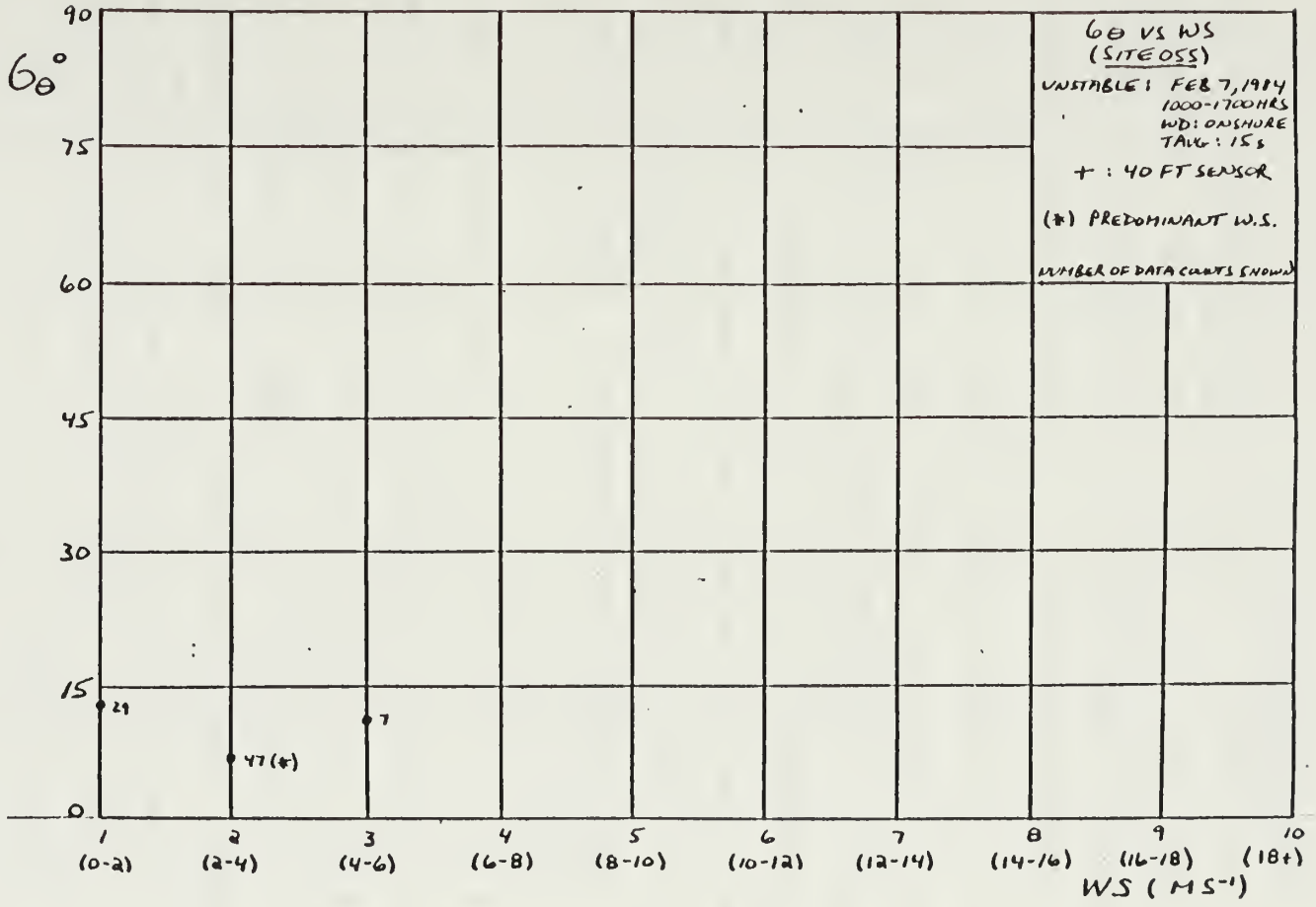

Figure 12(h). $\sigma\theta$ vs WS (Site 055) (2/7/84 (1000-1700)--Unstable)

specific sites (* = Predominant Wind Speed). The next section collectively examines $\sigma\theta$ differences between sites and $\sigma\theta$ dependences on wind speed relative to each site.

5. Terrain Dependence

The convective upwelling associated with the unstable onshore sea breeze flow in this case was most important in determining the dependence of $\sigma\theta$ on the terrain. Although the terrain effects were basically masked by the convective upwelling in this case, slightly lower $\sigma\theta$ values were found at the coastal sites versus inland. This was primarily due to the presence of the marine boundary layer along the coast which is accompanied by cooler less unstable air. As this air moves inland, it is modified by heating and the lower atmosphere becomes more unstable. This, together with the rougher inland terrain, contributed to slightly higher inland values of $\sigma\theta$.

Figure 13(a) summarizes the site $\sigma\theta$ results for various time averages as they relate to terrain characteristics. Coastal sites 300 and 301 showed relatively constant $\sigma\theta$ values with height while $\sigma\theta$ decreased with increasing height at the other sites. The change in $\sigma\theta$ with time averaging was least at sites 102 and 300 and most at the 12' sensor levels of sites 102 and 301. Coastal site 200 showed $\sigma\theta$ values higher than both sites 300 and 301 at the 12, 54, and 102' levels.

Figure 13(b) describes $\sigma\theta$ dependence on wind direction throughout the terrain. The figure shows that the lowest $\sigma\theta$

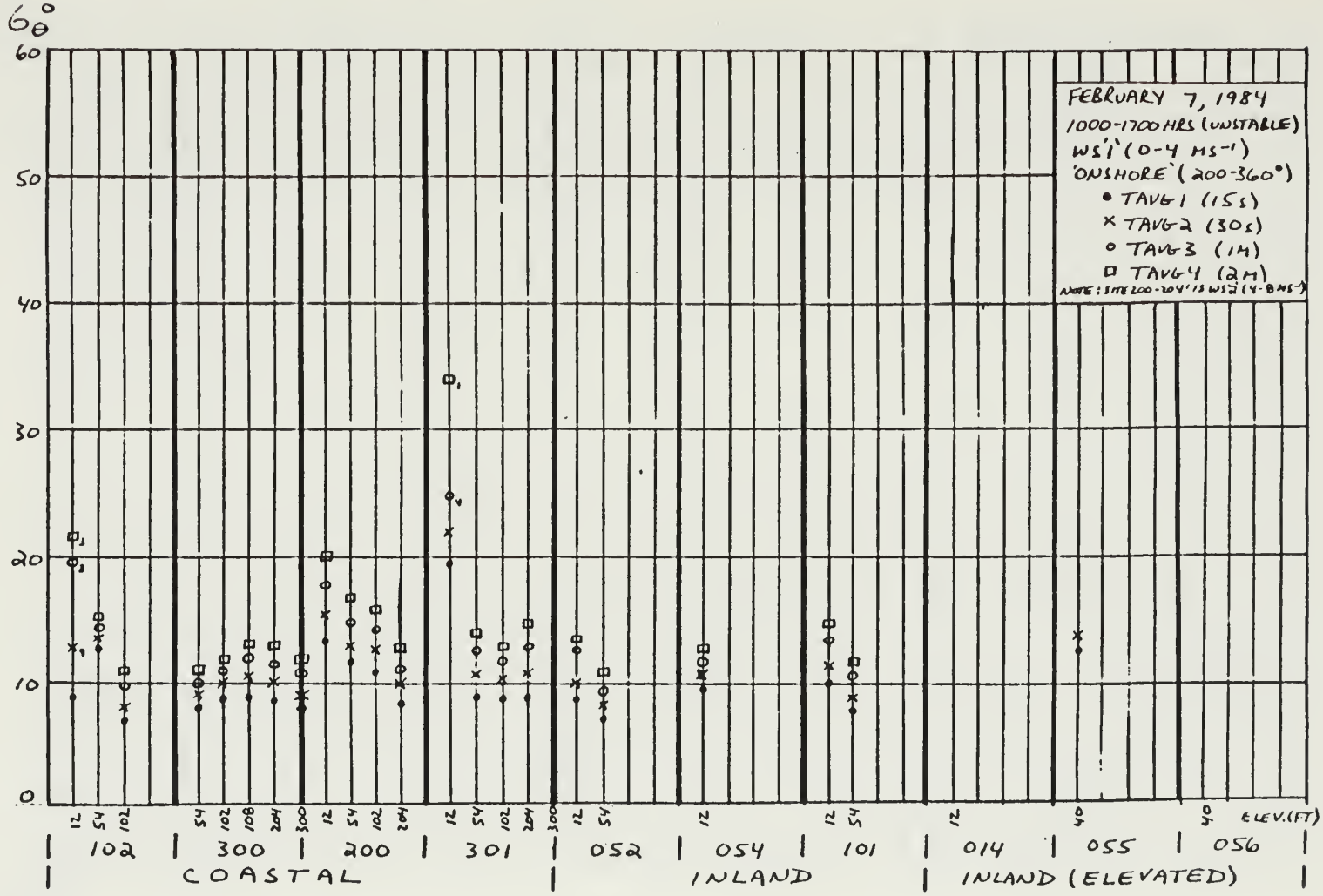

Figure 13(a). σθ vs TAVG (Terrain Analysis) (2/7/84 (1000-1700)--Unstable)

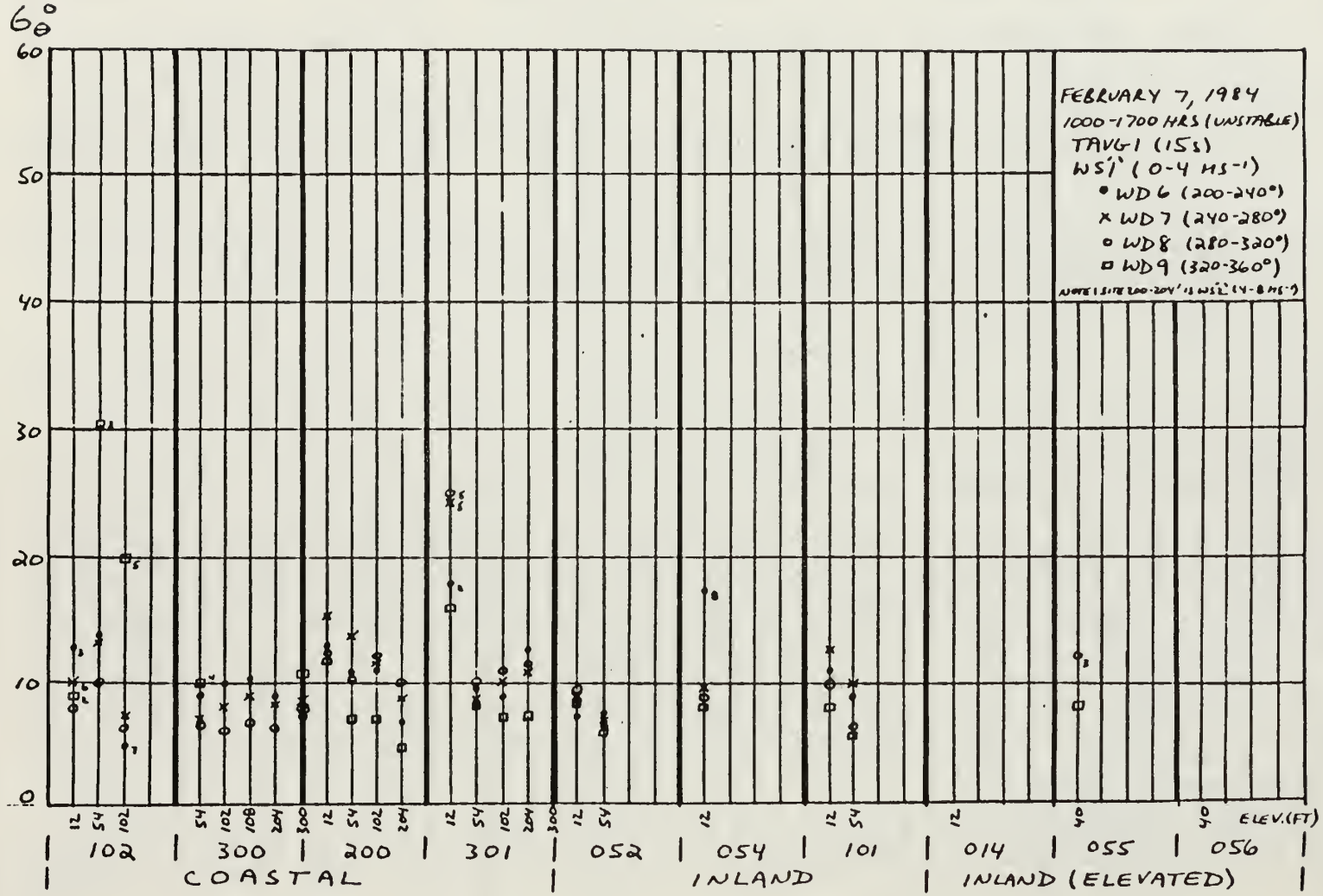

Figure 13(b). σθ vs WD (Terrain Analysis) (2/7/84 (1000-1700)--Unstable)

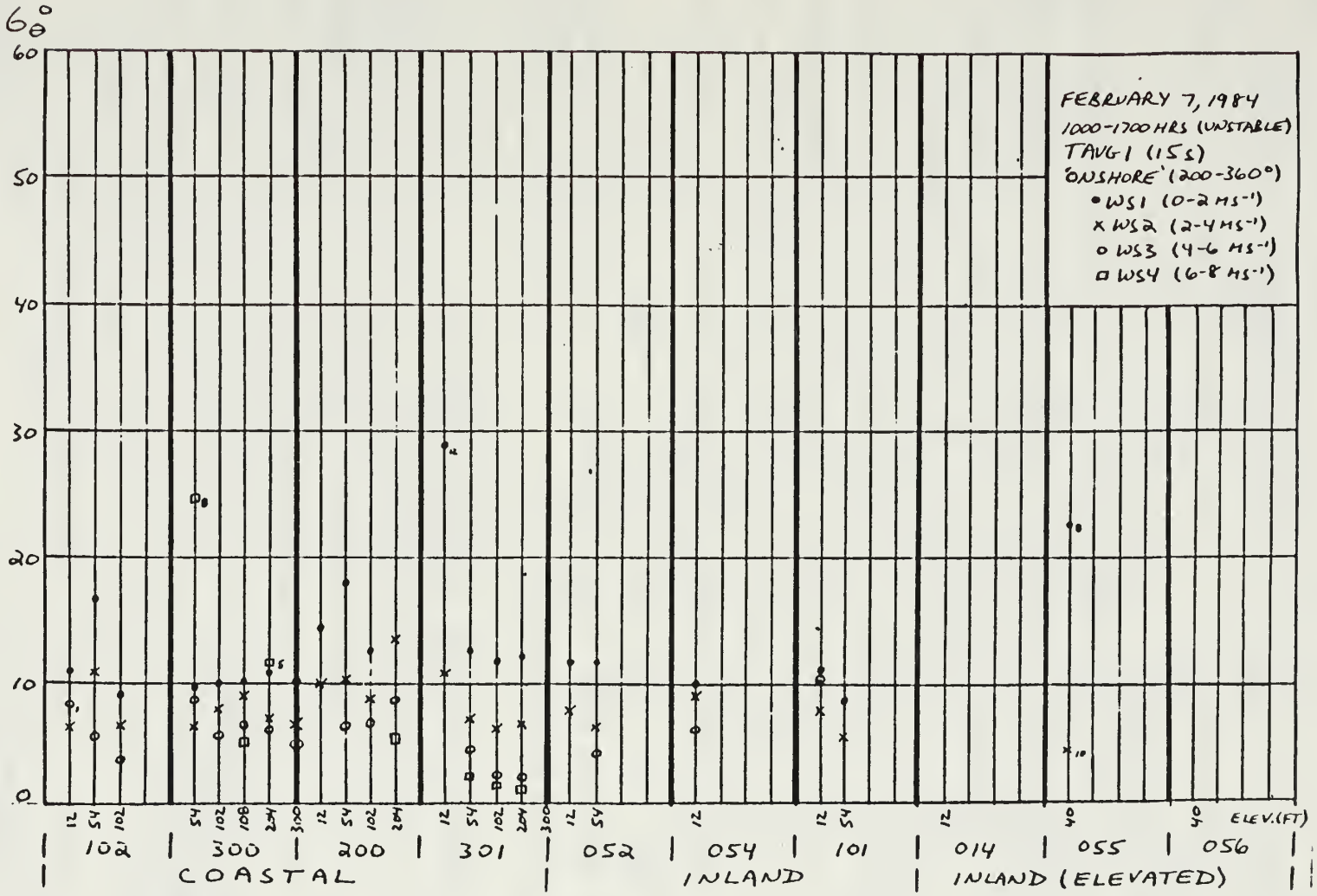

Figure 13(c). $\sigma\theta$ vs WS (Terrain Analysis) (2/7/84 (1000-1700)--Unstable)

values for all sites were related to the more north-northwesterly flow while the highest $\sigma\theta$ values were associated with the more southwesterly flow. Inland sites 052 and 054 showed the least variation in $\sigma\theta$ with wind direction.

Figure 13(c) illustrates site $\sigma\theta$ results for various wind speed categories as they relate to terrain characteristics. In general, the lowest $\sigma\theta$ values were associated with the highest wind speeds across the terrain. The lowest values of $\sigma\theta$ occurred with wind speeds of 6-8 ms^{-1} at the 54, 102, and 204' sensor levels of site 301. The highest values of $\sigma\theta$ (with a data count greater than 10) were evident at the 54' level of site 102 and at the 12, 54, and 102' levels of site 200. The least variation of $\sigma\theta$ with wind speed was found at sites 054, 101, and 300 while the greatest variation occurred at sites 200 and 301.

C. STABLE CASE STUDY (2/2/84, 0200-0800)

1. Synoptic Situation/Mean Flow

The Vandenberg weather in this case study was dominated by a 1032 mb high pressure center located over southern Idaho and a thermal trough along the California coast. Figure 14 shows no significant pressure gradient forcing over the central California coast with the 500 mb jet well north of the area (over western Canada). There was no precipitation in the Vandenberg area.

Max Temp: 50 °F Min Temp: 37 °F

AVG VBG Wind Direction (all sensors): Offshore (040-160°)

AVG VBG Wind Speed (all sensors): 0-8 ms^{-1}

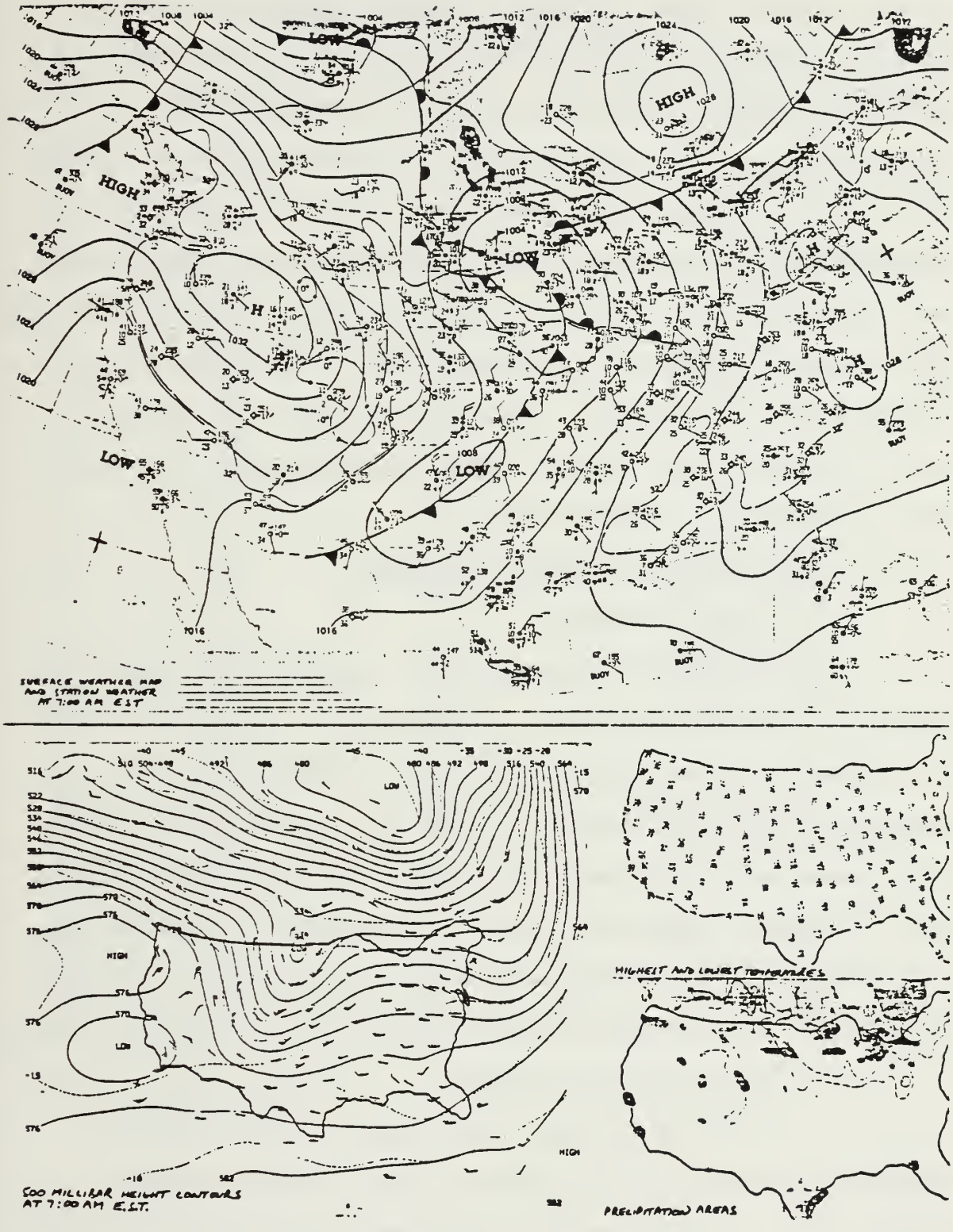

Figure 14. VBG Synoptic Situation (2/2/84--Stable)

Figure 15 illustrates the mean flow which occurred at the various sites and sensors in the Vandenberg area. Easterly, offshore flow was predominant along the coast due to land breeze/drainage flow effects. Downslope flow was apparent inland with southeasterly winds occurring at sites 055 and 101 and southerly breezes at site 014. Site 200 indicated possible channeling in accordance with the persistent easterly flow. The wind directions were generally uniform with height and higher wind speeds were in evidence at the higher sensor elevations. Tables XV and XVI list the mean flow wind directions and wind speeds according to site and sensor elevations, respectively.

2. $\sigma\theta$ Dependence on Time Averaging

a. General Results

Table XVII summarizes $\sigma\theta$ dependence on time averaging for time averages ranging from 15 s to 5 min. The $\sigma\theta$ values at all sensors at all sites increased as time averaging increased except at sites 052 and 301 where there was a decrease in the value of $\sigma\theta$ between the 1 and 2 minute time averages. Table XVIII shows the average $\sigma\theta$ values for all sensors for the designated time averaging values and the corresponding increase in their respective standard deviations.

b. Power Law Relationship

As stated before, the power law relationship examines the ratio of $\sigma\theta$ values at two averaging times. Figure 16(a) illustrates the relationship between the average

TABLE XV

VBG Mean Flow--By Site
(2/2/84 (0200-0800)--Stable)

Site	Level (Ft)	Sensor No.	Predominant Flow (WD/WS)
009	12	1	----------
014	12	2	160-200/2-4
055	40	13	120-160/4-6
056	40	14	----------
052	12	3	080-120/2-4
052	54	11	040-080/4-6
054	12	4	080-120/2-4
054	54	12	080-120/2-4
101	12	5	120-160/2-4
101	54	15	----------
103	12	7	----------
103	54	17	----------
102	12	6	080-120/2-4
102	54	16	040-080/2-4
102	102	21	----------
200	12	8	080-120/0-2
200	54	18	080-120/2-4
200	102	22	080-120/2-4
200	204	26	080-120/4-6
300	12	9	----------
300	54	19	080-120/2-4
300	102	23	080-120/2-4
299	108	24	080-120/4-6
300	204	27	080-120/4-6
300	300	29	080-120/4-6
301	12	10	080-120/2-4
301	54	20	120-160/4-6
301	102	25	120-160/4-6
301	204	28	120-160/4-6
301	300	30	----------

Note: WD (degrees)
WS (ms^{-1})

TABLE XVI

VBG Mean Flow--By Height
(2/2/84 (0200-0800)--Stable)

Level (Ft)	Sensor No.	Site	Predominant Flow (WD/WS)
12	1	009	----------
12	2	014	160-200/2-4
12	3	052	080-120/2-4
12	4	054	080-120/2-4
12	5	101	120-160/2-4
12	6	102	080-120/2-4
12	7	103	----------
12	8	200	080-120/0-2
12	9	300	----------
12	10	301	080-120/2-4
40	13	055	120-160/4-6
40	14	056	----------
54	11	052	040-080/4-6
54	12	054	080-120/2-4
54	15	101	----------
54	16	102	040-080/2-4
54	17	103	----------
54	18	200	080-120/2-4
54	19	300	080-120/2-4
54	20	301	120-160/4-6
102	21	102	----------
102	22	200	080-120/2-4
102	23	300	080-120/2-4
102	25	301	120-160/4-6
108	24	299	080-120/4-6
204	26	200	080-120/4-6
204	27	300	080-120/4-6
204	28	301	120-160/4-6
300	29	300	080-120/4-6
300	30	301	----------

Note: WD (degrees)
WS (ms^{-1})

TABLE XVII

σθ Dependence on Time Averaging
(2/2/84 (0200-0800)--Stable)

		TIME AVERAGING				
Sensor	Site-Ht	15 sec	30 sec	1 min	2 min	5 min
2	014-12'	9.1	11.9	14.6	17.0	19.5
3	052-12'	12.2	12.8	16.9	13.3	13.9
4	052-12'	11.8	15.7	19.5	23.7	27.3
6	102-12'	4.9	5.8	11.5	15.9	----
8	200-12'	5.0	5.7	6.6	7.9	9.4
10	301-12'	5.9	7.5	9.0	7.9	9.9
13	055-40'	6.2	6.6	6.9	7.1	7.5
11	052-54'	6.9	8.1	9.1	10.5	11.2
12	054-54'	5.9	7.9	9.9	12.0	15.7
16	102-54'	5.2	5.1	5.3	5.8	6.9
18	200-54'	4.8	5.5	6.5	7.7	9.4
19	300-54'	4.5	5.0	5.4	5.9	7.3
20	301-54'	10.7	11.6	12.0	12.3	12.5
22	200-102'	5.5	6.3	7.2	8.1	9.2
23	300-102'	13.1	13.2	13.3	13.5	13.9
25	301-102'	6.3	7.0	7.4	7.6	8.0
24	299-108'	5.4	6.1	6.6	7.1	9.2
26	200-204'	5.9	7.0	8.3	9.5	11.0
27	300-204'	9.1	10.8	11.6	12.4	13.0
28	301-204'	4.2	4.5	4.7	4.9	5.2
29	300-300'	5.7	6.0	6.5	7.0	7.7

Note: Most representative values listed above (σθ in degrees)
Wind Direction Offshore (040-160 degrees)
Wind Speed 0-4 ms^{-1} (Sensors 2,3,4,6,8,10,12,16,18, 19,22,23,29)
Wind Speed 4-8 ms^{-1} (Sensors 13,11,20,25,24,26,27,28)

TAVG = 15 sec: Mean σθ(DEG) = 7.1 Standard deviation (DEG) = 2.7

TAVG = 30 sec: Mean σθ(DEG) = 8.1 Standard deviation (DEG) = 3.1

TAVG = 1 min: Mean σθ(DEG) = 9.5 Standard deviation (DEG) = 3.9

TAVG = 2 min: Mean σθ(DEG) = 10.3 Standard deviation (DEG) = 4.5

TAVG = 5 min: Mean σθ(DEG) = 11.4 Standard deviation (DEG) = 4.9

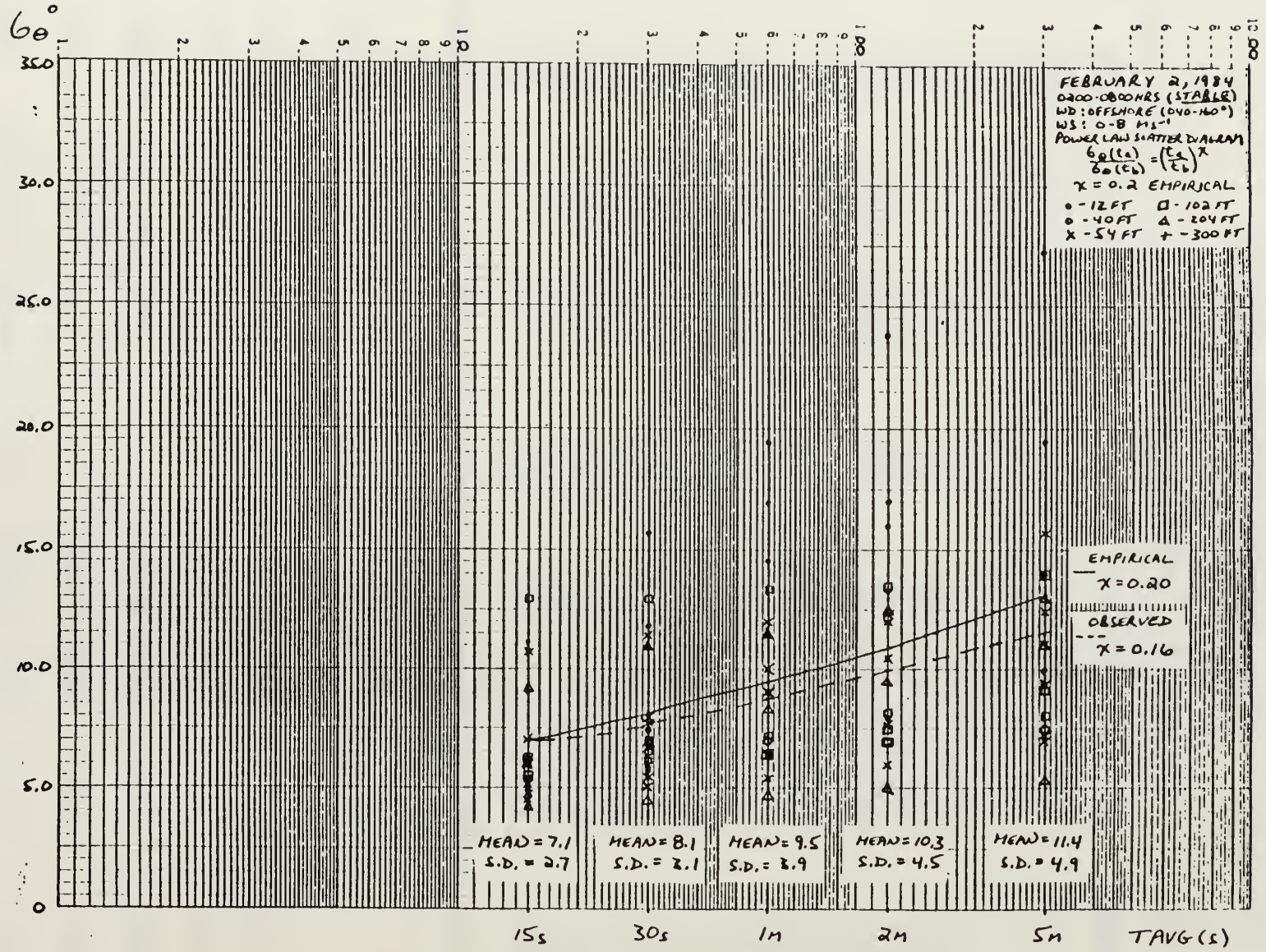

Figure 16(a). Power Law Relationship (All Sensors) (2/2/84 (0200-0800)--Stable)

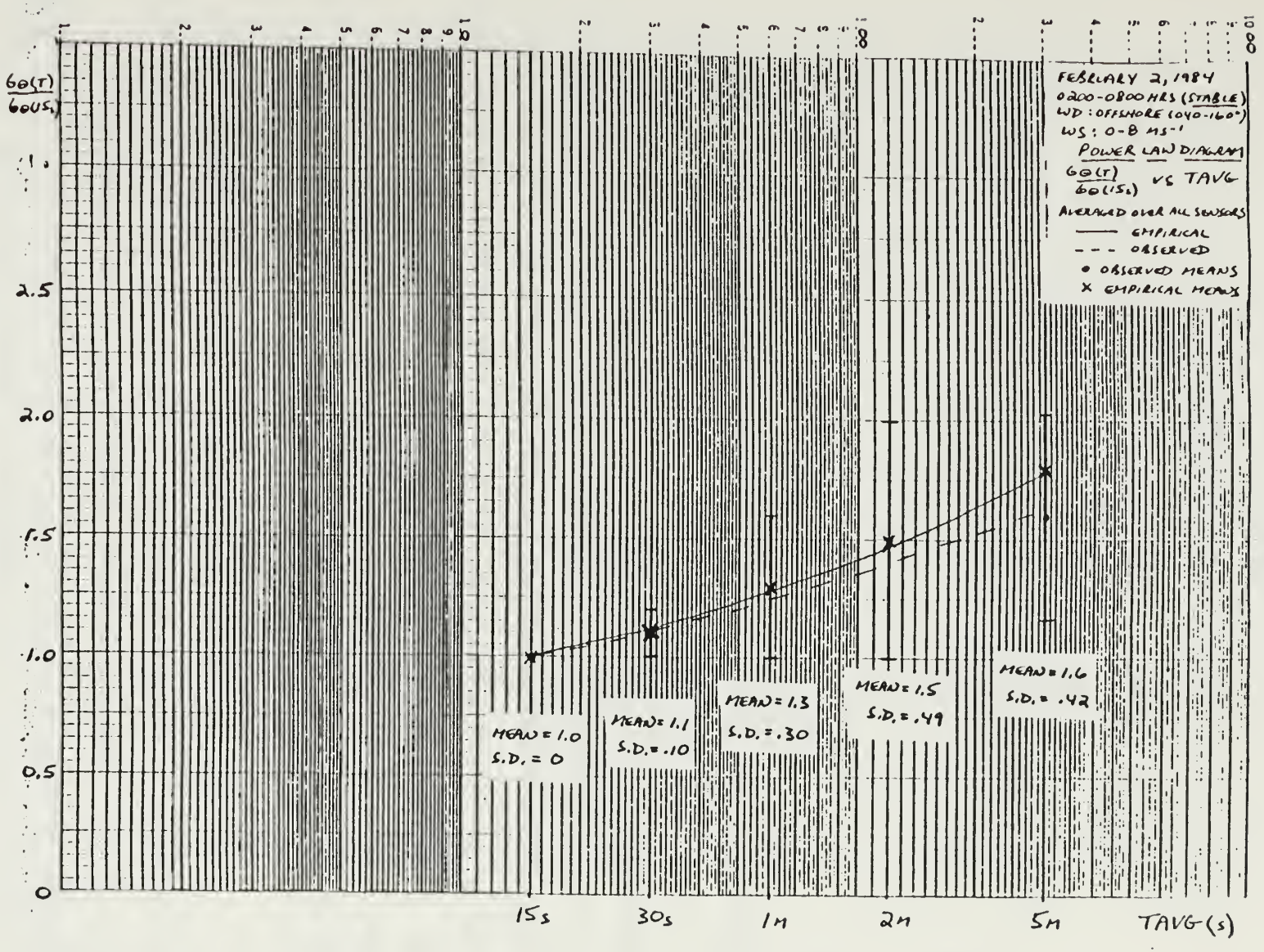

Figure 16(b). Power Law Ratio (All Sensors) (2/2/84 (0200-0800)--Stable)

TABLE XVIII

σθ vs TAVG (All Sensors)
(2/2/84 (0200-0800)--Stable)

TAVG	σθ (Deg)	S.D. (Deg)
15 s	7.1	2.7
30 s	8.1	3.1
1 m	9.5	3.9
2 m	10.3	4.5
5 m	11.4	4.9

observed power law value of x (x = 0.16) and the empirical x value (x = 0.20). In general, most of the sensors had x values between 0.07 and 0.22. This figure also shows the scatter of individual sensor σθ data at each time average and identifies the mean of the observed σθ values and its associated standard deviation for each time average. The difference between these two profiles gradually increased with increasing time averaging values (lower frequencies). The ratio (σθ (T)/σθ (15 s)) vs TAVG is shown in Figure 16(b).

c. Height Dependence

A summary of σθ dependence on time averaging as a function of sensor elevation is shown in Table XIX/Figure 17.

Table XIX shows a decrease in σθ values from sensor elevations 12 to 54', a slight increase in σθ values from 54 to 102', and a decrease in these values from 102 to 204' over all time averages. The difference in σθ from 15 s

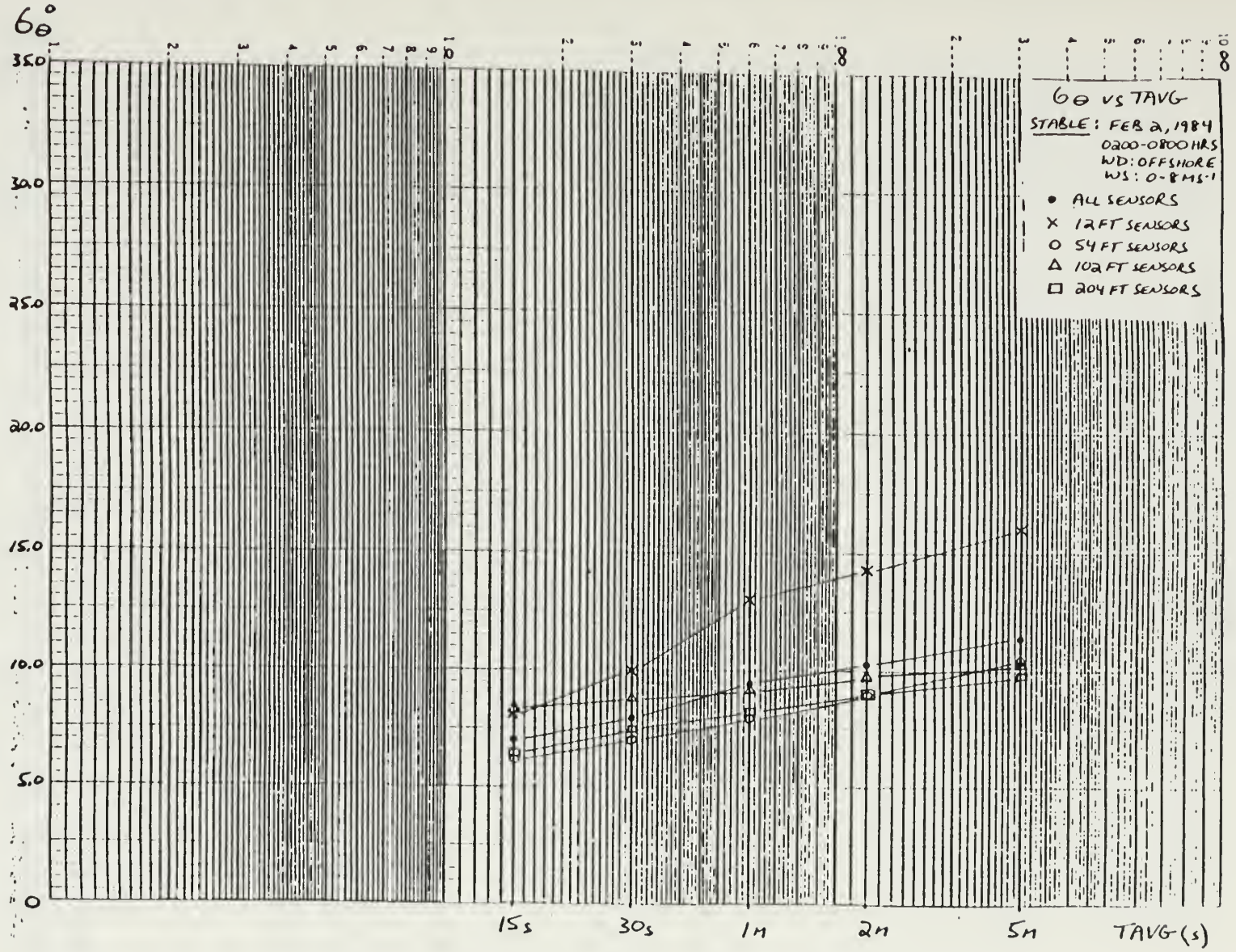

Figure 17. σθ vs TAVG (All Sites) (2/2/84 (0200-0800)--Stable)

TABLE XIX

$\sigma\theta$ vs TAVG (All Sites)
(2/2/84 (0200-0800)--Stable)

	Sensor Elevation (FT)			
TAVG	12	54	102	204
15 s	8.2	6.3	8.3	6.4
30 s	9.9	7.2	8.8	7.4
1 m	13.0	8.0	9.3	8.2
2 m	14.3	9.0	9.7	8.9
5 m	16.0	10.5	10.4	9.7

to 5 m time averaging decreased from the 12' levels to the 102' levels and then essentially remained constant from the 102 to the 204' levels.

d. Site/Sensor Elevation Dependence

Figures 18(a-h)/Tables C-(1-8) describe site specific $\sigma\theta$ dependence on time averaging for various sensor elevations. A terrain analysis later in this section will collectively examine $\sigma\theta$ differences between sites and $\sigma\theta$ dependence on time averaging relative to each site.

3. $\sigma\theta$ Dependence on Wind Direction

a. General Results

The predominant wind direction associated with most of the sensors in this stable offshore land breeze/ drainage flow regime was 080-120°. Exceptions to this included site 052 and 102 at 54' (winds from 120-160°), and

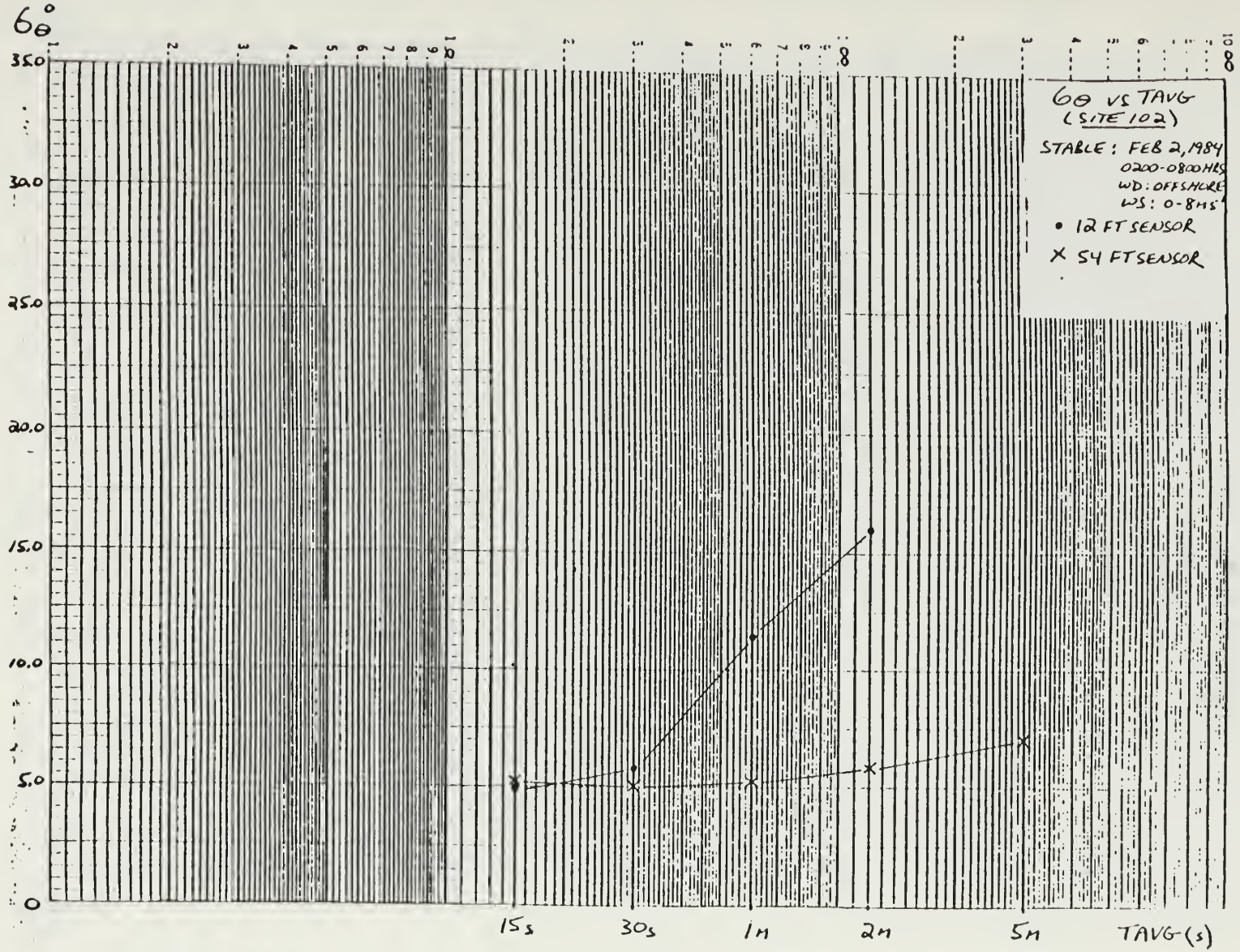

Figure 18(a). σθ vs TAVG (Site 102) (2/2/84 (0200-0800)--Stable)

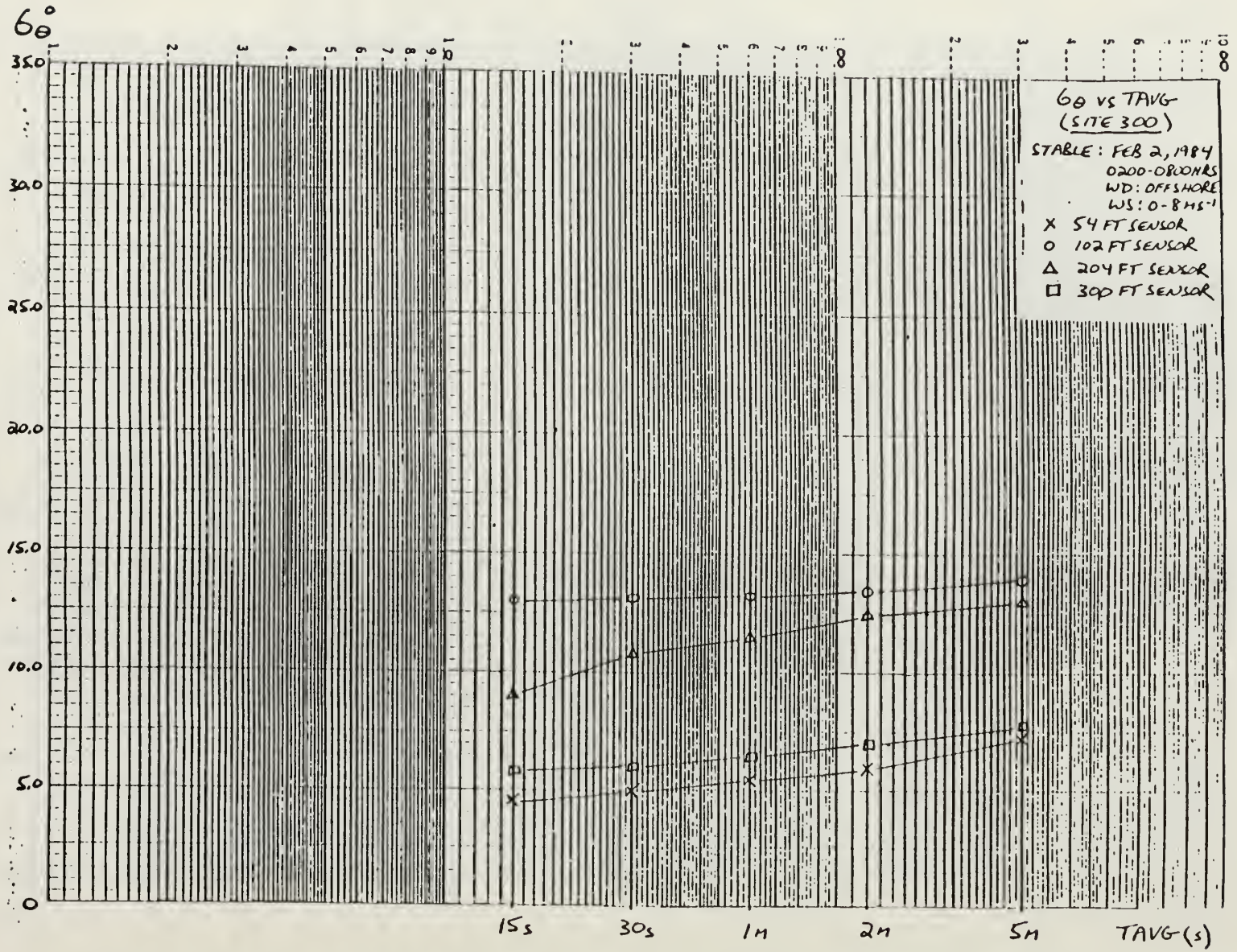

Figure 18(b). σθ vs TAVG (Site 300) (2/2/84 (0200-0800)--Stable)

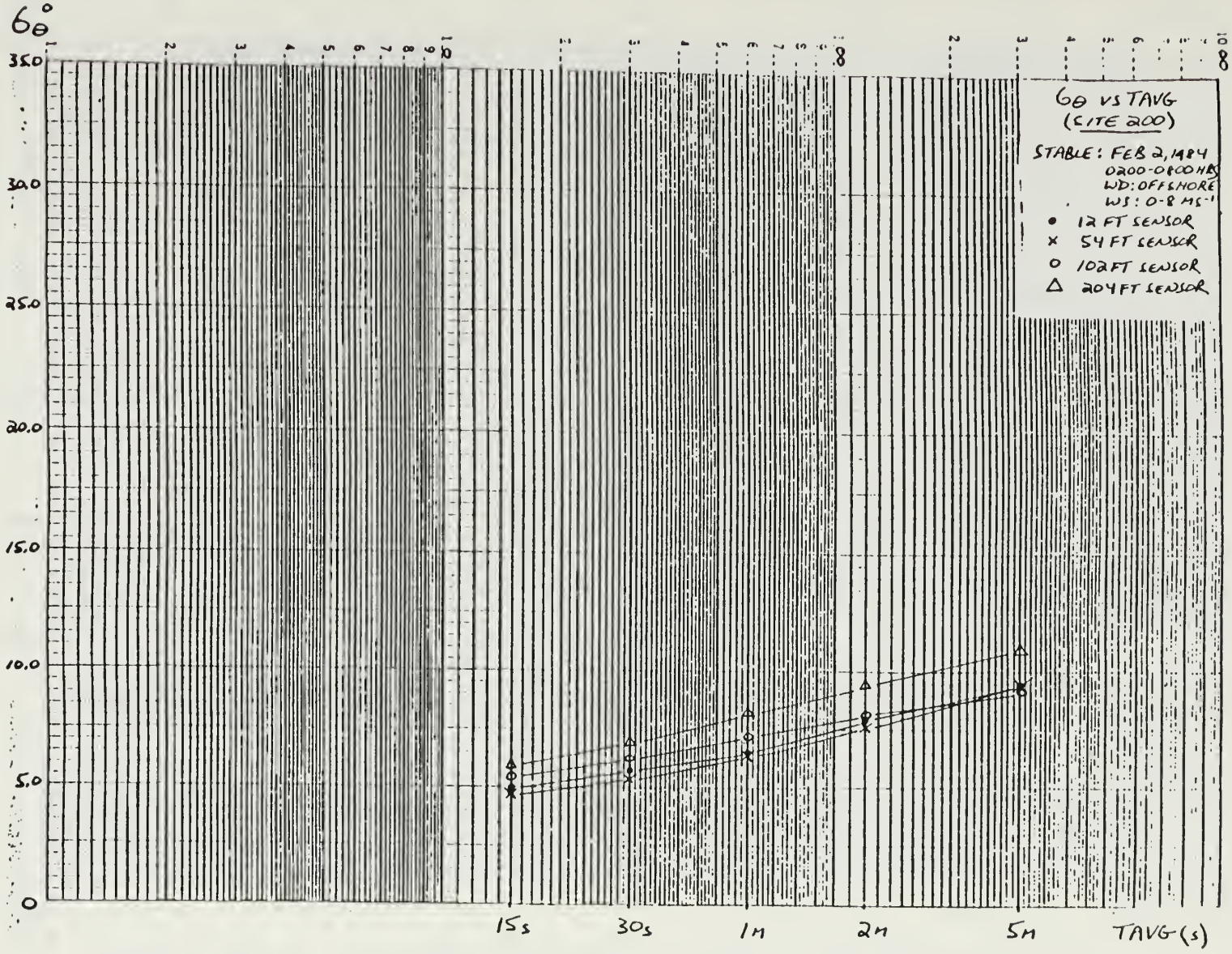

Figure 18(c). σθ vs TAVG (Site 200) (2/2/84 (0200-0800)--Stable)

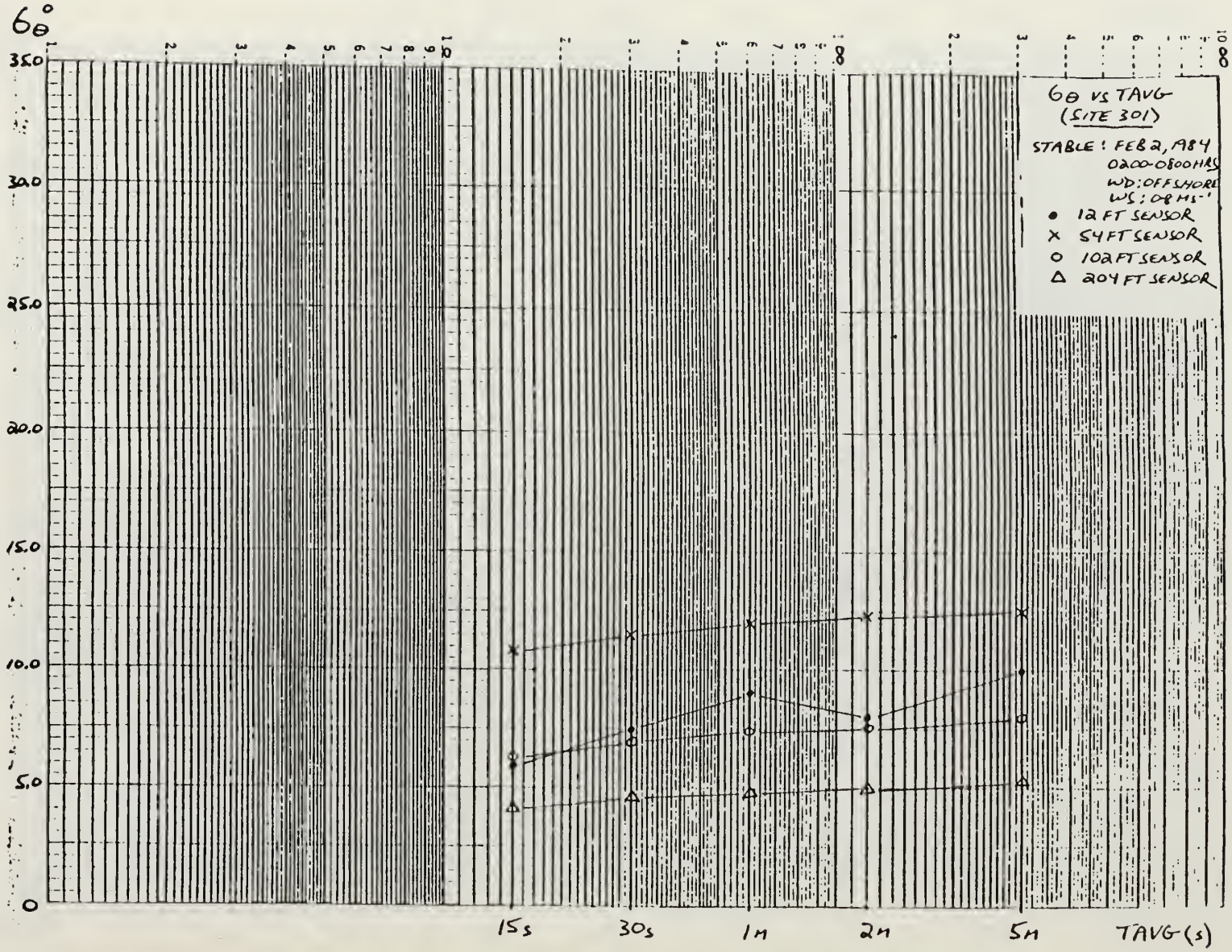

Figure 18(d). σθ vs TAVG (Site 301) (2/2/84 (0200-0800)--Stable)

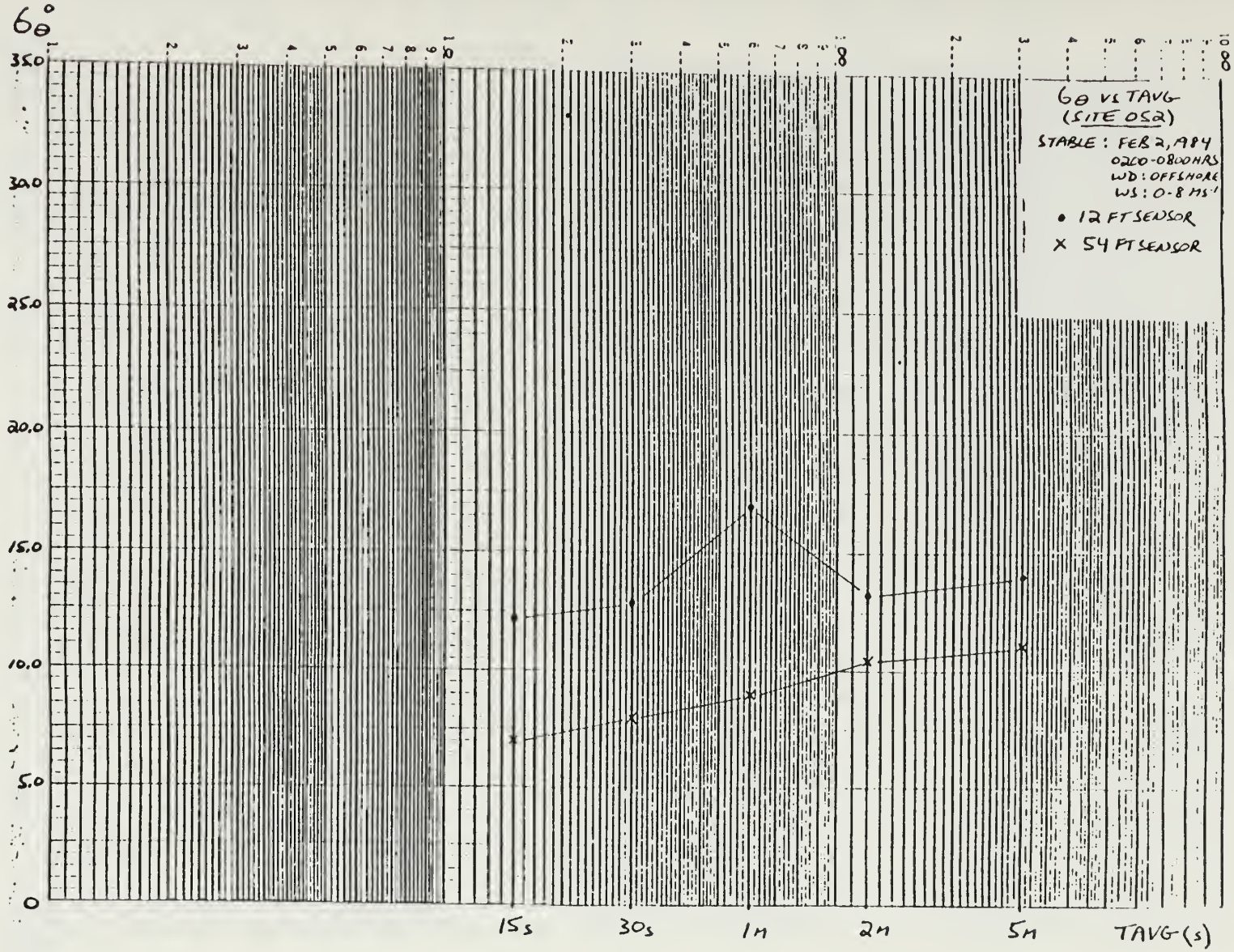

Figure 18(e). σθ vs TAVG (Site 052) (2/2/84 (0200-0800)--Stable)

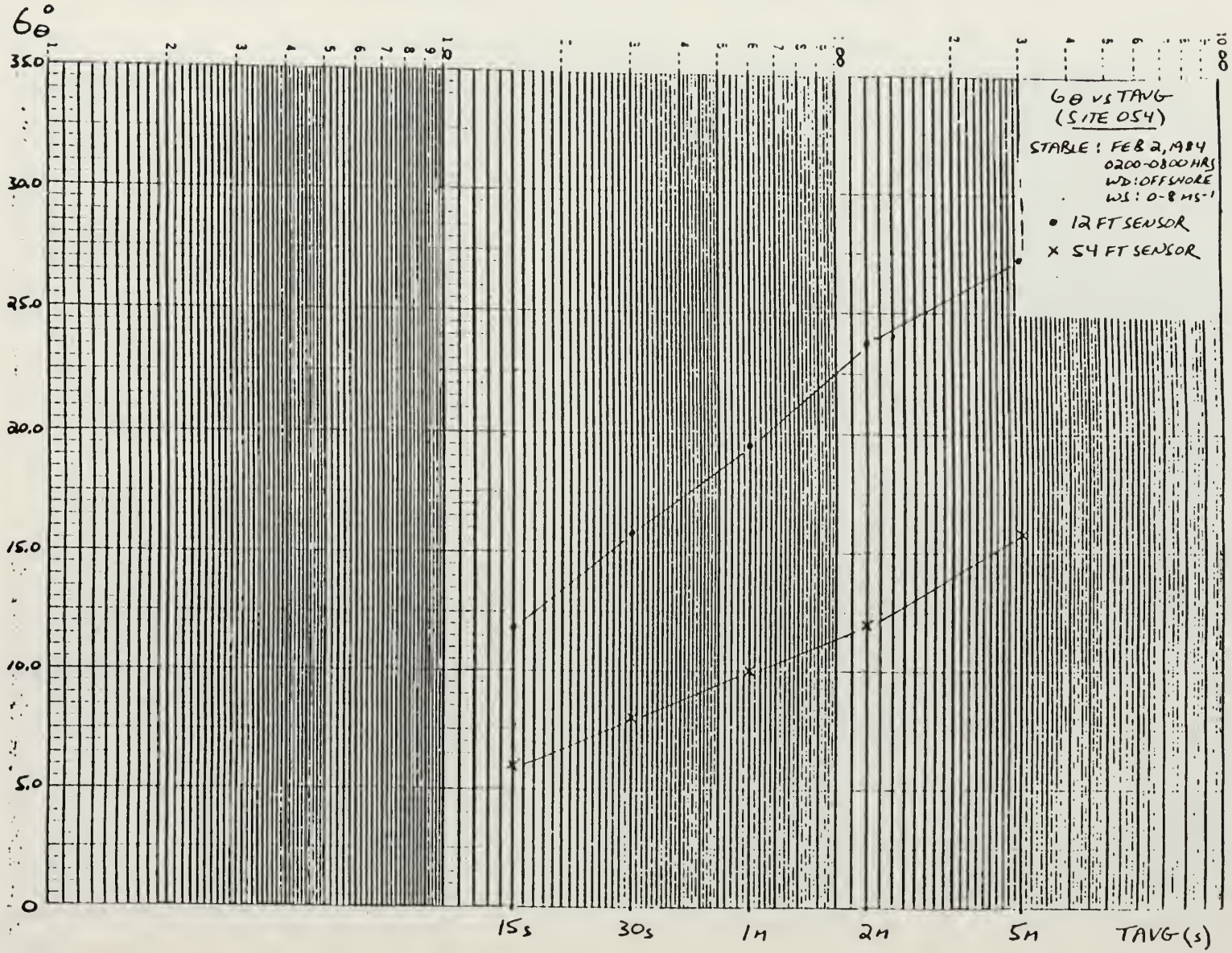

Figure 18(f). σθ vs TAVG (Site 054) (2/2/84 (0200-0800)--Stable)

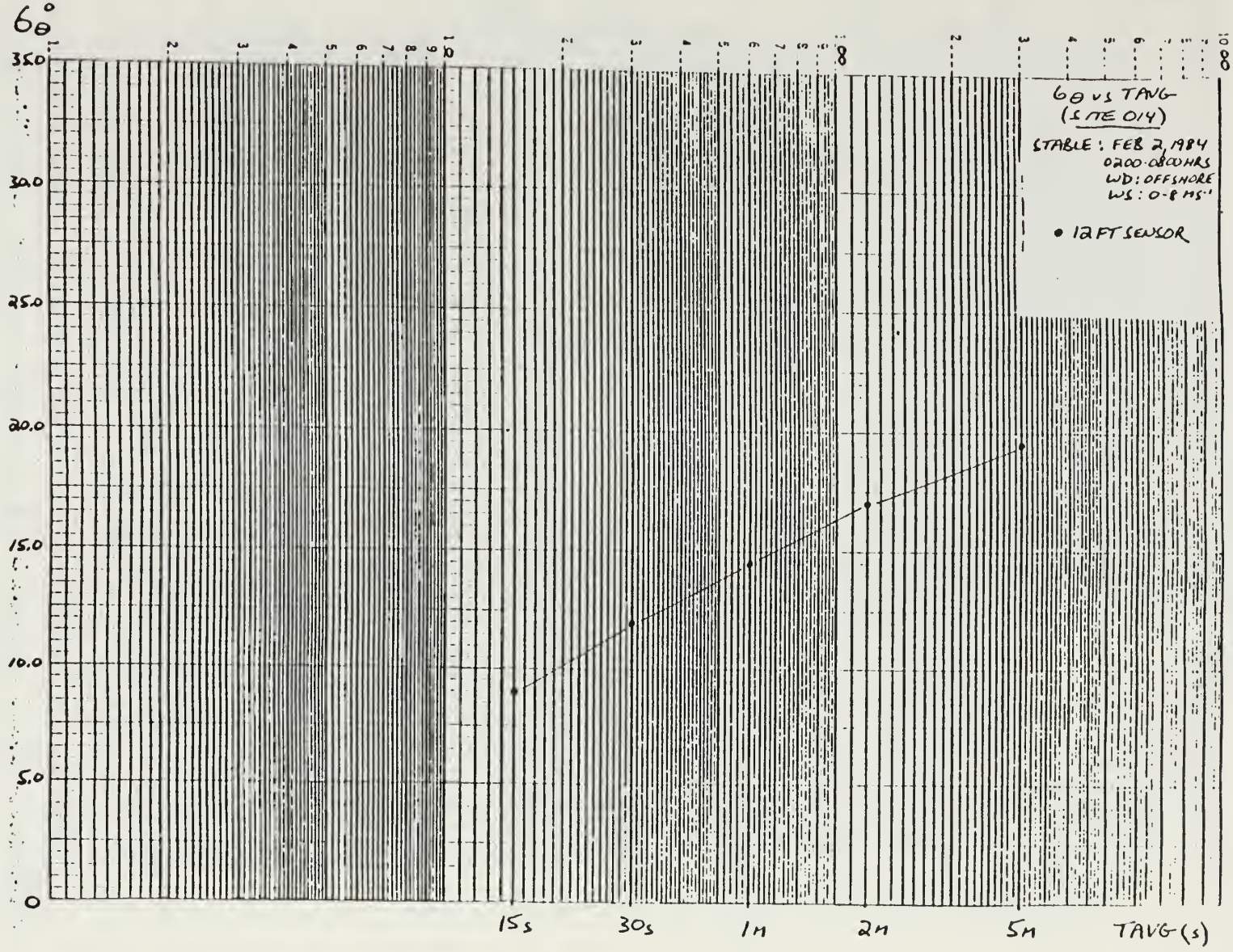

Figure 18(g). σθ vs TAVG (Site 014) (2/2/84 (0200-0800)--Stable)

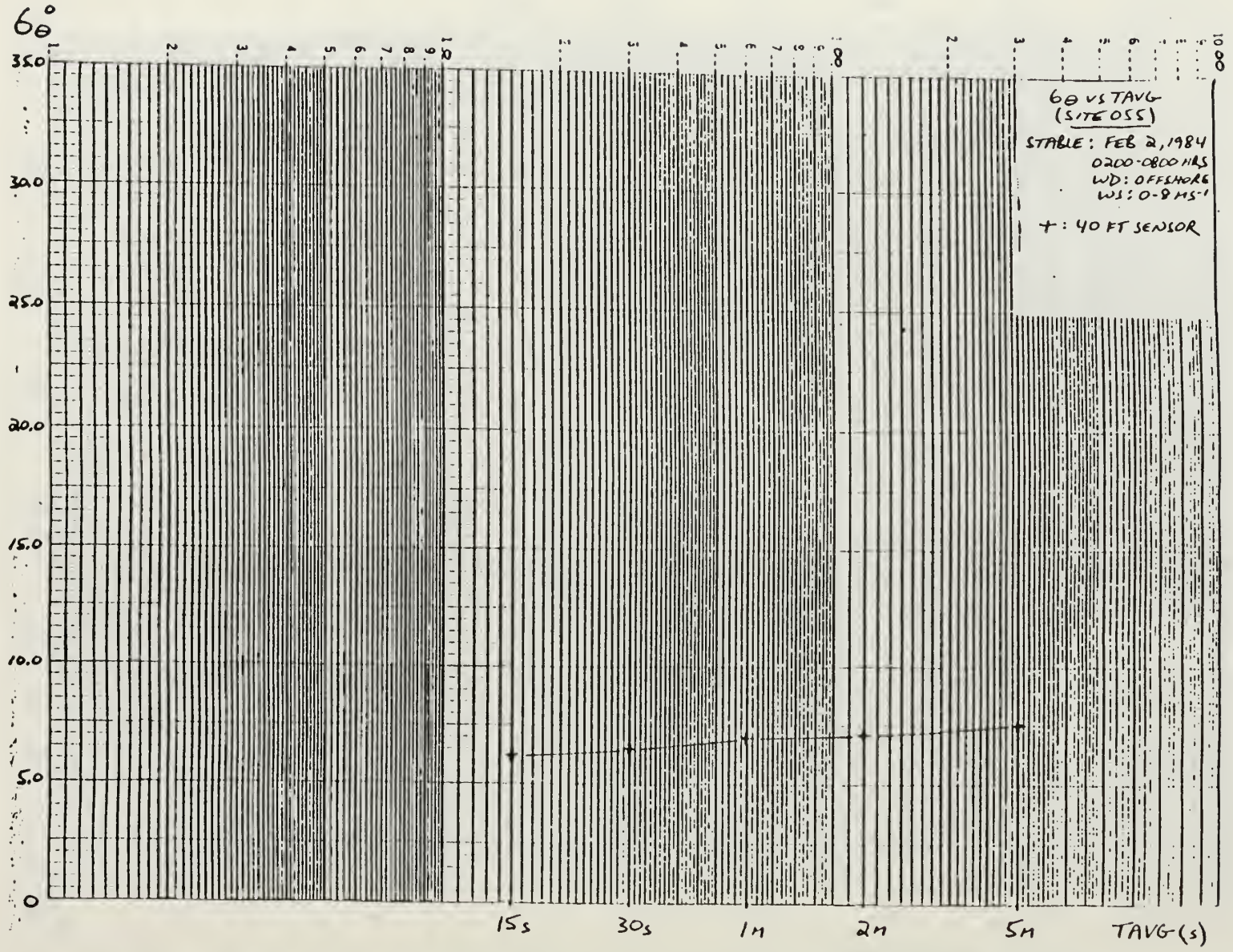

Figure 18(h). σθ vs TAVG (Site 055)--(2/2/84 (0200-0800)--Stable)

site 014-12' (winds from 160-200°). The lowest $\sigma\theta$ values appeared to be related with winds blowing from 080-120°, with higher $\sigma\theta$ values associated with winds blowing from 120-200°. The inland sites seemed to encounter the greatest $\sigma\theta$ variation with wind direction and the $\sigma\theta$ values appeared to vary with sensor height at all sites except site 200. Table XX describes $\sigma\theta$ dependence on wind direction at all sensors and indicates from which direction the predominant wind is blowing.

b. Site/Sensor Elevation Dependence

Figures 19(a-h)/Tables C-(9-16) show $\sigma\theta$ dependence on wind direction for various sensor elevations at specific sites (* = Predominant Wind Direction). A terrain analysis later in this section will collectively examine $\sigma\theta$ differences between sites and $\sigma\theta$ dependences on wind direction relative to each site.

4. $\sigma\theta$ Dependence on Wind Speed

a. General Results

The predominant wind speed for all sensors was 2-4 ms^{-1} with the exception of sensor 200-12' which had a predominant wind speed of 0-2 ms^{-1} and sensors 055-40', 052-54', 301-54' 102-204', 300-108, 204', and 200-204' which had predominant wind speeds of 4-6 ms^{-1}. In general, $\sigma\theta$ values decreased at the sensors as wind speed increased. Sensors 014-12', 052-54', and 054-54' showed a slight increase in the value of $\sigma\theta$ as wind speed increased and sensor

TABLE XX

$\sigma\theta$ Dependence on Wind Direction
(2/2/84 (0200-0800)--Stable)

		WIND DIRECTION			
Sensor	Site-Ht	2	3	4	5
2	014-12'	----	1.2	9.1	6.0*
3	052-12'	5.0	14.2*	18.0	----
4	054-12'	25.6	9.0*	29.2	71.9
6	102-12'	12.9	4.3*	4.8	----
8	200-12'	6.4	4.8*	5.5	14.0
10	301-12'	----	5.8*	6.3	----
13	055-40'	----	7.5	6.1*	5.7
11	052-54'	3.7*	9.0	23.6	----
12	054-54'	8.3	4.0*	18.0	----
16	102-54'	5.3*	4.6	7.9	16.2
18	200-54'	5.5	4.7*	5.0	----
19	300-54'	3.3	3.6*	6.0	----
20	301-54'	----	7.3	10.9*	8.2
22	200-102'	6.2	5.2*	7.7	----
23	300-102'	12.4	13.2*	13.0	----
25	301-102'	----	5.6	6.7*	----
24	299-108'	3.5	5.7*	5.3	----
26	200-204'	5.9	5.6*	6.2	2.3
27	300-204'	4.7	9.6*	13.8	----
28	301-204'	----	4.3	4.1*	----
29	300-300'	4.6	5.5*	6.9	----

Note: Most representative values listed above ($\sigma\theta$ in degrees)

* = Predominant Wind Direction

Time Averaging 15 seconds

Wind Speed 0-4 ms^{-1} (Sensors 2,3,4,6,8,10,12,16,18, 19,22,23,29)

Wind Speed 4-8 ms^{-1} (Sensors 13,11,20,25,24,26,27,28)

Wind Direction 2: 040-080 degrees

Wind Direction 3: 080-120 degrees

Wind Direction 4: 120-160 degrees

Wind Direction 5: 160-200 degrees

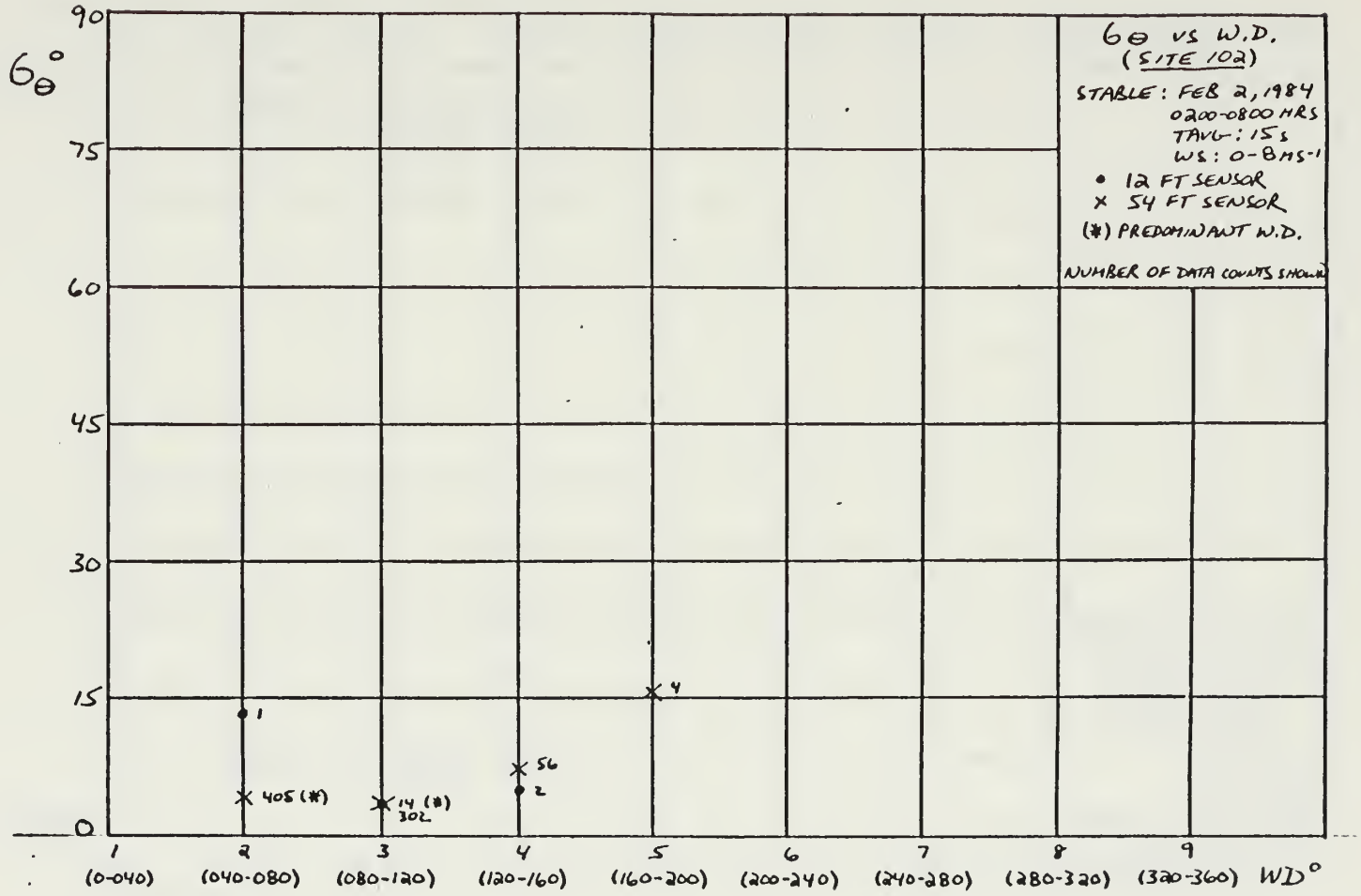

Figure 19(a). σθ vs WD (Site 102) (2/2/84 (0200-0800)--Stable)

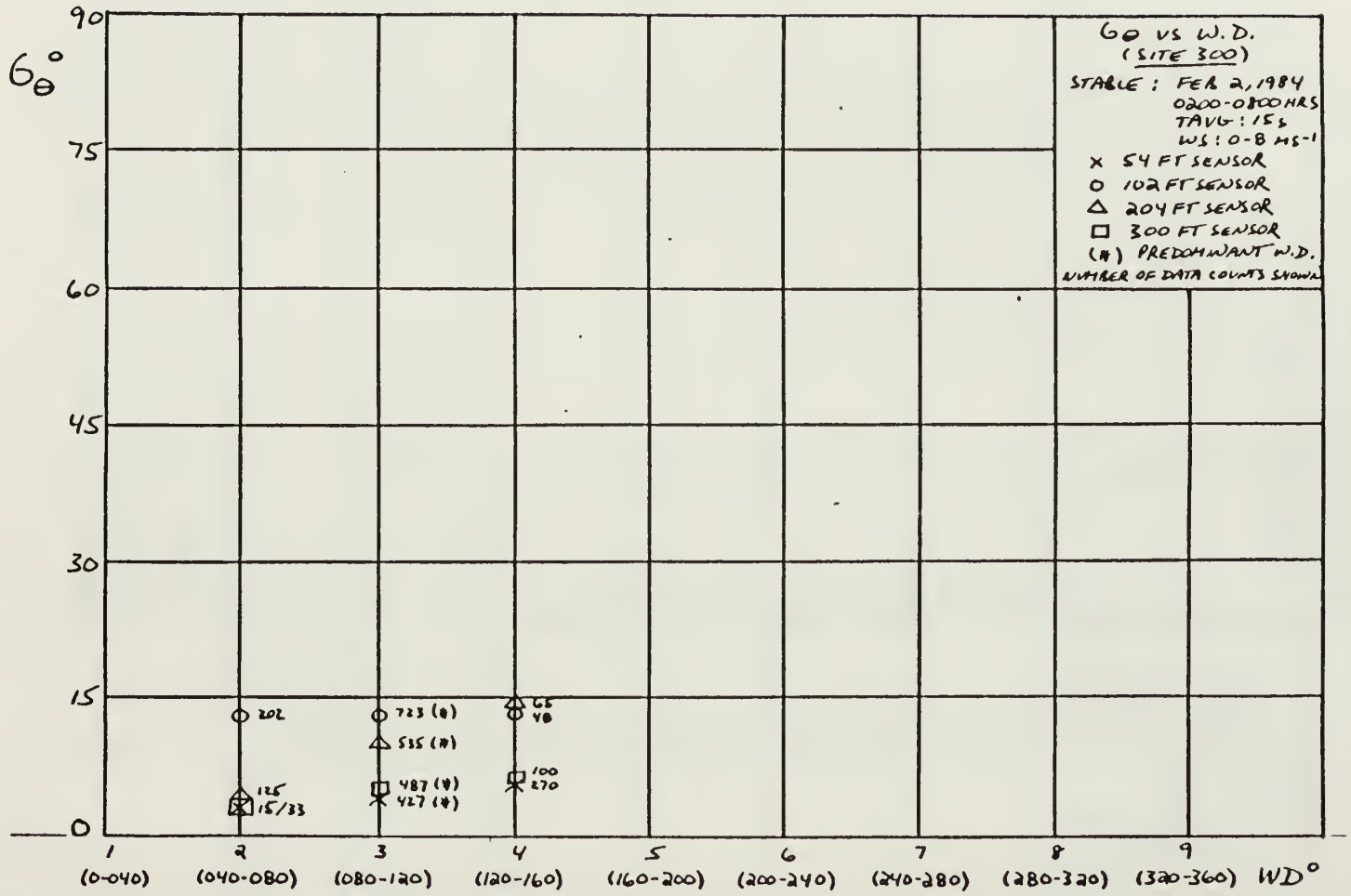

Figure 19(b). σθ vs WD (Site 300) (2/2/84 (0200-0800)--Stable)

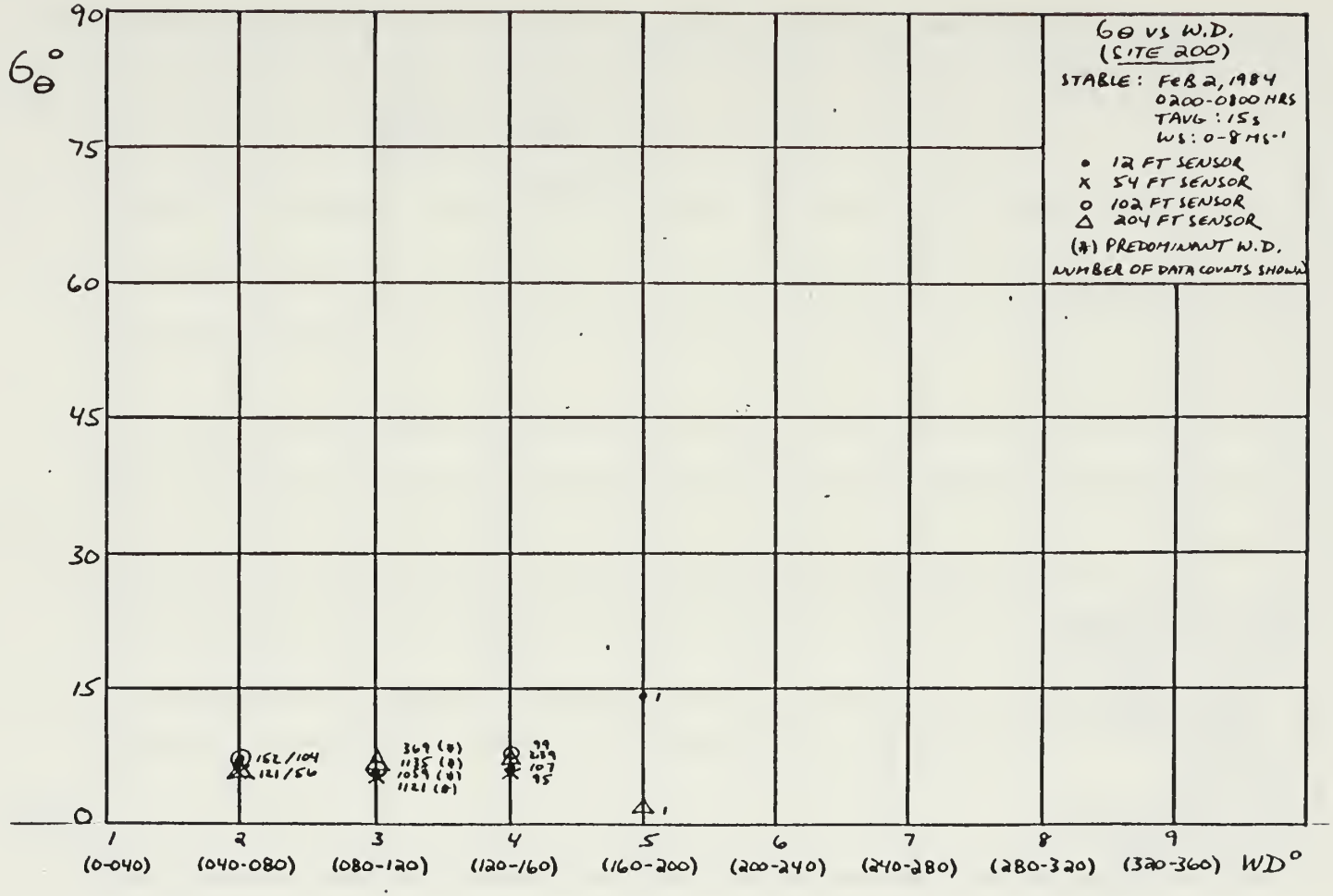

Figure 19(c). $\sigma\theta$ vs WD (Site 200) (2/2/84 (0200-0800)--Stable)

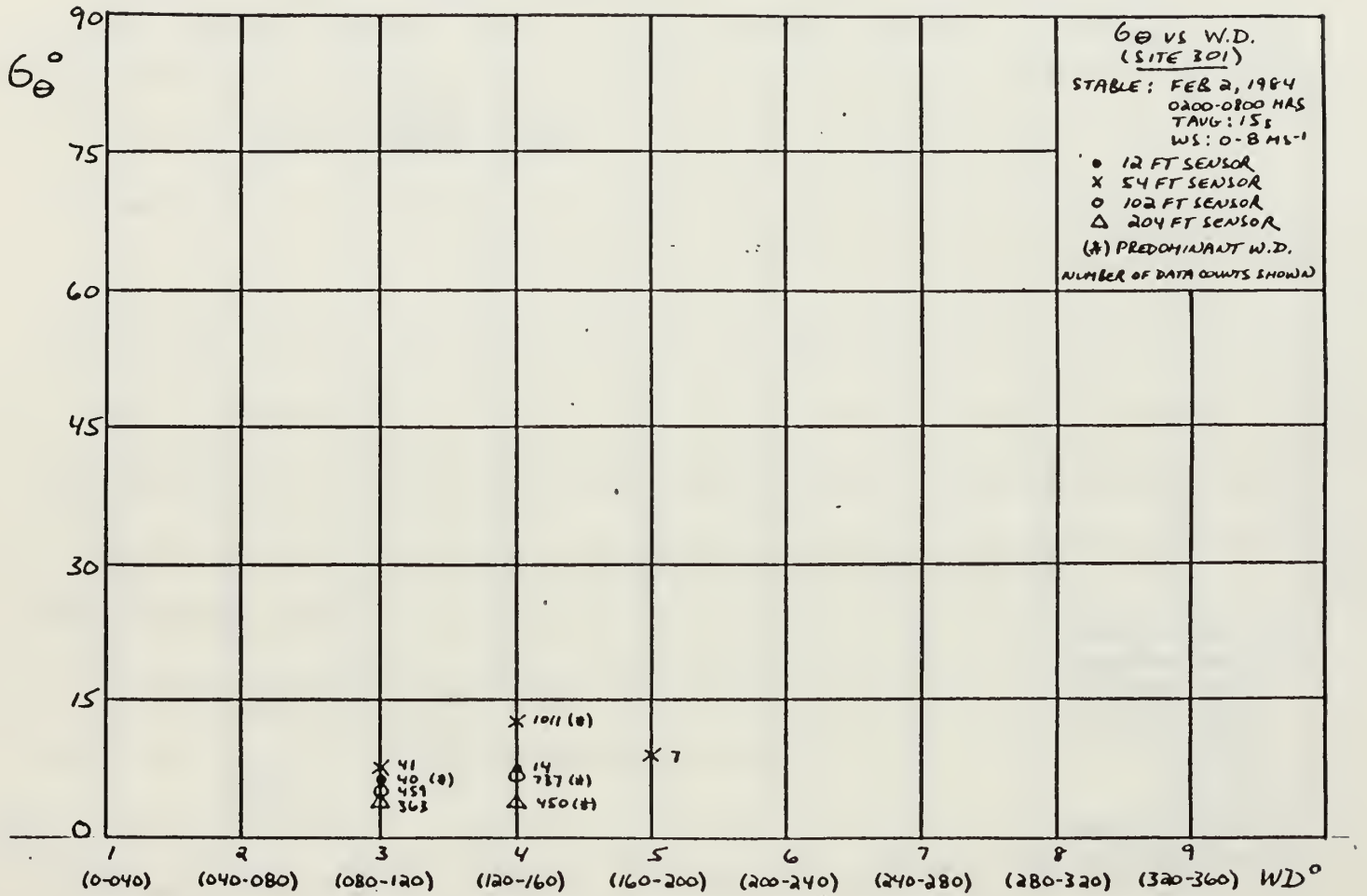

Figure 19(d). $\sigma\theta$ vs WD (Site 301) (2/2/84 (0200-0800)--Stable)

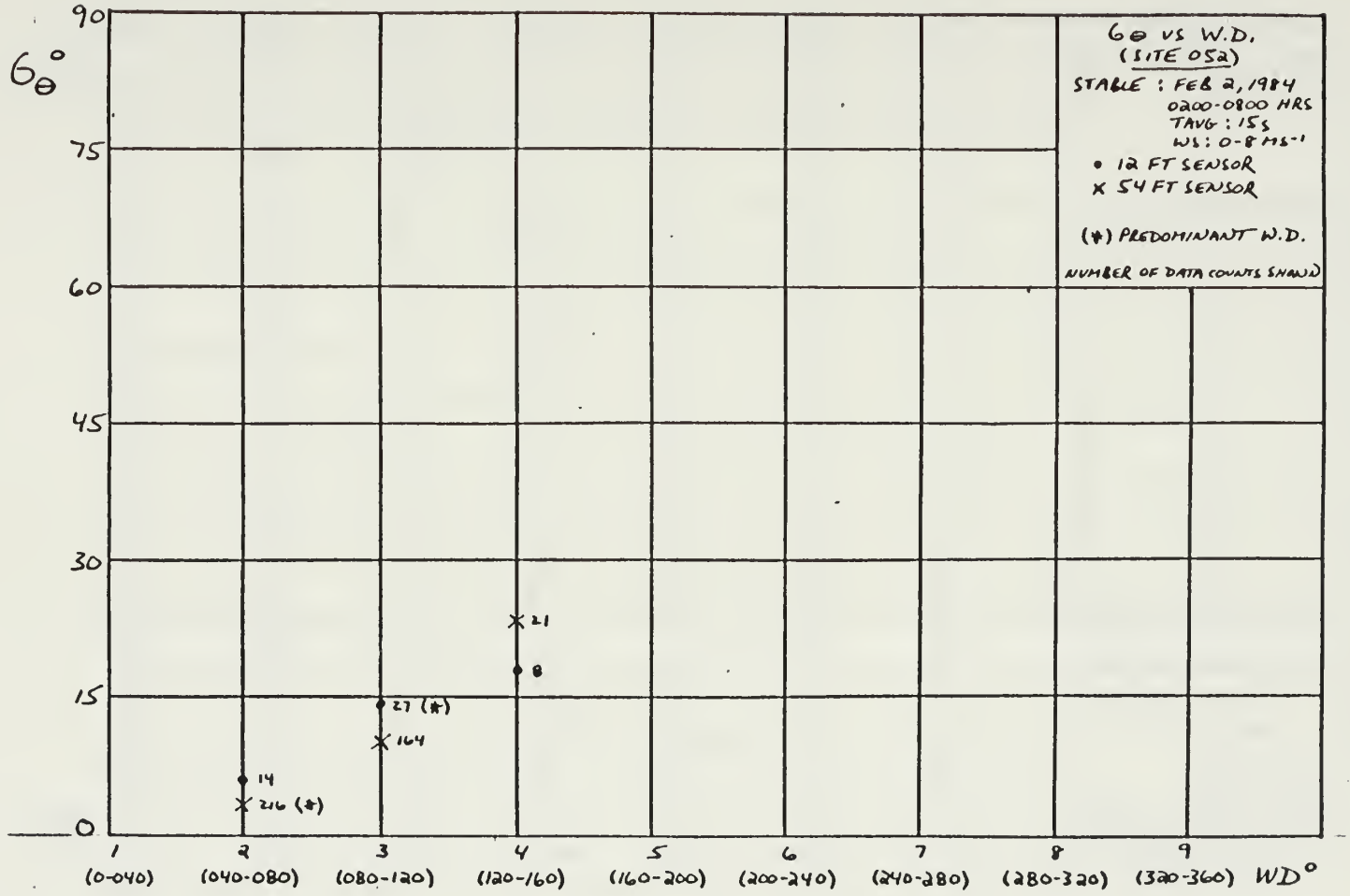

Figure 19(e). $\sigma\theta$ vs WD (Site 052) (2/2/84 (0200-0800)--Stable)

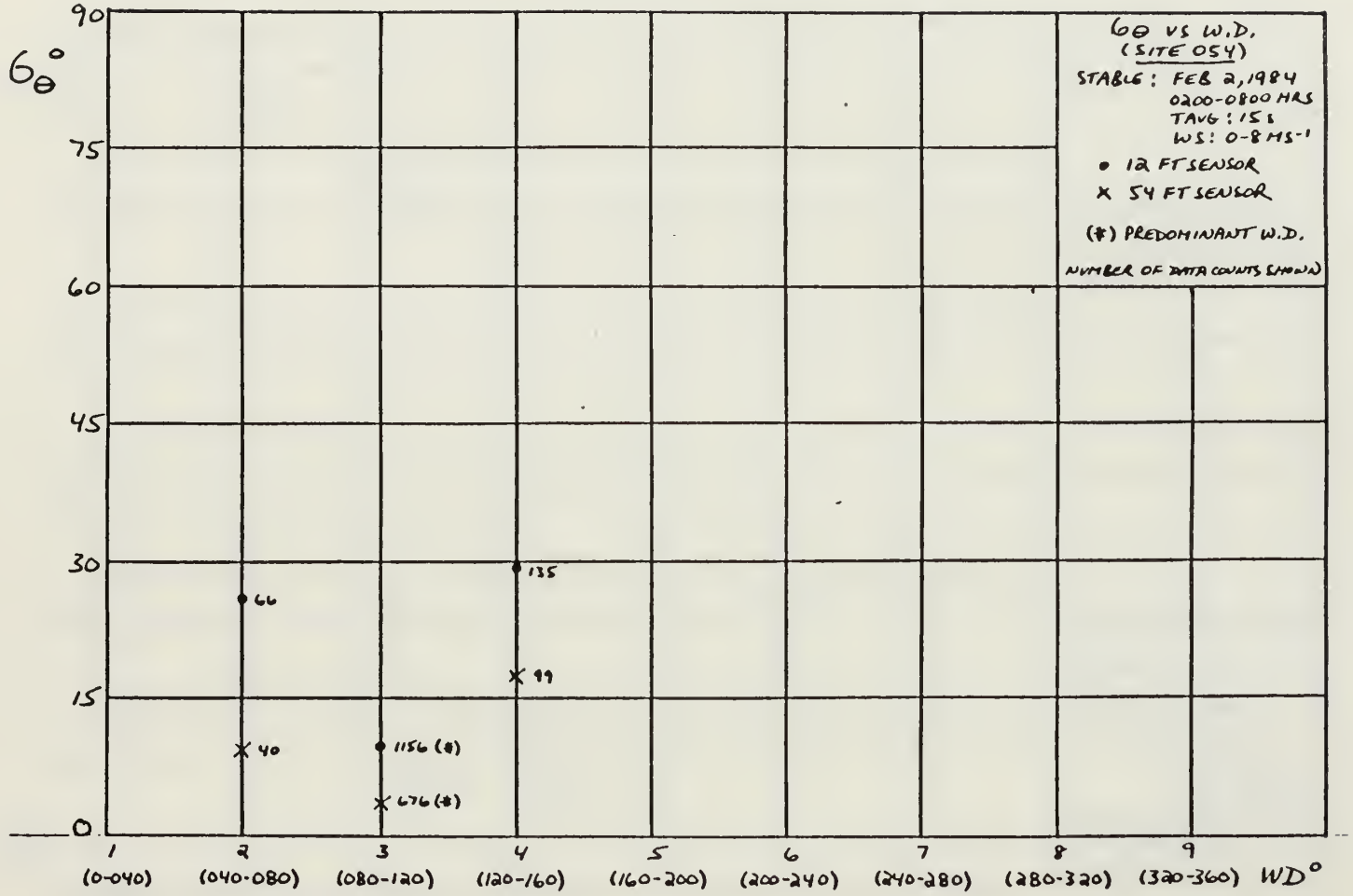

Figure 19(f). $\sigma\theta$ vs WD (Site 054) (2/2/84 (0200-0800)--Stable)

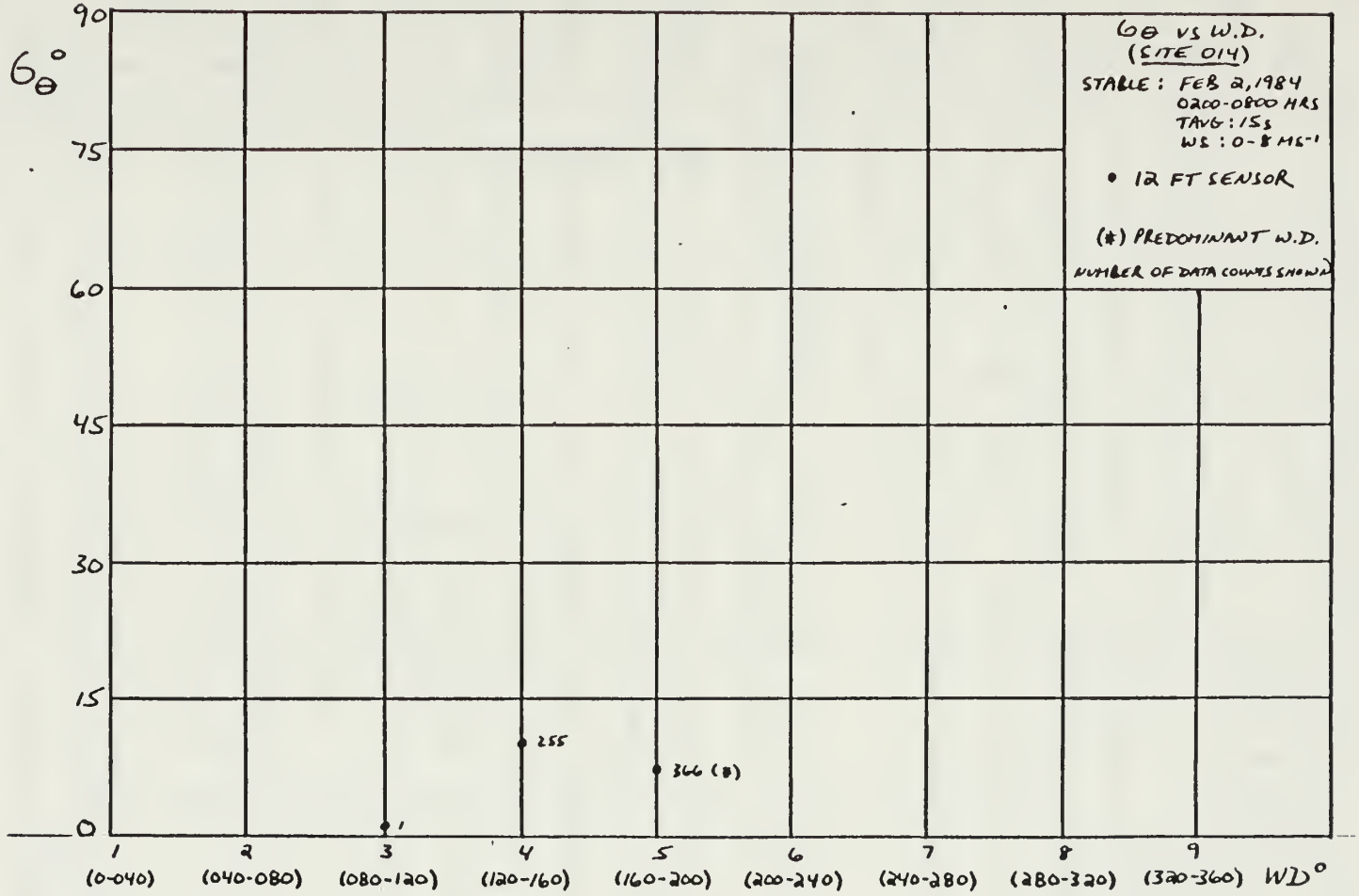

Figure 19(g). σθ vs WD (Site 014) (2/2/84 (0200-0800)--Stable)

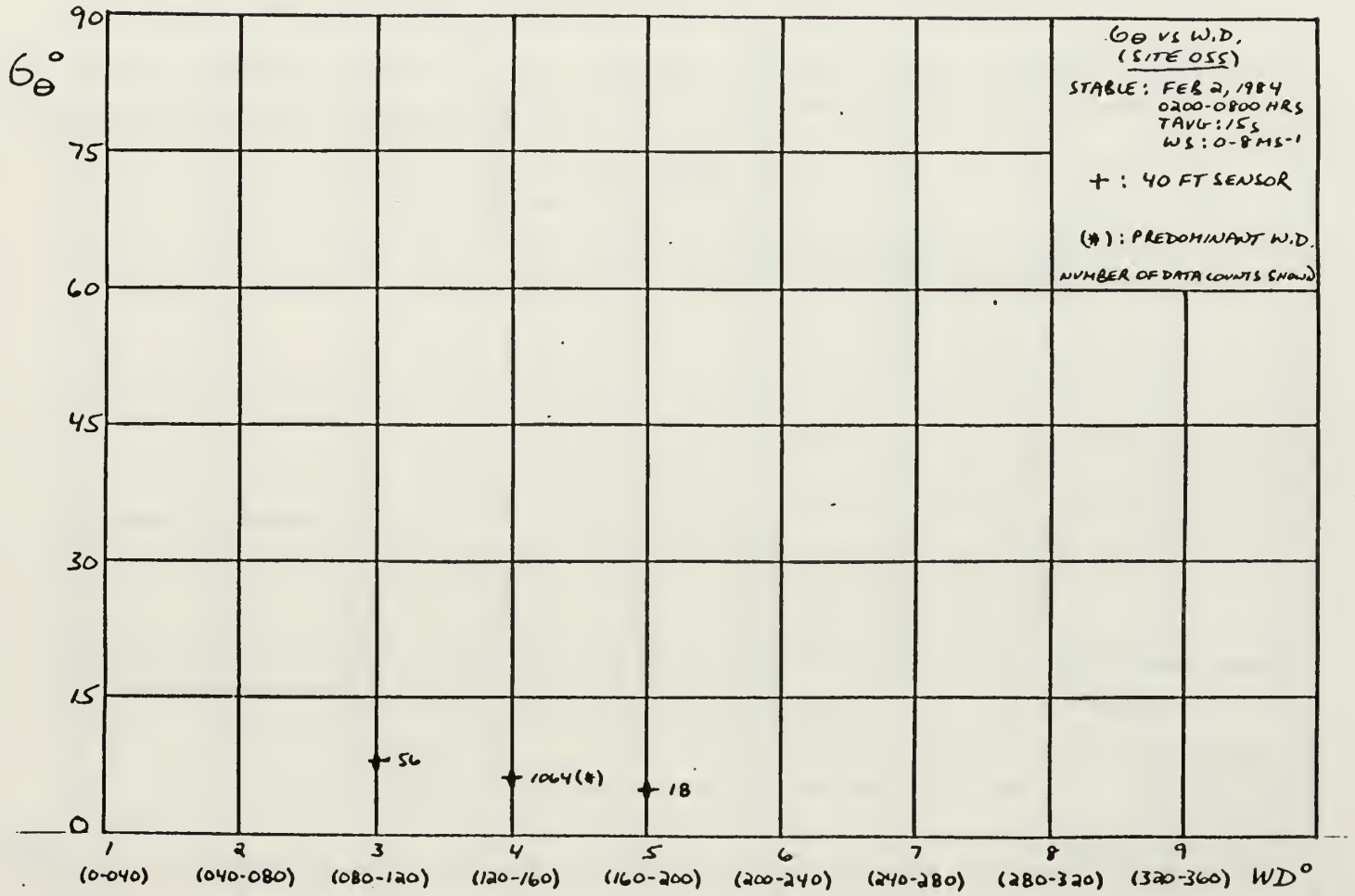

Figure 19(h). σθ vs WD (Site 055) (2/2/84 (0200-0800)--Stable)

301-54' exhibited a substantial increase in the $\sigma\theta$ value as wind speed increased. Table XXI describes the $\sigma\theta$ dependence on wind speed for all sensors and indicates the predominant wind speed at each sensor level as well.

b. Site/Sensor Elevation Dependence

Figures 20(a-h)/Tables C-(17-24) show $\sigma\theta$ dependence on wind speed for various sensor elevations at specific sites (* = Predominant Wind Speed). The following section examines $\sigma\theta$ differences between sites and $\sigma\theta$ dependence on wind speed relative to each site.

5. Terrain Dependence

The stable stratification associated with this case resulted in lower $\sigma\theta$ values, relative to the unstable case, and more sensitivity of $\sigma\theta$ to the terrain features. All of the schemes associated with this offshore land breeze/drainage flow regime showed higher values of $\sigma\theta$ inland versus at the coast and more sensitivity of $\sigma\theta$ to the terrain features inland. The coastal $\sigma\theta$ values appeared to be related to drainage flow from the mountains to the east. The inland sites were situated on elevated terrain and consequently appeared to be under the strongest influence of the land breeze.

Figure 21(a) summarizes the site $\sigma\theta$ results for various time averages as they relate to terrain characteristics. $\sigma\theta$ values were most uniform with height for all time averages at site 200, a coastal site located at the mouth of a long

TABLE XXI

$\sigma\theta$ Dependence on Wind Speed
(2/2/84 (0200-0800)--Stable)

		WIND SPEED			
Sensor	Site-Ht	1	2	3	4
2	014-12'	6.1	9.1*	18.6	28.8
3	052-12'	13.2	11.9*	7.4	----
4	054-12'	15.3	10.0*	22.8	----
6	102-12'	12.9	4.4*	----	----
8	200-12'	5.2*	4.7	----	----
10	301-12'	7.5	5.9*	----	----
13	055-40'	----	7.2	6.3*	5.3
11	052-54'	----	6.5	6.8*	11.3
12	054-54'	----	5.1*	5.4	----
16	102-54'	8.2	4.8*	3.4	----
18	200-54'	5.6	4.6*	3.2	----
19	300-54'	6.4	4.4*	3.5	----
20	301'54'	----	5.9	10.7*	12.1
22	200-102'	6.5	4.7*	4.2	----
23	300-102'	15.2	12.9*	7.1	----
25	301-102'	----	6.7	6.2*	8.1
24	299-108'	6.6	6.2	5.5*	4.6
26	200-204'	----	9.5	5.9*	5.1
27	300-204'	11.7	12.6	9.1*	----
28	301-204'	----	5.2	4.3*	3.6
29	300-300'	8.1	5.6*	4.1	2.5

Note: Most representative values listed above ($\sigma\theta$ in degrees)
* = Predominant wind speed
Time averaging 15 seconds
Wind Direction Offshore (040-160 degrees)
Wind Speed 1: 0-2 ms^{-1}
Wind Speed 2: 2-4 ms^{-1}
Wind Speed 3: 4-6 ms^{-1}
Wing Speed 4: 6-8 ms^{-1}

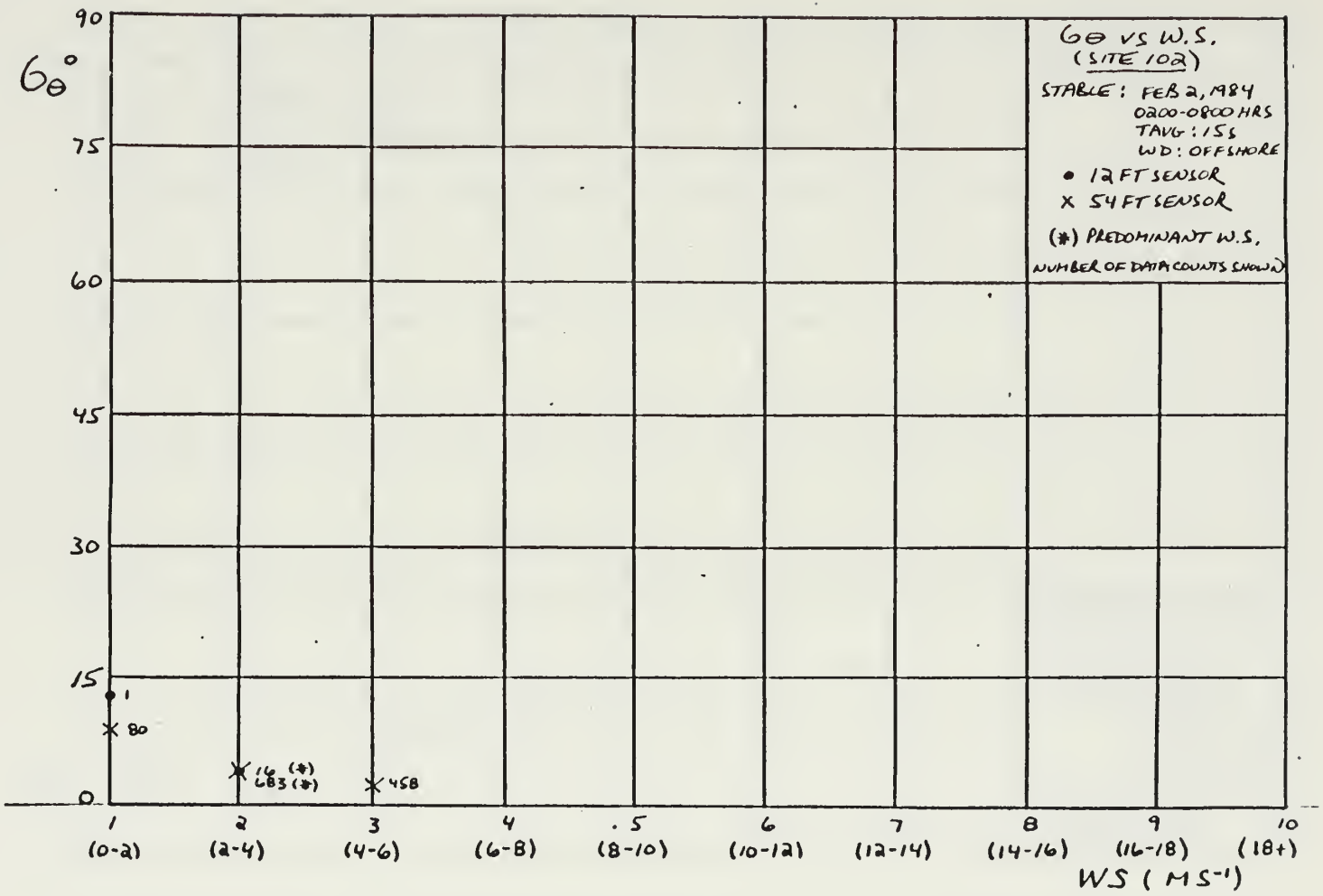

Figure 20(a). σθ vs WS (Site 102) (2/2/84 (0200-0800)--Stable)

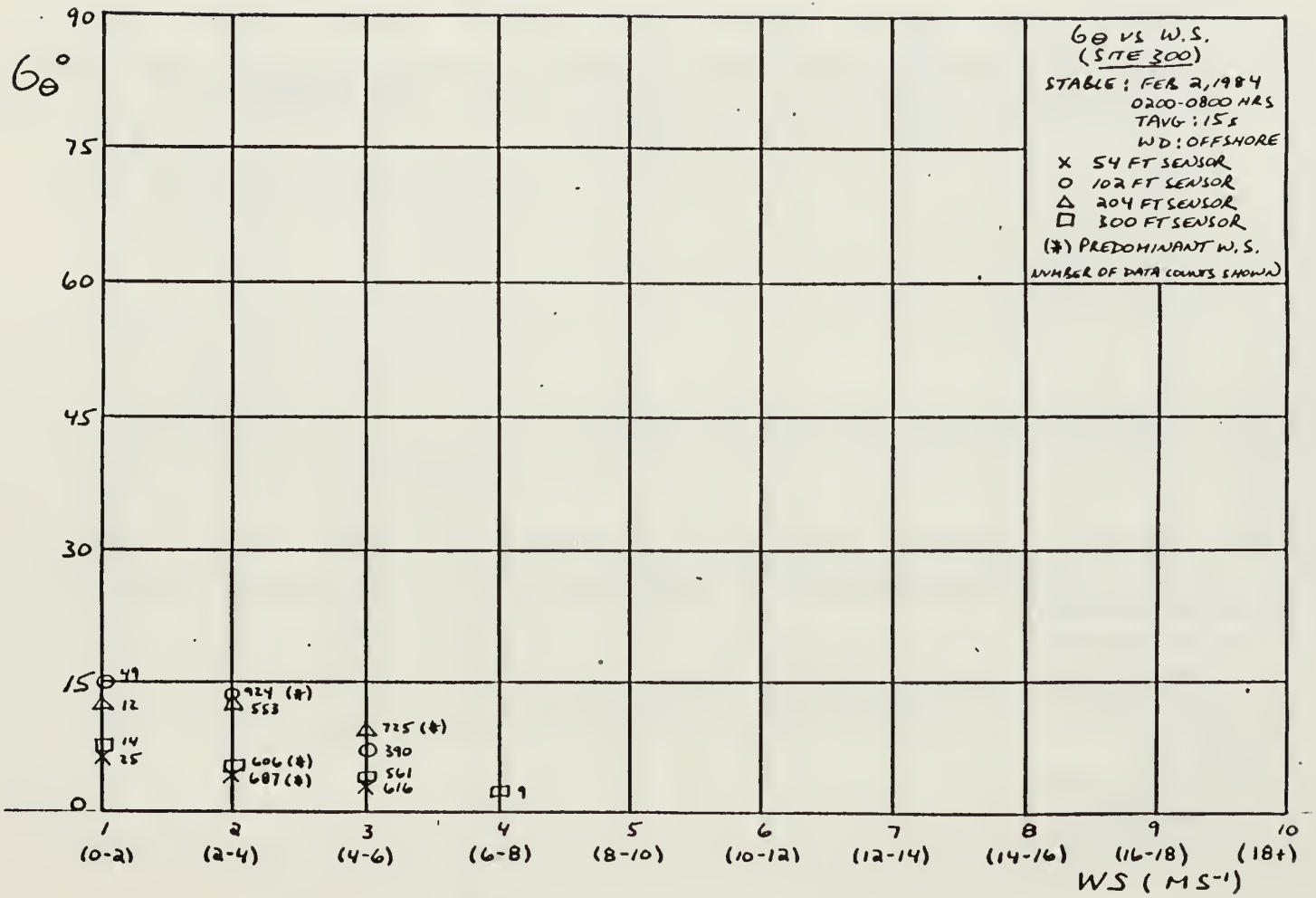

Figure 20(b). σθ vs WS (Site 300) (2/2/84 (0200-0800)--Stable)

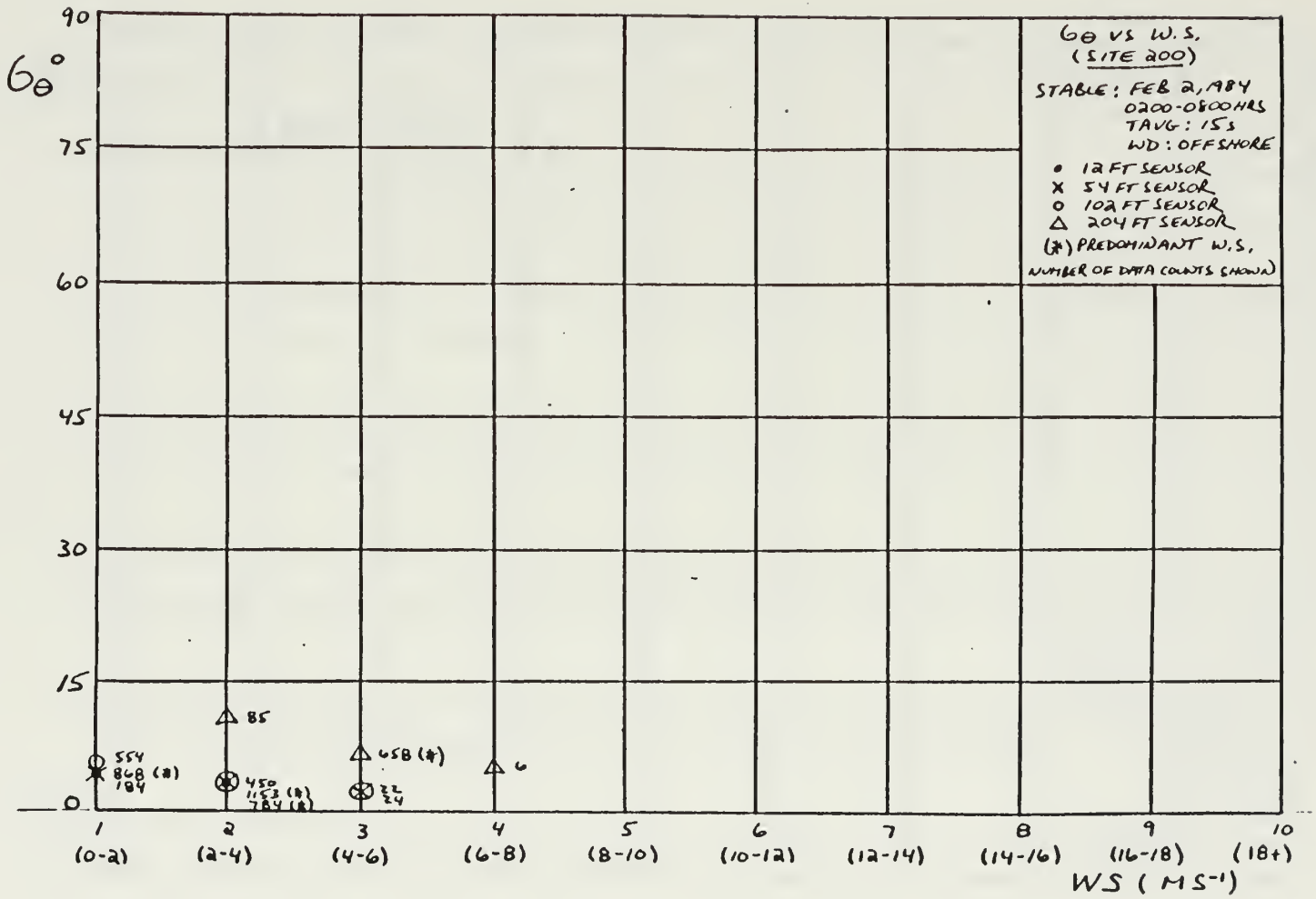

Figure 20(c). $\sigma\theta$ vs WS (Site 200) (2/2/84 (0200-0800)--Stable)

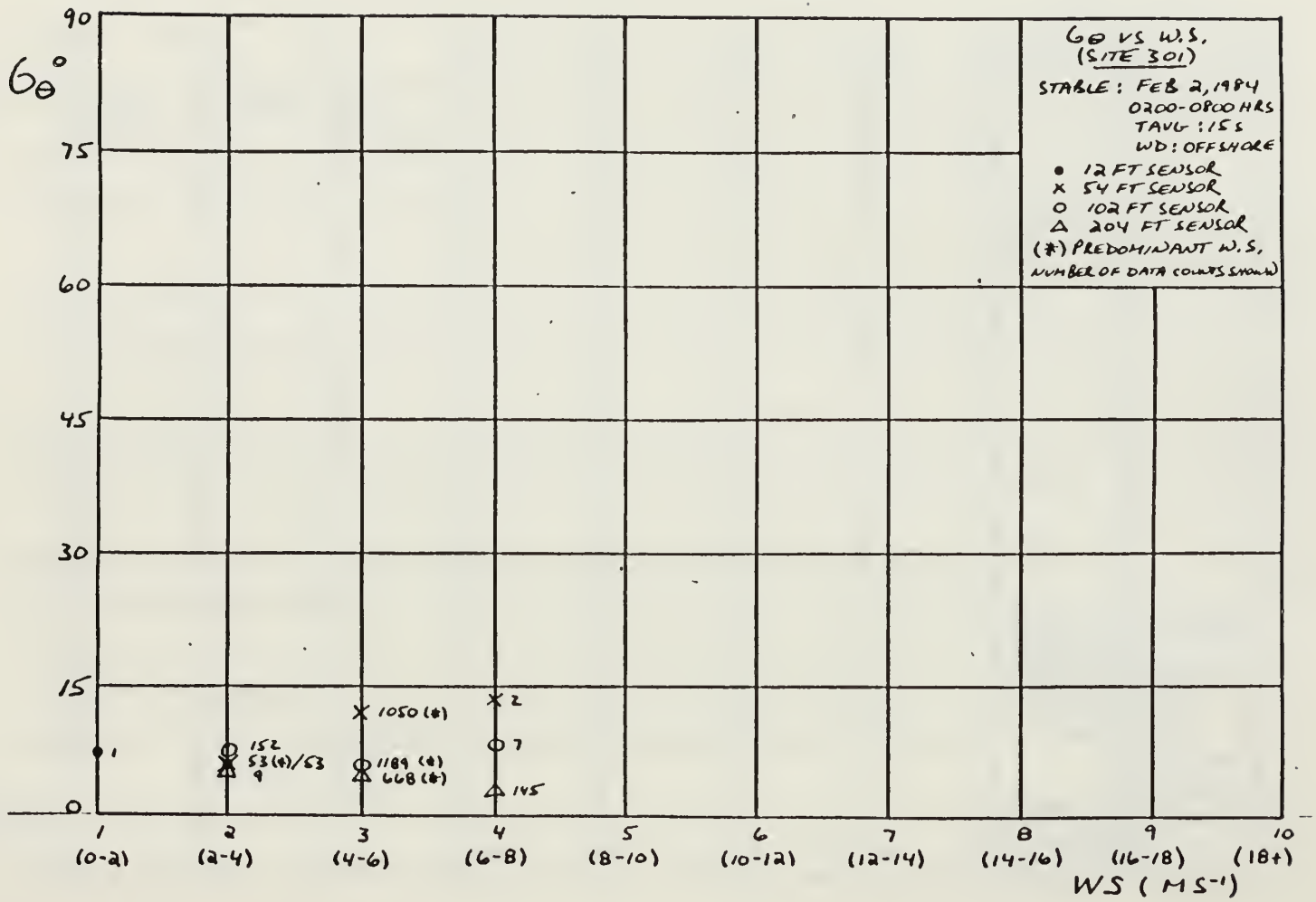

Figure 20(d). $\sigma\theta$ vs WS (Site 301) (2/2/84 (0200-0800)--Stable)

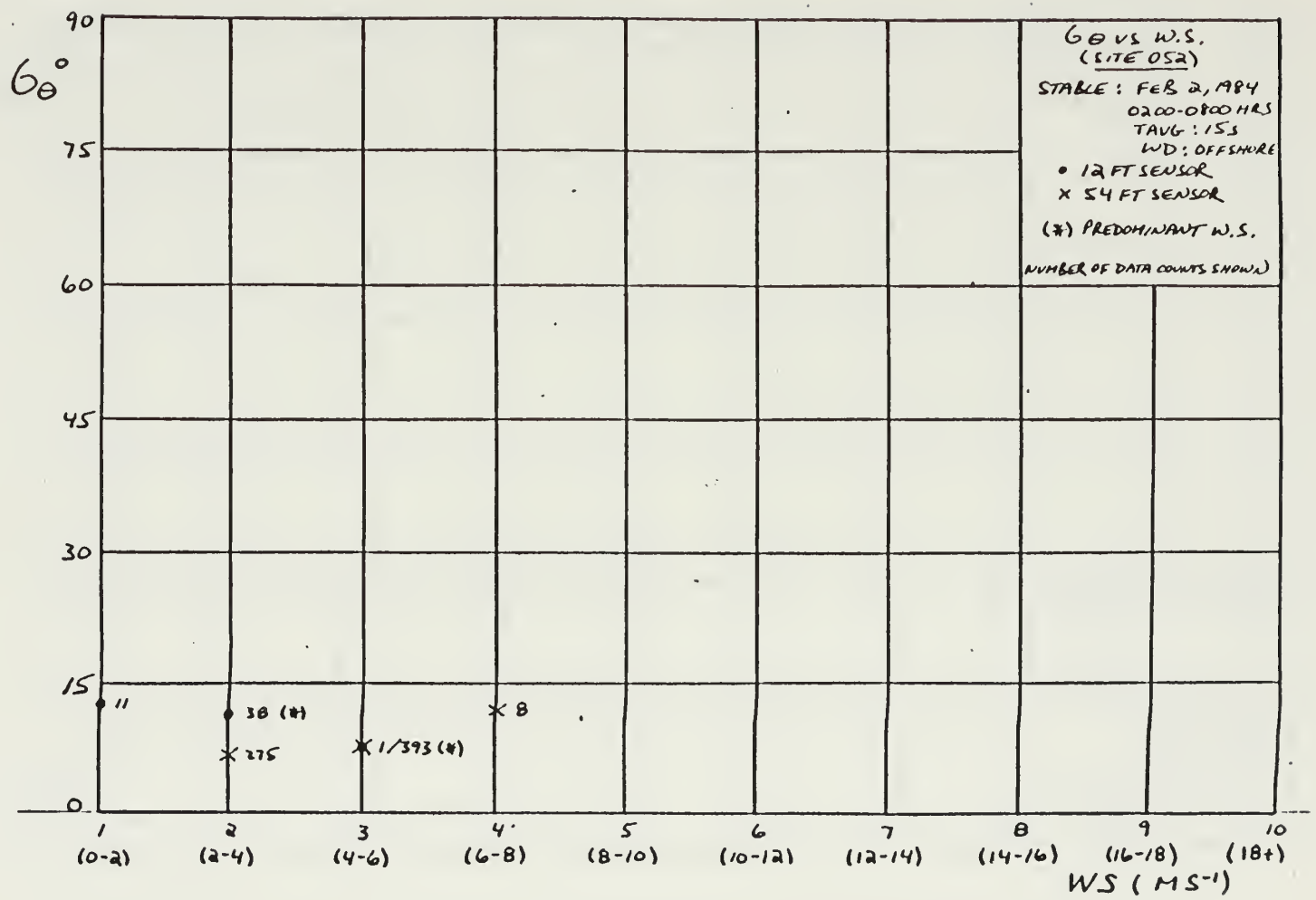

Figure 20(e). σθ vs WS (Site 052) (2/2/84 (0200-0800)--Stable)

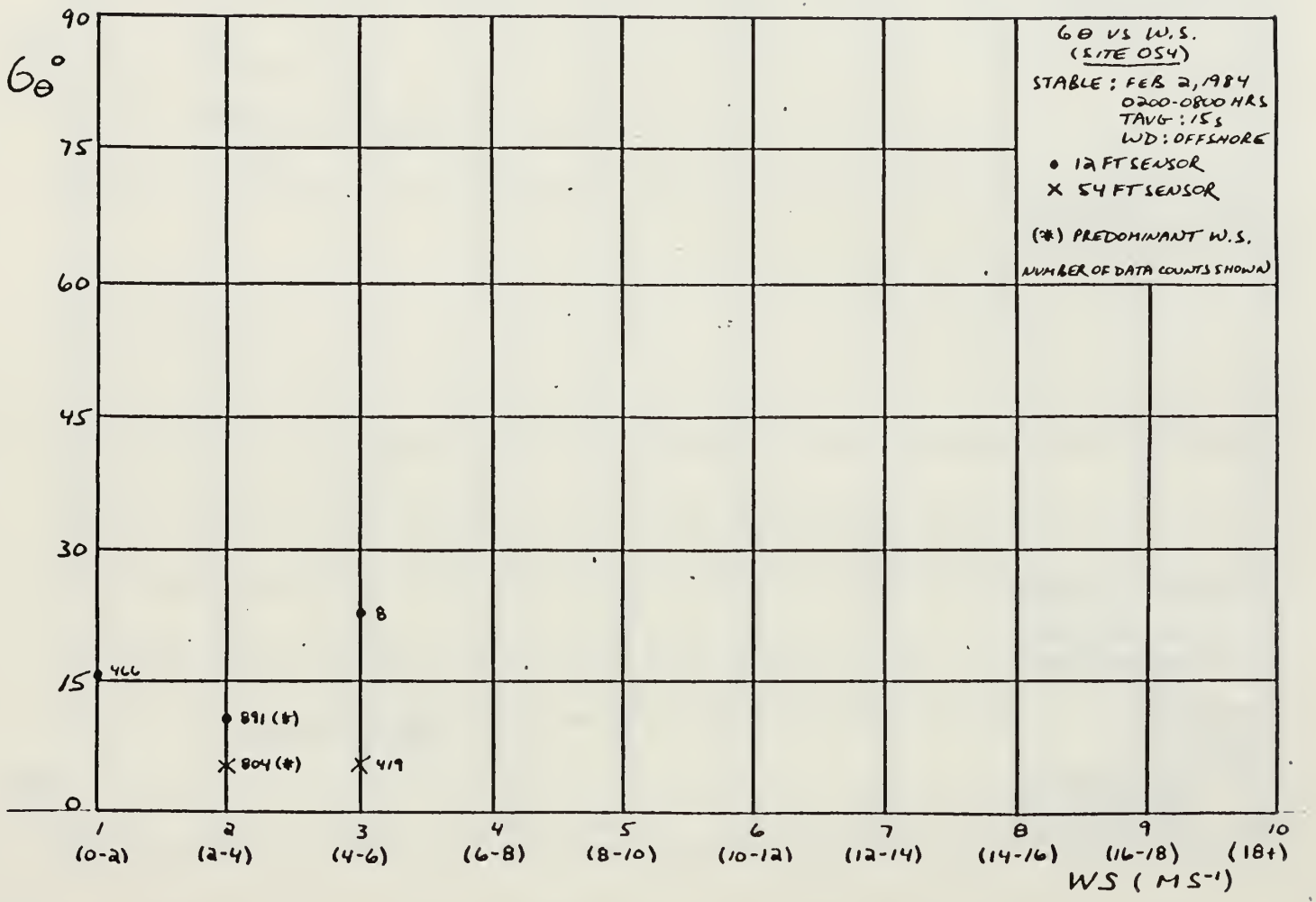

Figure 20(f). σθ vs WS (Site 054) (2/2/84 (0200-0800)--Stable)

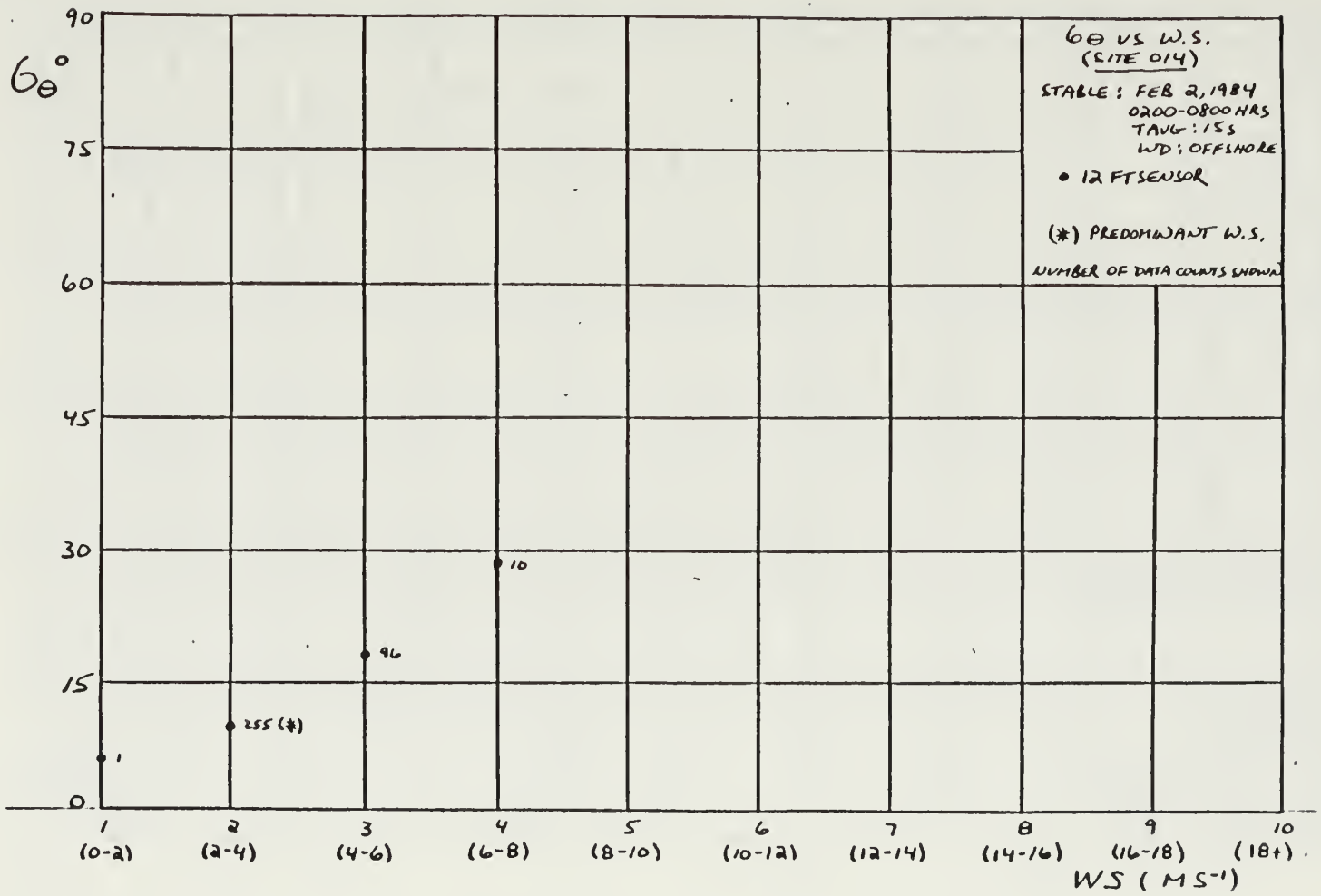

Figure 20(g). $\sigma\theta$ vs WS (Site 014) (2/2/84 (0200-0800)--Stable)

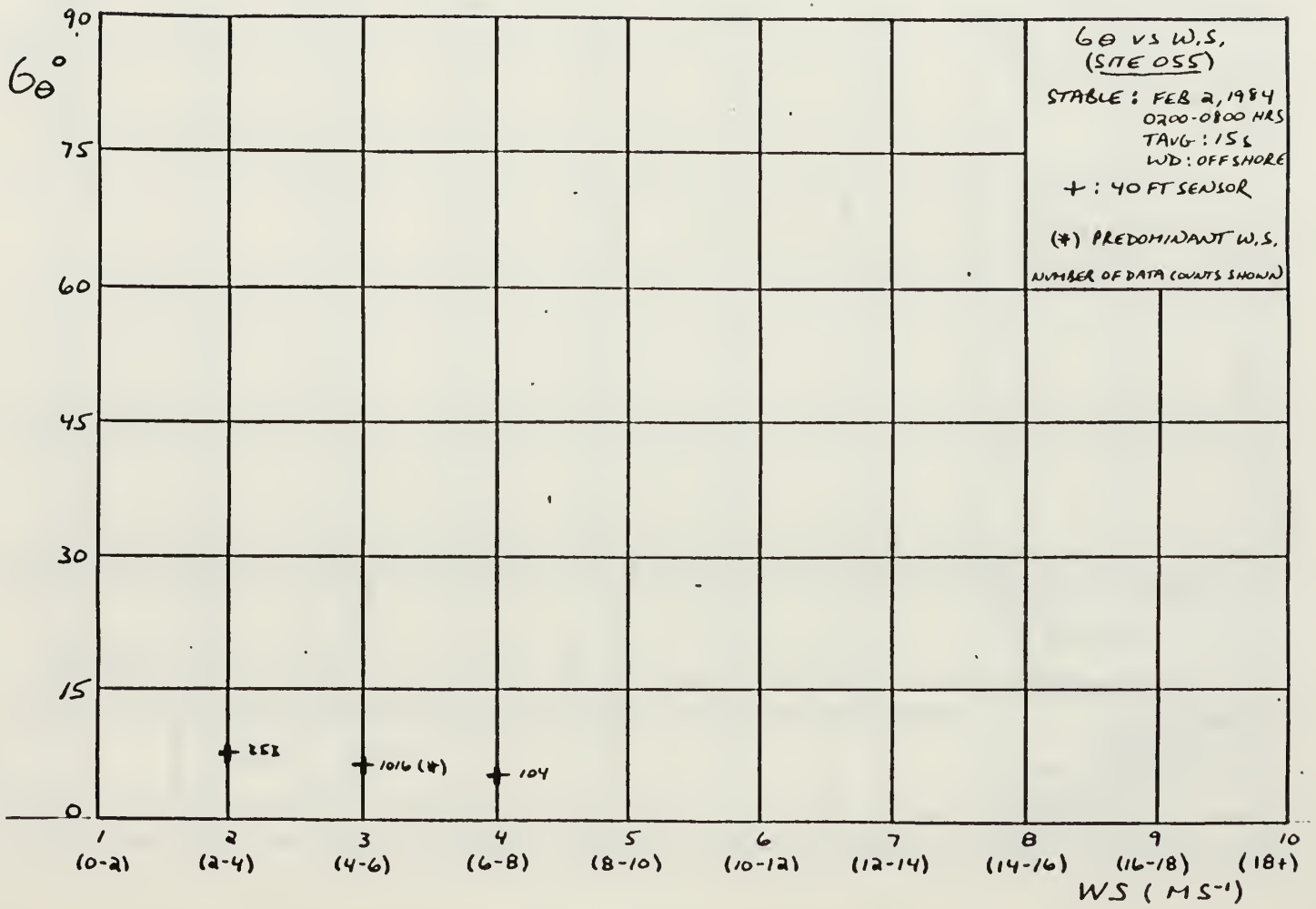

Figure 20(h). $\sigma\theta$ vs WS (Site 055) (2/2/84 (0200-0800)--Stable)

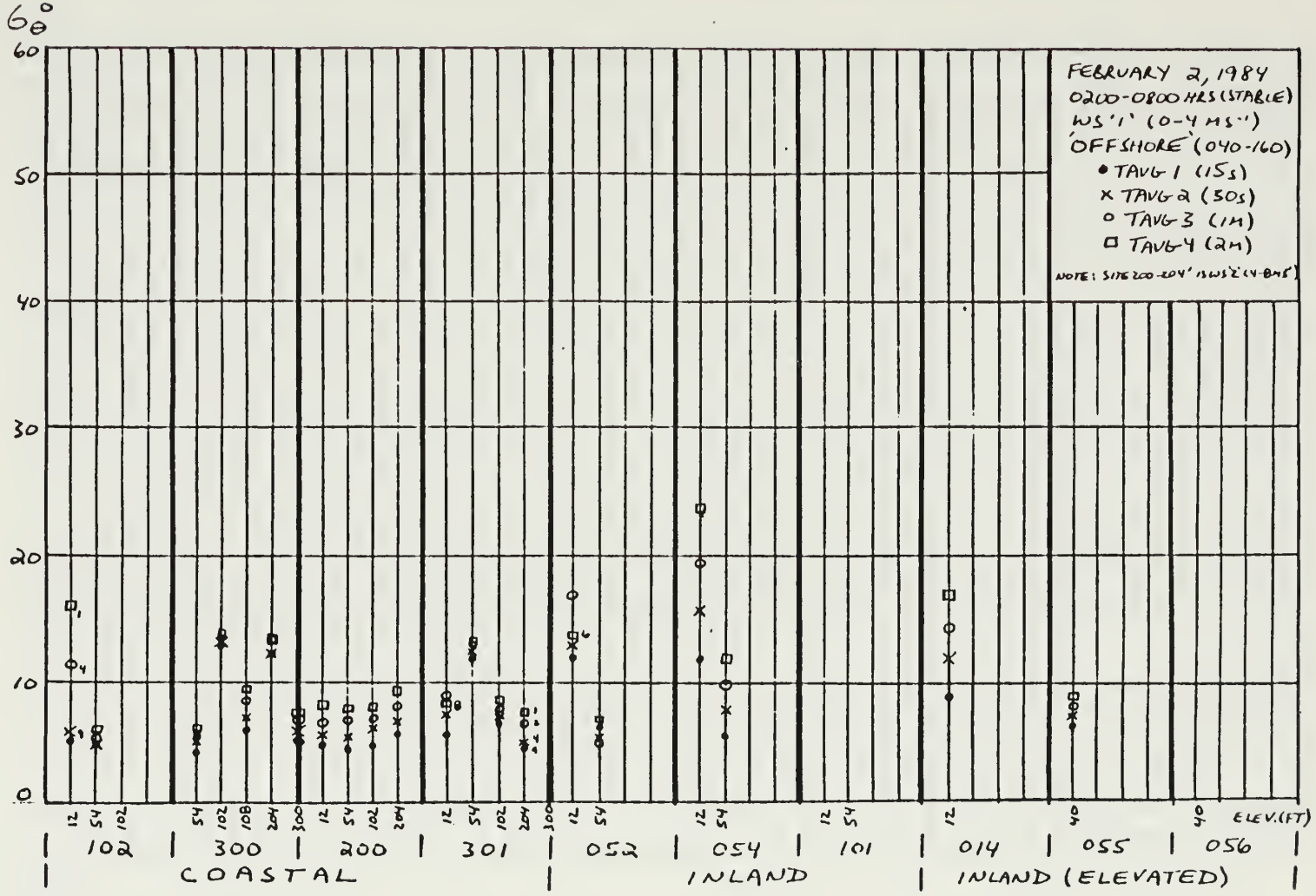

Figure 21(a). σθ vs TAVG (Terrain Analysis) (2/2/84 (0200-0800)--Stable)

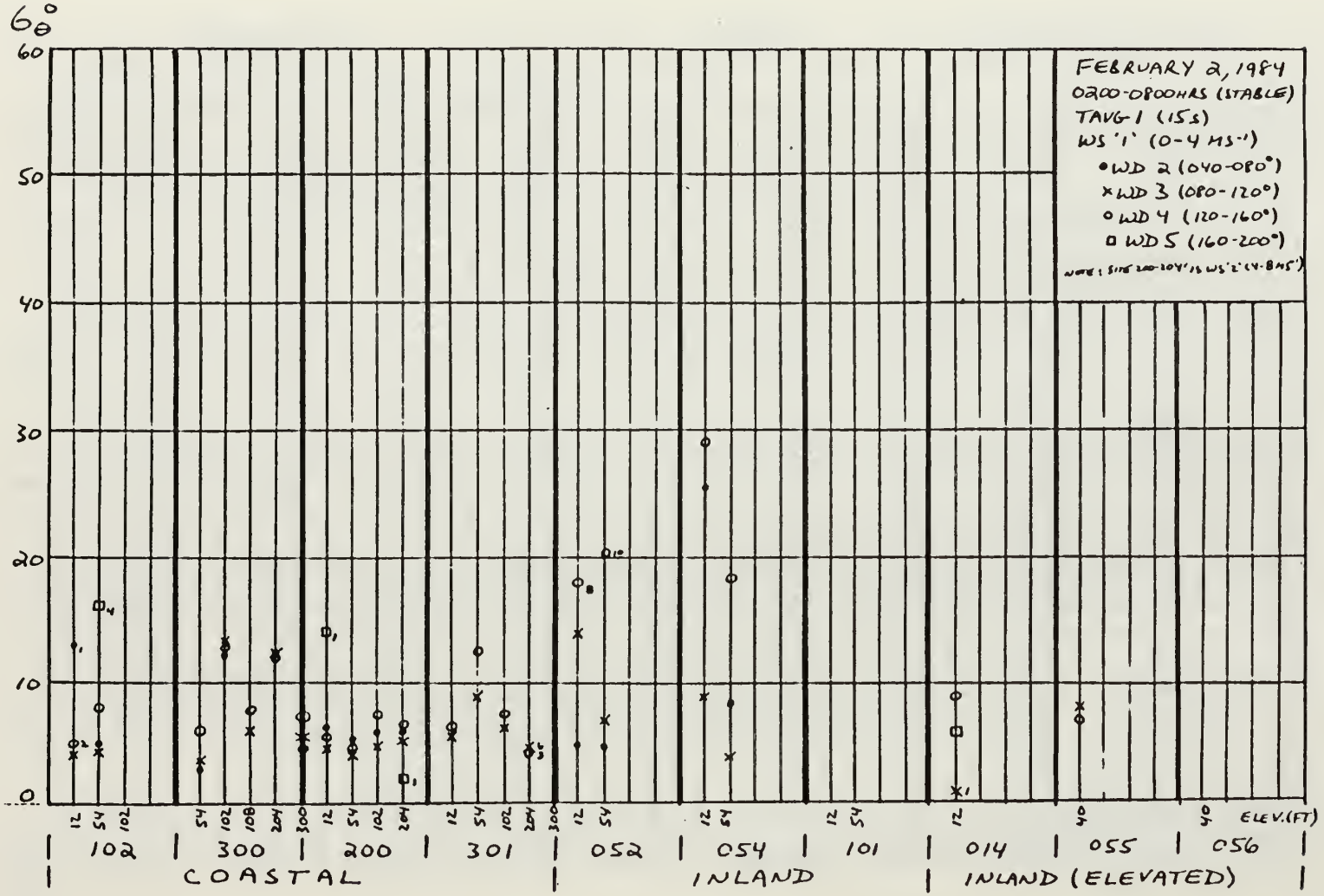

Figure 21(b). σθ vs WD (Terrain Analysis) (2/2/84 (0200-0800)--Stable)

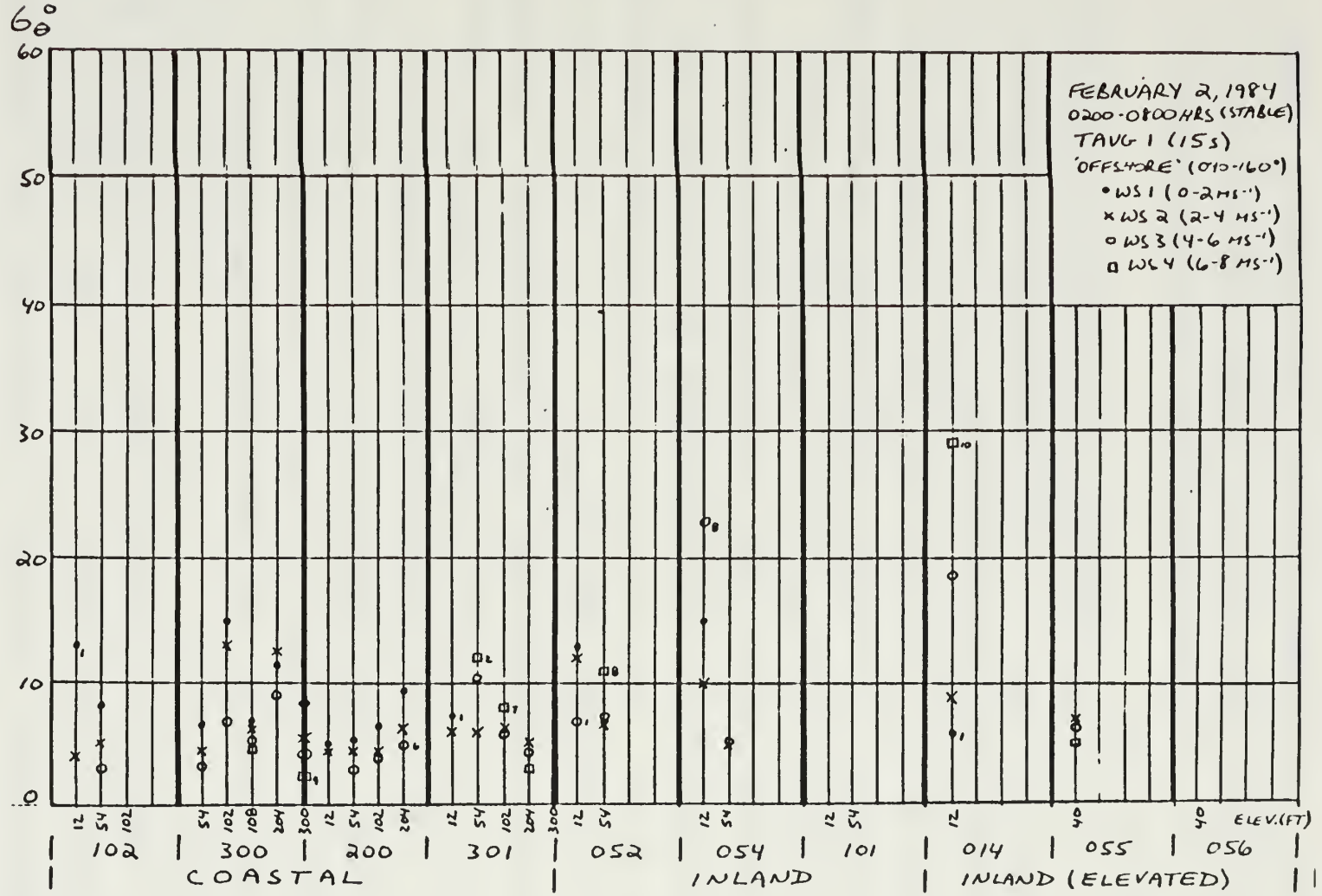

Figure 21(c). σθ vs WS (Terrain Analysis) (2/2/84 (0200-0800)--Stable)

valley, and least uniform with height at inland sites 052 and 054. The $\sigma\theta$ values showed the least amount of change with increasing time averaging at sites 102, 300, 301, 052, and 055 and they showed the greatest amount of change at site 054 and 014.

Figure 21(b) describes $\sigma\theta$ dependence on wind direction throughout the terrain. The lowest $\sigma\theta$ values associated with winds from the predominant direction of 040-080° were found at sites 102-54', 300-54 and 300', 200 (all levels), and 052-12 and 54'. The highest $\sigma\theta$ values under these conditions were in evidence at sites 102-12', 300-102 and 204', and 054-12'. The overall lowest $\sigma\theta$ values were associated with winds from 080-120° except at sensors 300-54 and 300' and 052-12 and 54', where the lowest values of $\sigma\theta$ were found with winds from 040-080", and at sensors 301-204' and 055-40' where these values were with winds from 120-160°. The highest $\sigma\theta$ values were generally associated with winds from 120-200°. Values of $\sigma\theta$ were most constant with height at site 200 and most variable with height at site 054. Sites 300, 200, 301 and 055 showed the least $\sigma\theta$ variation with wind direction while sites 052 and 054 experienced the most variation.

Finally, Figure 21(c) illustrates site $\sigma\theta$ results for various wind speed categories as they relate to terrain characteristics. The lowest $\sigma\theta$ values throughout the terrain were generally associated with higher wind speeds. The $\sigma\theta$

values were most uniform with sensor height at coastal sites 200 and 301. Sites 300, 200, 301, and 055 experienced less of a $\sigma\theta$ dependence on windspeed while there was more of such a dependence noted at inland sites 054 and 014.

D. NEUTRAL CASE STUDY (3/17/84, 0900-1800)

1. Synoptic Situation/Mean Flow

In this case study, the Vandenberg weather was dominated by strong postfrontal northwesterly flow associated with a cold frontal system which moved through the area earlier in the day. Figure 22 depicts strong pressure gradient forcing over the California central coast with the 500 mb jet extending west to east through northern California. Rainshowers were also in the Vandenberg area.

Max Temp: 66 °F Min Temp: Missing

AVG VBG Wind Direction (all sensors): 320-360°

AVG VBG Wind Speed (all sensors): 8+ ms^{-1}

Figure 23 illustrates the mean flow occurring at the various sites and sensors in the Vandenberg area. Strong north-northwesterly post-frontal flow (320-360°) was evident at all sites and at all sensor elevations. Wind speed increased with height at each site and a large range of wind speed values was apparent between the lower sensor levels and the higher sensor levels. The 12' sensors recorded average wind speeds of 6-8 ms^{-1} while the 300' sensors encountered average speeds of greater than 18 ms^{-1}. Tables XXII and XXIII list the mean flow wind directions and wind speeds according to site and sensor elevations, respectively.

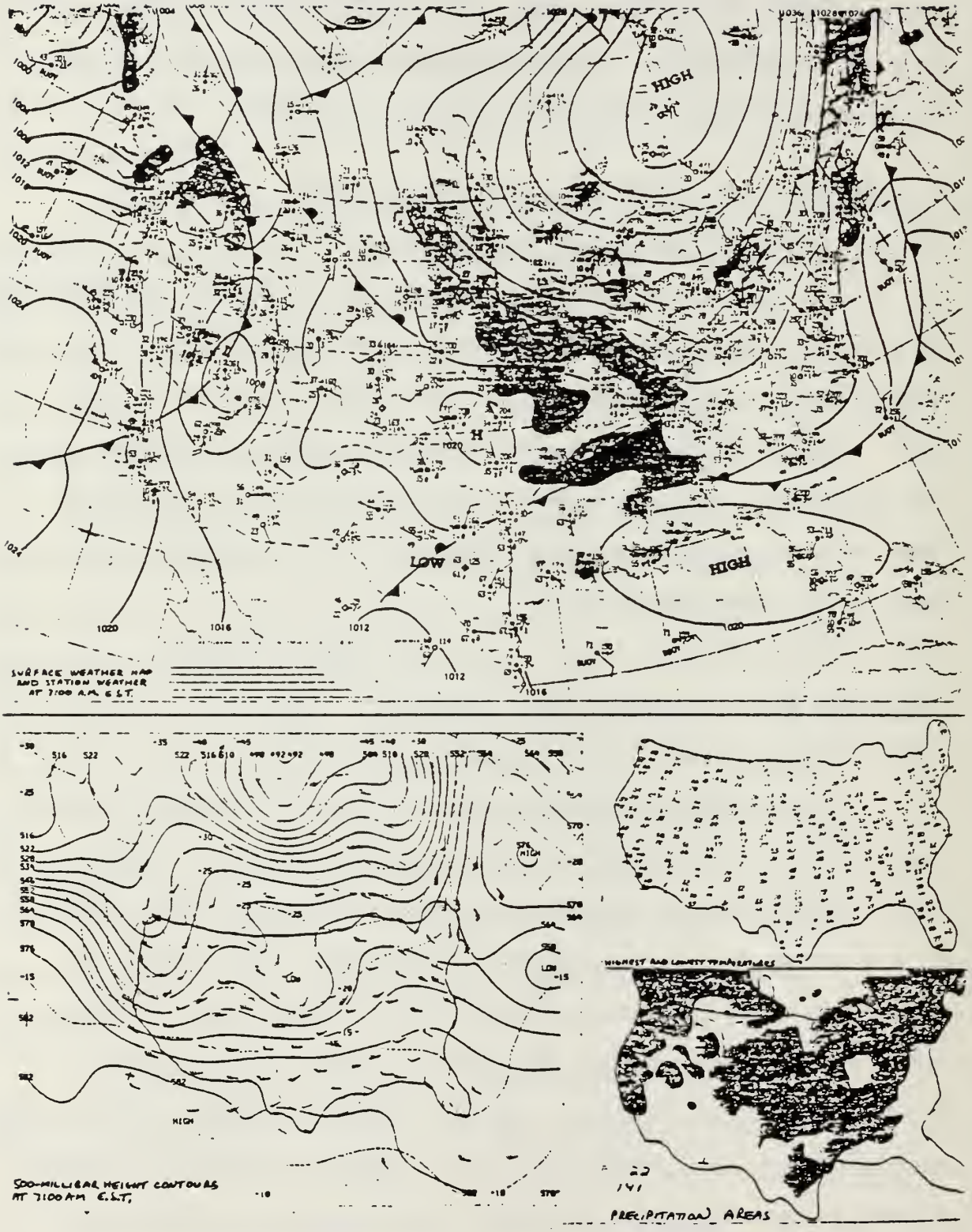

Figure 22. VBG Synoptic Situation (3/17/84 (0900-1800)--Neutral)

TABLE XXII

VBG Mean Flow--By Site
(3/17/84 (0900-1800)--Neutral)

Site	Level (Ft)	Sensor No.	Predominant Flow (WD/WS)
009	12	1	----------
014	12	2	----------
055	40	13	320-360/18+
056	40	14	040-080/4-6
052	12	3	320-360/8-10
052	54	11	320-360/10-12
054	12	4	320-360/8-10
054	54	12	320-360/8-12
101	12	5	320-360/8-10
101	54	15	320-360/8-12
103	12	7	----------
103	54	17	----------
102	12	6	320-360/4-6
102	54	16	----------
102	102	21	320-360/10-12
200	12	8	320-360/6-8
200	54	18	320-360/10-12
200	102	22	320-360/10-14
200	204	26	320-360/14-16
300	12	9	----------
300	54	19	----------
300	102	23	----------
299	108	24	320-360/18+
300	204	27	----------
300	300	29	----------
301	12	10	320-360/8-10
301	54	20	320-360/8-10
301	102	25	320-360/8-10
301	204	28	320-360/12-14
301	300	30	----------

Note: WD (degrees)
WS (ms^{-1})

TABLE XXIII

VBG Mean Flow--By Height
(3/17/84 (0900-1800)--Neutral)

Level (Ft)	Sensor No.	Site	Predominant Flow (WD/WS)
12	1	009	----------
12	2	014	----------
12	3	052	320-360/8-10
12	4	054	320-360/8-10
12	5	101	320-360/8-10
12	6	102	320-360/4-6
12	7	103	----------
12	8	200	320-360/6-8
12	9	300	----------
12	10	301	320-360/8-10
40	13	055	320-360/18+
40	14	056	040-080/4-6
54	11	052	320-360/10-12
54	12	054	320-360/8-12
54	15	101	320-360/8-12
54	16	102	----------
54	17	103	----------
54	18	200	320-360/10-12
54	19	300	----------
54	20	301	320-360/8-10
102	21	102	320-360/10-12
102	22	200	320-360/10-14
102	23	300	----------
102	25	301	320-360/8-10
108	24	299	320-360/18+
204	26	200	320-360/14-16
204	27	300	----------
204	28	301	320-360/12-14
300	29	300	----------
300	30	301	----------

Note: WD (degrees)
WS (ms^{-1})

TABLE XXIV

$\sigma\theta$ Dependence on Time Averaging
(3/17/84 (0900-1800)--Neutral)

		TIME AVERAGING				
Sensor	Site-Ht	15 sec	30 sec	1 min	2 min	5 min
3	052-12'	7.9	8.6	9.0	9.5	9.9
4	054-12'	7.3	8.0	8.6	8.9	9.2
5	101-12'	7.3	8.0	8.6	9.0	9.6
6	102-12'	7.5	7.6	8.9	11.0	10.6
8	200-12'	12.1	12.5	12.7	12.8	12.8
10	301-12	8.2	8.2	8.1	----	----
13	055-40'	4.1	4.6	5.1	5.4	5.5
12	054-54'	6.3	6.8	7.1	7.4	7.7
15	101-54'	5.9	6.6	7.1	7.6	8.2
18	200-54'	6.6	7.0	7.3	7.4	7.5
20	301-54'	10.0	10.6	11.3	12.4	12.7
21	102-102'	4.7	4.9	5.1	5.2	5.3
22	200-102'	5.0	5.3	5.4	5.5	5.6
25	301-102'	8.2	8.5	8.8	9.0	9.2
24	299-108'	5.4	5.7	5.9	6.1	6.2
26	200-204'	3.7	3.9	4.0	4.2	4.3
28	301-204'	6.5	6.8	7.0	7.1	7.2

Note: Most representative values listed above ($\sigma\theta$ in degrees)
Wind Direction Onshore (200-360 degrees)
Wind Speed 8+ ms^{-1} except for sensors 6 and 8 (4-8 ms^{-1})

TAVG = 15 sec: Mean $\sigma\theta$ (DEG) = 6.9 Standard deviation (DEG) = 2.1

TAVG = 30 sec: Mean $\sigma\theta$ (DEG) = 7.3 Standard deviation (DEG) = 2.1

TAVG = 1 min: Mean $\sigma\theta$ (DEG) = 7.6 Standard deviation (DEG) = 2.2

TAVG = 2 min: Mean $\sigma\theta$ (DEG) = 8.0 Standard deviation (DEG) = 2.5

TAVG = 5 min: Mean $\sigma\theta$ (DEG) = 8.2 Standard deviation (DEG) = 2.5

2. σθ Dependence on Time Averaging

a. General Results

Table XXIV summarizes σθ dependence on time averaging for time averages ranging from 15 s to 5 min. The σθ values at all sensors either increased slightly with increasing values of time averaging or virtually remained constant with increased time averaging values. Table XXV shows the general range of σθ values for all sensors and their standard deviations between 15 s and 5 min time averaging values. Along with the slight increase in σθ values with increased time averaging, there was also a slight increase in the standard deviation of σθ with increased time averaging.

TABLE XXV

σθ vs TAVG (All Sensors)
(3/17/84 (0900-1800)--Neutral)

TAVG	σθ (Deg)	S.D. (Deg)
15 s	6.9	2.1
30 s	7.3	2.1
1 m	7.6	2.2
2 m	8.0	2.5
5 m	8.2	2.5

b. Power Law Relationship

As stated before, the power law relationship examines the ratio of σθ values at two averaging times.

Figure 24(a) illustrates the relationship between the average observed power law value of x (x = 0.06) and the empirical x value (x = 0.20). This figure also shows the scatter of individual sensor $\sigma\theta$ data at each time average and identifies the mean of the observed $\sigma\theta$ values and its associated standard deviation for each time average. In general, all sensors without 'bad' data had x values between 0.02 and 0.11 with the exception of sensor 102-12' which had an x value of 0.16. The lowest x values appeared to be associated with the coastal sites with the highest x values linked with the inland sites. Figure 24(b) shows the ratio of ($\sigma\theta$ (T)/$\sigma\theta$ (15 s)) vs TAVG.

c. Height Dependence

A summary of $\sigma\theta$ dependence on time averaging as a function of sensor elevation is shown in Table XXVI/Figure 25.

TABLE XXVI

$\sigma\theta$ vs TAVG (All Sites)
(3/17/84 (0900-1800)--Neutral)

	SENSOR ELEVATION (FT)			
TAVG	12	54	102	204
15 s	8.4	7.2	6.0	5.1
30 s	8.8	7.8	6.2	5.4
1 m	9.3	8.2	6.4	5.5
2 m	10.2	8.7	6.6	5.7
5 m	10.4	9.0	6.7	5.8

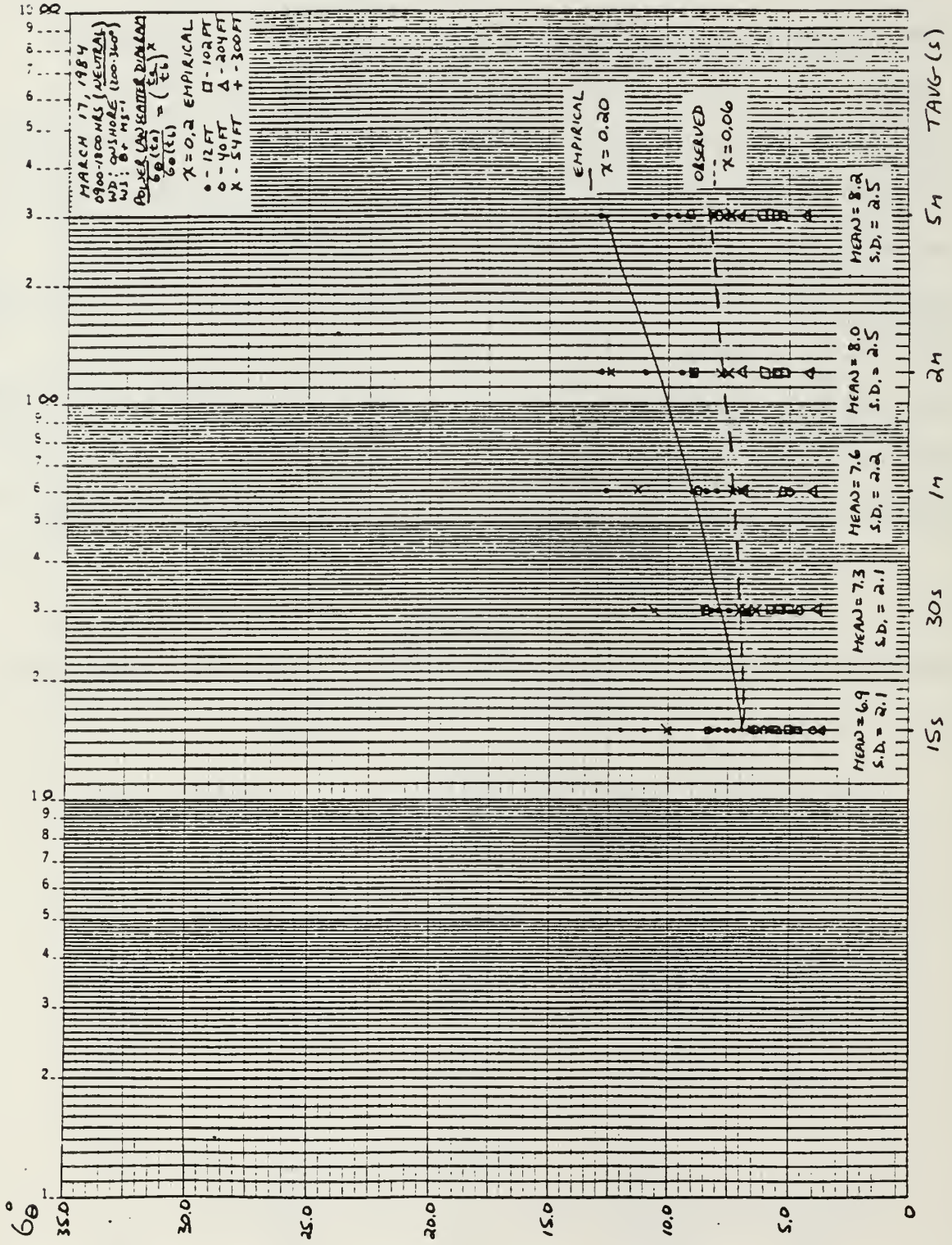

Figure 24(a). Power Law Relationship (All Sensors) (3/17/84 (0900-1800)--Neutral)

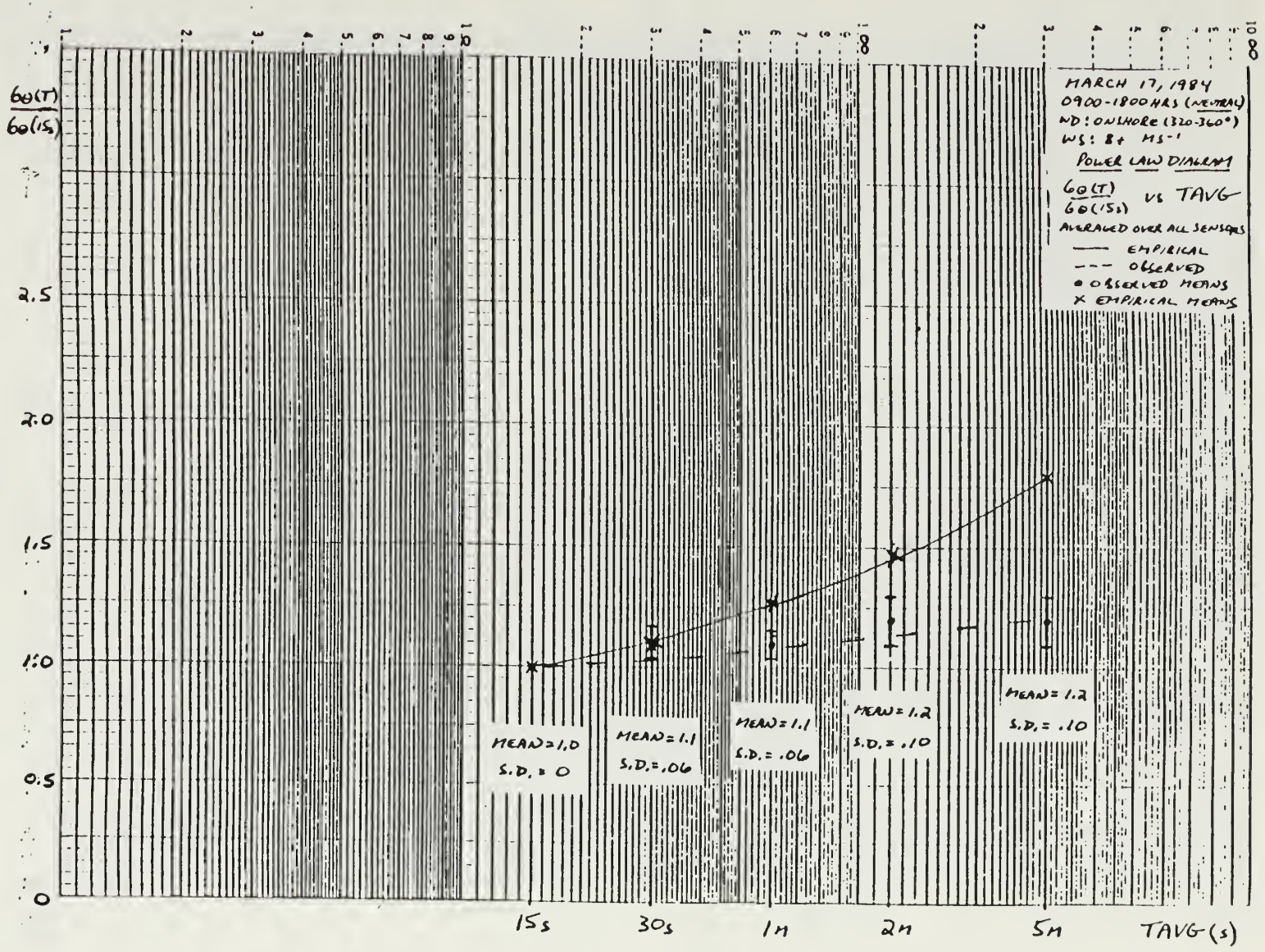

Figure 24(b). Powr Law Ratio (All Sensors) (3/17/84 (0900-1800)--Neutral)

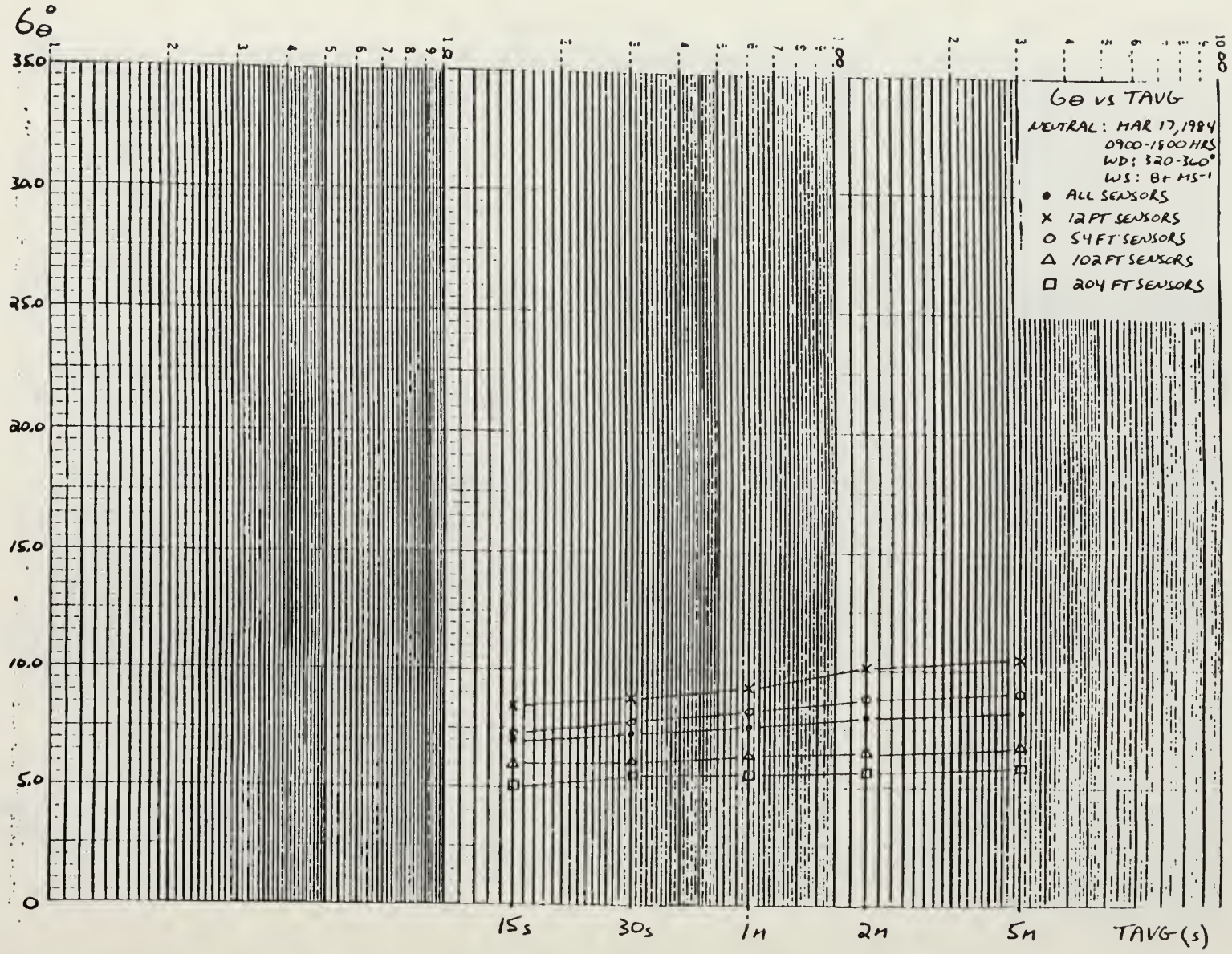

Figure 25. σθ vs TAVG (All Sites) (3/17/84 (0900-1800)--Neutral)

The above table shows a slight increase in values with increasing time averaging values for all sensor heights and a decrease in $\sigma\theta$ values with increasing sensor height over all time averages. The difference in $\sigma\theta$ values from 15 s to 5 m time averaging decreased slightly from the 12' levels to the 102' levels and then essentially remained constant from the 102 to the 204' level.

d. Site/Sensor Elevation Dependence

Figures 26(a-h)/Tables D-(1-8) show site specific $\sigma\theta$ dependence on time averaging for various sensor elevations. A terrain analysis later in this section will collectively examine $\sigma\theta$ differences between sites and $\sigma\theta$ dependences on time averaging relative to the sites.

3. $\sigma\theta$ Dependence on Wind Direction

a. General Results

The postfrontal flow associated with this neutral case resulted in predominant wind flow from 320-360° at all sensors at all sites. The lowest $\sigma\theta$ values were generally associated with winds from 320-040° with higher $\sigma\theta$ values occurring on either side of this braket (terrain influences). The highest values of $\sigma\theta$ appeared to be associated with the lower sensor elevations throughout the terrain. Table XXVII describes the $\sigma\theta$ dependence on wind direction at all sensors and indicates from which direction the predominant wind is blowing.

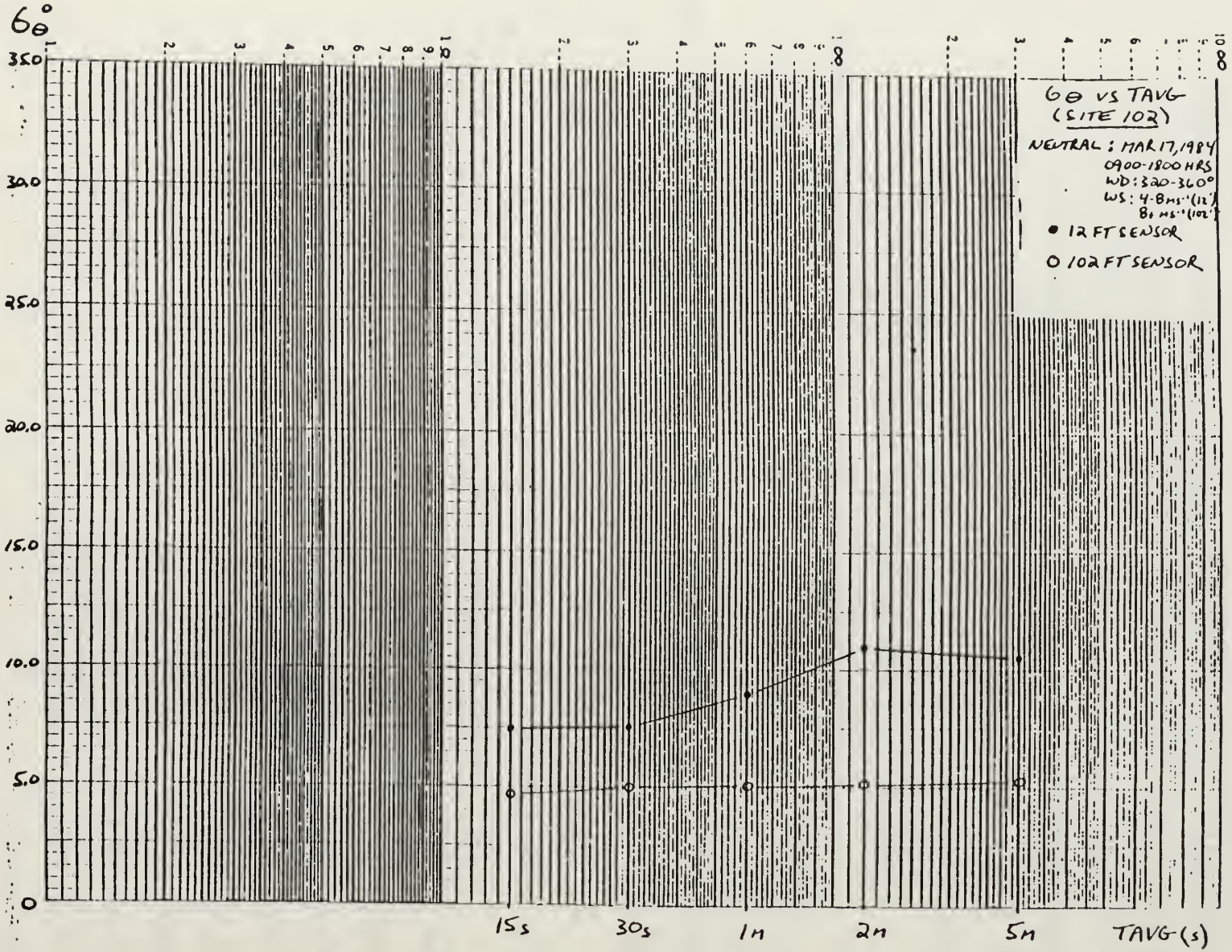

Figure 26(a). σθ vs TAVG (Site 102) (3/17/84 (0900-1800)--Neutral)

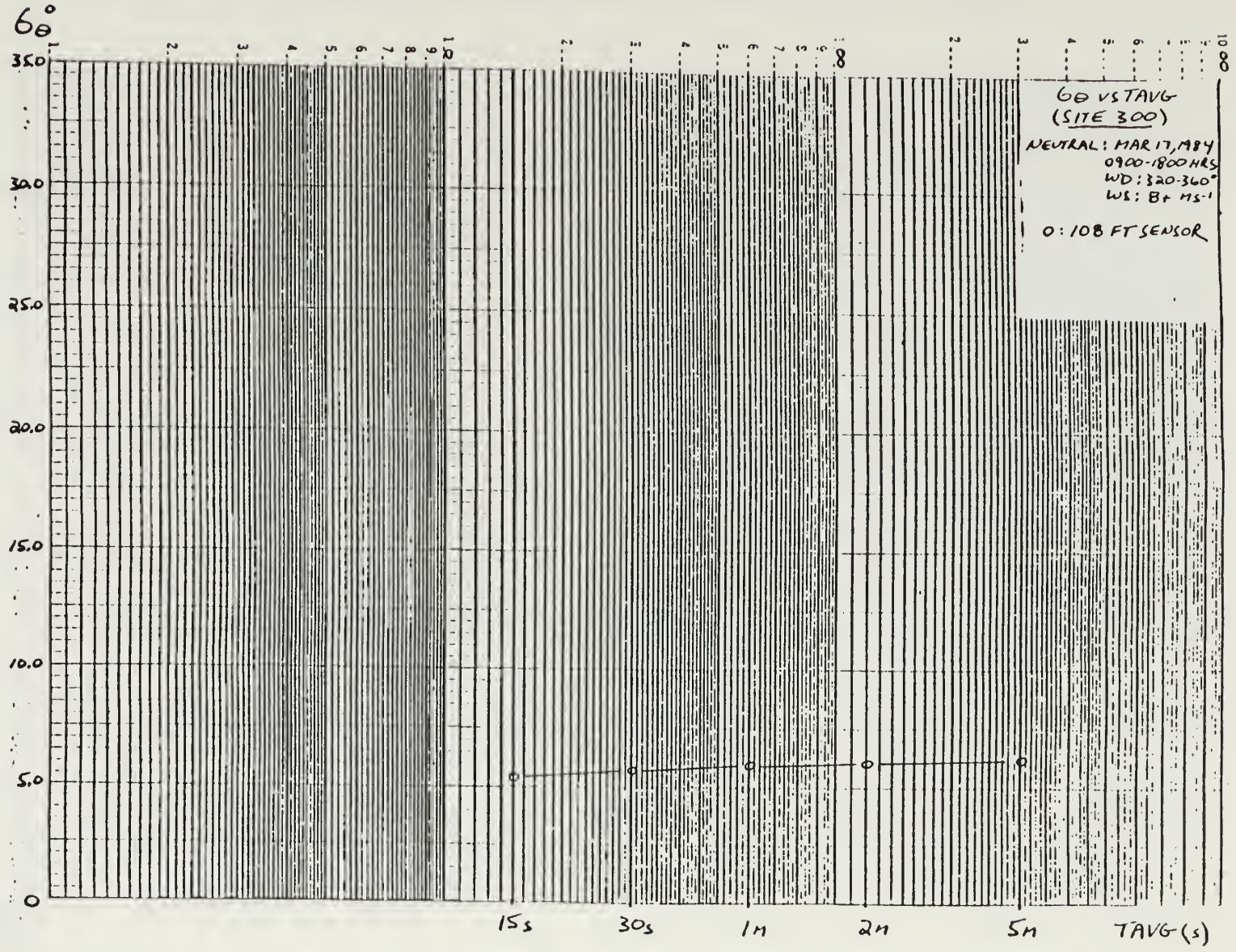

Figure 26(b). σθ vs TAVG (Site 300) (3/17/84 (0900-1800)--Neutral)

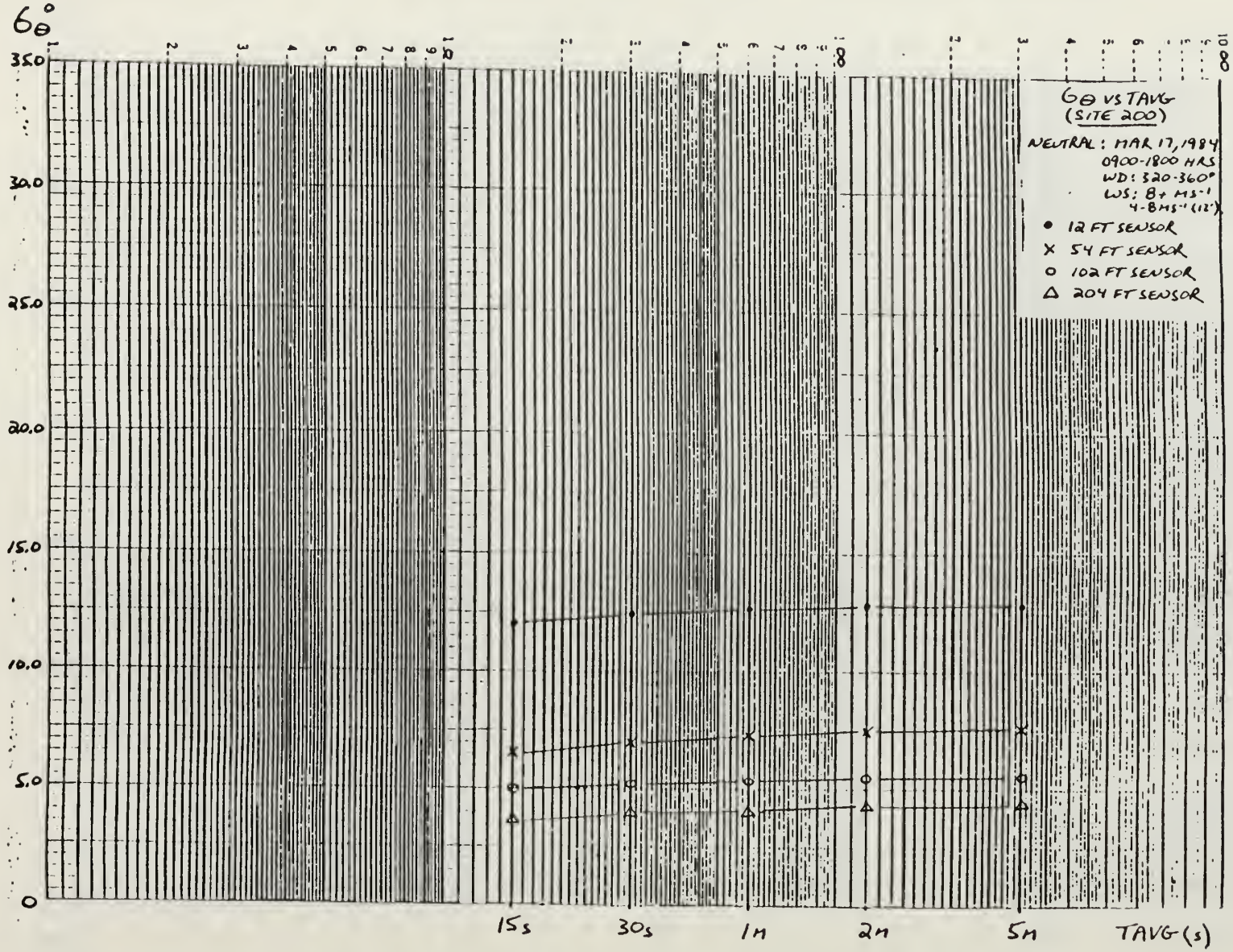

Figure 26(c). σθ vs TAVG (Site 200) (3/17/84 (0900-1800)--Neutral)

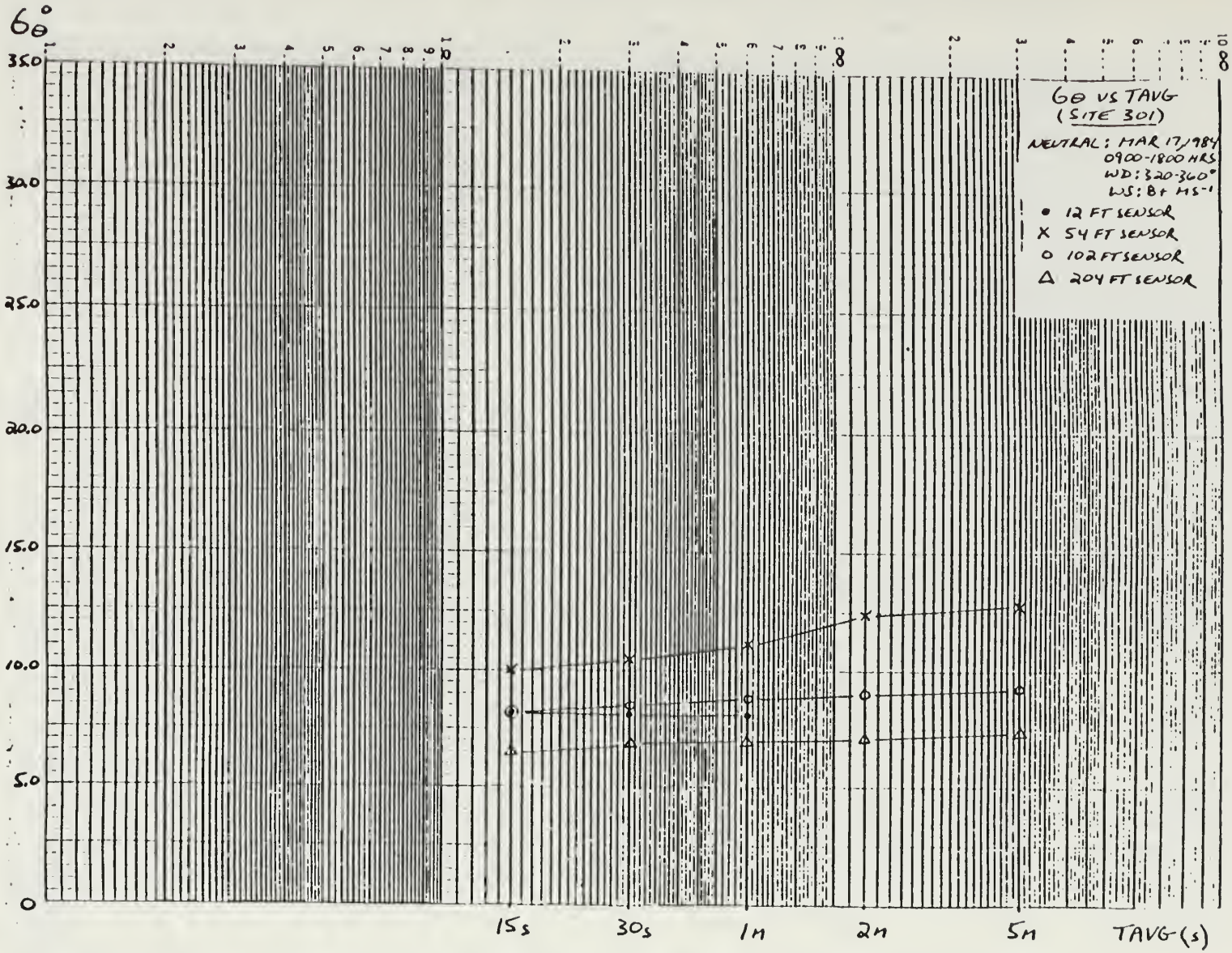

Figure 26(d). σθ vs TAVG (Site 301) (3/17/84 (0900-1800)--Neutral)

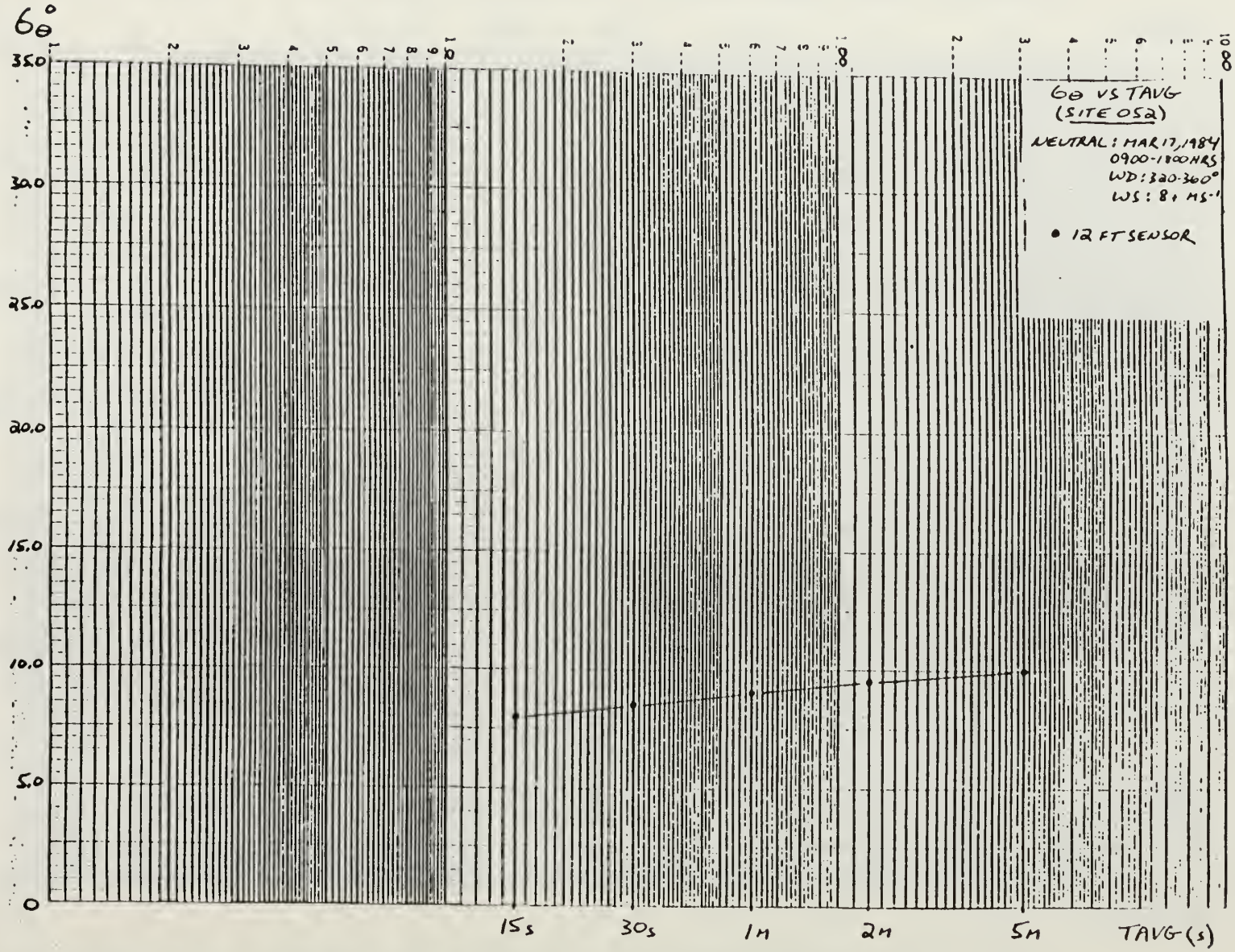

Figure 26(e). σθ vs TAVG (Site 052) (3/17/84 (0900-1800)--Neutral)

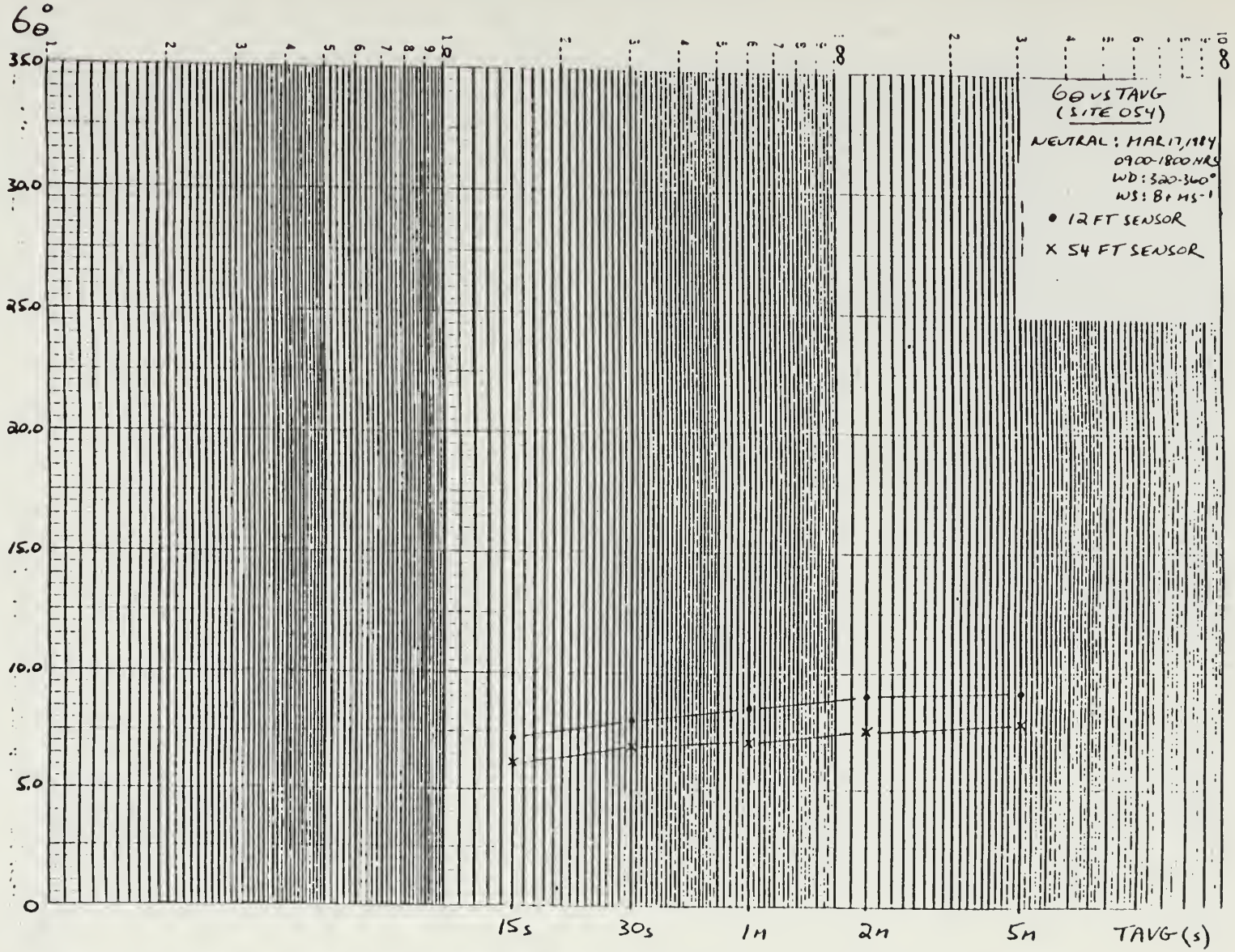

Figure 26(f). σθ vs TAVG (Site 054) (3/17/84 (0900-1800)--Neutral)

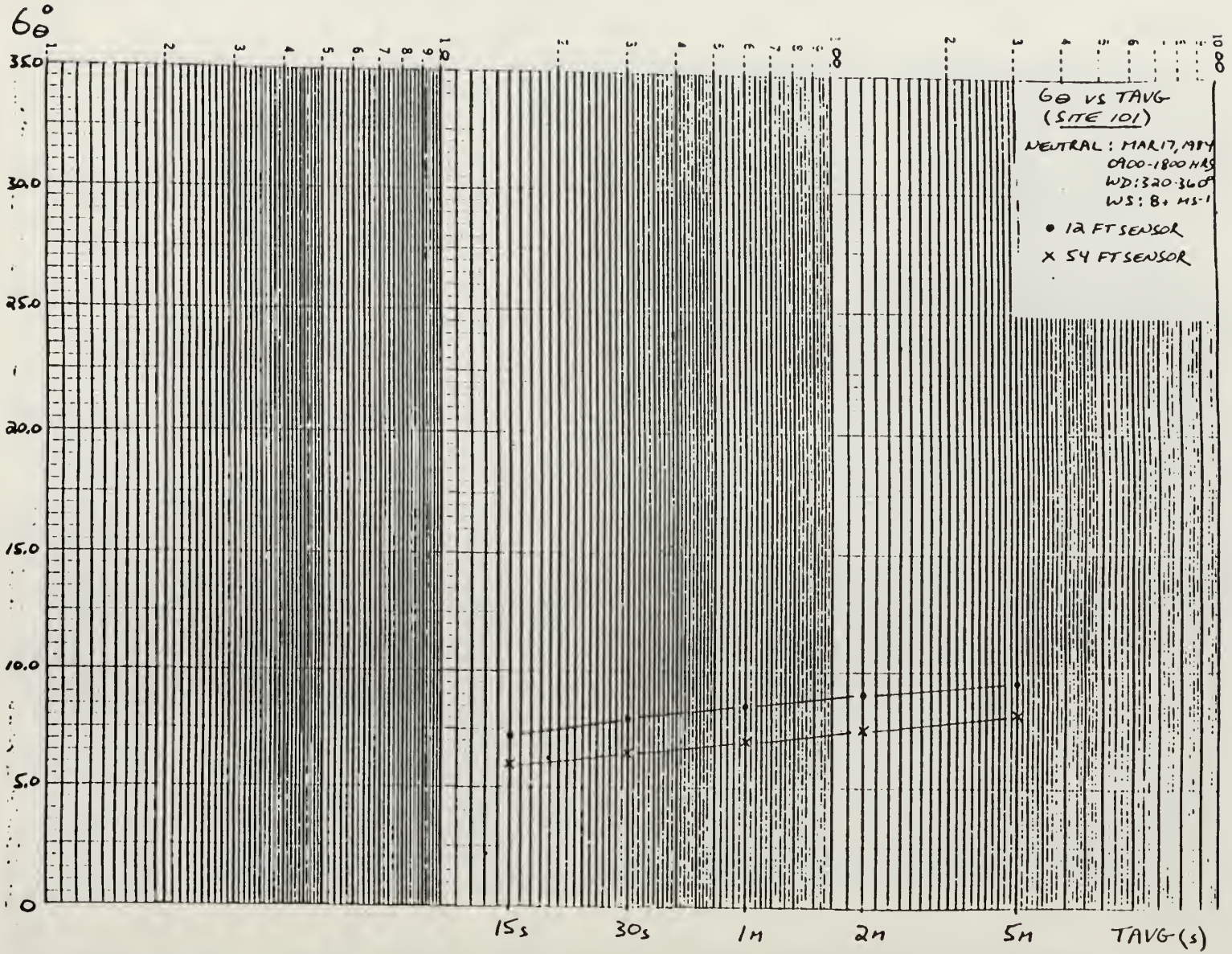

Figure 26(g). σθ vs TAVG (Site 101) (3/17/84 (0900-1800)--Neutral)

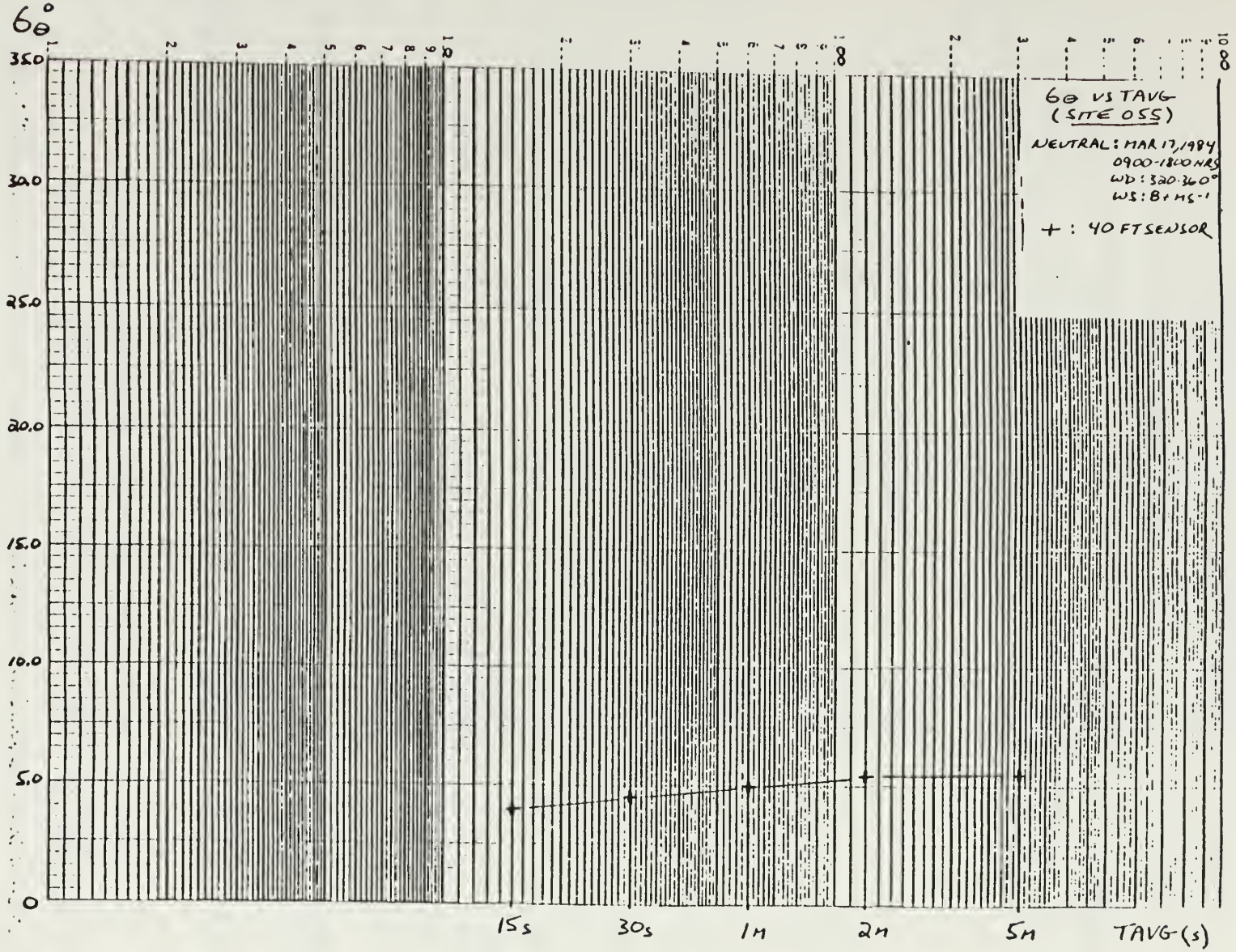

Figure 26(h). σθ vs TAVG (Site 055) (3/17/84 (0900-1800)--Neutral)

TABLE XXVII

$\sigma\theta$ Dependence on Wind Direction
(3/17/84 (0900-1800)--Neutral)

		WIND DIRECTION		
Sensor	Site-Ht	8	9	1
3	052-12'	7.7	7.9*	6.3
4	054-12'	8.7	7.2*	----
5	101-12'	14.1	7.3*	7.5
6	102-12'	7.5	7.8*	----
7	200-12'	12.1	12.2*	13.5
10	301-12'	----	8.2*	----
13	055-40'	----	4.1*	10.6
11	052-54'	7.8	5.9*	3.8
12	054-54'	8.3	6.2*	----
15	101-54'	6.4	5.9*	5.6
18	200-54'	6.8	6.6*	----
20	301-54'	----	10.0*	7.9
21	102-102'	4.8	4.7*	----
22	200-102'	5.9	5.0*	----
25	301-102'	----	8.2*	5.0
24	299-108'	6.0	5.3*	----
26	200-204'	3.3	3.7*	----
28	301-204'	10.9	6.5*	11.1

NOTE: Most representative values listed above ($\sigma\theta$ in degrees)
* = Predominant wind direction
Time averaging 15 seconds
Wind speed 8+ ms^{-1} except for sensors 6 and 8 (4-8 ms^{-1})
Wind Direction 8: 280-320 degrees
Wind Direction 9: 320-360 degrees
Wind Direction 1: 000-040 degrees

b. Site/Sensor Elevation Dependence

Figures 27(a-h)/Tables D-(9-16) show $\sigma\theta$ dependence on wind direction for various sensor elevations at specific sites (* = Predominant Wind Direction). A terrain analysis later in this section will examine $\sigma\theta$ differences between sites and $\sigma\theta$ dependence on wind direction relative to the sites.

4. $\sigma\theta$ Dependence on Wind Speed

a. General Results

The predominant wind speed for all sensors varied in this case depending mostly upon sensor elevation. The 12' sensors averaged 6-10 ms^{-1}, the 54' sensors averaged 8-12 ms^{-1}, the 102' sensors averaged 10-12 ms^{-1}, and the 204' sensors averaged 12-16 ms^{-1}. The lowest $\sigma\theta$ values were associated with the highest wind speeds at all sensors and, conversely, the highest $\sigma\theta$ values were associated with the lowest wind speeds. The range of $\sigma\theta$ values over all sensors and for all wind speeds was 4-12° and only a modest decrease in these values was evident with increasing height and with increasing wind speed. Table XXVIII describes the $\sigma\theta$ dependence on wind speed for all sensors and indicates the predominant wind speed at each sensor level as well.

b. Site/Sensor Elevation Dependence

Figures 28(a-h)/Tables D-(17-24) show $\sigma\theta$ dependence on wind speed for various sensor elevations at specific sites (* = Predominant Wind Speed). The following section examines

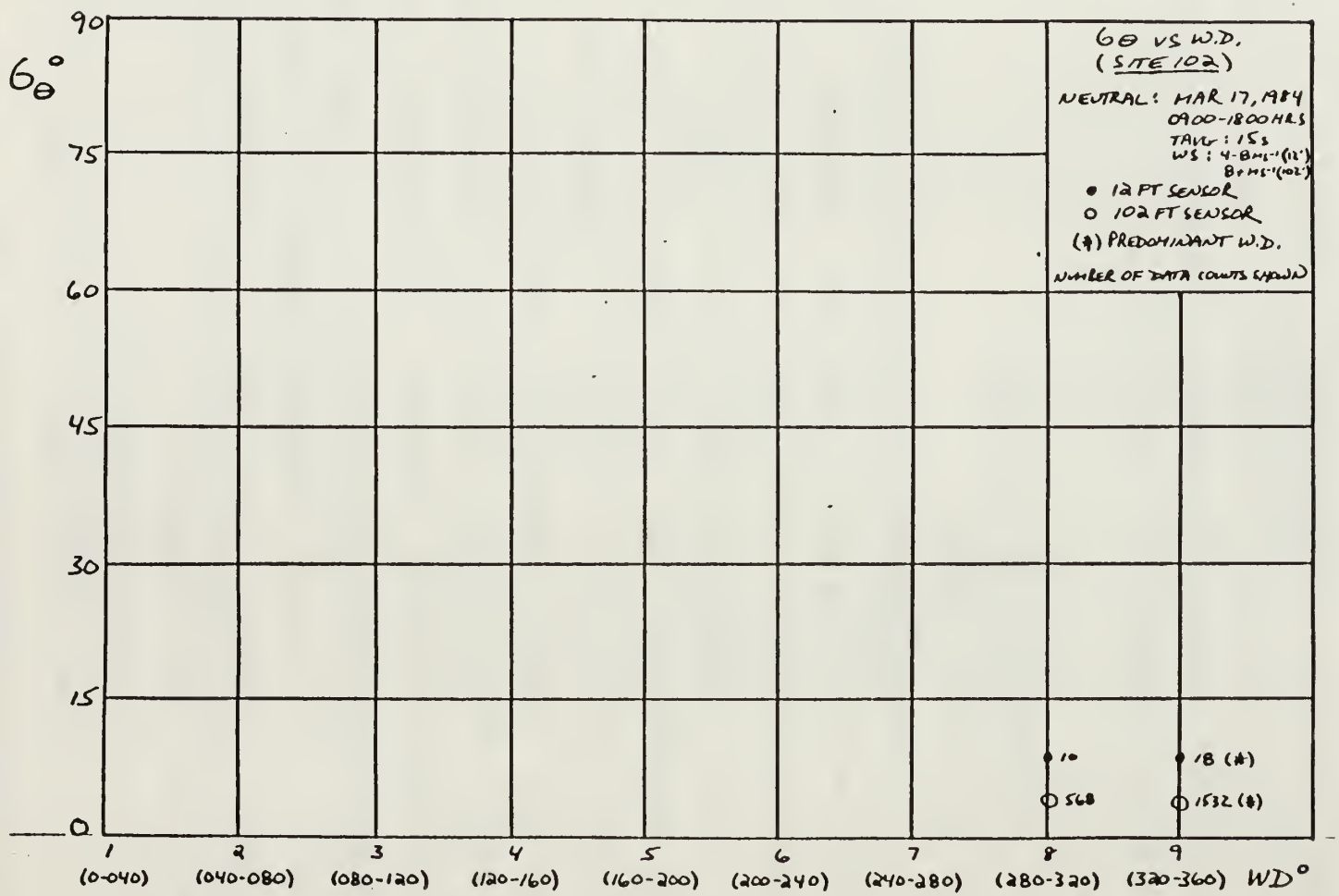

Figure 27(a). $\sigma\theta$ vs WD (Site 102) (3/17/84 (0900-1800)--Neutral)

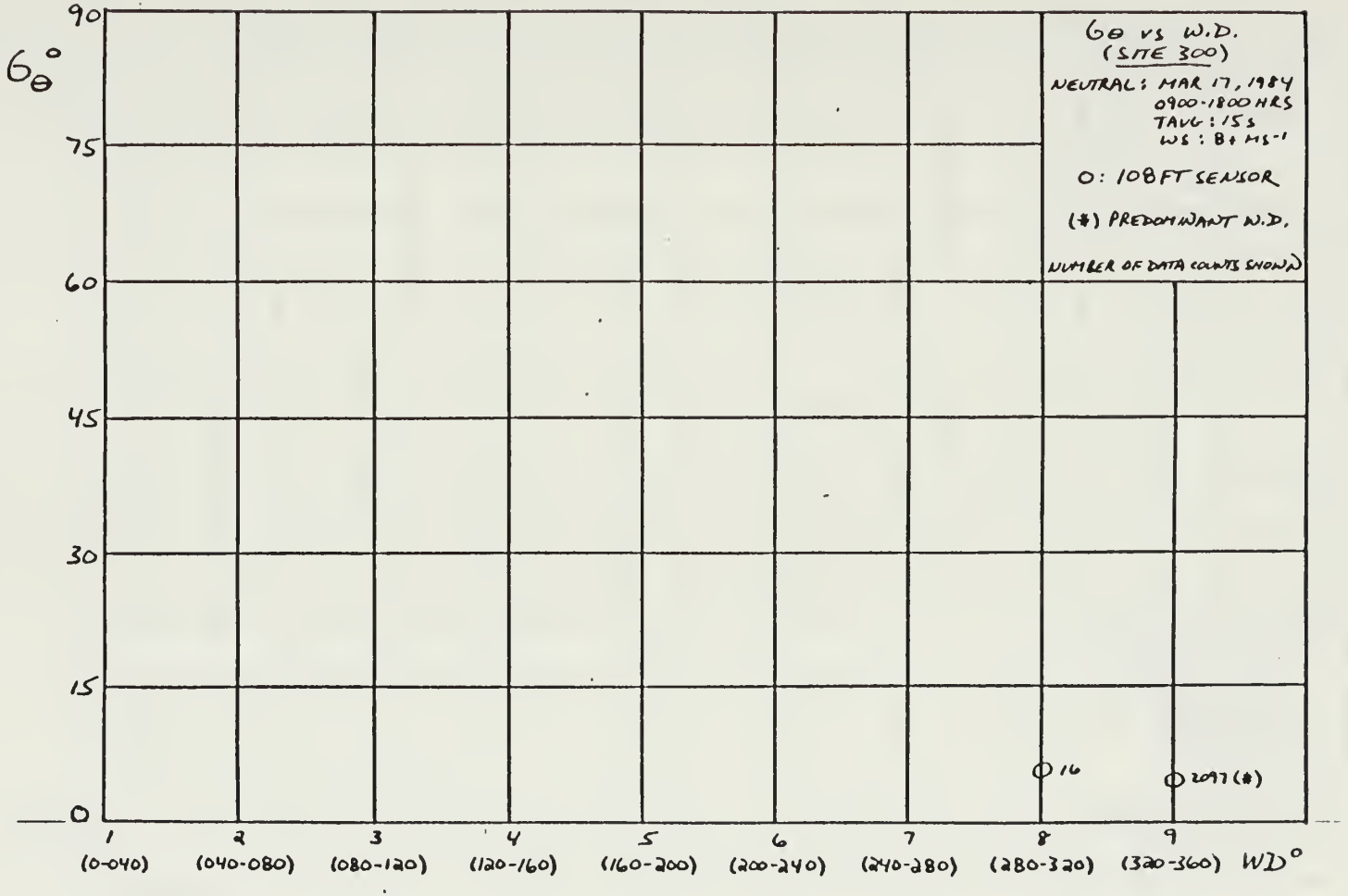

Figure 27(b). σθ vs WD (Site 300) (3/17/84 (0900-1800)--Neutral)

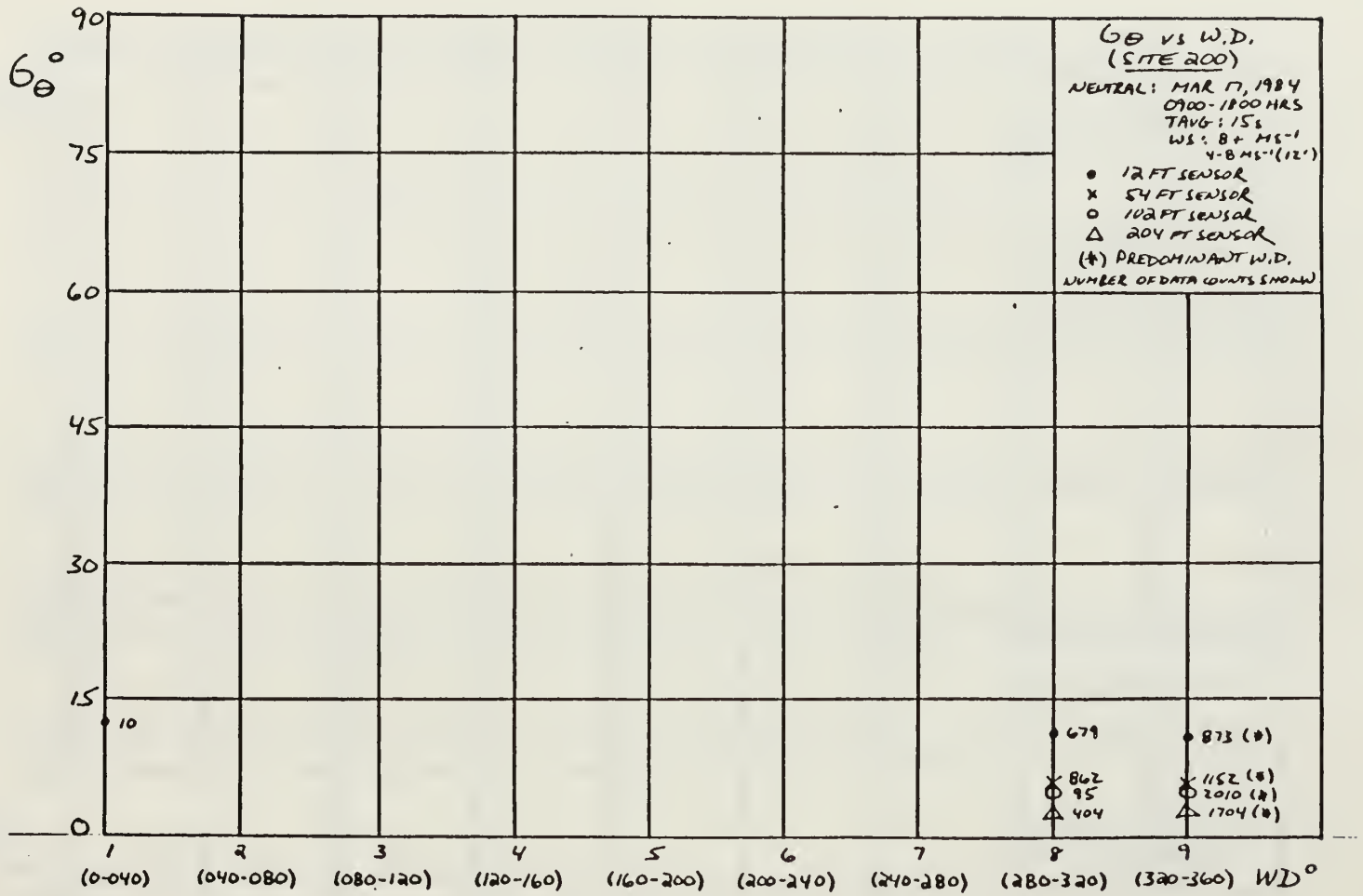

Figure 27(c). σθ vs WD (Site 200) (3/17/84 (0900-1800)--Neutral)

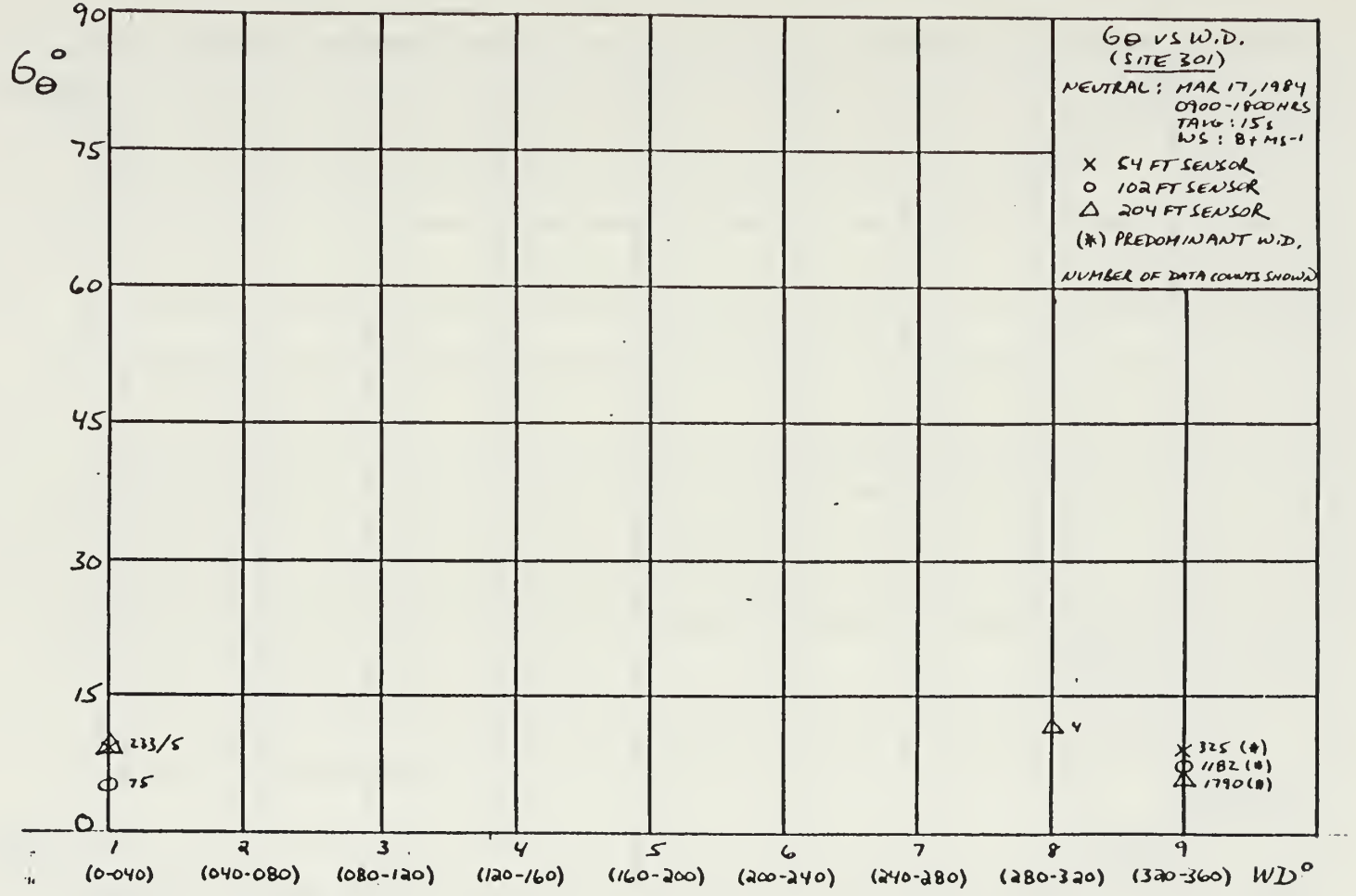

Figure 27(d). $\sigma\theta$ vs WD (Site 301) (3/17/84 (099-1800)--Neutral)

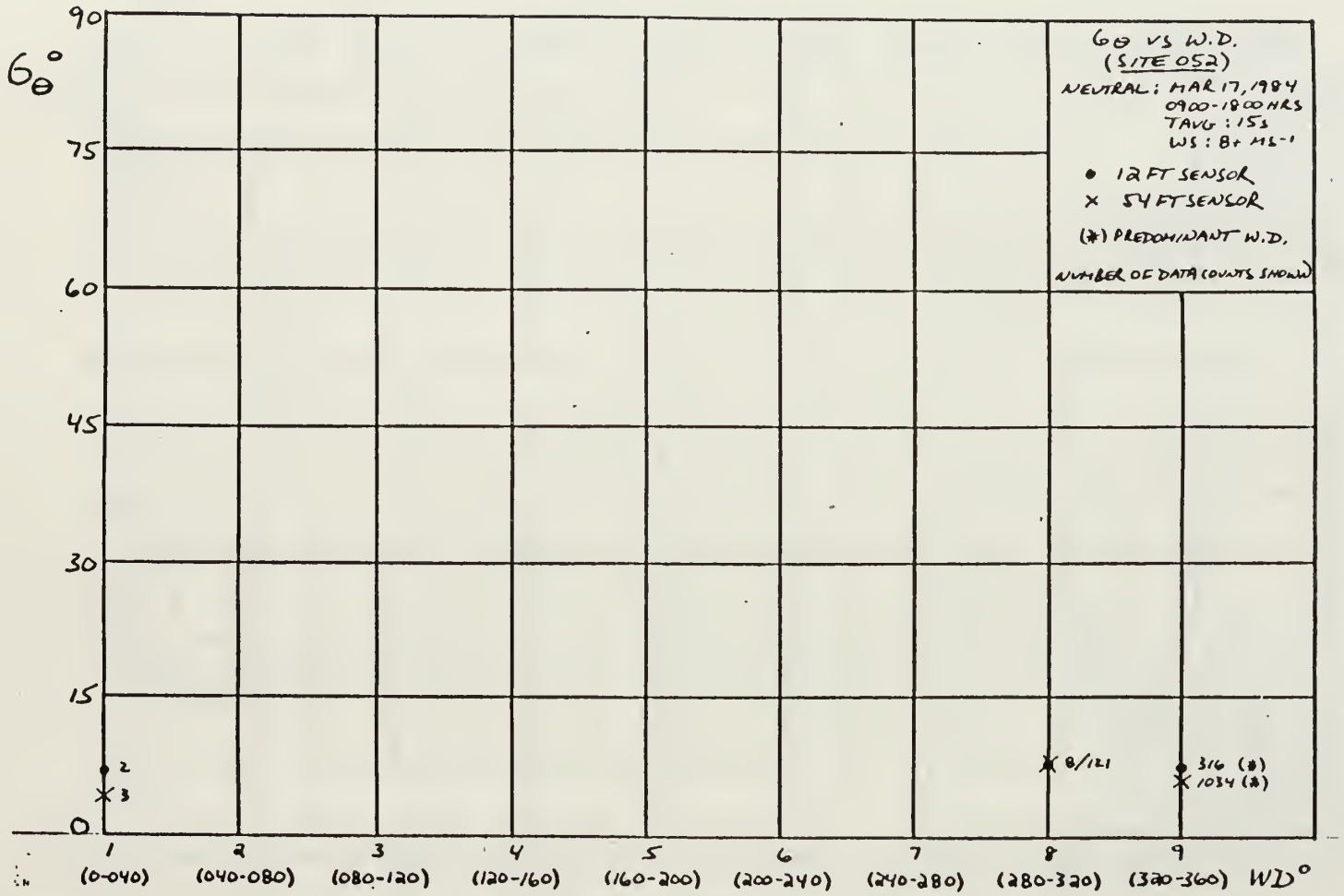

Figure 27(e). σθ vs WD (Site·052) (3/17/84 (0900-1800)--Neutral)

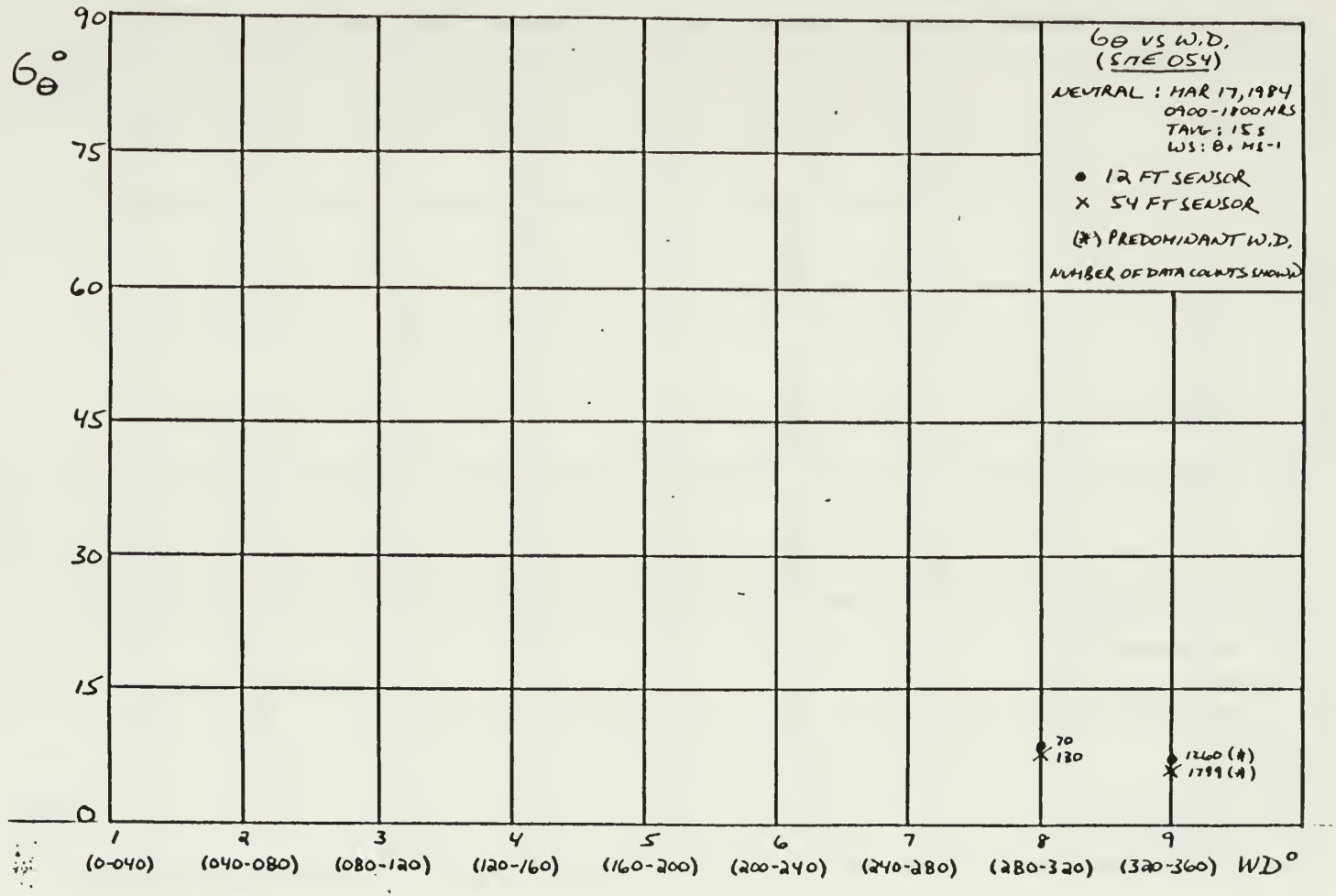

Figure 27(f). σθ vs WD (Site 054) (3/17/84 (0900-1800)--Neutral)

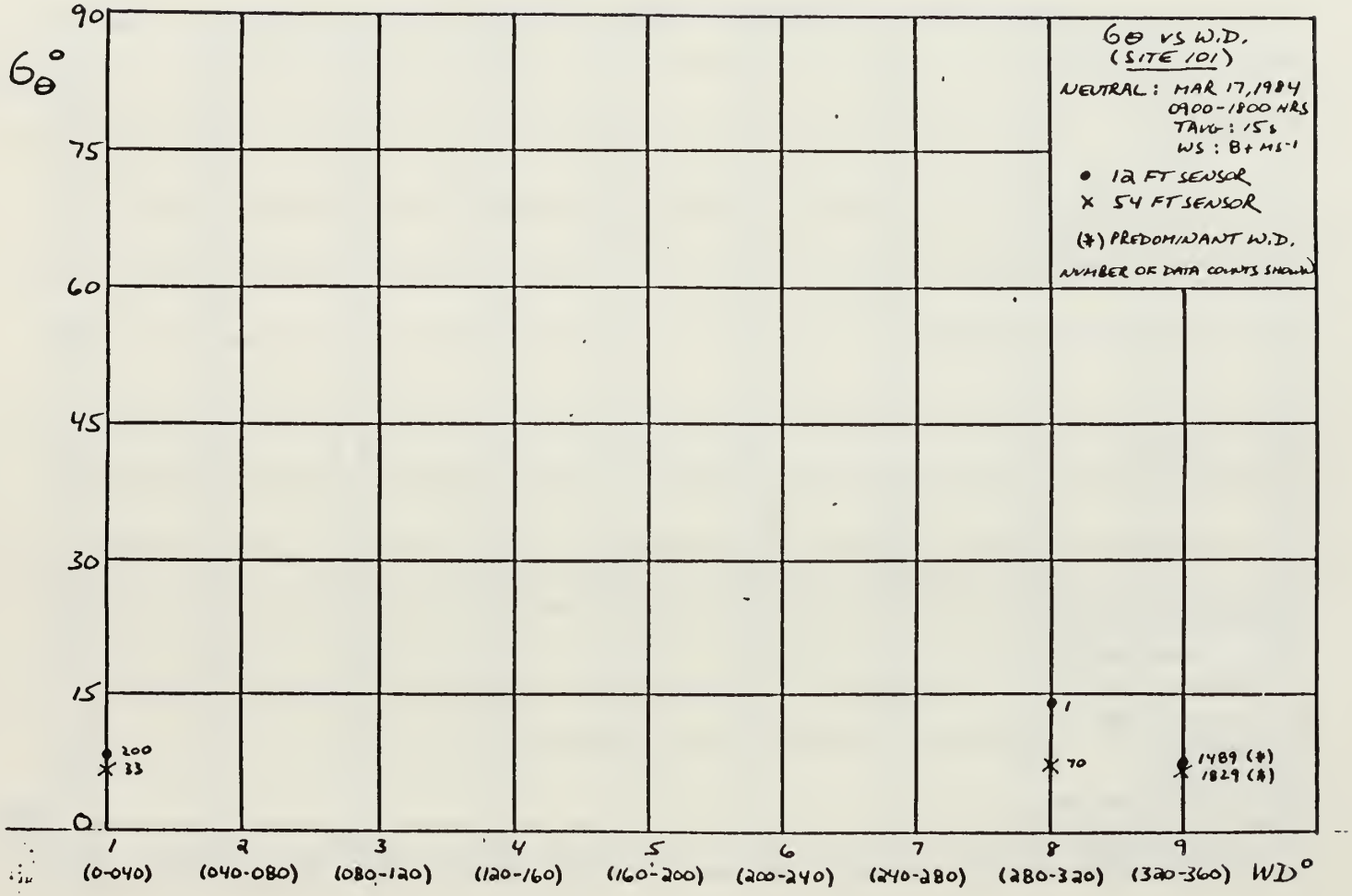

Figure 27(g). σθ vs WD (Site 101) (3/17/84 (0900-1800)--Neutral)

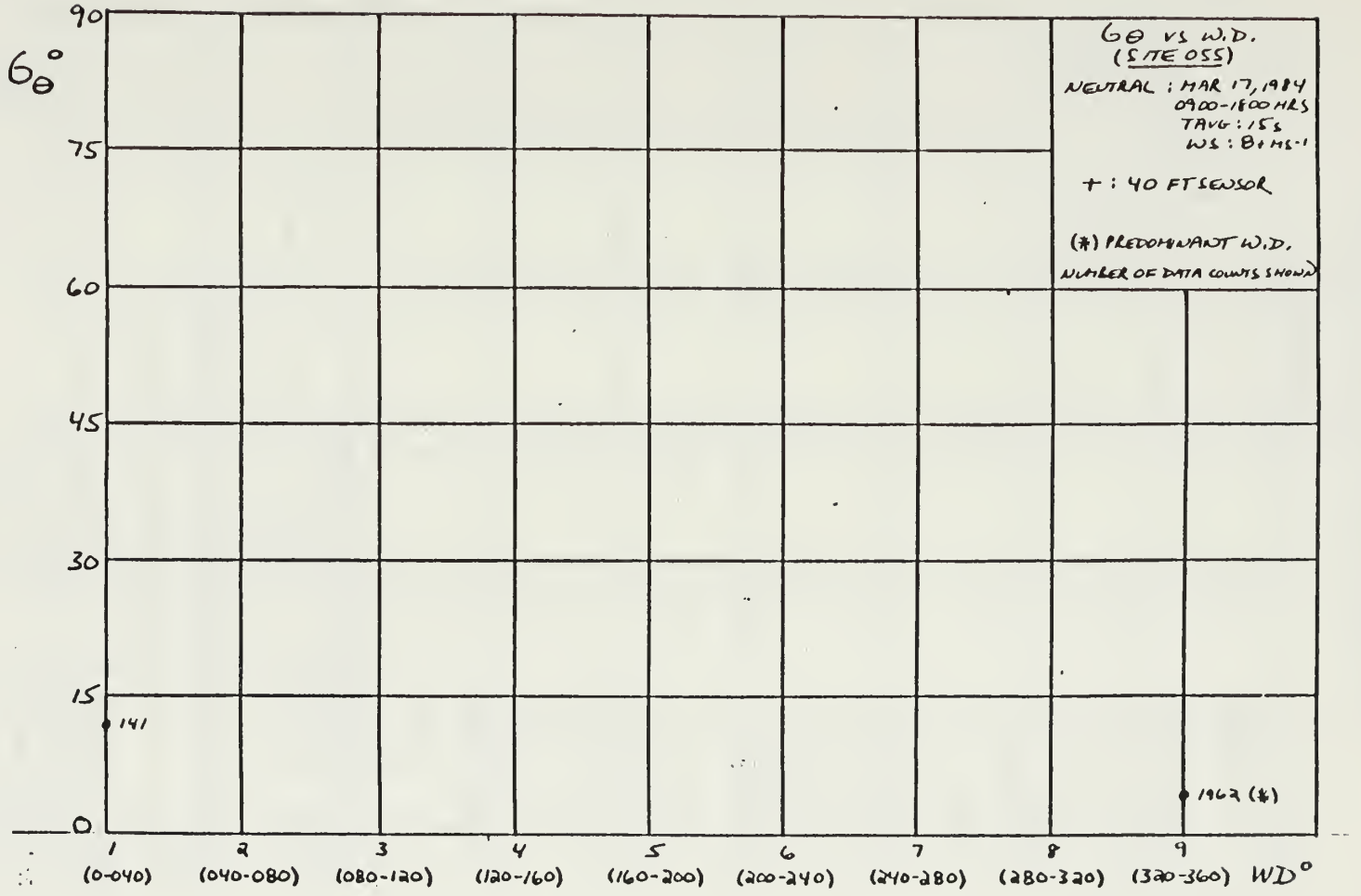

Figure 27(h). $\sigma\theta$ vs WD (Site 055) (3/17/84 (0900-1800)--Neutral)

TABLE XXVIII

$\sigma\theta$ Dependence on Wind Speed
(3/17/84 (0900-1800)--Neutral)

		WIND SPEED				
Sensor	Site-Ht	4	5	6	7	8
3	052-12'	9.4	8.0*	7.7	7.3	6.5
4	054-12'	10.1	7.7*	6.0	4.5	----
5	101-12'	9.8	7.9*	6.5	6.1	----
6	102-12'	5.7	----	----	----	----
8	200-12'	11.5*	9.9	8.4	----	----
10	301-12'	----	8.2*	----	----	----
13	055-40'	----	----	8.9	8.1	6.1
11	052-54'	12.8	8.2	6.3*	5.1	4.0
12	054-54'	9.2	7.5	5.6*	4.4	3.4
15	101-54'	9.0	6.8*	5.1	4.6	3.9
18	200-54'	10.2	8.1	6.5*	5.3	4.9
20	301-54'	13.4	11.4*	8.5	5.8	7.2
21	102-102'	8.3	6.7	5.1*	4.1	3.2
22	200-102'	7.5	6.6	5.4*	4.4	3.9
25	301-102'	11.1	10.0*	7.4	5.5	4.5
24	299-108'	----	----	7.2	6.5	6.4
26	200-204'	----	----	6.0	4.6	3.4*
28	301-204'	11.3	9.2	7.3	5.8*	5.4

NOTE: Most representative values listed above ($\sigma\theta$ in degrees)
* = Predominant wind speed
Time averaging 15 seconds
Wind direction onshore (200-360 degrees)
Sensor 6: Predominant WD 4-6 ms^{-1}
Sensor 13: Predominant WS 18+ ms^{-1}
Sensor 24: Predominant WS 18+ ms^{-1}
Wind Speed 4: 6-8 ms^{-1}
Wind Speed 5: 8-10 ms^{-1}
Wind Speed 6: 10-12 ms^{-1}
Wind Speed 7: 12-14 ms^{-1}
Wind Speed 8: 14-16 ms^{-1}

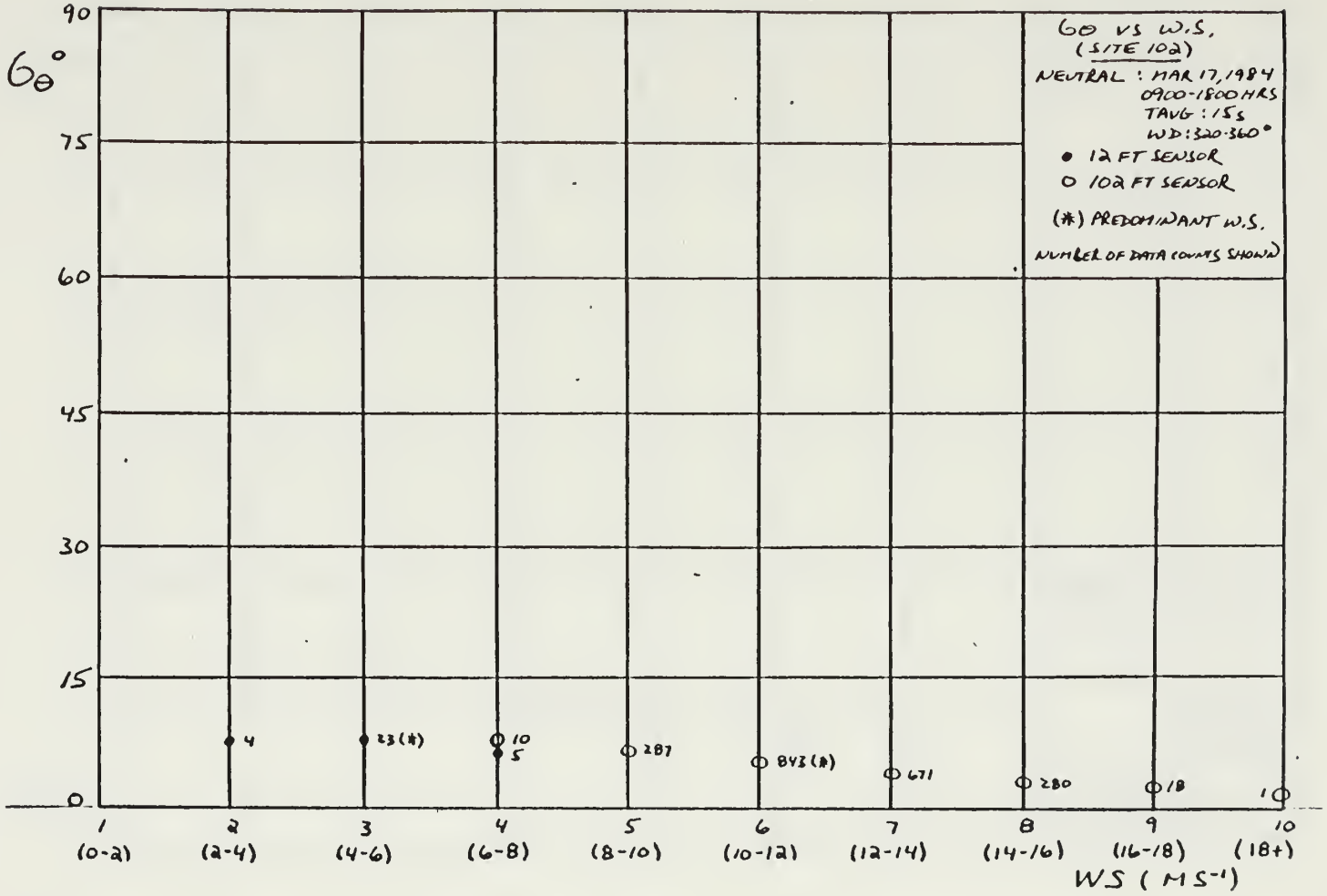

Figure 28(a). σθ vs WS (Site 102) (3/17/84 (0900-1800)--Neutral)

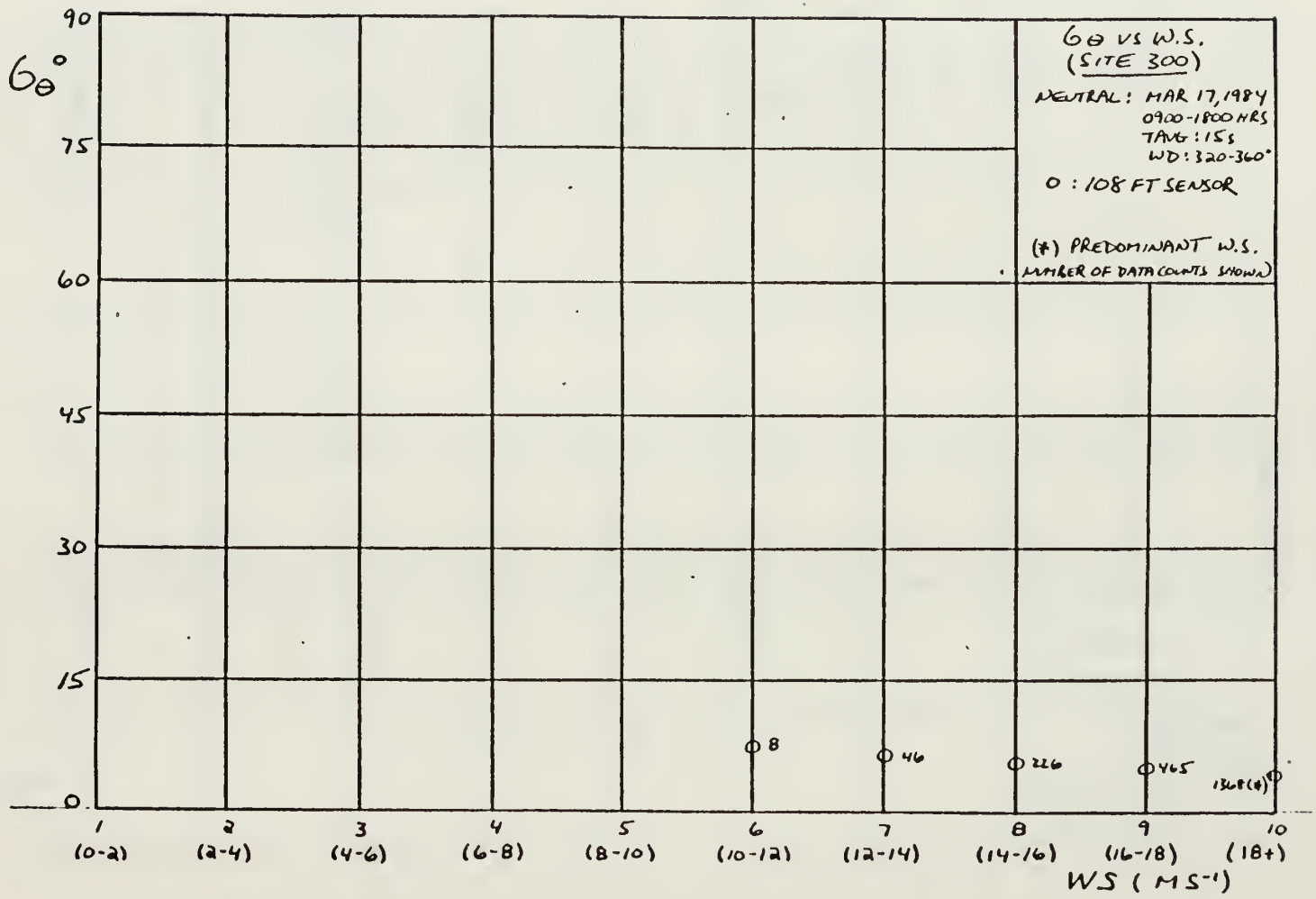

Figure 28(b). σθ vs WS (Site 300) (3/17/84 (0900-1800)--Neutral)

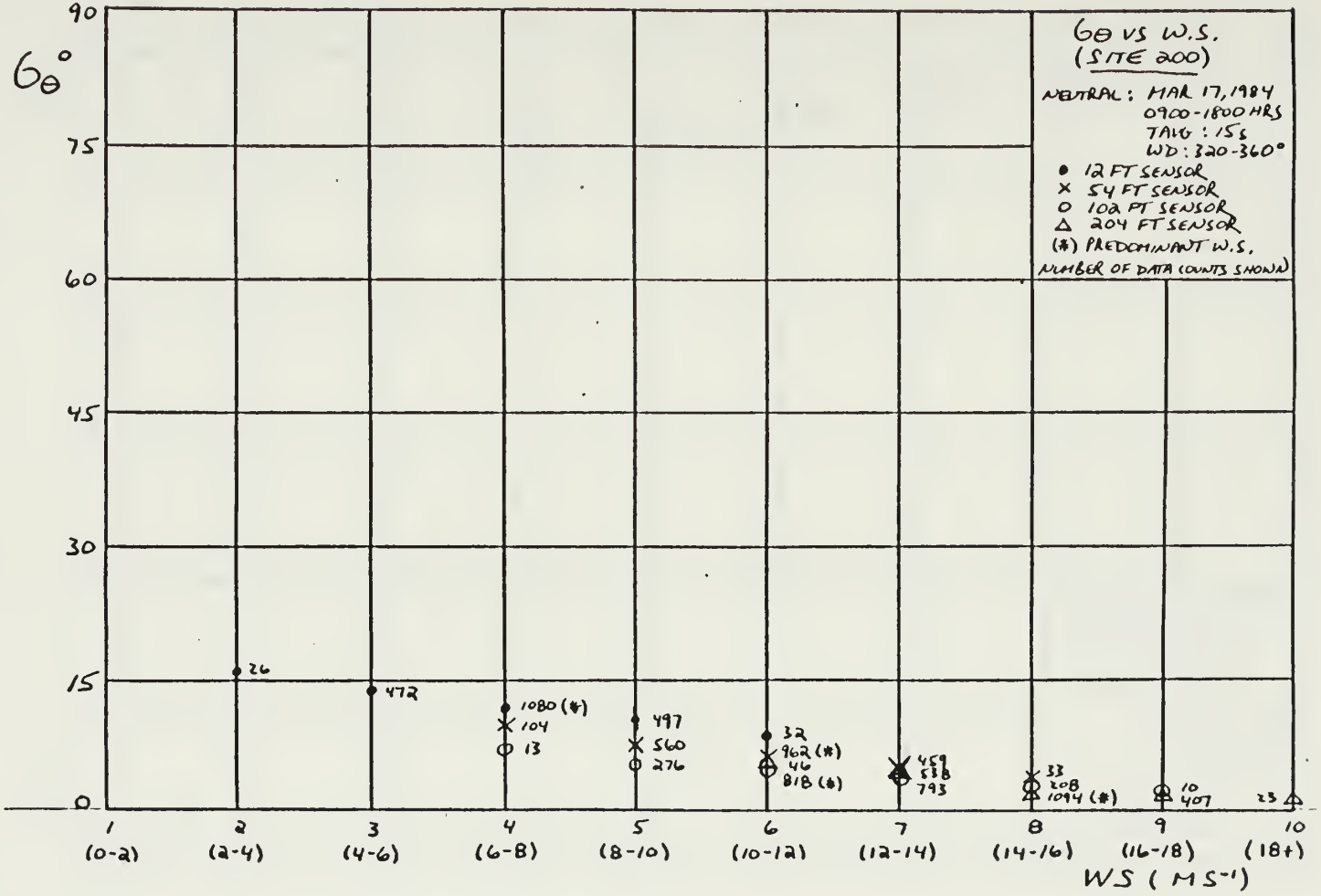

Figure 28(c). σθ vs WS (Site 200) (3/17/84 (0900-1800)--Neutral)

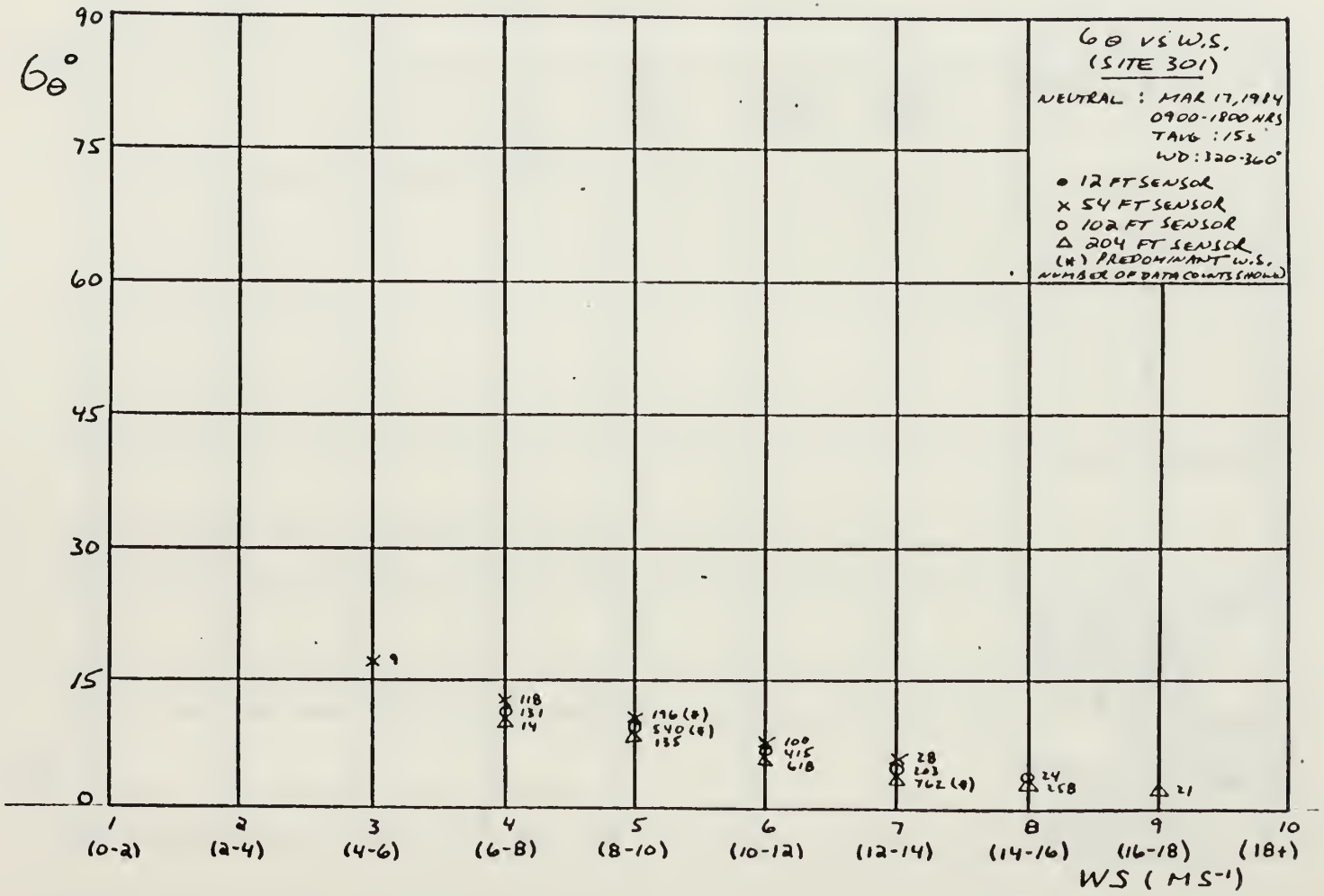

Figure 28(d). σθ vs WS (Site 301) (3/17/84 (0900-1800)--Neutral)

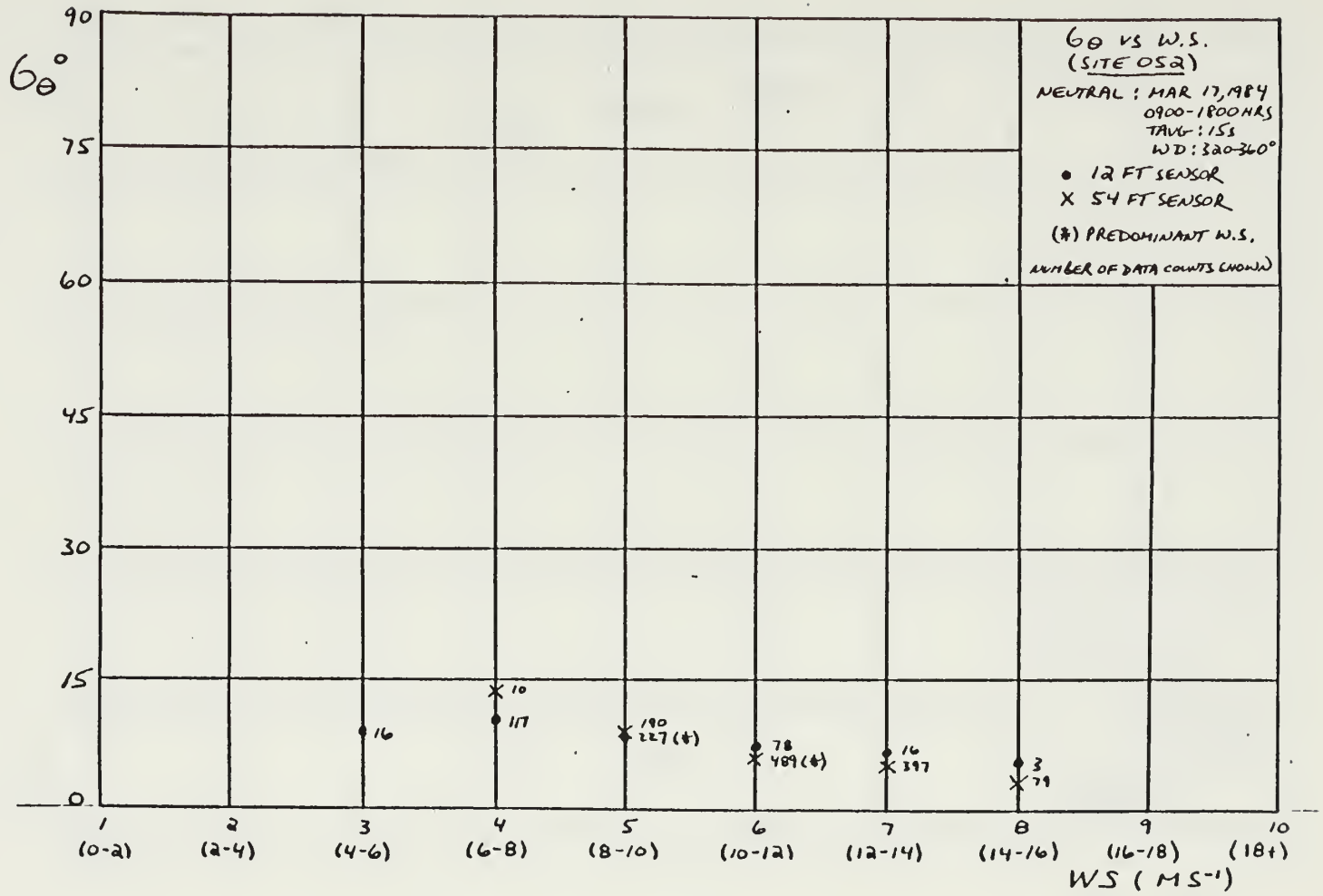

Figure 28(e). $\sigma\theta$ vs WS (Site 052) (3/17/84 (0900-1800)--Neutral)

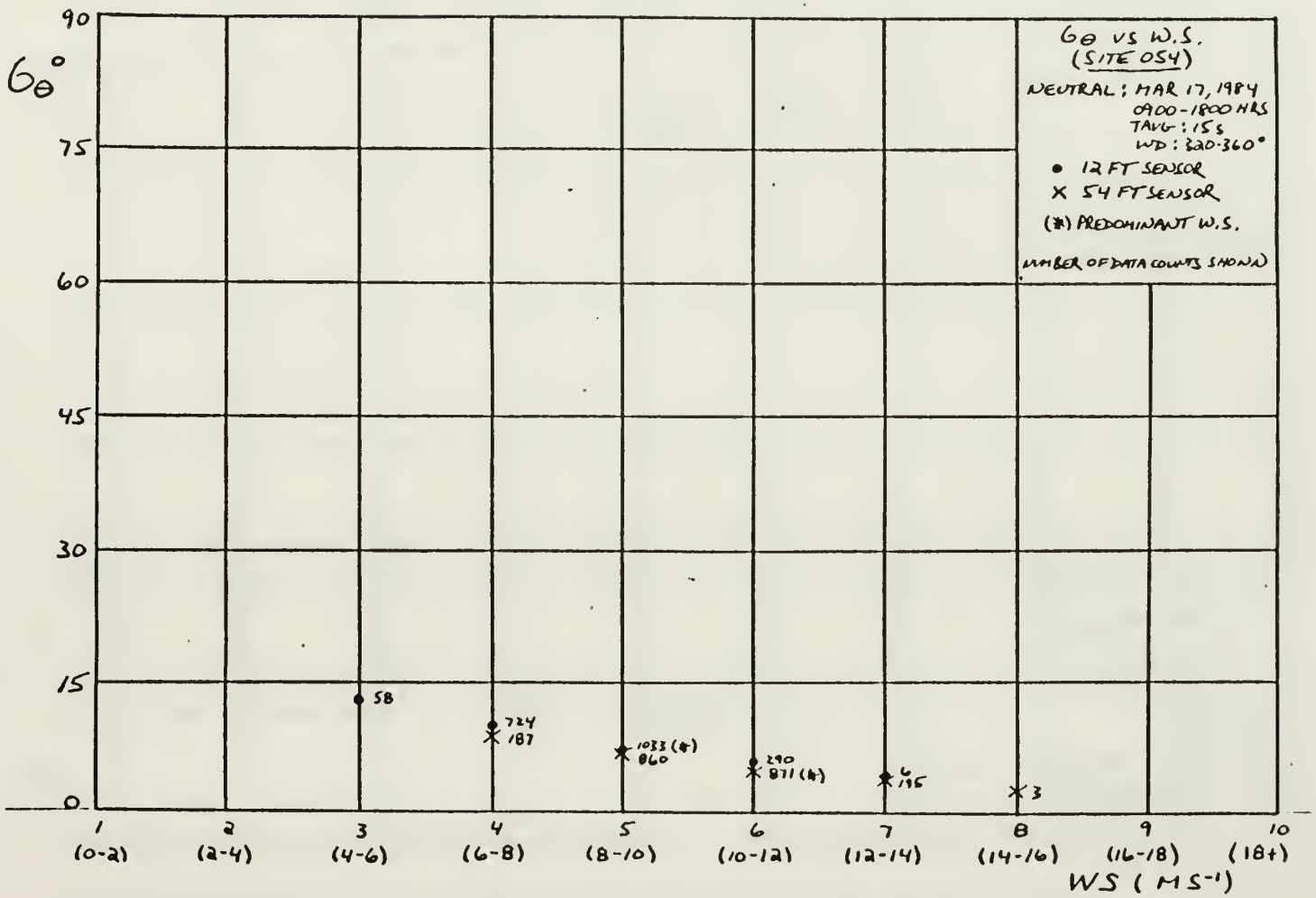

Figure 28(f). σθ vs WS (Site 054) (3/17/84 (0900-1800)--Neutral)

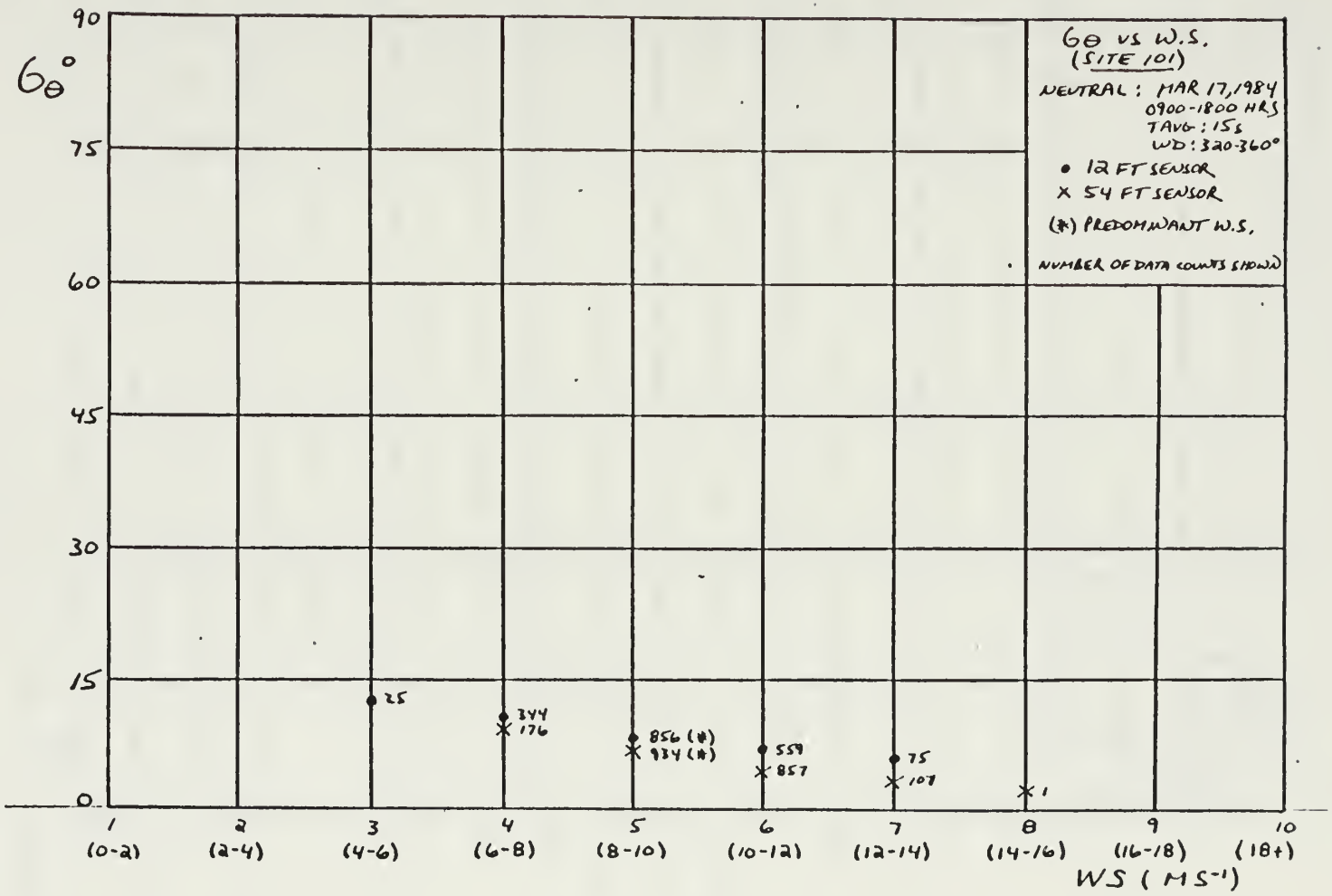

Figure 28(g). σθ vs WS (Site 101) (3/17/84 (0900-1800)--Neutral)

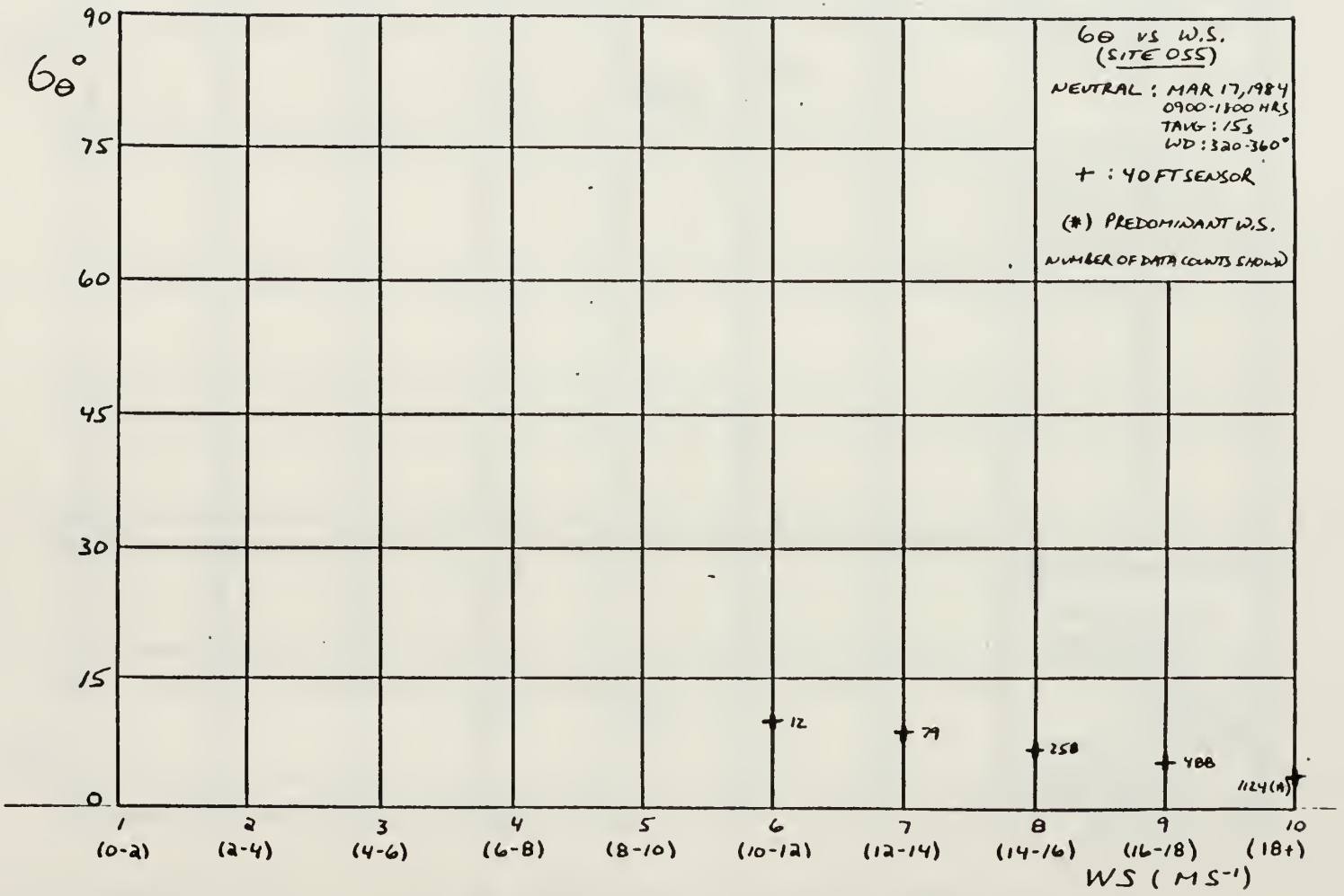

Figure 28(h). σθ vs WS (Site 055) (3/17/84 (0900-1800)--Neutral)

the $\sigma\theta$ differences between sites and $\sigma\theta$ dependences on wind speed relative to the sites.

5. Terrain Dependence

Figure 29(a) summarizes the site $\sigma\theta$ results for various time averages as they relate to terrain characteristics. In this neutral case, $\sigma\theta$ values were between 4 and 12° at all sites/sensors and over all time averages. The minimal change in $\sigma\theta$ values with increased time averaging at all sites/sensors throughout the terrain is indicative of the strong and persistent flow associated with this case. It also shows that most of the energy is contained at the higher frequencies or shorter time averages with little change occurring with increasing time average. The $\sigma\theta$ values over all averaging times decreased with height at all sites. The relative lowest $\sigma\theta$ values were associated with the upper sensor levels at each site and the relative maximum values were associated with the lower sensor elevations at each site. Because of the strength, nature, and persistence of this flow, there was no significant $\sigma\theta$ dependence on terrain and very little dependence on time averaging.

Figure 29(b) describes $\sigma\theta$ dependence on wind direction throughout the terrain. This figure shows the lowest $\sigma\theta$ values to be associated with winds from 320-340° with higher $\sigma\theta$ values occurring with winds from 280-320° and 040-080°. The values of $\sigma\theta$ showed the least variation with wind direction at sites 102, 300, 200, and 101 with more of a variation

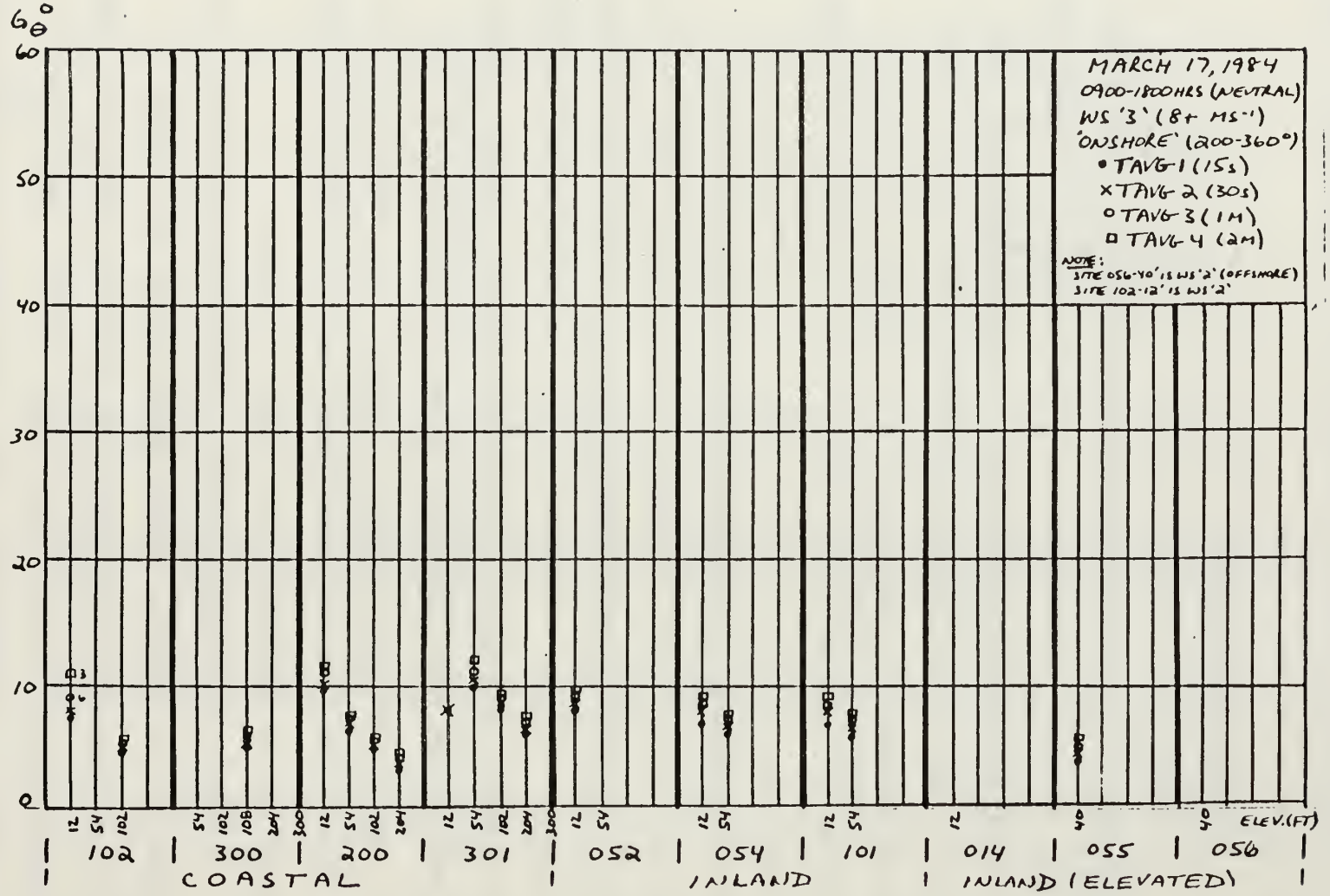

Figure 29(a). σθ vs TAVG (Terrain Analysis) (3/17/84 (0900-1800)--Neutral)

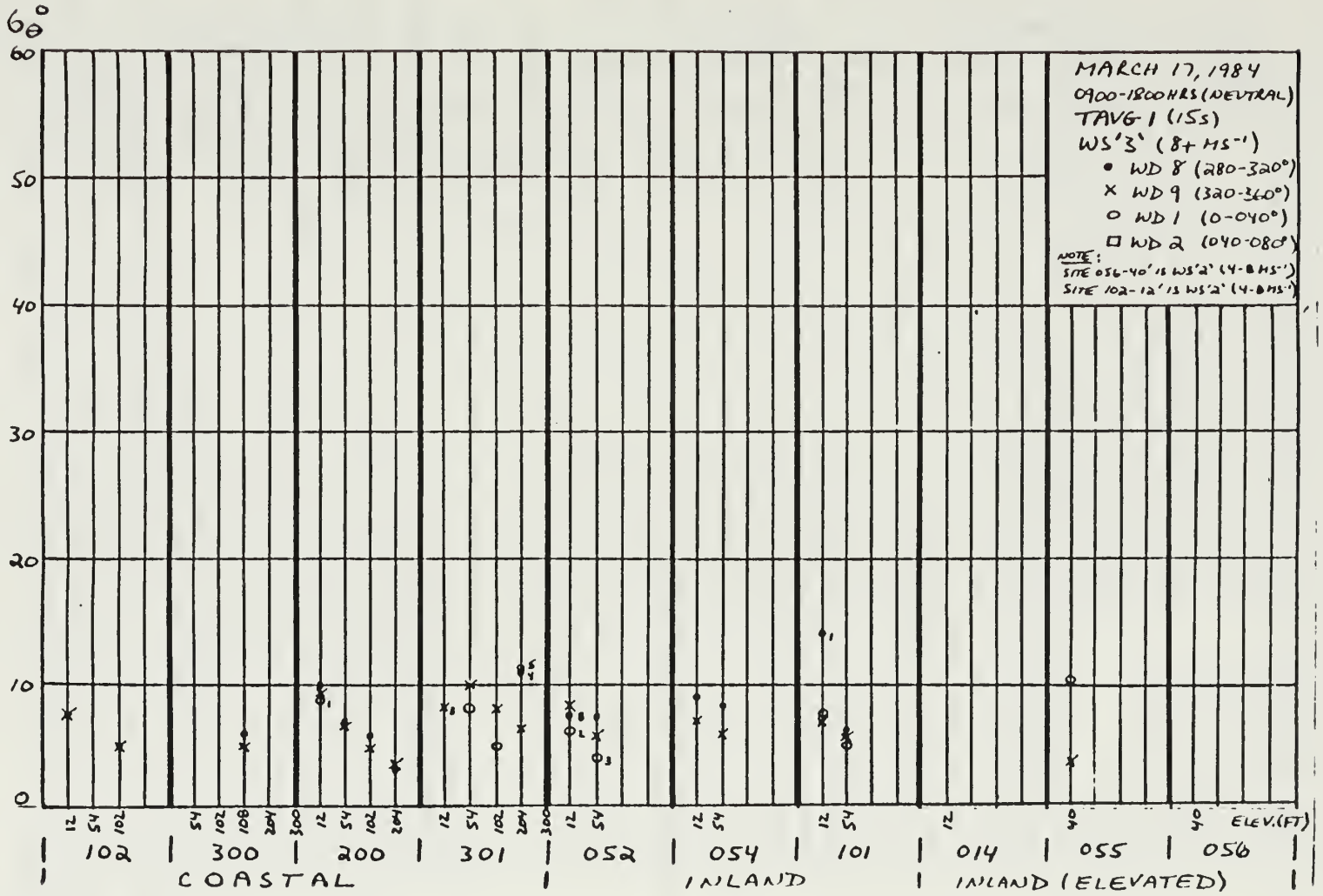

Figure 29(b). $\sigma\theta$ vs WD (Terrain Analysis) (3/17/84 (0900-1800)--Neutral)

REPRODUCED AT GOVERNMENT EXP

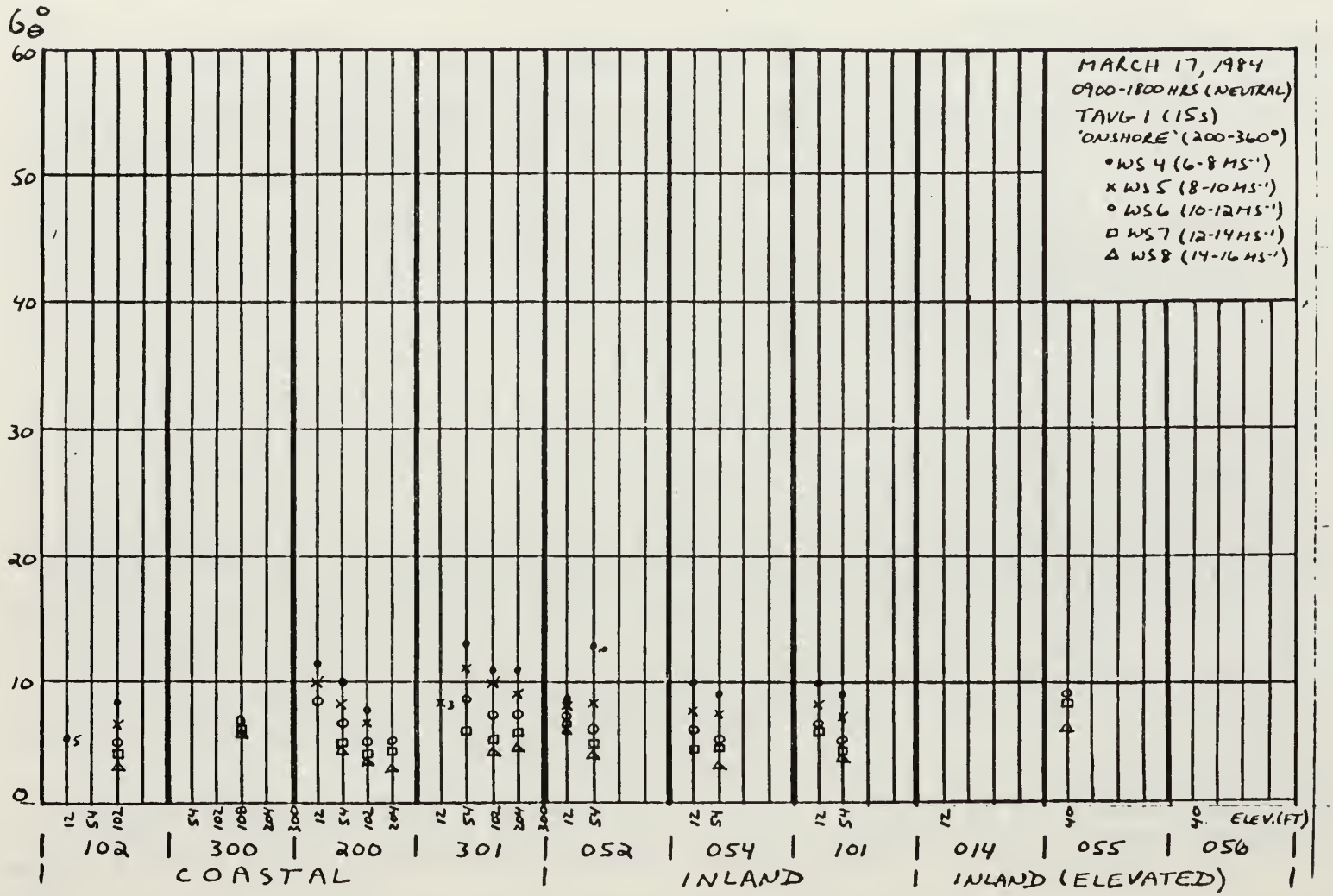

Figure 29(c). σθ vs WS (Terrain Analysis) (3/17/84 (0900-1800)--Neutral)

with wind direction occurring at sites 301, 052, 054, and 055. $\sigma\theta$ values decreased with increasing height throughout the terrain.

Finally, Figure 29(c) illustrates site $\sigma\theta$ results for various wind speed categories as they relate to terrain characteristics. This figure shows that $\sigma\theta$ does depend on wind speed in this case but that this dependence does not vary that much throughout the terrain. The lowest $\sigma\theta$ values were generally associated with the higher wind speeds at all sites. For all wind speeds, the $\sigma\theta$ values were less than 12 throughout the terrain and less than 6 when wind speeds exceeded 14 ms^{-1}. The values of $\sigma\theta$ also decreased slightly with increasing height at all sites with surface roughness characteristics apparently a factor in this difference.

E. INTERSTABILITY COMPARISON

Figure 30(a) illustrates the differences in the time averaging power law curves for the three stability cases studied. The highest $\sigma\theta$ values were apparent with the unstable case with the lower $\sigma\theta$ values associated with the stable and neutral cases. The observed unstable profile was closest to the empirical $x = 0.20$ profile with the next best fit associated with the observed stable profile ($x = 0.16$) and the worst fit in conjunction with the neutral profile ($x = 0.06$). The neutral case exhibited the largest difference between the observed and empirical profiles at long time averaging values (low frequencies).

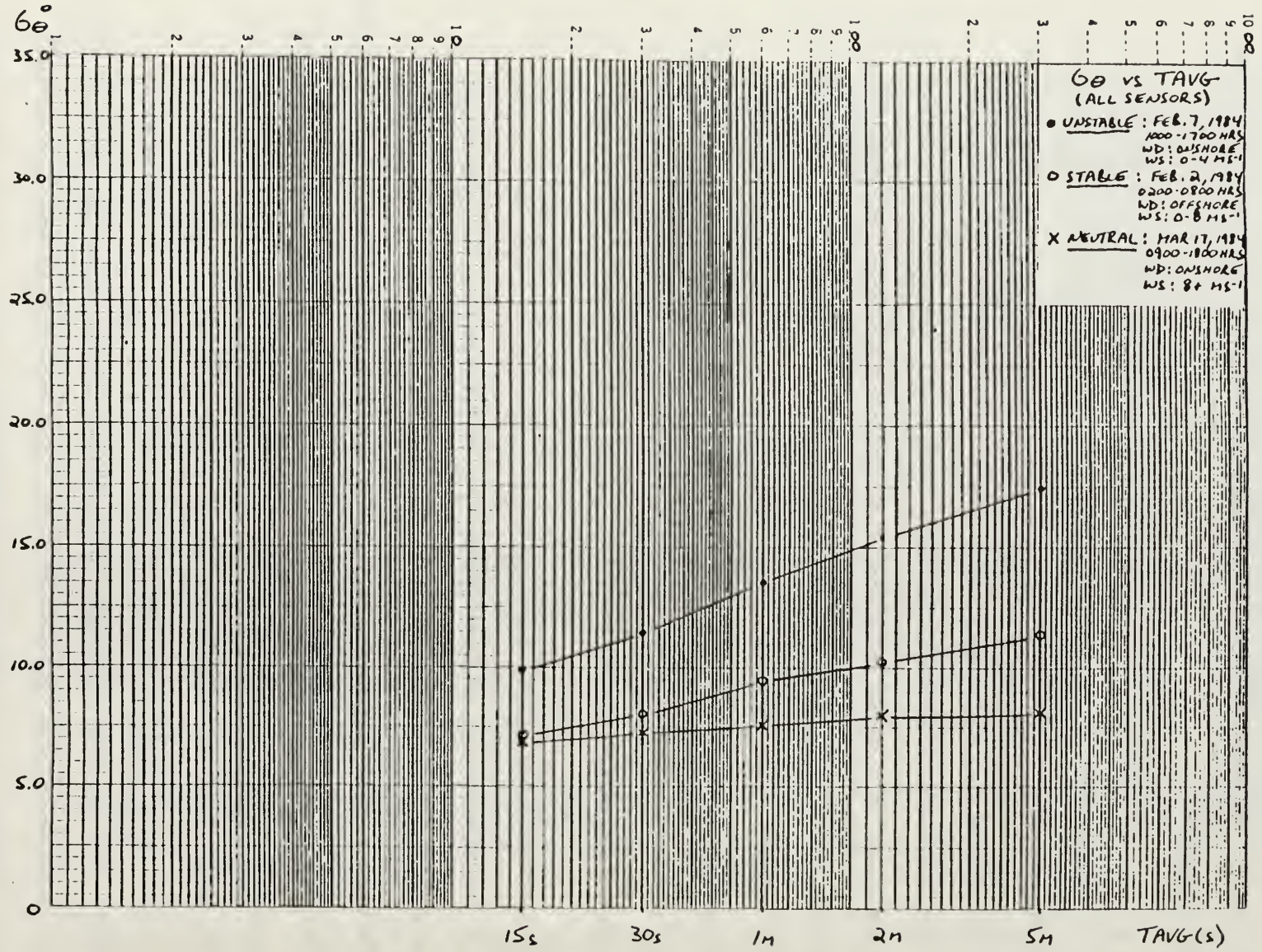

Figure 30(b). σθ vs TAVG (Interstability--All Sensors)

Figure 30(b)/Table XXIX shows an intercomparison of $\sigma\theta$ dependence on time averaging between the three stability case studies. The standard deviations of the $\sigma\theta$ values are noted in parentheses.

TABLE XXIX

$\sigma\theta$ vs TAVG (Interstability--All Sensors)

TAVG	Unstable	Neutral	Stable
15 s	9.9 (2.7)	6.9 (2.1)	7.1 (2.7)
30 s	11.5 (3.0)	7.3 (2.1)	8.1 (3.1)
1 m	13.6 (3.5)	7.6 (2.2)	9.5 (3.9)
2 m	15.4 (5.0)	8.0 (2.5)	10.3 (4.5)
5 m	17.4 (5.4)	8.2 (2.5)	11.4 (4.9)

This figure/table shows $\sigma\theta$ increasing with time averaging over all stabilities. The range of $\sigma\theta$ values between the 15 s and 5 m time averaging values decreased from unstable to stable to neutral stabilities. The largest $\sigma\theta$ values were found for the unstable case, lower for stable, and the lowest for neutral stability.

Figures 30(c-f)/Tables E-(1-4) highlight interstability $\sigma\theta$ dependence on time averaging for sensors at elevations of 12, 54, 102, and 204', respectively. Both the stable and the unstable cases exhibited decreasing $\sigma\theta$ values from the 12 to the 54' levels, increasing values from the 54 to the 102' levels, and decreasing values from the 102 to the 204' levels. The neutral case showed decreasing $\sigma\theta$ values with

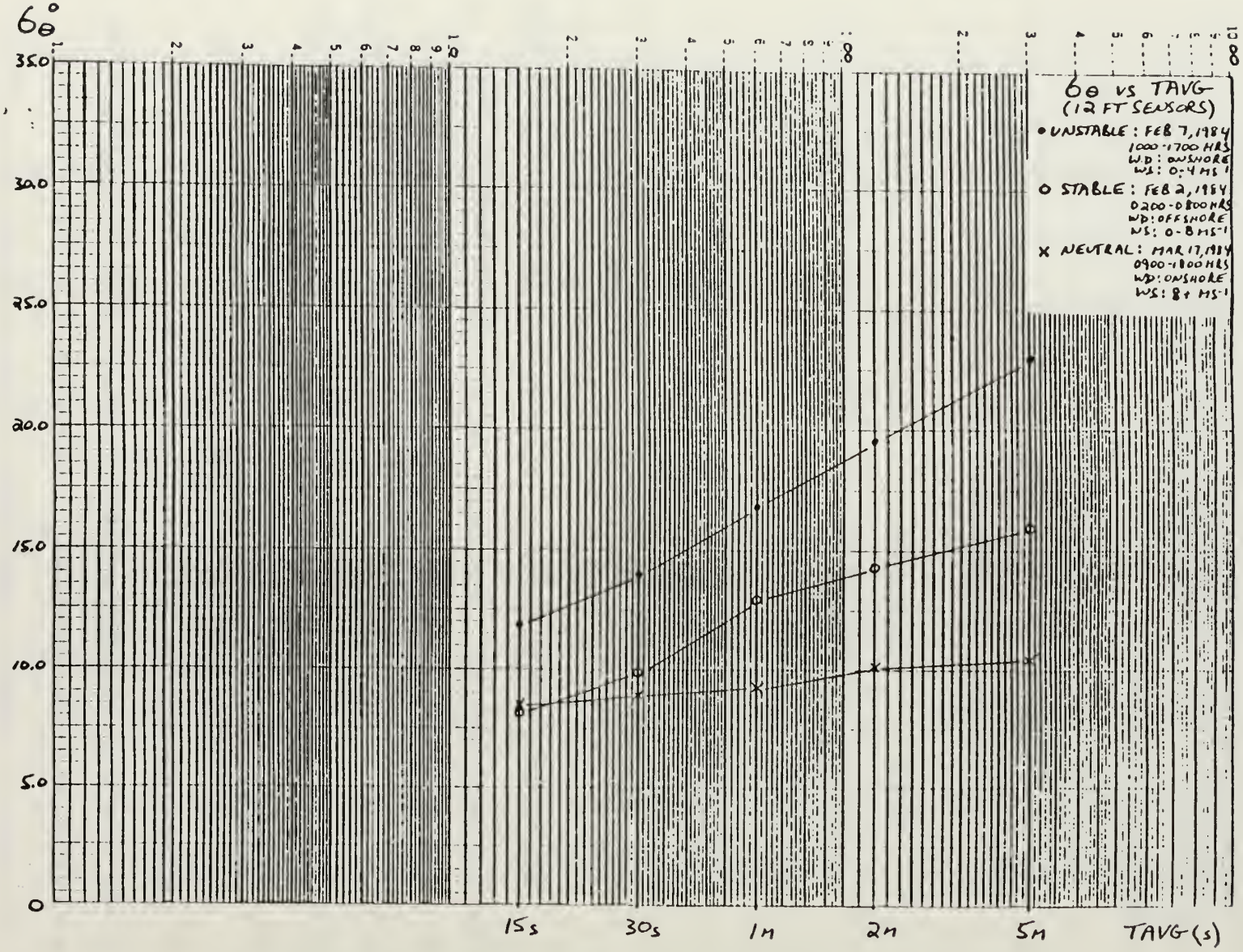

Figure 30(c). σθ vs TAVG (Interstability--12' Sensors)

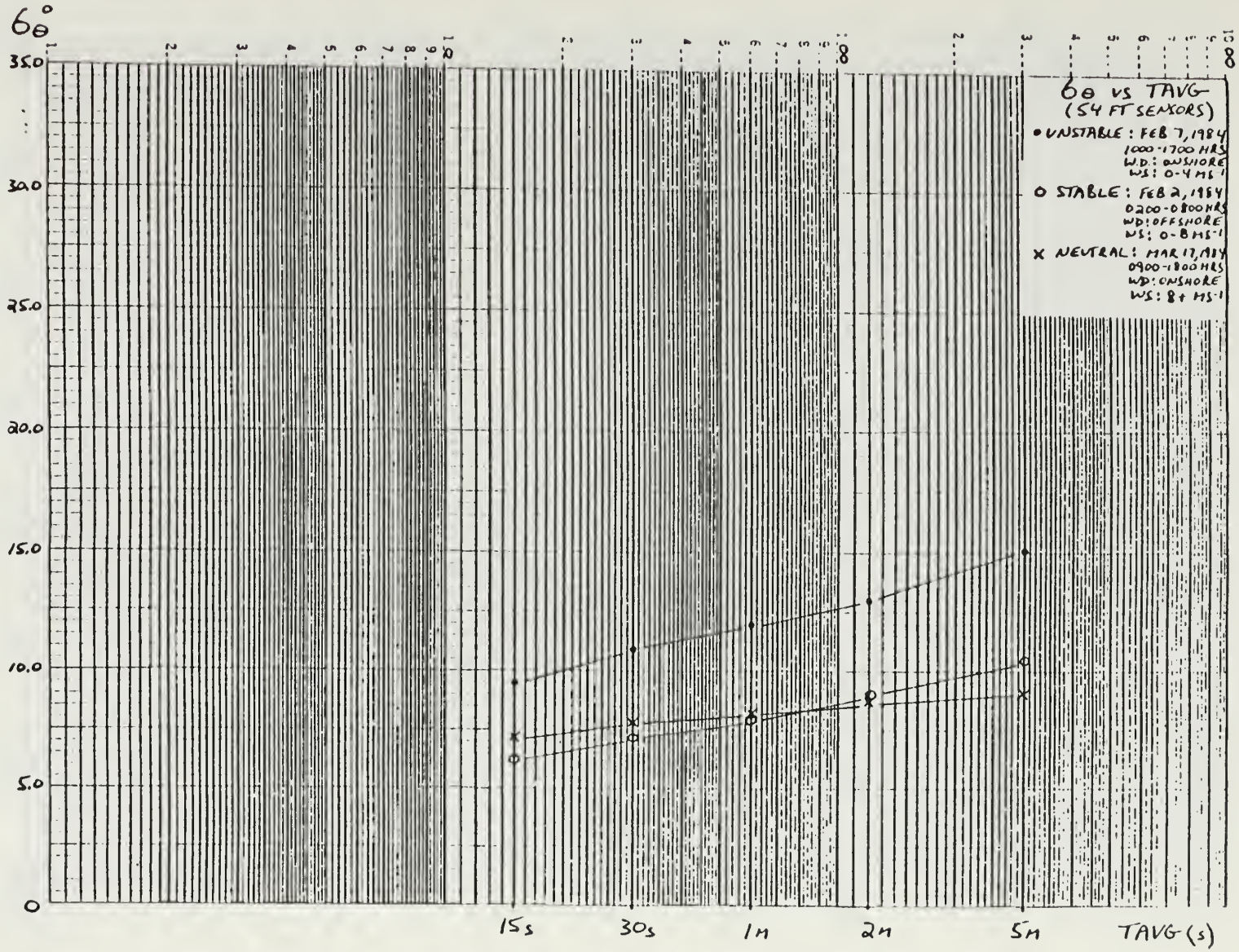

Figure 30(d). σθ vs TAVG (Interstability--54' Sensors)

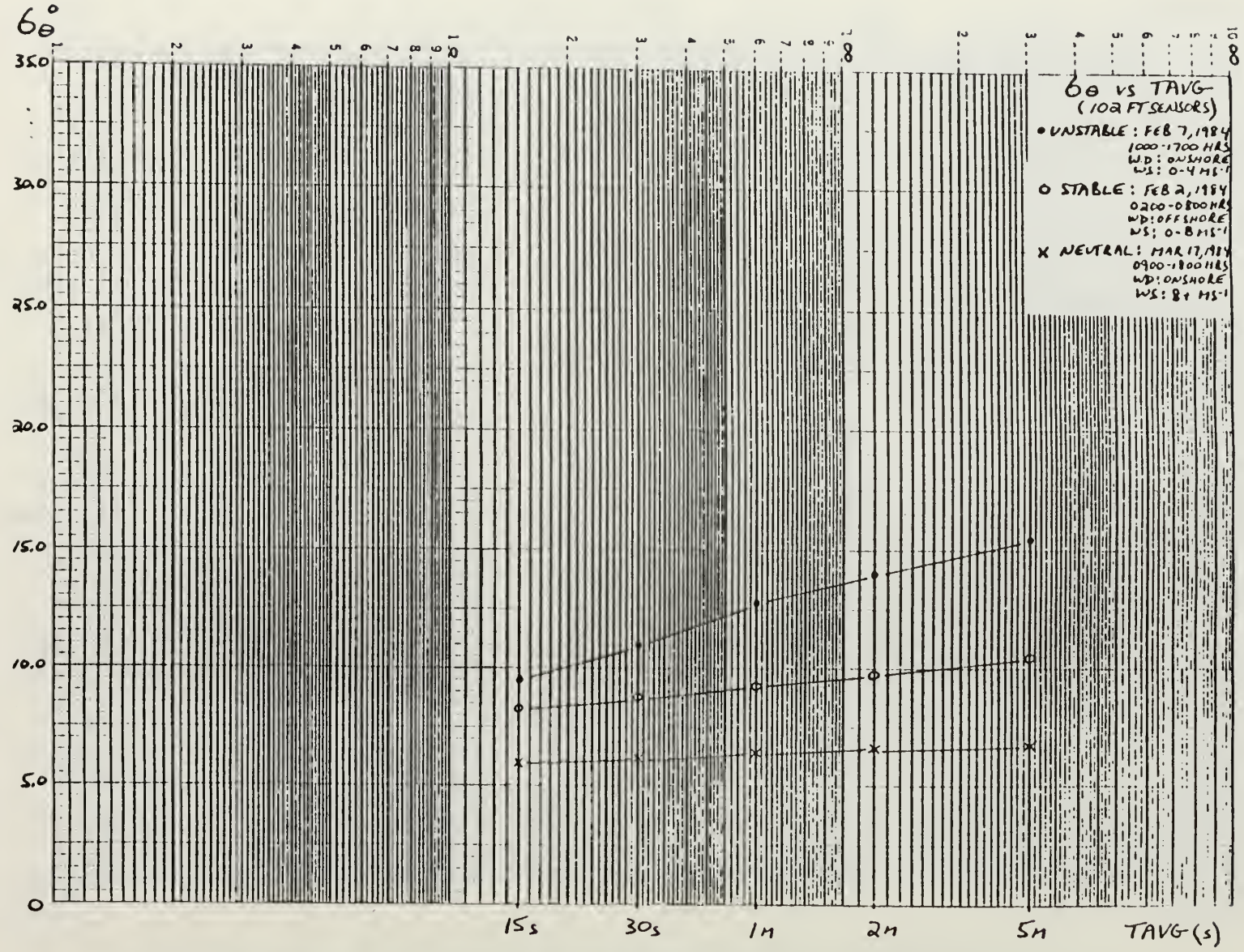

Figure 30(e). σθ vs TAVG (Interstability--102' Sensors)

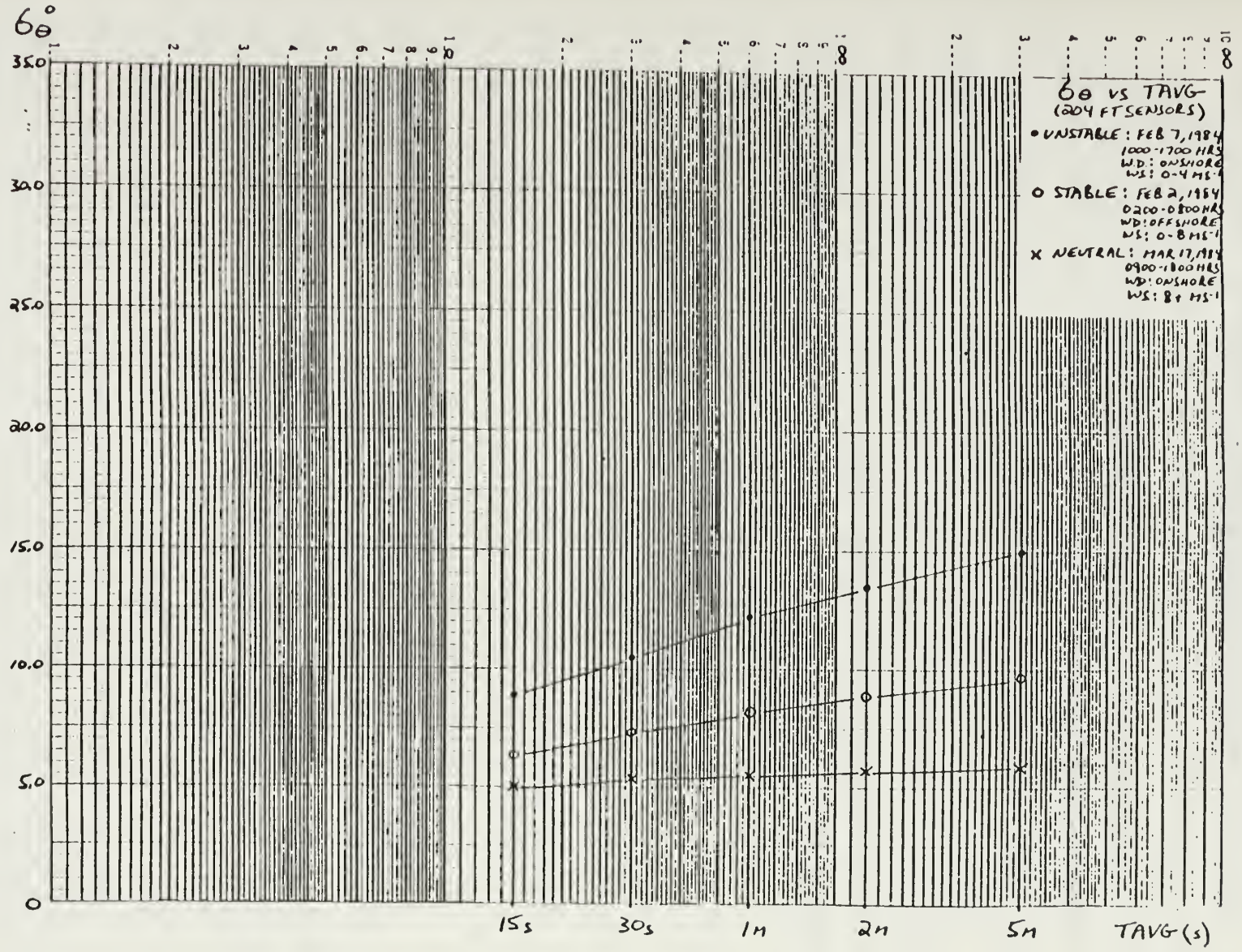

Figure 30(f). σθ vs TAVG (Interstability--204' Sensors)

increasing height. In the unstable case, the $\sigma\theta$ spread of values over all time averages studied decreased from 12 to 54' and then remained constant with height. In the neutral case, this spread was constant from 12 to 54', decreased from 54 to 102', and then was constant up to 204'. And in the stable case, this spread decreased from 12 to 102' and then increased from 102 to 204'.

Finally, Tables E-(5-13) in the Appendix describe inter-stability $\sigma\theta$ dependence on time averaging for sensors at specific sites. Terrain influences, flow persistence, and land/sea breeze effects are all evident in this summary.

IX. DISCUSSION AND INTERPRETATION

A. GENERAL REMARKS

In examining $\sigma\theta$ dependence on various meteorological parameters at sites located throughout the complex terrain of Vandenberg AFB, it was apparent that similarity theory applied only on a local scale. As a result, each stability case study was considered quasi-stationary but not isotropic. The effect of wind speed in each of the case studies was very important in determining $\sigma\theta$ values or turbulence intensities and this effect was found to vary with stability. The lateral wind fluctuation standard deviation, σv, from the relationship $\sigma\theta \sim (\sigma v/U)$, was assumed constant with height in the surface layer. Finally, specific flow regimes were found to be related with the stability case studies chosen in this report.

B. UNSTABLE CASE

The unstable case chosen for this study was the longest and most consistent unstable condition available. The period of analysis was coincident with an onshore sea breeze regime. Relatively high $\sigma\theta$ values (versus those for the stable and neutral cases) were found for this stability condition and flow regime. This apparently was due to the buoyancy and convective mixing associated with this flow. Sea surface temperatures caused cooling of the lower atmosphere along

the coast which, consequently, resulted in a more stable or neutral atmosphere and implied lower values of $\sigma\theta$ relative to the inland sites. As this air moved inland, convective mixing became more of a factor and this, together with the rougher terrain, contributed to higher inland values of $\sigma\theta$. The turbulent internal boundary layer (TIBL), which often forms with onshore sea breeze flow and increases in depth with distance inland, also may contribute to higher values of $\sigma\theta$ inland although all of the towers in this case study were assumed to be within this layer.

Mean flow directed from the west along the coast and from the south at sites 055 and 056 appeared to result in convergence near the inland sites of 101 and 014. An east-west canyon east of site 200 may have contributed to this effect. The variable flow direction with height at site 200 apparently was influenced by terrain effects as it fell between predominantly westerly flow at site 300 and predominantly northwesterly flow at site 301.

Various schemes indicated that the largest $\sigma\theta$ values were found near the ground (12' level). There was no major statistical difference between the empirical and observed curves ($\sigma\theta$ vs TAVG) in the power law study. A certain amount of scatter did occur in the data, however, because of the use of different sites in this study (22 independent measurements) and because of the uncertainty in the wind vanes themselves.

An examination of $\sigma\theta$ dependence on time averaging resulted in information regarding spectral energy which itself is proportional to turbulence intensity. In studying height dependence, $\sigma\theta$ values near the ground (12') were found to be much higher than those aloft (54, 102, and 204'). The decrease in $\sigma\theta$ values from 54 to 204' was not significant. As surface similarity laws were assumed not applicable at the 12' level, the larger surface values of $\sigma\theta$ were attributed basically to lower wind speeds near the surface.

Site 102 showed a rapid increase in energy from the higher frequencies to the lower frequencies at the 12' level. The relatively high amount of energy at this level between 30 s and 2 m averaging time appeared to be a result of flow around a surface obstacle.

Site 300 along the coast showed a standard spectrum of energy without topographical influences, under the influence of cooler marine air. The $\sigma\theta$ values were generally constant with height and there were only small changes in the mean horizontal wind speed with height.

Coastal site 200 showed generally higher values of $\sigma\theta$ than those at site 300 apparently due to rougher surface at site 200. Topographical influences, together with the variability in wind direction with height, resulted in the relatively high $\sigma\theta$ values at the 12' level. The difference in the $\sigma\theta$ profiles with height was caused by the difference in wind speeds at these heights. This is shown through the

relationship $\sigma\theta \sim \sigma v/U$, where U is the mean horizontal wind speed and σv is assumed constant with height in the surface layer.

Site 301 showed uniform profiles of $\sigma\theta$ with averaging time for elevations of 54, 102, and 204'. The large amount of energy at the 12' level appeared to be due to topographical influence and low mean wind speeds.

Inland sites 052, 054, and 101 all showed larger values of $\sigma\theta$ than those at the coast apparently due to increased roughness. Variation in wind speed with height caused a larger difference between the $\sigma\theta$ profiles at different sensor levels than was evident at the coastal sites.

Site 055 exhibited unrealistic values of $\sigma\theta$ with increasing averaging time apparently due to flow around large structures in the vicinity of the tower.

Local topography was the most important factor in examining $\sigma\theta$ dependence on wind direction. The lowest values were generally associated with winds from the north-northwest. With an averaging time of 15 s, small scale influences determined the magnitude of the $\sigma\theta$ values at each site.

Site 102 encountered some turning of the wind flow with height and experienced the lowest $\sigma\theta$ values when winds were from 280-320°.

Site 300 experienced more of a neutral stability in the cool coastal air. The $\sigma\theta$ values did not vary much with wind direction or height and small surface roughness was implied.

Site 200 recorded slightly higher $\sigma\theta$ values than the other coastal sites apparently due to terrain effects.

Coastal site 301 showed terrain and eddy effects with winds evident from all directions. Higher values of $\sigma\theta$ were associated with winds from the east (off the mountain).

$\sigma\theta$ dependence on wind speed was similar throughout the terrain. The lowest $\sigma\theta$ values were found with the highest wind speeds which were associated with the greater heights. Conversely, the highest values of $\sigma\theta$ were found in conjunction with the lowest wind speeds. The lower sensor levels generally recorded higher $\sigma\theta$ values due to topographical effects and low wind speeds. Finally, lower values of $\sigma\theta$ were found along the coast in the cool, neutral marine layer while relatively higher values were found inland where the convective upwelling associated with the general instability of the case study had some effect.

C. STABLE CASE

The stable case selected for this study also was chosen because of the consistent stability conditions which existed across the terrain. The period of analysis was coincident with evening land breeze/drainage flow. Higher $\sigma\theta$ values were found inland where the land breeze had more of an effect and lower $\sigma\theta$ values were found along the coast where drainage flow was evident. Coastal sites 200 and 300 experienced increasing $\sigma\theta$ values with height, apparently due to stable drainage flow at the lower levels and land breeze influence aloft.

With no significant synoptic pressure gradient forcing involved with this case study, the mean flow associated with this time period was well representative of a land breeze/ drainage flow regime. Winds along the coast were generally out of the east with more variable flow occurring in the mountainous terrain. Winds at site 301 were from the southeast, exactly opposite to the daytime sea breeze flow occurring at this site.

The power law study indicated an observed dependence on averaging time slightly less than the empirical relation. The lower elevations experienced higher values of $\sigma\theta$ and the upper elevations experienced lower $\sigma\theta$ values. There was a lower amount of energy at the lower frequencies than in the unstable case.

As in the unstable case, an examination of $\sigma\theta$ dependence on averaging time revealed higher $\sigma\theta$ values at the 12' level than at the 54, 102 and 204' levels. The high $\sigma\theta$ values at the lower levels were apparently due to the lower wind speeds at those levels.

As in the unstable case, site 102 again showed relatively high values of $\sigma\theta$ at the 12' level between averaging times of 30 s and 1 m. Flow around an obstacle appeared to contribute to this. The 54' level exhibited a more gradual increase in $\sigma\theta$ values with an increase in averaging time.

Site 300 had low values of $\sigma\theta$ at the 54' level apparently due to drainage flow or topography. The relatively high

values of $\sigma\theta$ at the 204' level appeared to be a result of wind shear induced turbulence aloft.

Site 200 showed a uniform $\sigma\theta$ vs TAVG profile with height which is indicative of a steady increase in wind speed with height. Channeling was also apparent at this site with flow coming through the canyon to the east.

Site 301 also showed evidence of channeling with very little change in $\sigma\theta$ occurring with increasing averaging time. Small scale turbulence was also apparent here either due to drainage flow or topographical influences.

Very little topographical or drainage flow was evident at site 052. The large value of $\sigma\theta$ for the one minute averaging time for the 12' sensor appears to be the result of bad data.

Inland sites 054 and 014 exhibited high values of $\sigma\theta$ at the lower frequencies at their respective sensor levels. Large topographical influences apparently were responsible for this. Site 055 showed evidence of shear produced small scale turbulence due to flow distortion caused by structures in the area. All of the energy at this site was apparent at the 15 s averaging time and no significant change in $\sigma\theta$ occurred with increasing averaging time.

An investigation of $\sigma\theta$ dependence on wind direction across the terrain revealed no significant $\sigma\theta$ dependence on this parameter at coastal sites 102, 300, 200 and 301. Inland sites 052 and 054 showed higher $\sigma\theta$ values with winds from

the southeast versus east, apparently due to local topography. Site 014 exhibited more drainage flow than land breeze flow with the predominant wind direction perpendicular to the terrain. Another inland site, 055, encountered persistent flow from the southeast and appeared to be dominated by land breeze flow.

An analysis of $\sigma\theta$ dependence on wind speed indicated slightly decreasing $\sigma\theta$ values with increasing wind speed at most sites. Erratically high values of $\sigma\theta$ at low wind speeds may be attributed to instrument performance. The lowest $\sigma\theta$ values associated with the lower sensor elevations at the coastal sites resulted from drainage flow. Inland site 014 did show some $\sigma\theta$ dependence on wind speed with $\sigma\theta$ values increasing with increasing wind speed. Local terrain effects appeared to be responsible for this.

Overall, the terrain effects suggested that topographical elements such as the mountains caused low frequency turbulence inland whereas the coastal sites encountered turbulence as a result of mechanical shear production. The higher surface roughness inland resulted in higher values of $\sigma\theta$ inland versus along the coast. There was also more $\sigma\theta$ dependence on wind direction and wind speed inland than there was along the coast.

D. NEUTRAL CASE

The neutral case examined here also was selected from a time period of consistent stability across the terrain

based on Richardson Number calculations. The period of analysis was coincident with a regime of strong postfrontal northwesterly (320-360°) flow. In this case study, $\sigma\theta$ values were most dependent on height or wind speed as there was a significant difference in the speed of the flow aloft versus at the lower elevations.

Unlike the stable and unstable case studies where synoptic pressure gradient forcing was negligible, this case study was totally dominated by synoptic forcing. Wind flow was consistently from 320-360° at all sites and sensors during this time period.

The power law study indicated a large difference between the empirical and observed $\sigma\theta$ vs TAVG plots. This apparently is because most of the energy under neutral stability conditions is contained in the higher frequencies and no significant change in $\sigma\theta$ occurs as averaging time increases.

An examination of $\sigma\theta$ dependence on averaging time revealed similar plots of $\sigma\theta$ increase with averaging time for the various sensor levels. The flow was persistent at all levels and any change in $\sigma\theta$ with height could only be attributable to changes in wind speed. The lower sensor elevations showed more $\sigma\theta$ dependence on time averaging than the upper levels.

An investigation of $\sigma\theta$ dependence on wind direction across the terrain revealed that such dependence did not exist under these stability conditions. The predominant flow

at all sites/sensors was from 320-360° and this flow was persistent and strong enough that very little variation either in wind direction or in values of $\sigma\theta$ was evident.

An analysis of $\sigma\theta$ dependence on wind speed indicated decreasing values of $\sigma\theta$ with increasing wind speed at all sites and sensors. Although there were large differences in wind speed with height at the given sites, the values of $\sigma\theta$ at the different sensor levels were virtually constant at each site under conditions of constant wind speed. Differences between $\sigma\theta$ values for sensors at the same elevation, with the same wind direction, and with the same wind speed were found to be primarily due to differences in surface roughness. Higher surface roughness values caused higher values of $\sigma\theta$.

All sites showed very little $\sigma\theta$ dependence on either averaging time or wind direction, due to the strength and persistence of the flow, although significant $\sigma\theta$ dependences on wind speed/height were observed.

E. INTERSTABILITY COMPARISON

A comparison of the three stability cases studied revealed higher values of $\sigma\theta$ for the unstable case than for either the stable or neutral cases. The $\sigma\theta$ values recorded under stable and neutral conditions were similar in magnitude, with the stable values generally slightly greater than the neutral values. A similar investigation of $\sigma\theta$ dependence on stability was performed recently at a site in New Zealand

(Wratt et al [Ref. 11]) with a similar trend reported. In the work reported here, the larger $\sigma\theta$ values associated with the unstable case were primarily due to convective mixing. Lower $\sigma\theta$ values were found at the coastal sites (versus the inland sites) because of the characteristics of the marine layer atmosphere. The turbulence intensity values found for the stable case study were significantly less than those associated with the unstable case. The variations in $\sigma\theta$ values across the terrain were primarily due to land breeze versus drainage flow influences which, in turn, were terrain related. The neutral case study examined showed $\sigma\theta$ values lower than those found in either the stable or unstable case studies. Higher wind speeds, normally associated with this category, were primarily responsible for these lower values. Variations in $\sigma\theta$ were minimal with respect to time averaging, wind direction, and terrain although differences were noted relative to sensor elevation which were a result of $\sigma\theta$ dependence on wind speed.

In addition to the overall $\sigma\theta$ dependence on stability, $\sigma\theta$ was found to be a function of averaging time, wind direction, wind speed, elevation and terrain within the three stabilities. The amount of $\sigma\theta$ dependence on each of these parameters was dependent upon the given stability/flow regime. $\sigma\theta$ dependence on averaging time was stronger in both the unstable and stable cases than in the neutral case due to the suppression of low frequency turbulence under high wind

conditions. $\sigma\theta$ was also more dependent on wind direction in the stable and unstable cases than in the neutral case. The strong persistent flow associated with the neutral case was responsible for this lack of dependence. Terrain influence and surface roughness contributed to the variation in $\sigma\theta$ with wind direction in both the stable and unstable cases. $\sigma\theta$ dependence on wind speed and height was found for all three stability case studies with the neutral case exhibiting the greatest dependence. Surface roughness contributed primarily to the changing wind speed with height associated with the neutral wind profile and the changing wind speed, in turn, resulted in the variation of $\sigma\theta$ with height.

$\sigma\theta$ dependence on terrain was felt more for the stable and neutral cases than for the unstable case. The convective mixing occurring in the unstable case appeared to mask the overall terrain effects. In the stable case, the $\sigma\theta$ values appeared to be more sensitive to the terrain, apparently due to the suppression of lower frequency turbulence and to the low wind speeds.

X. SUMMARY AND CONCLUSIONS

This investigation was an attempt to characterize the mean flow and the standard deviation of wind direction fluctuations ($\sigma\theta$) over the complex terrain of Vandenberg AFB under specified stability conditions. $\sigma\theta$ values were analyzed across the terrain as functions of averaging time, wind direction, wind speed, elevation and terrain. The following is a list of assumptions and/or observations that were made relative to this analysis:

1. Because of the complexity of the terrain, direct $\sigma\theta$ measurements were made rather than applying similarity theory which, in this case, could only be applied on a local scale. Each stability case studied was assumed stationary.

2. Each stability case studied was chosen solely from Richardson Number criteria which, in itself, is correlated with mean flow and turbulence in the atmosphere. The cases were:

UNSTABLE: February 7, 1984 (1000-1700 hrs)

STABLE: February 2, 1984 (0200-0800 hrs)

NEUTRAL: March 17, 1984 (0900-1800 hrs)

3. The stability cases chosen turned out to be related to specific flow regimes. The unstable case was an onshore afternoon sea breeze flow where convective mixing was important, particularly inland. The stable case, which also was only weakly influenced by synoptic pressure gradient

forcing, was an evening land breeze and drainage flow regime. And the neutral case was representative of strong and persistent postfrontal synoptic flow.

4. $\sigma\theta$ dependence on stability: The largest $\sigma\theta$ values were found for the unstable case with lower values associated with the stable case and the lowest during the neutral case. The convective mixing, together with larger eddies aloft and overall lower wind.speeds (relative to other stabilities) contributed to large $\sigma\theta$ values. Stable stratification causes a reduction in all turbulence scales (smaller eddies) and lower $\sigma\theta$'s. Mechanical energy production dominates buoyancy production in the neutral case as wind speeds become large and increase with height due to wind shear. The lowest $\sigma\theta$ values were associated with this case due to suppression of meander.

5. $\sigma\dot{\theta}$ dependence on time averaging: The unstable case showed the most dependence on time averaging with less dependence evident in the stable case and the least in the neutral case due to lack of meander. $\sigma\theta$ values increased with increasing averaging time regardless of stability. $\sigma\theta$ values were more dependent on time averaging at the lower levels than aloft primarily due to surface roughness and small scale terrain effects.

6. $\sigma\theta$ dependence on wind direction: The unstable case showed predominant winds from 240-280° with the lowest $\sigma\theta$ values associated with winds from 280-360°. This dependence

was limited though in that buoyancy masks the terrain effects. Under stable conditions, the winds were predominantly from 080-120° with the lowest $\sigma\theta$ values associated with winds from that direction. Higher $\sigma\theta$ values were found with winds from 120-200°, apparently due to terrain effects. Greater $\sigma\theta$ dependence on wind direction was found inland than along the coast. Strong flow from 320-360° occurred at all sites in the neutral case study. The lowest $\sigma\theta$ values were found with winds from 320-360° with slightly higher values occurring with winds from directions on either side of this braket. No significant $\sigma\theta$ dependence on wind direction was found in this case because of the strength and persistence of the flow.

7. $\sigma\theta$ dependence on wind speed: $\sigma\theta$ dependence on wind speed was very important in the neutral case where wind speeds were more variable with height. The stable and unstable cases showed relatively little $\sigma\theta$ dependence on wind speed, the only significant dependence being at the inland sites. $\sigma\theta$ values generally decreased with increasing wind speed in all three of the case studies. Predominant wind speeds were 2-4 ms^{-1} at all levels in the unstable case, 2-4 ms^{-1} at the lower levels and 4-6 ms^{-1} aloft in the stable case, and ranging from 6 ms^{-1} at lower levels to greater than 18 ms^{-1} aloft in the neutral case.

8. $\sigma\theta$ dependence on height: The unstable and stable case studies showed much higher values of $\sigma\theta$ at the 12'

level than at the other levels. This presumably was due to terrain effects. The stable case showed a variation of $\sigma\theta$ values with height at all sites except site 200 where channeling was apparent. The $\sigma\theta$ values were also found to vary with height at all sites in the unstable case. The neutral case exhibited variation in $\sigma\theta$ with height at all sites due to variations in wind speed with height and terrain effects.

9. $\sigma\theta$ dependence on terrain: All three case studies showed an increase in turbulence with rougher terrain. The terrain effects in the unstable case were basically masked by the convective mixing which, itself, was more dominant inland. Lower $\sigma\theta$ values were found along the coast where the cooler marine air induced more of a stable or neutral stability regime. The stable case showed much more $\sigma\theta$ sensitivity to the terrain, particularly at the inland sites. Lower $\sigma\theta$ values were generally found near the coast where drainage flow was dominant. Land breeze flow further inland generally resulted in higher $\sigma\theta$ values at these sites. The neutral case showed $\sigma\theta$ dependence on terrain due to the variability of the wind speeds with height which depends on local roughness.

Tables F-(1-3) in the Appendix summarize the most likely $\sigma\theta$ values to occur at each site under the given stability condition. The first three $\sigma\theta$ values listed for each site represent the most likely $\sigma\theta$ values found from examining the

schemes involving $\sigma\theta$ dependence on time averaging, wind direction, and wind speed, holding other parameters constant. The minimum and maximum values of $\sigma\theta$ with respect to wind direction are listed for each site under given stability conditions. Finally, the power law values of 'x' are listed for each site and stability. Abbreviations and categorizations mentioned in these tables are explained in Table V.

XI. APPLICATIONS TO DIFFUSION MODELING

Analysis of mean flow and turbulence fields under a variety of conditions is necessary for current and future diffusion modeling endeavors. Previous model development has been primarily based on data collected from homogeneous terrain areas and from a limited number of sites/towers. Periods of analysis have generally been arbitrary and void of any particular synoptic relationship.

The work reported here was performed not only as input for specific diffusion modeling over the coastal complex terrain of Vandenberg AFB but also as a preliminary effort to build a data base for a wide range of complex terrain modeling efforts. Future work with the Vandenberg data will hopefully result in better predictions of turbulence intensities under given synoptic conditions and results which are more generic in applicability.

Fully parameterizing the flow and turbulence fields is a necessary first step for many diffusion models. For example, Puff modeling, based on theory suggested by Smith and Hay [Ref. 12], requires flow and turbulence fields as initial input for its operation. Turbulence intensity information, derived from an analysis of $\sigma\theta$ values as was done in this report, must be representative of the terrain being studied and the synoptic conditions if it is to be truly useful in

the diffusion modeling process. Flow and turbulence fields must also be parameterized for use with Monte Carlo and Gaussian diffusion models and for validation of 3-D numerical models. Finally, imbedded models have been developed at White Sands which analyze flow scales ranging from synoptic to mesoscale to local site specific to vegetation scales. This effort needs detailed knowledge on flow and turbulence on several scales, emphasizing the need for obtaining more data over complex terrain and under specific synoptic conditions.

Improved flow and turbulence field parameterization will result in improved diffusion modeling and a better understanding of our turbulent atmosphere.

DATE	FLOW	GRADIENT STRENGTH	SYNOPTIC FEATURES
9	N	MDT	(H: off N. CA coast; L: over central CA & NW Mexico)
10	NW	MDT	(Trof thru central CA; H: off NW U.S.)
11	--	---	(H: off NW U.S. & over Nevada)
12	NW	MDT	(H: off NW U.S. & over N. Arizona)
13	N	WK	(H: off NW U.S. & over Montana; L: over Gulf of CA)
14	NW	MDT	(H: off NW U.S. & over N. Nevada; L: over Gulf of CA)
15	--	---	(Trof thru N-S CA)
16	--	---	(Trof thru N-S CA)
17	--	---	(Trof thru N-S CA)
18	--	---	(L: over N. CA and Gulf of CA)
19	--	---	(L: over SW Idaho and Gulf of CA)
20	NW	WK	(front thru Nevada; L: over S. CA; H: off NW U.S.)
21	NW	WK	(H: off NW U.S.; L: over S. Nevada)
22	NNW	MDT	(H: off NW U.S. & over Idaho; L: over Gulf of CA)
23	NNW	MDT	(H: off NW U.S. & over Idaho; L: over Gulf of CA)
24	NW	MDT	(H: off Oregon; L: over S. Nevada & N. Gulf of CA)
25	NW	MDT	(H: off central CA; trofing thru E. CA)
26	NNW	STR	(front thru central CA; H: off central CA; L: over Gulf of CA)
27	N	MDT	(L: over N. Gulf of CA)
28	N	MDT	(H: off central CA coast; L: over Gulf of CA)
29	NW	WK	(H: off S. CA coast; L: over S. CA & off NW U.S.)
30	--	---	(H: off S. CA coast & over Colorado; L: off NW U.S.)
31	--	---	(L: off NW CA & over Gulf of CA)

SEPTEMBER

1	N	MDT	(H: off central CA; L: over SW Ariz.)
2	N	MDT	(H: over Oregon; L: over N. Gulf of CA)
3	NNW	STR	(H: off NW U.S.; L: over Gulf of CA)
4	NW	STR	(H: off NW U.S.; L: over Gulf of CA)
5	NW	MDT	(H: off NW U.S.; L: over N. & S. CA)
6	NW	WK	(H: off NW U.S.; L: over N. & S. CA)
7	NW	STR	(front thru N. CA; H: off NW U.S. & S. CA)
8	NW	STR	(front thru N. CA; H: off NW U.S. & S. CA)
9	NNE	STR	(front thru central CA; H: off NW U.S.; L: over Gulf of CA)
10	NNE	STR	(H: over Montana; L: over NW Mexico)
11	NNW	STR	(H: off Oregon coast; L: over N. Gulf of CA)
12	NW	WK	(L: over central CA & N. Gulf of CA)
13	--	---	(L: over central CA & N. Gulf of CA)
14	NW	WK	(L: over central CA; H: off NW U.S.)
15	NW	WK	(L: over central CA; H: off NW U.S.)
16	NW	WK	(H: off NW U.S.; L: over S. CA)
17	NW	WK	(H: off NW U.S.; L: over S. CA)
18	NNW	MDT	(H: off central CA coast; L: over S. CA)
19	--	---	(front thru central CA; T.S. off Baha; H: over Arizona)
20	E	WK	(T.S. L: off SW CA; H: over SW Montana)
21	--	---	(L: off Oregon coast; stationary front thru Nevada)
22	--	---	(L: over Gulf of CA; H: over NW Montana)
23	--	---	(L: over Gulf of CA; H: over NW U.S.)
24	N	WK	(H: off NW U.S.; L: over S. Nevada)
25	NW	MDT	(L: over N. CA)
26	--	---	(front approach NW U.S.; L: over Gulf of CA)
27	NW	WK	(front thru N. CA; H: off NW U.S.; L: over Gulf of CA)

28	NW	MDT	(L: over Gulf of CA)
29	NW	MDT	(L: over S. Nevada & N. Gulf of CA)
30	--	---	(L: over N. CA, N. Nevada & N. Gulf of CA)

OCTOBER

1	--	---	(L: over VBG)
2	NW	WK	(front thru N. CA; H. over E. Arizona)
3	--	---	(L: over N. CA & Gulf of CA)
4	--	---	(H: off NW U.S. & over Utah; L: over Gulf of CA)
5	--	---	(H: over E. Utah; L: over Gulf of CA)
6	--	---	(H: over S. Utah)
7	--	---	(H: over SE Utah; L: over NW Gulf of CA)
8	--	---	(L: over N. CA & Gulf of CA)
9	--	---	(H: off SW CA)
10	--	---	(H: off NW CA; L: over Gulf of CA)
11	NE	MDT	(L: over Gulf of CA; H: over NW U.S.)
12	NNE	MDT	(L: over Gulf of CA; H: over N Idaho)
13	NNW	STR	(front thru VBG)
14	NNW	STR	(front thru S. CA)
15	NW	STR	(front thru Arizona)
16	NW	MDT	(front approach NW U.S.)
17	NNW	MDT	(front thru NW U.S.; L: over Gulf of CA
18	NNW	MDT	(H: over NW U.S.; L: over Gulf of CA)
19	NE	MDT	(H: over E. Idaho; L: over Gulf of CA)
20	NE	WK	(front thru N. CA; L: over Gulf of CA)
21	--	---	(front approach NW U.S.; L: over Gulf of CA)
22	NE	WK	(front thru N. CA; L: over Gulf of CA)
23	--	---	(stationary front thru N. CA)
24	NNE	WK	(staionary front NW CA--SE CA)
25	ESE	STR	(STR H: over Colorado; L: over Gulf of CA)
26	SE	STR	(H: over Utah & Texas; L: over Gulf of CA)

27	SE	WK	(H: over Utah; L: over Gulf of CA)
28	--	---	(H: over N. Mexico; L: over Gulf of CA)
29	--	---	(H: over Idaho; L: over Gulf of CA)
30	--	---	(front thru N. CA; L: over Gulf of CA)
31	--	---	(front thru N. CA; L: over Gulf of CA)

NOVEMBER

1	--	---	(front thru N. CA; L: over Gulf of CA)
2	NNE	WK	(front thru Nevada; H: off central CA coast)
3	E	MDT	(H: over NE Utah; L: over Gulf of CA)
4	--	---	(front thru N. CA; L: over Gulf of CA)
5	--	---	(front thru Nevada; H: over Arizona)
6	--	---	(front thru N. CA)
7	NNE	STR	(front thru VBG)
8	N	MDT	(front thru S. CA)
9	--	---	(front thru N. CA; H: over N. Colorado)
10	SW	STR	(front thru N. CA)
11	SW	STR	(front thru VBG)
12	SW	STR	(front thru N. CA; H: off Baha)
13	WSW	MDT	(front thru VBG
14	N	MDT	(front thru VBG and S. CA)
15	NW	WK	(H: off E. Utah & off SW CA)
16	W	WK	(front thru N. CA; H: off SW CA)
17	W	MDT	(front thru N. CA; H: off SW CA)
18	NNE	STR	(front thru VBG)
19	NE	MDT	(front thru N. CA; H: over Utah)
20	NW	STR	(front thru VBG)
21	NW	STR	(front thru Arizona)
22	NNW	MDT	(front approach NW U.S.)
23	NW	WK	(front thru N.CA)
24	WSW	STR	(front thru central CA)
25	NNW	STR	(front thru S. CA)
26	NNE	STR	(H: over Oregon; L: over NE New Mexico)

27	NE	MDT	(H: over N. Nevada; L: over SW New Mexico)
28	ESE	WK	(H: over Utah)
29	--	---	(H: off SW CA; L: over Utah)
30	SW	STR	(front approach N. CA)

DECEMBER

1	SE	STR	(front approach SW CA)
2	NNW	STR	(front thru VBG)
3	W	STR	(front thru N. CA)
4	NNW	STR	(front thru S. CA)
5	NNE	MDT	(H: off central CA)
6	--	---	(H: off S. CA & over S. Utah)
7	--	---	(front approach N. CA; H: over SE Utah)
8	SE	WK	(front thru N. CA)
9	WSW	STR	(front thru N. CA)
10	W	WK	(front thru S. CA)
11	SW	STR	(front thru N. CA)
12	N	STR	(front thru Arizona)
13	E	STR	(H: over central CA)
14	NE	STR	(H: off central CA coast)
15	NE	STR	(stationary front thru N. CA)
16	--	---	(stationary front thru N. CA)
17	NW	MDT	(stationary front thru Nevada)
18	NNE	MDT	(H: over NW Mexico)
19	NNW	MDT	(front thru N. CA)
20	N	STR	(front thru VBG)
21	NNW	STR	(front thru S. CA)
22	NNW	MDT	(stationary front thru N. & S. CA)
23	SW	WK	(stationary front thru N. CA)
24	SW	STR	(front approach N. CA)
25	SW	STR	(front thru VBG)
26	W	MDT	(stationary frontthru N. CA)
27	W	MDT	(stationary front thru N. CA)
28	N	WK	(stationary front thru W. CA)

29	NW	WK	(front approach NW U.S.)
30	--	---	(front thru N. CA)
31	NE	WK	(H: over ONT & E. Utah)

JANUARY

1	ESE	MDT	(H: over Idaho; L: over Gulf of CA)
2	SE	WK	(H: over Utah; L: over NW Mexico)
3	SE	WK	(H: over Utah; L: over Gulf of CA)
4	ESE	MDT	(H: over Utah; L: over Gulf of CA)
5	ESE	MDT	(H: over Utah; L: over N Gulf of CA)
6	--	---	(L: over N. CA & over Gulf of CA)
7	--	---	(front approach N. CA; H: over Utah)
8	NW	WK	(dissipating front thru N. CA; H: off central CA coast)
9	--	---	(H: over Idaho; L: over Texas)
10	--	---	(front thru N. CA; H: over Utah; L: over Gulf of CA)
11	NE	STR	(front thru S. CA; H: off Oregon coast)
12	SE	MDT	(H: over Utah; L: over Gulf of CA)
13	NNW	WK	(L: over Gulf of CA)
14	--	---	(L: over S. Nevada)
15	--	---	(H: over Washington; L: over N. CA coast & over NW Mexico)
16	--	---	(trof along CA coast; H: over Idaho; L: over N. Mexico)
17	--	---	(L: over N. CA & over N. Mexico)
18	--	---	(H: over Utah; L: over N. Mexico)
19	--	---	(H: over Utah; L: over N. Mexico)
20	--	---	(H: over Idaho; L: over N. Mexico)
21	NW	MDT	(front thru N. CA)
22	NE	MDT	(H: over Utah & off CA coast; L: over NW Mexico)
23	NE	MDT	(H: over Oregon; L: over Texas)
24	E	MDT	(H: over Utah & off CA coast; L: over NW Mexico)
25	ENE	MDT	(trof thru NW U.S.; H: over Utah; L: in S. CA)

26	ENE	STR	(H: off Oregon coast)
27	ESE	STR	(H: over Nevada; L: over Baha)
28	ESE	MDT	(H: over Nevada; L: over Baha)
29	E	MDT	(H: over Nevada; L: over Baha)
30	--	---	(trof along CA coast; H: over Utah)
31	--	---	(L: off Oregon coast & in S. CA)

FEBRUARY

1	NW	WK	(L: off Oregon coast & in S. CA)
2	--	---	(H: over Idaho; L: in S. CA)
3	--	---	(H: over Idaho; L: in Gulf of CA)
4	ESE	WK	(H: over Idaho; L: in Gulf of CA)
5	--	---	(H: off S. CA coast & over Idaho)
6	E	WK	(H: over Utah; L: over Gulf of CA)
7	ESE	WK	(H: over Idaho; L: over NW Mexico)
8	SE	WK	(front thru N. CA; H: over Utah; L: over Gulf of CA)
9	NW	WK	(front thru central CA; H: over S. CA)
10	NW	STR	(front thru S. CA; H: off S. CA)
11	NNE	MDT	(front approach NW U.S.; H: over Idaho)
12	--	---	(front approach NW U.S.; H: over Utah)
13	--	---	(front thru N. CA)
14	N	STR	(front thru S. CA)
15	--	---	(front approach N. CA; H: over Utah)
16	NW	STR	(front thru S. CA)
17	NNE	STR	(H: off central CA coast; L: over N. Mexico)
18	ENE	MDT	(H: off Oregon & SW Canada)
19	--	---	(H: off Oregon & SW Canada)
20	--	---	(H: off central CA coast & over Utah)
21	NW	STR	(front thru central CA)
22	NE	STR	(L: over Nevada; H: off N. CA coast)
23	E	MDT	(H: over Utah; L: over Gulf of CA)
24	NE	WK	(H: over Utah; front thru central CA)

25	N	STR	(front thru S. CA)
26	ENE	MDT	(H: over NE Oregon; L: over Texas)
27	--	---	(H: over E. Idaho; L: over Baha)
28	--	---	(front thru N. CA)
29	NNE	WK	(front dissipates; H: off CA coast & over Utah)

MARCH

1	NNE	WK	(H: over Utah; L: over S. Nevada)
2	NE	MDT	(H: off N. CA coast & over Utah; L: over S. Nevada)
3	ENE	MDT	(H: over Washington; L: over S. CA)
4	ESE	WK	(H: over SW Canada; L: over SW New Mexico)
5	--	---	(H: over Idaho; L: off N. CA coast)
6	NW	WK	(H: off S. CA & over Idaho; L: over Gulf of CA)
7	NW	WK	(H: off S. CA & over Idaho; L: over Gulf of CA)
8	--	---	(H: over Idaho; L: off NW U.S.)
9	NNE	WK	(H: off NW CA; L: over N. Mexico)
10	NE	MDT	(front thru N. CA; H: off CA coast & over Idaho)
11	NNE	STR	(front thru S. CA; H: over Oregon; L: over Gulf of CA)
12	NW	MDT	(H: off CA coast; L: over Gulf of CA)
13	WSW	MDT	(front thru N. CA)
14	NW	STR	(front thru S. CA)
15	NW	STR	(front thru central CA)
16	NW	MDT	(H: off central CA coast)
17	NNE	STR	(front thru central CA)
18	NE	STR	(H: off central CA coast)
19	NE	MDT	(H: over Utah)
20	NE	WK	(H: off central CA coast & over Utah; L: over S. CA)
21	N	STR	(front thru central CA)
22	NNE	STR	(H: over Oregon)
23	E	WK	(front thru N. CA; H: over Utah)

24	N	MDT	(front dissipates; H: off Washington & over Arizona)
25	NNW	MDT	(H: over Idaho)
26	NW	STR	(stationary front thru N. CA; L: over NW Arizona)
27	N	STR	(H: off Oregon coast)
28	NE	MDT	(front thru N. CA)
29	NNE	STR	(front dissipates; H: off Oregon coast; L: over NW Mexico)
30	NNE	MDT	(L: over SE Utah)
31	NW	MDT	(front thru central CA)

APRIL

1	NNW	STR	(front thru S. CA; H: off NW coast; L: over Utah)
2	NNW	MDT	(H: off CA coast; L: over Colorado)
3	--	---	(front thru NW CA; H: over Idaho)
4	NW	WK	(H: off S. CA coast & over N. Colorado)
5	NW	MDT	(H: off S. CA coast; L: over central Nevada)
6	NNE	STR	(H: off Oregon coast; L: over Nevada & Gulf of CA)
7	NNE	MDT	(H: over Idaho & off S. CA coast)
8	NW	STR	(front thru central CA)
9	NW	WK	(front thru S. CA; H: over N. CA)
10	NNW	STR	(front thru central CA)
11	NNE	STR	(H: off central CA coat)
12	NNE	STR	(front thru N. CA; H: off central CA coast)
13	NNE	STR	(H: off central CA coast & over Idaho)
14	NNW	MDT	(H: off central CA coast & over Idaho)
15	NNW	WK	(front thru N. CA; H: off S. CA coast)
16	NNE	MDT	(front thru central CA)
17	NNE	STR	(front thru S. CA; H: off S. CA coast)
18	NNE	MDT	(front thru N. CA)
19	NNW	STR	(front thru central CA)

20	NNE	STR	(H: off central CA coast)
21	NE	MDT	(front thru Washington; L: over Oklahoma)
22	N	MDT	(L: over NW Mexico)
23	N	MDT	(front thru N. CA; H: off Washington coast)
24	NNW	STR	(front thru central CA; L: over Nevada)
25	NNE	STR	(front thru S. CA; L: over Colorado)
26	NNW	STR	(front thru S. CA; L: over Colorado)
27	NNW	MDT	(H: off Washington coast & over Arizona)
28	NNW	MDT	(H: off Washington coast; L: over N. Mexico)
29	NW	WK	(H: off central CA coast; L: over N. Utah)
30	NW	MDT	(H: off S. CA coast; L: over S. Nevada)
MAY			
1	NNW	STR	(front thru N. CA; H: off S. CA; L: over Nevada)
2	NNW	STR	(front dissipating in central CA)
3	NNE	MDT	(front dissipating)
4	NNE	STR	(H: off S. CA coast; L: over Nevada)
5	NNE	STR	(H: off S. CA coast; L: over Nevada)
6	NNE	STR	(H: off Washington coast)
7	WNW	MDT	(front approach NW U.S.; H: over Idaho)
8	NNE	WK	(fron thru N. CA; H: over Utah)
9	NNE	STR	(front thru central CA)
10	N	STR	(H: over Oregon; L: over S. Arizona)
11	NNE	STR	(H: off CA coast; L: over Gulf of CA)
12	NE	STR	(dissipating front thru central CA)
13	NNE	MDT	(front thru N. CA; L: over Arizona)
14	N	STR	(front thru central CA)
15	N	STR	(H: off Oregon coast; L: over Nevada)
16	NNE	STR	(H: off Oregon coast; L: over Gulf of CA)

17	NNE	MDT	(front thru N. CA; L: over S. CA)
18	NNE	MDT	(H: over Washington; L: over Gulf of CA)
19	NNW	MDT	(H: off S. CA coast & over S. Idaho)
20	NNE	MDT	(front thru central CA)
21	NNW	STR	(front thru S. CA; H: over Oregon)
22	NNW	MDT	(front approach NW U.S.; H: over Idaho)
23	NNW	STR	(front thru N. CA)
24	N	STR	(front thru S. CA)
25	NNE	STR	(front approach NW U.S.)
26	NNE	STR	(front thru N. CA)
27	NW	MDT	(front dissipates in central CA)
28	--	---	(L: over N. CA & Gulf of CA)
29	NNW	WK	(front thru N. CA; L: over N. & S. CA)
30	NNW	WK	(front thru N. CA)
31	NNW	STR	(front thru central CA)

JUNE

1	NW	MDT	(H: off Washington coast; L: over S. ARizona)
2	NW	STR	(H: off Washington coast; L: over S. Arizona)
3	NNW	STR	(L: over S. Nevada)
4	N	STR	(front thru N. CA; L: over Nevada)
5	NNW	STR	(front thru central CA)
6	NW	MDT	(front thru N. CA; H: off S. CA coast)
7	N	STR	(front dissipates; H: off S. CA; L: over Utah)
8	NNE	STR	(H: off Oregon coast; L: over Nevada)
9	NNE	STR	(H: off Oregon coast; L: over Nevada)
10	NNE	STR	(H: off Oregon coast; L: over Gulf of CA)
11	N	MDT	(H: off CA coast; L: over Gulf of CA)
12	N	MDT	(H: off Washington coast; L: over Gulf of CA)
13	NNW	STR	(H: off Washington coast; L: over Nevada)
14	NW	STR	(H: off Washington coast; L: over Nevada)

15	NNW	STR	(H: off Washington coast; L: over Nevada)
16	NW	MDT	(H: off Washington coast; L: over Gulf of CA)
17	NNW	MDT	(H: off Washington coast; L: over Gulf of CA)
18	NW	STR	(H: off Washington coast; L: over Gulf of CA)
19	NW	STR	(H: off N. CA coast; L: over Gulf of CA)
20	NNW	STR	(H: off N. CA coast; L: over Gulf of CA)
21	NNW	STR	(H: off N. CA coast; L: over Gulf of CA)
22	NNW	MDT	(H: over Oregon; L: over Gulf of CA)
23	NNW	MDT	(L: over N. CA and Gulf of CA)
24	NNW	MDT	(L: over N. CA and Gulf of CA)
25	N	MDT	(H: off central CA coast; L: over Gulf of CA)
26	NNW	MDT	(front thru NW U.S.; H: off central CA & over Nevada)
27	N	STR	(H: over Washington; L: over Gulf of CA)
28	NNW	STR	(H: off central CA coast; L: over Gulf of CA)
29	NNW	STR	(dissipating front thru N. CA; L: over Arizona)
30	NNW	STR	(H: over Washington
JULY			
1	NW	MDT	(H: over Idaho; L: over Gulf of CA)
2	NW	WK	(L: over central CA)
3	NW	MDT	(L: over central CA)
4	NW	WK	(L: over Gulf of CA)
5	NW	STR	(front approach NW U.S.; L: over Gulf of CA)
6	NW	MDT	(front thru N. CA)
7	NW	WK	(L: over N. CA)
8	NNW	MDT	(L: over Nevada & NW Mexico)

9	NNW	MDT	(H: off Washington; L: over S. Nevada)
10	NNW	MDT	(H: off Washington; front thru Nevada)
11	NNW	MDT	(H: off Washington; L: over S. CA)
12	NW	MDT	(H: off Washington; L: over central CA)
13	NW	WK	(L: over N. CA & Gulf of CA)
14	NW	WK	(L: over N. CA & off SW CA coast)
15	--	---	(L: over N. CA & over Gulf of CA)
16	--	---	(L: over N. CA & over Gulf of CA)
17	--	---	(L: over N. CA & over Gulf of CA)
18	--	---	(front thru N. CA)
19	--	---	(L: over N. CA & over Gulf of CA)
20	NW	MDT	(L: over N. CA & over Gulf of CA)
21	NW	MDT	(L: over N. CA & over S. Nevada)
22	NW	MDT	(trof thru central CA)

APPENDIX B

SITE SPECIFIC $\sigma\theta$ DEPENDENCY TABLES
(2/7/84 (1000-1700)--UNSTABLE)

TABLES B-(1-8). $\sigma\theta$ vs TAVG for Sites Indicated

TABLE B-1 (Site 102)

TAVG	SENSOR ELEVATION (FT) 12	54
15 s	8.7	12.9
30 s	13.4	13.7
1 m	19.8	14.4
2 m	21.7	15.2
5 m	30.6	15.5

TABLE B-2 (Site 300)

TAVG	SENSOR ELEVATION (FT) 54	102	108	204	300
15 s	7.9	8.7	8.8	8.6	8.0
30 s	9.0	10.0	10.6	10.2	9.4
1 m	10.1	11.1	12.0	11.6	10.7
2 m	11.3	12.2	13.3	12.6	12.0
5 m	13.2	13.4	14.8	13.7	13.7

TABLE B-3 (Site 200)

SENSOR ELEVATION (FT)

TAVG	12	54	102	204
15 s	13.6	11.5	11.0	8.5
30 s	15.6	13.3	12.8	10.0
1 m	17.8	15.3	14.6	11.4
2 m	20.1	16.7	15.9	12.7
5 m	22.3	18.7	17.7	14.5

TABLE B-4 (Site 301)

SENSOR ELEVATION (FT)

TAVG	12	54	102	204
15 s	19.6	9.0	8.9	9.5
30 s	22.2	10.8	10.4	11.3
1 m	24.8	12.6	12.3	13.6
2 m	34.0	14.2	13.4	15.2
5 m	34.3	16.6	15.3	16.7

TABLE B-5 (Site 052)

SENSOR ELEVATION (FT)

TAVG	12	54
15 s	8.7	7.5
30 s	10.2	8.5
1 m	12.9	9.6
2 m	13.6	10.8
5 m	18.3	12.5

TABLE B-6 (Site 054)

SENSOR ELEVATION (FT)

TAVG	12
15 s	9.7
30 s	10.7
1 m	11.9
2 m	12.8
5 m	14.0

TABLE B-7 (SITE 101)

	SENSOR ELEVATION (FT)	
TAVG	12	54
15 s	10.3	8.1
30 s	11.7	9.3
1 m	13.7	10.7
2 m	15.3	11.8
5 m	18.9	14.7

TABLE B-8 (SITE 055)

	SENSOR ELEVATION (FT)
TAVG	40
15 s	8.5
30 s	8.9
1 m	14.8
2 m	19.4
5 m	----

TABLES B-(9-16). $\sigma\theta$ vs WD for Sites Indicated
(* = Predominant Wind Direction)

TABLE B-9 (Site 102)

	SENSOR ELEVATION (FT)	
WD	12	54
5	----	----
6	13.1	14.0
7	9.8	13.8*
8	7.8*	10.2
9	8.8	30.6

TABLE B-10 (SITE 300)

SENSOR ELEVATION (FT)

WD	54	102	108	204	300
5	7.7	9.0	10.5	9.0	6.4
6	9.0	10.1	10.5	9.4	7.6
7	7.4*	7.7*	8.9*	8.6*	8.3*
8	7.4	5.8	7.3	6.5	7.7
9	9.9	----	----	----	10.8

TABLE B-11 (SITE 200)

SENSOR ELEVATION (FT)

WD	12	54	102	204
5	15.7	10.1	6.5	----
6	13.5	10.8*	11.4	7.0
7	15.6	13.9	11.5*	8.9
8	13.2*	11.0	12.3	10.2*
9	11.7	7.5	6.8	5.4

TABLE B-12 (SITE 301)

SENSOR ELEVATION (FT)

WD	12	54	102	204
5	----	13.7	9.0	8.1
6	18.0	9.5	8.9	13.0
7	24.5	8.8	10.4	10.9
8	25.1	10.0	11.1	11.5
9	16.0*	8.6*	7.6*	7.9*

TABLE B-13 (Site 052)

	SENSOR ELEVATION (FT)	
WS	12	54
5	9.1	6.4
6	7.7	7.8
7	8.7*	7.5*
8	9.3	7.4
9	8.6	7.1

TABLE B-14 (SITE 054)

	SENSOR ELEVATION (FT)
WD	12
5	----
6	17.5
7	9.8*
8	9.4
9	8.5

TABLE B-15 (SITE 101)

	SENSOR ELEVATION (FT)	
WD	12	54
5	11.1	10.1
6	11.1*	8.9*
7	12.6	10.0
8	9.9	6.8
9	7.8	6.3

TABLE B-16 (SITE 055)

	SENSOR ELEVATION (FT)
WD	40
5	5.0*
6	----
7	----
8	----
9	----

Wind Direction 5: 160-200 degrees

Wind Direction 6: 200-240 degrees

Wind Direction 7: 240-280 degrees

Wind Direction 8: 280-320 degrees

Wind Direction 9: 320-360 degrees

TABLES B-(17-24). $\sigma\theta$ vs WS for Sites Indicated
(* = Predominant Wind Speed)

TABLE B-17 (SITE 102)

SENSOR ELEVATION (FT)

WS	12	54
1	10.9	16.7
2	6.8*	10.6*
3	8.7	5.9
4	----	----

TABLE B-18 (SITE 300)

SENSOR ELEVATION (FT)

WS	54	102	108	204	300
1	9.8	10.1	10.4	10.7	10.3
2	7.3*	8.0*	8.6*	7.8*	6.8*
3	9.1	6.2	7.2	6.7	5.7
4	----	----	5.5	----	----

TABLE B-19 (SITE 200)

SENSOR ELEVATION (FT)

WS	12	54	102	204
1	15.0*	17.8	12.7*	----
2	9.9	10.3*	9.2	13.9
3	----	7.0	6.8	8.6*
4	----	----	----	5.9

TABLE B-20 (SITE 301)

SENSOR ELEVATION (FT)

WS	12	54	102	204
1	29.1	12.6	12.0	12.5
2	10.9*	7.7*	7.0*	7.3*
3	----	4.7	3.1	2.8
4	----	3.6	2.4	1.9

TABLE B-21 (SITE 052)

SENSOR ELEVATION (FT)

WS	12	54
1	11.9	11.9
2	8.1*	7.3*
3	----	4.6
4	----	----

TABLE B-22 (SITE 054)

SENSOR ELEVATION (FT)

WS	12
1	10.2
2	9.5*
3	6.6
4	----

TABLE B-23 (SITE 101)

SENSOR ELEVATION (FT)

WS	12	54
1	11.4*	8.8*
2	8.2	6.4
3	10.7	----
4	----	----

TABLE B-24 (SITE 055)

SENSOR ELEVATION (FT)

WS	40
1	12.4
2	6.1*
3	10.5
4	---

Wind Speed 1: 0-2 ms^{-1}
Wind Speed 2: 2-4 ms^{-1}
Wind Speed 3: 4-6 ms^{-1}
Wind Speed 4: 6-8 ms^{-1}

APPENDIX C

SITE SPECIFIC $\sigma\theta$ DEPENDENCY TABLES
(2/2/84 (0200-0800)--STABLE)

TABLES C-(1-8). $\sigma\theta$ vs TAVG for Sites Indicated

TABLE C-1 (SITE 102)

TAVG	SENSOR ELEVATION (FT) 12	54
15 s	4.9	5.2
30 s	5.8	5.1
1 m	11.5	5.3
2 m	15.9	5.8
5 m	----	6.9

TABLE C-2 (SITE 300)

TAVG	SENSOR ELEVATION (FT) 54	102	108	204	300
15 s	4.5	13.1	5.4	9.1	5.7
30 s	5.0	13.2	6.1	10.8	6.0
1 m	5.4	13.3	6.6	11.6	6.5
2 m	5.9	13.5	7.1	12.4	7.0
5 m	7.3	13.9	9.2	13.0	7.7

TABLE C-3 (SITE 200)

SENSOR ELEVATION (FT)

TAVG	12	54	102	204
15 s	5.0	4.8	5.5	5.9
30 s	5.7	5.5	6.3	7.0
1 m	6.6	6.5	7.2	8.3
2 m	7.9	7.7	8.1	9.5
5 m	9.4	9.4	9.2	11.0

TABLE C-4 (SITE 301)

SENSOR ELEVATION (FT)

TAVG	12	54	102	204
15 s	5.9	10.7	6.3	4.2
30 s	7.5	11.6	7.0	4.5
1 m	9.0	12.0	7.4	4.7
2 m	7.9	12.3	7.6	4.9
5 m	9.9	12.5	8.0	5.2

TABLE C-5 (SITE 052)

SENSOR ELEVATION (FT)

TAVG	12	54
15 s	12.2	6.9
30 s	12.8	8.1
1 m	16.9	9.1
2 m	13.3	10.5
5 m	13.9	11.2

TABLE C-6 (SITE 054)

SENSOR ELEVATION (FT)

TAVG	12	54
15 s	11.8	5.9
30 s	15.7	7.9
1 m	19.5	9.9
2 m	23.7	12.0
5 m	27.3	15.7

TABLE C-7 (SITE 014)

	SENSOR ELEVATION (FT)
TAVG	12
15 s	9.1
30 s	11.9
1 m	14.6
2 m	17.0
5 m	19.5

TABLE C-8 (SITE 055)

	SENSOR ELEVATION (FT)
TAVG	40
15 s	6.2
30 s	6.6
1 m	6.9
2 m	7.1
5 m	7.5

TABLES C-(9-16). $\sigma\theta$ vs WD for Sites Indicated
(* = Predominant Wind Direction)

TABLE C-9 (SITE 102)

	SENSOR ELEVATION (FT)	
WD	12	54
2	12.9	5.3*
3	4.3*	4.6
4	4.8	7.9
5	----	16.2

TABLE C-10 (SITE 300)

	SENSOR ELEVATION (FT)				
WD	54	102	108	204	300
2	3.3	12.4	3.5	4.7	4.6
3	3.6*	13.2*	5.7*	9.6*	5.5*
4	6.0	13.0	5.3	13.8	6.9
5	----	----	----	----	----

TABLE C-11 (SITE 200)

SENSOR ELEVATION (FT)

WD	12	54	102	204
2	6.4	5.5	6.2	5.9
3	4.8*	4.7*	5.2*	5.6*
4	5.5	5.0	7.7	6.2
5	14.0	----	----	2.3

TABLE C-12 (SITE 301)

SENSOR ELEVATION (FT)

WS	12	54	102	204
2	----	----	----	----
3	5.8*	7.3	5.6	4.3
4	6.3	10.9*	6.7*	4.1*
5	----	8.2	----	----

TABLE C-13 (SITE 052)

SENSOR ELEVATION (FT)

WD	12	54
2	5.0	3.7*
3	14.2*	9.0
4	18.0	23.6
5	----	----

TABLE C-14 (SITE 054)

SENSOR ELEVATION (FT)

WD	12	54
2	25.6	8.3
3	9.0*	4.0*
4	20.2	18.0
5	71.9	----

TABLE C-15 (SITE 014)

WD	SENSOR ELEVATION (FT) 12
2	----
3	1.2
4	9.1
5	6.0*

TABLE C-16 (SITE 055)

WD	SENSOR ELEVATION (FT) 40
2	----
3	7.5
4	6.1*
5	5.7

Wind Direction 2: 040-080 degrees
Wind Direction 3: 080-120 degrees
Wind Direction 4: 120-160 degrees
Wind Direction 5: 160-200 degrees

TABLES C-(17-24). $\sigma\theta$ vs WS for Sites Indicated
(* = Predominant Wind Speed)

TABLE C-17 (SITE 102)

WS	SENSOR ELEVATION (FT) 12	54
1	12.9	8.2
2	4.4*	4.9*
3	----	3.4
4	----	----

TABLE C-18 (SITE 300)

SENSOR ELEVATION (FT)

WS	54	102	108	204	300
1	6.4	15.2	6.6	11.7	8.1
2	4.4*	12.9*	6.2	12.6	5.6*
3	3.5	7.1	5.5*	9.1*	4.1
4	----	----	4.6	----	2.5

TABLE C-19 (SITE 200)

SENSOR ELEVATION (FT)

WS	12	54	102	204
1	5.2*	5.6	6.5	----
2	4.7	4.6*	4.7*	9.5
3	----	3.2	4.2	5.9*
4	----	----	----	5.1

TABLE C-20 (SITE 301)

SENSOR ELEVATION (FT)

WS	12	54	102	204
1	7.5	----	----	----
2	5.9*	5.9	6.7	5.2
3	----	10.7*	6.2*	4.3*
4	----	12.1	8.1	3.6

TABLE C-21 (SITE 052)

WS	SENSOR ELEVATION (FT) 12	54
1	13.2	----
2	11.9*	6.5
3	7.4	6.8*
4	----	11.3

TABLE C-22 (SITE 054)

WS	SENSOR ELEVATION (FT) 12	54
1	15.3	----
2	10.0*	5.1*
3	22.8	5.4
4	----	----

TABLE C-23 (SITE 014)

WS	SENSOR ELEVATION (FT) 12
1	6.1
2	9.1*
3	18.6
4	28.8

TABLE C-24 (SITE 055)

WS	SENSOR ELEVATION (FT) 40
1	----
2	7.2
3	6.3*
4	5.3

Wind Speed 1: 0-2 ms^{-1}
Wind Speed 2: 2-4 ms^{-1}
Wind Speed 3: 4-6 ms^{-1}
Wind Speed 4: 6-8 ms^{-1}

APPENDIX D

SITE SPECIFIC $\sigma\theta$ DEPENDENCY TABLES
(3/17/84 (0900-1800)--Neutral)

TABLES D-(1-8). $\sigma\theta$ vs TAVG for Sites Indicated

TABLE D-1 (SITE 102)

TAVG	SENSOR ELEVATION (FT) 12	102
15 s	7.5	4.7
30 s	7.6	4.9
1 m	8.9	5.1
2 m	11.0	5.2
5 m	10.6	5.3

TABLE D-2 (SITE 300)

TAVG	SENSOR ELEVATION (FT) 108
15 s	5.4
30 s	5.7
1 m	5.9
2 m	6.1
5 m	6.2

TABLE D-3 (SITE 200)

SENSOR ELEVATION (FT)

TAVG	12	54	102	204
15 s	12.1	6.6	5.0	3.7
30 s	12.5	7.0	5.3	3.9
1 m	12.7	7.3	5.4	4.0
2 m	12.8	7.4	5.5	4.2
5 m	12.8	7.5	5.6	4.3

TABLE D-4 (SITE 301)

SENSOR ELEVATION (FT)

TAVG	12	54	102	204
15 s	8.2	10.0	8.2	6.5
30 s	8.2	10.6	8.5	6.8
1 m	8.1	11.3	8.8	7.0
2 m	----	12.4	9.0	7.1
5 m	----	12.7	9.2	7.2

TABLE D-5 (SITE 052)

SENSOR ELEVATION (FT)

TAVG	12
15 s	7.9
30 s	8.6
1 m	9.0
2 m	9.5
5 m	9.9

TABLE D-6 (SITE 054)

SENSOR ELEVATION (FT)

TAVG	12	54
15 s	7.3	6.3
30 s	8.0	6.8
1 m	8.6	7.1
2 m	8.9	7.4
5 m	9.2	7.7

TABLE D-7 (SITE 101)

	SENSOR ELEVATION (FT)	
TAVG	12	54
15 s	7.3	5.9
30 s	8.0	6.6
1 m	8.6	7.1
2 m	9.0	7.6
5 m	9.6	8.2

TABLE D-8 (SITE 055)

	SENSOR ELEVATION (FT)
TAVG	40
15 s	4.1
30 s	4.6
1 m	5.1
2 m	5.4
5 m	5.5

TABLES D-(9-16). $\sigma\theta$ vs WD for Sites Indicated
(* = Predominant Wind Direction)

TABLE D-9 (SITE 102)

	SENSOR ELEVATION (FT)	
WD	12	102
8	7.5	4.8
9	7.8*	4.7*
1	----	----

TABLE D-10 (SITE 300)

	SENSOR ELEVATION (FT)
WD	108
8	6.0
9	5.3*
1	----

TABLE D-11 (SITE 200)

	SENSOR ELEVATION (FT)			
WD	12	54	102	204
8	12.1	6.8	5.9	3.3
9	12.2*	6.6*	5.0*	3.7*
1	13.5	----	----	----

TABLE D-12 (SITE 301)

SENSOR ELEVATION (FT)

WD	12	54	102	204
8	----	----	----	10.9
9	8.2*	10.0*	8.2*	6.5*
1	----	7.9	5.0	11.1

TABLE D-13 (SITE 052)

SENSOR ELEVATION (FT)

WD	12	54
8	7.7	7.8
9	7.9*	5.9*
1	6.3	3.8

TABLE D-14 (SITE 054)

SENSOR ELEVATION (FT)

WD	12	54
8	8.7	8.3
9	7.2*	6.2*
1	----	----

TABLE D-15 (SITE 101)

SENSOR ELEVATION (FT)

WD	12	54
8	14.1	6.4
9	7.3*	5.9*
1	7.5	5.6

TABLE D-16 (SITE 055)

SENSOR ELEVATION (FT)

WD	40
8	----
9	4.1*
1	10.6

Wind Direction 8: 280-320 degrees
Wind Direction 9: 320-360 degrees
Wind Direction 1: 000-040 degrees

TABLES D-(17-24). $\sigma\theta$ vs WS for Sites Indicated
(* = Predominant Wind Speed)

TABLE D-17 (SITE 102)

WS	SENSOR ELEVATION (FT) 12	102
4	5.7	8.3
5	----	6.7
6	----	5.1*
7	----	4.1
8	----	3.2

TABLE D-18 (SITE 300)

WS	SENSOR ELEVATION (FT) 108
4	----
5	----
6	7.2
7	6.5
8	6.4

TABLE D-19 (SITE 200)

WS	SENSOR ELEVATION (FT) 12	54	102	204
4	11.5*	10.2	7.5	----
5	9.9	8.1	6.6	----
6	8.4	6.5*	5.4*	6.0
7	----	5.3	4.4	4.6
8	----	4.9	3.9	3.4*

TABLE D-20 (SITE 301)

WS	SENSOR ELEVATION (FT) 12	54	102	204
4	----	13.4	11.1	11.3
5	8.2*	11.4*	10.0*	9.2
6	----	8.5	7.4	7.3
7	----	5.8	5.5	5.8*
8	----	7.2	4.5	5.4

TABLE D-21 (SITE 052)

SENSOR ELEVATION (FT)

WS	12	54
4	9.4	12.8
5	8.0*	8.2
6	7.7	6.3*
7	7.3	5.1
8	6.5	4.0

TABLE D-22 (SITE 054)

SENSOR ELEVATION (FT)

WS	12	54
4	10.1	9.2
5	7.7*	7.5
6	6.0	5.6*
7	4.5	4.4
8	----	3.4

TABLE D-23 (SITE 101)

SENSOR ELEVATION (FT)

WS	12	54
4	9.8	9.0
5	7.9*	6.8*
6	6.5	5.1
7	6.1	4.6
8	----	3.9

TABLE D-24 (SITE 055)

SENSOR ELEVATION (FT)

WS	40
4	----
5	----
6	8.9
7	8.1
8	6.1

102-12': Predominant W.S. 4-6 ms^{-1}
300-108': Predominant W.S. 18+ ms^{-1}
055-40': Predominant W.S. 18+ ms^{-1}
Wind Speed 4: 6-8 ms^{-1}
Wind Speed 5: 8-10 ms^{-1}
Wind Speed 6: 10-12 ms^{-1}
Wind Speed 7: 12-14 ms^{-1}
Wind Speed 8: 14-16 ms^{-1}

APPENDIX E

SITE/ELEVATION SPECIFIC $\sigma\theta$ DEPENDENCY TABLES (INTERSTABILITY)

TABLES E-(1-4). $\sigma\theta$ vs TAVG for Heights Indicated (Interstability)

TABLE E-1 (12' Sensors)

TAVG	UNSTABLE	NEUTRAL	STABLE
15 s	11.8	8.4	8.2
30 s	14.0	8.8	9.9
1 m	16.8	9.3	13.0
2 m	19.6	10.2	14.3
5 m	23.1	10.4	16.0

TABLE E-2 (54' Sensors)

TAVG	UNSTABLE	NEUTRAL	STABLE
15 s	9.5	7.2	6.3
30 s	10.8	7.8	7.2
1 m	12.1	8.2	8.0
2 m	13.3	8.7	9.0
5 m	15.2	9.0	10.5

TABLE E-3 (102' Sensors)

TAVG	UNSTABLE	NEUTRAL	STABLE
15 s	9.5	6.0	8.3
30 s	11.1	6.2	8.8
1 m	12.7	6.4	9.3
2 m	13.9	6.6	9.7
5 m	15.5	6.7	10.4

TABLE E-4 (204' Sensors)

TAVG	UNSTABLE	NEUTRAL	STABLE
15 s	8.9	5.1	6.4
30 s	10.5	5.4	7.4
1 m	12.2	5.5	8.2
2 m	13.5	5.7	8.9
5 m	15.0	5.8	9.7

TABLES E-(5-13). $\sigma\theta$ vs TAVG for Sites Indicated (Insterstability)

TABLE E-5 (SITE 102)

HT	TAVG	UNSTABLE	NEUTRAL	STABLE
12'	15 s	8.7	7.5	4.9
	30 s	13.4	7.6	5.8
	1 m	19.8	8.9	11.5
	2 m	21.7	11.0	15.9
	5 m	30.6	10.6	----
54'	15 s	12.9	----	5.2
	30 s	13.7	----	5.1
	1 m	14.4	----	5.3
	2 m	15.2	----	5.8
	5 m	15.5	----	6.9
102'	15 s	----	4.7	----
	30 s	----	4.9	----
	1 m	----	5.1	----
	2 m	----	5.2	----
	5 m	----	5.3	----

TABLE E-6 (SITE 300)

HT	TAVG	UNSTABLE	NEUTRAL	STABLE
	15 s	7.9	----	4.5
	30 s	9.0	----	5.0
54'	1 m	10.1	----	5.4
	2 m	11.3	----	5.9
	5 m	13.2	----	7.3
	15 s	8.7	----	13.1
	30 s	10.0	----	13.2
102'	1 m	11.1	----	13.3
	2 m	12.2	----	13.5
	5 m	13.4	----	13.9
	15 s	8.8	5.4	5.4
	30 s	10.6	5.7	6.1
108'	1 m	12.0	5.9	6.6
	2 m	13.3	6.1	7.1
	5 m	14.8	6.2	9.2
	15 s	8.6	----	9.1
	30 s	10.2	----	10.8
204'	1 m	11.6	----	11.6
	2 m	12.6	----	12.4
	5 m	13.7	----	13.0
	15 s	8.0	----	5.7
	30 s	9.4	----	6.0
300'	1 m	10.7	----	6.5
	2 m	12.0	----	7.0
	5 m	13.7	----	7.7

TABLE E-7 (SITE 200)

HT	TAVG	UNSTABLE	NEUTRAL	STABLE
	15 s	13.6	12.1	5.0
	30 s	15.6	12.5	5.7
12'	1 m	17.8	12.7	6.6
	2 m	20.1	12.8	7.9
	5 m	22.3	12.8	9.4
	15 s	11.5	6.6	4.8
	30 s	13.3	7.0	5.5
54'	1 m	15.3	7.3	6.5
	2 m	16.7	7.4	7.7
	5 m	18.7	7.5	9.4
	15 s	11.0	5.0	5.5
	30 s	12.8	5.3	6.3
102'	1 m	14.6	5.4	7.2
	2 m	15.9	5.5	8.1
	5 m	17.7	5.6	9.2
	15 s	8.5	3.7	5.9
	30 s	10.0	3.9	7.0
204'	1 m	11.4	4.0	8.3
	2 m	12.7	4.2	9.4
	5 m	14.5	4.3	11.0

TABLE E-8 (SITE 301)

HT	TAVG	UNSTABLE	NEUTRAL	STABLE
	15 s	19.6	8.2	5.9
	30 s	22.2	8.2	7.5
12'	1 m	24.8	8.1	9.0
	2 m	34.0	----	7.9
	5 m	34.3	----	9.9
	15 s	9.0	10.0	10.7
	30 s	10.8	10.6	11.6
54'	1 m	12.6	11.3	12.0
	2 m	14.2	12.4	12.3
	5 m	16.6	12.7	12.5
	15 s	8.9	8.2	6.3
	30 s	10.4	8.5	7.0
102'	1 m	12.3	8.8	7.4
	2 m	13.4	9.0	7.6
	5 m	15.3	9.2	8.0
	15 s	9.5	6.5	4.2
	30 s	11.3	6.8	4.5
204'	1 m	13.6	7.0	4.7
	2 m	15.2	7.1	4.9
	5 m	16.7	7.2	5.2

TABLE E-9 (SITE 052)

HT	TAVG	UNSTABLE	NEUTRAL	STABLE
	15 s	8.7	7.9	12.2
	30 s	10.2	8.6	12.8
12'	1 m	12.9	9.0	16.9
	2 m	13.6	9.5	13.3
	5 m	18.3	9.9	13.9
	15 s	7.5	----	6.9
	30 s	8.5	----	8.1
54'	1 m	9.6	----	9.1
	2 m	10.8	----	10.5
	5 m	12.5	----	11.2

TABLE E-10 (SITE 054)

HT	TAVG	UNSTABLE	NEUTRAL	STABLE
	15 s	9.7	7.3	11.8
	30 s	10.7	8.0	15.7
12'	1 m	11.9	8.6	19.5
	2 m	12.8	8.9	23.7
	5 m	14.0	9.2	27.3
	15 s	----	6.3	5.9
	30 s	----	6.8	7.9
54'	1 m	----	7.1	9.9
	2 m	----	7.4	12.0
	5 m	----	7.7	15.7

TABLE E-11 (SITE 101)

HT	TAVG	UNSTABLE	NEUTRAL	STABLE
	15 s	10.3	7.3	----
	30 s	11.7	8.0	----
12'	1 m	13.7	8.6	----
	2 m	15.3	9.0	----
	5 m	18.9	9.6	----
	15 s	8.1	5.9	----
	30 s	9.3	6.6	----
54'	1 m	10.7	7.1	----
	2 m	11.8	7.6	----
	5 m	14.7	8.2	----

TABLE E-12 (SITE 014)

HT	TAVG	UNSTABLE	NEUTRAL	STABLE
	15 s	----	----	9.1
	30 s	----	----	11.9
12'	1 m	----	----	14.6
	2 m	----	----	17.0
	5 m	----	----	19.5

TABLE E-13 (SITE 055)

HT	TAVG	UNSTABLE	NEUTRAL	STABLE
	15 s	8.5	4.1	6.2
	30 s	8.9	4.6	6.6
40'	1 m	14.8	5.1	6.9
	2 m	19.4	5.4	7.1
	5 m	15.9	5.5	7.5

APPENDIX F

SENSOR SPECIFIC $\sigma\theta$ CHARACTERIZATION TABLES (INTERSTABILITY)

NOTE: See Table V "Vandenberg Data Binning' for Abbreviation and Categorization Information.

TABLE F-1 (UNSTABLE CASE)

SENSOR 3 (052-12'):	TAVG 1/WS '1' (on):	8.7
	WD 7/TAVG '1' (WS '1'):	8.7
	WS 2/TAVG '1' (on):	8.1
	MIN $\sigma\theta$ (WD 6):	7.7
	MAX $\sigma\theta$ (WD 8):	9.3
	Power Law (x):	.25
SENSOR 4 (054-12'):	TAVG 1/WS '1' (on):	9.7
	WD 7/TAVG '1' (WS '1'):	9.8
	WS 2/TAVG '1' (on):	9.5
	MIN $\sigma\theta$ (WD 9):	8.5
	MAX $\sigma\theta$ (WD 6):	17.5
	Power Law (x):	.12
SENSOR 5 (101-12'):	TAVG 1/WS '1' (on):	10.3
	WD 6/TAVG '1' (WS '1'):	11.1
	WS 1/TAVG '1' (on):	11.4
	MIN $\sigma\theta$ (WD 9):	7.8
	MAX $\sigma\theta$ (WD 7):	12.6
	Power Law (x):	.20
SENSOR 6 (102-12'):	TAVG 1/WS '1' (on):	8.7
	WD 8/TAVG '1' (WS '1'):	7.8
	WS 2/TAVG '1' (on):	6.8
	MIN $\sigma\theta$ (WD 8):	7.8
	MAX $\sigma\theta$ (WD 6):	13.1
	Power Law (x):	.42
SENSOR 8 (200-12'):	TAVG 1/ WS '1' (on):	13.6
	WD 8/TAVG '1' (WS '1'):	13.2
	WS 1/TAVG '1' (on):	15.0
	MIN $\sigma\theta$ (WD 9):	11.7
	MAX $\sigma\theta$ (WD 5):	15.7
	Power Law (x):	.17
SENSOR 10 (301-12'):	TAVG 1/WS '1' (0n):	19.6
	WD 9/TAVG '1' (WS '1'):	16.0
	WS 2/TAVG '1' (on):	10.9
	MIN $\sigma\theta$ (WD 9):	16.0
	MAX $\sigma\theta$ (WD 8):	25.1
	Power Law (x):	.19

SENSOR 13 (055-40'):	TAVG 1/WS'1' (off):	8.5
	WD 5/TAVG '1' (WS '2'):	5.0
	WS 2/TAVG '1' (0ff):	6.1
	MIN σθ (WD 5):	5.0
	MAX σθ (WD 4):	12.7
	Power Law (x):	.21
SENSOR 11 (052-54'):	TAVG 1/WS '1' (0n):	7.5
	WD 7/TAVG '1' (WS '1'):	7.5
	WS 2/TAVG '1' (on):	7.3
	MIN σθ (WD 5):	6.4
	MAX σθ (WD 6):	7.8
	Power Law (x):	.17
SENSOR 15 (101-54'):	TAVG 1/WS '1' (on):	8.1
	WD 6/TAVG '1' (WS '1'):	8.9
	WS 1/TAVG '1' (on):	8.8
	MIN σθ (WD 9):	6.3
	MAX σθ (WD 4):	11.8
	Power Law (x):	.20
SENSOR 16 (102-54'):	TAVG 1/WS '1' (on):	12.9
	WD 7/TAVG '1' (WS '1'):	13.8
	WS 2/TAVG '1' (0n):	10.6
	MIN σθ (WD 8):	10.2
	MAX σθ (WD 6):	14.0
	Power Law (x):	.06
SENSOR 18 (200-54'):	TAVG 1/WS '1' (on):	11.5
	WD 6/TAVG '1' (WS '1'):	10.8
	WS 3/TAVG '1' (on):	10.3
	MIN σθ (WD 9):	7.5
	MAX σθ (WD 7):	13.9
	Power Law (x):	.16
SENSOR 19 (300-54'):	TAVG 1/WS '1' (on):	7.9
	WD 7/TAVG '1' (WS '1'):	7.4
	WS 2/TAVG '1' (on):	7.3
	MIN σθ (WD 7&8):	7.4
	MAX σθ (WD 6):	9.0
	Power Law (x):	.17
SENSOR 20 (301-54'):	TAVG 1/WS '1' (on):	9.0
	WD 9/TAVG '1' (WS '1'):	8.6
	WS 2/TAVG '1' (on):	7.7
	MIN σθ (WD 1):	8.2
	MAX σθ (WD 8):	10.0
	Power Law (x):	.20

SENSOR 22 (200-102'):	TAVG 1/WS '1' (on):	11.0
	WD 7/TAVG '1' (WS '1'):	11.5
	WS 1/TAVG '1' (on):	12.7
	MIN σθ (WD 9):	6.8
	MAX σθ (WD 8):	12.3
	Power Law (x):	.16
SENSOR 23 (300-102'):	TAVG 1/WS '1' (on):	8.7
	WD 7/TAVG '1' (WS '1'):	7.7
	WS 2/TAVG '1' (on):	8.0
	MIN σθ (WD 8):	5.8
	MAX σθ (WD 6):	10.1
	Power Law (x):	.14
SENSOR 25 (301-102'):	TAVG 1/WS '1' (on):	8.9
	WD 9/TAVG '1' (WS '1'):	7.6
	WS 2/TAVG '1' (on):	7.0
	MIN σθ (WD 1&9):	7.5
	MAX σθ (WD 8):	11.1
	Power Law (x):	.18
SENSOR 24 (300-108'):	TAVG 1/WS '1' (on):	8.8
	WD 7/TAVG '1' (WS '1'):	8.9
	WS 2/TAVG '1' (on):	8.6
	MIN σθ (WD 8):	7.3
	MAX σθ (WD 6):	10.5
	Power Law (x):	.17
SENSOR 26 (200-204'):	TAVG 1/WS '2' (on):	8.5
	WD 8/TAVG '1' (WS '2'):	10.2
	WS 3/TAVG '1' (on):	8.6
	MIN σθ (WD 9):	5.4
	MAX σθ (WD 8):	10.2
	Power Law (x):	.18
SENSOR 27 (300-204'):	TAVG 1/WS '1' (on):	8.6
	WD 7/TAVG '1' (WS '1'):	8.6
	WS 2/TAVG '1' (on):	7.8
	MIN σθ (WD 8):	6.5
	MAX σθ (WD 6):	9.4
	Power Law (x):	.16
SENSOR 28 (301-204'):	TAVG 1/WS '1' (on):	9.5
	WD 9/TAVG '1' (WS '1'):	7.9
	WD 2/TAVG '1' (on):	7.3
	MIN σθ (WD 9):	7.9
	MAX σθ (WD 6):	13.0
	Power Law (x):	.19
SENSOR 29 (300-300'):	TAVG 1/WS '1' (on):	8.0
	WD 7/TAVG '1' (WS '1'):	8.3
	WS 2/TAVG '1' (on):	6.8
	MIN σθ (WD 5):	6.4
	MAX σθ (WD 7):	8.3
	Power Law (x):	.18

TABLE F-2 (STABLE CASE)

SENSOR 2 (014-12'):	TAVG 1/WS '1' (off):	9.1
	WD 5/TAVG '1' (WS '2'):	6.4
	WS2/TAVG '1' (off):	9.1
	MIN σθ (WD 6):	5.7
	MAX σθ (WD 4):	19.8
	Power Law (x):	.25
SENSOR 3 (052-12'):	TAVG 1/WS '1' (off):	12.2
	WD 3/TAVG '1' (WS '1'):	14.2
	WS 2/TAVG '1' (off):	11.9
	MIN σθ (WD 2):	5.0
	MAX σθ (WD 4):	18.0
	Power Law (x):	.04
SENSOR 4 (054-12'):	TAVG 1/WS '1' (off):	11.8
	WD 3/TAVG '1' (WS '1'):	9.0
	WS 2/TAVG '1' (off):	10.0
	MIN σθ (WD 3):	9.0
	MAX σθ (WD 4):	29.2
	Power Law (x):	.28
SENSOR 6 (102-12'):	TAVG 1/WS '1' (off):	4.9
	WD 3/TAVG '1' (WS '1'):	4.3
	WS 2/TAVG '1' (off):	4.4
	MIN σθ (WD 3):	4.3
	MAX σθ (WD 2):	12.9
	Power Law (x):	.40
SENSOR 8 (200-12'):	TAVG 1/WS '1' (off):	5.0
	WD 3/TAVG '1' (WS '1'):	4.8
	WS 1/TAVG '1' (off):	5.2
	MIN σθ (WD 3):	4.8
	MAX σθ (WD 2):	6.4
	Power Law (x):	.21
SENSOR 10 (301-12'):	TAVG 1/WS '1' (off):	5.9
	WD 3/TAVG '1' (WS '1'):	5.8
	WS 2/TAVG '1' (off):	5.9
	MIN σθ (WD 3):	5.8
	MAX σθ (WD 4):	6.3
	Power Law (x):	.17
SENSOR 13 (055-40'):	TAVG 1/WS '2' (off):	6.2
	WD 4/TAVG '1' (WS '2'):	6.1
	WS 3/TAVG '1' (off):	6.3
	MIN σθ (WD 5):	5.7
	MAX σθ (WD 3):	7.5
	Power Law (x):	.14

SENSOR 11 (052-54'):	TAVG 1/WS '2' (off):	6.9
	WD 2/TAVG '1' (WS '2'):	3.7
	WS 3/TAVG '1' (off):	6.8
	MIN σθ (WD 2):	3.7
	MAX σθ (WD 4):	23.6
	Power Law (x):	.16
SENSOR 12 (054-54'):	TAVG 1/WS '1' (off):	5.9
	WD 3/TAVG '1' (WS '1'):	4.0
	WS 2/TAVG '1' (off):	5.1
	MIN σθ (WD 3):	4.0
	MAX σθ (WD 4):	18.0
	Power Law (x):	.33
SENSOR 16 (102-54'):	TAVG 1/WS '1' (off):	5.2
	WD 2/TAVG '1' (WS '1'):	5.3
	WS 2/TAVG '1' (off):	4.9
	MIN σθ (WD 3):	4.6
	MAX σθ (WD 4):	7.9
	Power Law (x):	.09
SENSOR 18 (200-54'):	TAVG 1/WS '1' (off):	4.8
	WD 3/TAVG '1' (WS '1'):	4.7
	WS 2/TAVG '1' (off):	4.6
	MIN σθ (WD 3):	4.7
	MAX σθ (WD 2):	5.5
	Power Law (x):	.22
SENSOR 19 (300-54'):	TAVG 1/WS '1' (off):	4.5
	WD 3/TAVG '1' (WS '2'):	3.0
	WS 2/TAVG '1' (off):	4.4
	MIN σθ (WD 2):	2.2
	MAX σθ (WD 4):	6.0
	Power Law (x):	.16
SENSOR 20 (301-54'):	TAVG 1/WS '2' (off):	10.7
	WD 4/TAVG '1' (WS '2'):	10.9
	WS 3/TAVG '1' (off):	10.7
	MIN σθ (WD 3):	7.3
	MAX σθ (WD 4):	10.9
	Power Law (x):	.05
SENSOR 22 (200-102'):	TAVG 1/WS '1' (off):	5.5
	WD 3/TAVG '1' (WS '1'):	5.2
	WS 2/TAVG '1' (off):	4.7
	MIN σθ (WD 3):	5.2
	MAX σθ (WD 4):	7.7
	Power Law (x):	.17
SENSOR 23 (300-102'):	TAVG 1/WS '1' (off):	13.1
	WD 3/TAVG '1' (WS '1'):	13.2
	WS 2/TAVG '1' (off):	12.9
	MIN σθ (WD 2):	12.4
	MAX σθ (WD 3):	13.2
	Power Law (x):	.02

SENSOR 25 (301-102'):	TAVG 1/WS '2' (off):	6.3
	WD 4/TAVG '1' (WS '2'):	6.7
	WS 3/TAVG '1' (off):	6.2
	MIN σθ (WD 3):	5.6
	MAX σθ (WD 4):	6.7
	Power Law (x):	.08
SENSOR 24 (299-108'):	TAVG 1/WS '2' (off):	5.4
	WD 3/TAVG '1' (WS '2'):	5.7
	WS 3/TAVG '1' (off):	5.5
	MIN σθ (WD 2):	3.5
	MAX σθ (WD 3):	5.7
	Power Law (x):	.18
SENSOR 26 (200-204'):	TAVG 1/WS '2' (off):	5.9
	WD 3/TAVG '1' (WS '2'):	5.6
	WS 3/TAVG '1' (off):	5.9
	MIN σθ (WD 3):	5.6
	MAX σθ (WS 4):	6.2
	Power Law (x):	.21
SENSOR 27 (300-204'):	TAVG 1/WS '2' (off):	9.1
	WD 3/TAVG '1' (WS '2'):	9.6
	WS 3/TAVG '1' (off):	9.1
	MIN σθ (WD 2):	4.7
	MAX σθ (WD 4):	13.8
	Power Law (x):	.12
SENSOR 28 (301-204'):	TAVG 1/WS '2' (off):	4.2
	WD 4/TAVG '1' (WS '2'):	4.1
	WS 3/TAVG '1' (off):	4.3
	MIN σθ (WD 4):	4.1
	MAX σθ (WD 3):	4.3
	Power Law (x):	.07
SENSOR 29 (300-300'):	TAVG 1/WS '1' (off):	5.7
	WD 3/TAVG '1' (WS '1'):	5.5
	WS 2/TAVG '1' (off):	5.6
	MIN σθ (WD 2):	4.6
	MAX σθ (WD 4):	6.9
	Power Law (x):	.10

TABLE F-3 (NEUTRAL CASE)

SENSOR 3 (052-12'):	TAVG 1/WS '3' (on):	7.9
	WD 9/TAVG '1' (WS '3'):	7.9
	WS 5/TAVG '1' (on):	8.0
	Power Law (x):	.08
SENSOR 4 (054-12'):	TAVG 1/WS '3' (on):	7.3
	WD 9/TAVG '1' (WS '3'):	7.2
	WS 5/TAVG '1' (on):	7.7
	Power Law (x):	.08
SENSOR 5 (101-12'):	TAVG 1/WS '3' (on):	7.3
	WD 9/TAVG '1' (WS '3'):	7.3
	WS 5/TAVG '1' (on):	7.9
	Power Law (x):	.09
SENSOR 6 (102-12'):	TAVG 1/WS '2' (on):	7.5
	WD 9/TAVG '1' (WS '2'):	7.5
	WS 3/TAVG '1' (on):	7.8
	Power Law (x):	.16
SENSOR 8 (200-12'):	TAVG 1/WS '2' (on):	12.1
	WD 9/TAVG '1' (WS '2'):	12.2
	WS 4/TAVG '1' (on):	11.5
	Power Law (x):	.02
SENSOR 10 (301-12'):	TAVG 1/WS '3' (on):	8.2
	WD 9/TAVG '1' (WS '3'):	8.2
	WS 5/TAVG '1' (on):	8.2
	Power Law (x):	----
SENSOR 13 (055-40'):	TAVG 1/WS '3' (on):	4.1
	WD 9/TAVG '1' (WS '3'):	4.1
	WS 10/TAVG '1' (on):	3.2
	Power Law (x):	.10
SENSOR 11 (052-54'):	TAVG 1/WS '3' (on):	----
	WD 9/TAVG '1' (WS '3'):	5.9
	WS 6/TAVG '1' (on):	6.3
	Power Law (x):	----
SENSOR 12 (054-54'):	TAVG 1/WS '3' (on):	6.3
	WD 9/TAVG '1' (WS '3'):	6.2
	WS (5&6)/TAVG '1' (on):	7.5-5.6
	Power Law (x):	.07
SENSOR 15 (101-54'):	TAVG 1/WS '3' (on):	5.9
	WD 9/TAVG '1' (WS '3'):	5.9
	WS (5&6)/TAVG '1' (on):	6.8-5.1
	Power Law (x):	.11

SENSOR 18 (200-54'):	TAVG 1/WS '3' (on):	6.6
	WD 9/TAVG '1' (WS '3'):	6.6
	WS 6/TAVG '1' (on):	6.5
	Power Law (x):	.04
SENSOR 20 (301-54'):	TAVG 1/WS '3' (on):	10.0
	WD 9/TAVG '1' (WS '3'):	10.0
	WS 5/TAVG '1' (on):	11.4
	Power Law (x):	.08
SENSOR 21 (102-102'):	TAVG 1/WS '3' (on):	4.7
	WD 9/TAVG '1' (WS '3'):	4.7
	WS 6/TAVG '1' (on):	5.1
	Power Law (x):	.04
SENSOR 22 (200-102'):	TAVG 1/WS '3' (on):	5.0
	WD9/ TAVG '1' (WS '3'):	5.0
	WS (6&7)/ TAVG '1' (on):	5.4-4.4
	Power Law (x):	.04
SENSOR 25 (301-102'):	TAVG 1/WS '3' (on):	8.2
	WD 9/TAVG '1' (WS '3'):	8.2
	WS 5/TAVG '1' (on):	10.0
	Power Law (x):	.04
SENSOR 24 (299-108'):	TAVG 1/WS '3' (on):	5.4
	WD 9/TAVG '1' (WS '3'):	5.3
	WS 10/TAVG '1' (on):	5.0
	Power Law (x):	.05
SENSOR 26 (200-204'):	TAVG 1/WS '3' (on):	3.7
	WD 9/TAVG '1' (WS '3'):	3.7
	WS 8/TAVG '1' (on):	3.4
	Power Law (x):	.05
SENSOR 28 (301-204'):	TAVG 1/WS '3' (on):	6.5
	WD 9/TAVG '1' (WS '3'):	6.5
	WS 7/TAVG '1' (on):	5.8
	Power Law (x):	.03

LIST OF REFERENCES

1. Schacher, G.E. and Stanton, T.P., Mean Flow and Turbulence in Complex Terrain (NPS/Vandenberg Measurement System), Naval Postgraduate School, Monterey, California, March 1984.

2. Hanna, S.R., "Diurnal Variation of Horizontal Wind Direction Fluctuations in Complex Terrain at Geysers, CAL.," Boundary-Layer Meteorology, V. 21, pp. 207-213, 1981.

3. Scientific Report 7 (ISSN 0112-2398), Measurements on a Thirty Metre Tower at the New Zealand Synthetic Fuels Corporation Plant, Motunui, with Applications to Atmospheric Dispersion, by D.S. Wratt and L.F. Homes, New Zealand, June 1984.

4. Slade, D.H., Meteorology and Atomic Energy 1968, p. 53, USAEC Technical Information Center, Oak Ridge, Tennessee, July 1968.

5. Wratt, D.S., Hadfield, M.G., Homes, L.F., and Isacc, P., Pollution Dispersion Predictions from Meteorological Tower Measurements, from Proceedings, Eighth International Clean Air Conference, Melbourne, Australia, p. 533, May 1984.

6. Panofsky, H.A., Egolf, C.A., and Lipschutz, R., "On Characteristics of Wind Direction Fluctuations in the Surface Layer," Boundary-Layer Meteorology, V. 15, pp. 439-446, 1978.

7. Air Force Cambridge Research Laboratories (AFCRL-65-637), Summary of One Year of Data from the Cape Kennedy WIND System, by J. Dwyer and G.L. Tucker, Capt, USAF, August 1965.

8. Schacher, G.E. and Stanton, T.P., Mean Flow and Turbulence in Complex Terrain (NPS/Vandenberg Measurement System), Naval Postgraduate School, Monterey, California, pp. 57-66, March 1984.

9. Scientific Report 8 (ISSN 0112-2398), Using Information from Meteorological Towers in Complex Terrain, by D.S. Wratt, M.G. Hadfield, L.F. Homes, and P. Isaac, July 1984.

10. Institute for Aerospace Studies, University of Toronto, Canada, Utias Review No. 32, Characteristics of the Mean Wind and Turbulence in the Planetary Boundary Layer, by H.W. Teunissen, pp. 13-14, October 1970.

11. Wratt, D.S., Hadfield, M.G., Homes, L.F., and Isacc, P., Pollution Dispersion Predictions from Meteorological Tower Measurements, from Proceedings, Eighth International Clean Air Conference, Melbourne, Australia, p. 542, May 1984.

12. Smith, F.B. and Hay, J.S., "The Expansion of Clusters of Particles in the Atmosphere," Quarterly Journal of the Royal Meteorological Society, V. 87, p. 82, 1961.

INITIAL DISTRIBUTION LIST

		No. Copies
1.	Defense Technical Information Center Cameron Station Alexandria, Virginia 22314	2
2.	Library, Code 0142 Naval Postgraduate School Monterey, California 93943	2
3.	Capt. Michael J. Buell Det 30 2 Weather Squadron Vandenberg Air Force Base California 93437	5
4.	Chairman, Code 63Rd Department of Meteorology Naval Postgraduate School Monterey, CA 93943	1
5.	Professor G.E. Schacher, Code 61Sg Department of Physics Naval Postgraduate School Monterey, California 93943	3
6.	Professor Torben Mikkelsen, Code 63Mk Department of Meteorology Naval Postgraduate School Monterey, California 93943	2
7.	Professor W. Shaw, Code 63Sr Department of Meteorology Naval Postgraduate School Monterey, California 93943	1
8.	Professor K.L. Davidson, Code 63Ds Department of Meteorology Naval Postgraduate School Monterey, California 93943	1
9.	Mr. Chuck Skupniewicz, Code 61 Department of Physics Naval Postgraduate School Monterey, California 93943	1

10. Capt. Betchart — 1
SD/CFAT
Headquarters Space Division
P.O. Box 92960
Worldway Postal Center
Los Angeles, California 90009

11. Dr. Ray Bernberg — 2
The Aerospace Corporation
Space Launch Vehicle Division
P.O. Box 92957
Los Angeles, California 90009

12. Dr. Ron Cionco — 1
Atmospheric Sciences Lab
WSMR, New Mexico 80002

13. Lt. Col. William Bihner — 2
WSMC/WE
Vandenberg Air Force Base
California 93437

DUDLEY KNOX LIBRARY
NAVAL POSTGRADUATE SCHOOL
MONTEREY, CALIFORNIA 93943-5002

219245

Thesis
B83746 Buell
c.1 Mean flow and turbulence in complex terrain.

219245

Thesis
B83746 Buell
c.1 Mean flow and turbulence in complex terrain.

thesB83746
Mean flow and turbulence in complex terr
3 2768 000 67187 9
DUDLEY KNOX LIBRARY